MAP Kinase Phosphatase-2 in Vascular Smooth Muscle Cell Function

Emma Torrance

A thesis submitted in the fulfilment of the

requirements for the degree of Doctor of Philosophy

Department of Cell Biology

Strathclyde Institute of Pharmacy and Biomedical Science

October 2013

This thesis is the result of the author's original research. It has been composed by the author and has not been previously submitted for examination which has led to the award of a degree.

Signed:

Date:

Acknowledgements

First and foremost, I would like to thank Robin for all his help, support and humour in the writing of this thesis. I truly attribute my development, not only as a scientist but as a person to his openness and belief in me. Furthermore, I would like to serve my gratitude to Andy, who is always readily on hand for advice and sheer banter. I have had amazing lab mates always ready for advice and biscuits; Gary, Roy, Juliane, Yuen, Ali, Sulaiman, Thikryat, Lindsay and Dave. I would especially like to thank Katy, who has been a great friend and I believe that if cell culture hoods had ears, we'd have our own TV show by now. I would also like to apologise to everyone for three years of blaring music in the cell culture room...Particularly Pat Benatar – Love is a Battlefield.

I am blessed to belong to a large family, where each and every one of you has supported me in your own way. I would like to thank my parents, who have a unique talent of making me feel as though they are always around the corner, no matter how far they really are. Not only that, from a young age they have instilled an attitude in me that anything be achieved with hard work and kindness. This is a mantra that I hope I can spread to those I meet.

I have a great network of friends who really must be applauded for enduring with me throughout my Ph.D. The sacred Tuesday meets with Shell, Leigh, Fiona, Ruth and Kirsty have definitely ensured my sanity and for this they must be commended. I also must thank all my SIPBS friends for their support, partying and office banter. Particularly Mark and Hutchy; whether it was trying to keep Hutchy in her proverbial cage or fighting in the office with Mark over Cyclin D1, every little moment amounts to an excellent three years. A worthy mention must also go to Karen who somehow managed to put up with living with me, even when we were finding Western blot film on the bathroom floor. Not to forget Douglas, I thank him for all his love and support throughout the writing of this thesis; particularly for being so patient with my 2am questions of "what's another word for…".

I thank you all for your belief in me – it really has carried me through.

This is for you all.

Abbreviations

Adv	Adenovirus
APC	Anaphase Promoting Complex
ApoE	Apolipoprotein E
Asp	Aspartic Acid
ATP	Adenosine Triphosphate
BSA	Bovine Serum Albumin
CAR	Coxsackie Adenovirus Receptor
cdc	Cell Division Cycle
CDK	Cyclin Dependant Kinase
CI	Catalytically Inactive
CT	Computer Tomography
DEN	Diethylnitrosamine
DMEM	Dulbecco's Modified Eagle's Medium
DNA	Deoxyribonucleic Acid
DTT	Dithiothreitol
DUSP	Dual-Specificity Phosphatase
EC	Endothelial Cell
ECL	Enhanced Chemiluminescence
ECM	Extracellular Matrix
EDRF	Endothelial Derived Relaxing Factors
EDTA	Ethylenediaminetetraacetic acid
EGF	Epidermal Growth Factor
ERK	Extracellular Regulated Kinase
ES	Embryonic Stem Cells
ESCRT	Endosomal Sorting Complex Required for Transport
FCS	Fetal Calf Serum
FGF	Fibroblast Growth Factor
FOXO1	Forkhead Box O1
GAPDH	Glyceraldehyde 3-phosphate dehydrogenase
GAX	Growth Arrest Homeobox
GDP	Guanosine Diphosphate
GPCR	G-Protein Coupled Receptor
GTP	Guanosine Triphosphate
HASMC	Human Aortic Smooth Muscle Cells
HCC	Hepatocellular Carcinoma
HEK	Human Embryonic Kidney Cells
ICAM-1	Intercellular Adhesion Molecule
IGF-1	Insulin Growth Factor
IL-1	Interleukin-1
IL-6	Interleukin-6
ILK	Integrin-Linked Kinase
INCEP	Inner Centromere Protein
iNOS	Nitric Oxide Synthase
JNK	c-Jun N-terminal kinase

KIM	Kinase Interaction Motif
KO	Knockout
LDL	Low Density Lipoprotein
LPS	Lipopolysaccharide
MAP	Mitogen Activated Protein
MASMC	Mouse Aortic Smooth Muscle Cells
MCM6	Minichromosome maintenance protein 6
MCP-1	Monocyte Chemoattractant Protein
MEF	Mouse Embryonic Fibroblast
MEM	Modified Eagle's Medium
MKB	MAP Kinase Binding Domain
MKLP1	Motor Kinesin-Like Protein
MKP	Mitogen Activated Protein Kinase Phosphatase
MLC	Myosin Light Chain
MLCK	Myosin Light Chain Kinase
MPF	Mitosis Promoting Factor
mRNA	Messenger Ribonucleic Acid
MSK	Mitogen and Stress Activated Protein Kinase
mTOR	Mammalian Target of Rapamycin
NES	Nuclear Export Sequence
NLS	Nuclear Localisation Sequence
NO	Nitric Oxide
PAGE	Polyacrylamide Gel Electrophoresis
PBS	Phosphate Buffered Saline
PCNA	Proliferating Cell Nuclear Antigen
PCR	Polymerase Chain Reaction
PDGF	Platelet Derived Growth Factor
PLK1	Polo-Like Kinase
pRb	Retinoblastoma protein
PRL	Phosphatase of Regenerating Liver
PTEN	Phosphatase and Tensin Homolog
PTP	Protein Tyrosine Phosphatase
RGD	Arginine-Glycine-Aspartate
RTK	Receptor Tyrosine Kinase
SAPK	Stress Activated Protein Kinase
SDS	Sodium Dodecyl Sulphate
SEM	Standard Error Mean
Ser	Serine
siRNA	Small interfering RNA
SMA	Smooth Muscle Actin
SMC	Smooth Muscle Cell
TEMED	N,N,N',N'-tetramethylenediamine
TGF	Transforming Growth Factor
Thr	Threonine
TNF-α	Tumour Necrosis Factor
Tyr	Tyrosine

VCAM-1	Vascular Cell Adhesion Molecule
VHR	VH-1-related phosphatase
VRK1	Vaccinia-Related Kinase 1
Vs.	Versus
VSMC	Vascular Smooth Muscle Cell
WT	Wild-type
ZIPK	Zipper-Interacting Protein

Abstract

MAP kinase phosphatase-2: a role in vascular function and disease

The progression of major cardiovascular disorders are a consequence of a pathophysiological modification within the blood vessel; a process often driven by vascular smooth muscle cell hyperproliferation. A major mechanism by which smooth muscle cell proliferation occurs involves ligand-induced activation of MAP kinase signalling (Schad et al., 2011). MAP kinases have been noteworthy but troublesome targets in cardiovascular therapeutics; thus exploration of targeting endogenous regulatory dual specificity proteins namely MAP kinase phosphatases has been advancing in recent years. Mitogen-activated protein kinase phosphatase-2 (MKP-2) is a type 1 nuclear phosphatase with the ability to dephosphorylate and ultimately inactivate MAP kinases ERK and JNK in vitro (Lawan et al., 2012). Therefore, by the use of a novel MKP-$2^{-/-}$ mouse, we assess a role for MKP-2 in smooth muscle proliferation as a potential future therapeutic target in cardiovascular disease.

Contrary to current literature, mouse aortic smooth muscle cells cultured from a novel Dusp4 knockout mouse exhibit no significant difference in MAP kinase signalling profiles when compared with wild-type. Interestingly however, a significant reduction in proliferation rate corresponded with MKP-2 knockout cells and further cell cycle investigation elucidated a significant accumulation of MKP-$2^{-/-}$ cells in G2/M phase of the cell cycle. With levels of p-cdc-2 comparable between MKP-2 wild-type and knockout cells, mitotic entry was unaffected by MKP-2 deficiency which therefore diverted our study downstream to cytokinesis. Utilising time-lapse microscopy, smooth muscle cells lacking in MKP-2 exhibited a delay in cytokinesis and failure in abscission, resulting in the dividing cells connected by an intercellular bridge. The molecular mechanism of cytokinesis requires phosphorylation of the mitotic kinase aurora B for successful division of two daughter cells. However nocodazole-arrest studies reveal MKP-2 is required for aurora B phosphorylation and its downstream target histone H3, thus identifying MKP-2 as essential in the effective completion of cytokinesis.

Within this thesis, an early investigation into the possible use of Adv.WT-MKP-2 as a vascular therapeutic in human aortic smooth muscle cells (HASMCs) was conducted. The over-expression of MKP-2 negated ERK signalling and consequently resulted in a reduction in cellular proliferation. Furthermore, the reduction in cellular proliferation was shown to be caused by a G1/S accumulation in the cell cycle. Collectively, these data suggest a novel role for MKP-2 in mouse aortic smooth muscle cell proliferation, providing new insights into the understanding of MKP-2 in the completion of cytokinesis. Furthermore, MKP-2 kinase binding domain is required for successful completion of cytokinesis but may not involve the inactivation of ERK or JNK. Therefore, modification of MKP-2 expression or function may represent a new approach in reducing SMC hyperproliferation in vascular disease states.

Publications

1. Lawan A, **Torrance E**, Al-Harthi S, Shweash M, Alnasser S, Neamatallah T, Schroeder J, Plevin R. (2012) MKP-2: out of the DUSP-bin and back into the limelight. *Biochem Soc Trans*. 40.235–9

2. **Emma Torrance**, Louise Collins, Eileen Miller, Gwyn Gould, Patrick Hadoke, Robin Plevin (2013) MAP kinase phosphatase-2: a critical component in smooth muscle cell cytokinesis. EMBO Europhosphatase, Rehovot, Israel.

3. **Emma Torrance**, Louise Collins, Eileen Miller, Gwyn Gould, Patrick Hadoke, Robin Plevin (2013). A critical role for MAP kinase phosphatase-2 in smooth muscle cell cytokinesis. Scottish Cardiovascular Forum, Glasgow, Scotland.

4. **Emma Torrance**, Louise Collins, Eileen Miller, Gwyn Gould, Patrick Hadoke, Robin Plevin (2012). An essential role for MAP kinase phosphatase-2 in smooth muscle proliferation and cell cycle progression. Scottish Cardiovascular Forum, Dundee, Scotland.

5. Sameer Al-Harthi, **Emma Torrance,** Robin Plevin (2011). Differential role of MAP kinase phosphatase-2 over-expression in endothelial apoptosis and smooth muscle cell proliferation. European Vascular Biology and Medicine, Krakow, Poland.

Table of Contents

1.0 Introduction **1**
1.1 Vascular Disease 1
1.1.1 Atherosclerosis 1
1.1.1.1 History 1
1.1.1.2 Pathophysiology 2
1.1.2 Restenosis 4
1.1.2.1 Pathophysiology 4
1.2 Physiological Structure of Blood Vessels 8
1.2.1 Blood Vessel Composition 8
1.2.2 Vascular Smooth Muscle Cells 10
1.2.2.1 Contractility of VSMC 10
1.2.2.2 VSMC Phenotype 11
1.2.2.3 VSMC Proliferation 14
1.3 Cell Cycle 16
1.3.1 G0/G1 Transition 17
1.3.2 G1/S Transition 18
1.3.3 S/G2 Transition 19
1.3.4 G2/M Transition 20
1.3.5 Mitosis 20
1.3.6 Cytokinesis 24
1.3.7 Abscission 26
1.4 MAP Kinase Signalling 29
1.4.1 Extracellular Signal Regulated Kinase Signalling 31
1.4.1.1 Architectural Features of ERK Signalling 31
1.4.1.2 ERK in Hyperproliferative Disease 33
1.4.2 c-Jun N-terminal Kinase Signalling 33
1.4.2.1 Architectural Features of JNK Signalling 33
1.4.2.2 JNK in Hyperproliferative Disease 34
1.4.3 p38 MAP Kinase Signalling 35
1.4.3.1 Architectural Features of p38 MAP Kinase 35

1.4.3.2 p38 MAP Kinase Signalling in Hyperproliferative Disease 35
1.4.4 MAP Kinase Signalling in Atherosclerosis..... 36
1.4.5 MAP Kinase Signalling in Restenosis 37
1.5 Regulation of MAP Kinase Signalling Pathways by Protein Phosphatases 41
1.5.1 The Protein Tyrosine Phosphatase Family (PTPs) 41
1.6 MAP Kinase Phosphatase 42
1.6.1 MKP Structure 42
1.6.2 Classification of MKPs 44
1.6.3 Physiological Role of MKPs..... 47
1.6.3.1 MKP-1..... 47
1.6.3.1.1 MKP-1 in Disease 48
1.6.3.1.1.1. MKP-1 in Cancer 48
1.6.3.1.1.2 MKP-1 in Cardiovascular Disease 49
1.6.3.2 MKP-2..... 49
1.6.3.2.1 MKP-2 in Disease 50
1.6.3.2.2 MKP-2 in Cancer 50
1.6.3.2.3 MKP-2 in Cellular Studies..... 51
1.6.3.3 MKP-3..... 52
1.6.3.4 MKP-5..... 53
1.7 Aims and Objectives 54

2.0 Materials and Methods..... 55
2.1 Reagents 55
2.1.1 General Reagents 55
2.1.2 Reagents for Cell Culture..... 55
2.1.3 Antibodies 56
2.1.4 Plasmids 56
2.1.5 Radiochemicals 56
2.2 Cell Culture 57
2.2.1 MASMC..... 57
2.2.1.1 Culturing MASMC 57

2.2.2 HEK293 Cells 58
2.2.3 HASMC 58
2.3 Generation of MKP-2 Deficient Mice 58
2.3.1 Ethical Approval 59
2.4 DNA Preparation for Mouse Genotyping 60
2.4.1 DNA Extraction 60
2.4.2 PCR 60
2.4.3 DNA Detection 60
2.5 Preparation of Recombinant Adenoviruses 61
2.5.1 Adenoviral Crude Lysates 61
2.5.2 Generation and Purification of High Titre Adenovirus 61
2.5.3 Adenoviral Titration 62
2.5.4 Infection SMCs with Adenovirus 65
2.6 Detection and Analysis of Proteins (Western Blotting) 65
2.6.1 Preparation of samples for SDS-PAGE and Immunoblotting 65
2.6.2 SDS-PAGE 66
2.7 Cell Population Synchronisation using Nocodazole 67
2.8 Proliferation Rate of SMC 67
2.9 Doubling Time of SMC 68
2.10 Cell Cycle Analysis 68
2.11 Histological Sectioning and Staining of Vascular Tissue 68
2.11.1 Fixation, Wax Embedding and Cutting of Tissues 68
2.11.2 Rehydration and Dehydration of Tissue Slides 69
2.11.3 Haematoxylin and Eosin 69
2.12 Immunofluorescent Microscopy 71
2.13 Time Lapse Microscopy 71
2.14 Determination of Protein Concentration 71
2.15 Expression and Purification of GST-c-Jun Construct 71
2.15.1 Growth of GST-c-Jun 72
2.15.2 Purification of GST-Fusion Proteins 72
2.15.3 Elution of GST-Fusion Proteins 73
2.15.4 Electrophoretic Analysis of GST-Fusion Proteins 73
2.16 Scanning and Densitometry 75
2.17 Statistical Analysis 75

3.0 Characterisation of Cellular Functions of MKP-2 in Primary Mouse Aortic Smooth Muscle Cells 76
3.1 Introduction 76
3.2 Results 78
3.2.1 Dusp4 Knockout Mouse Characterisation 78
3.2.1.1 MKP-2 Knockout Generation 78
3.2.1.2 Aorta Dissected from WT and KO MASMC Exhibit No Significant Differences 80
3.2.1.3 Characterisation of SMC Derived from Mouse Aorta 80
3.2.1.4 SMC Phenotype is Comparable between WT and KO MASMC 83
3.2.2 Induction of MKP-2 85
3.2.2.1 Induction of MKP-2 in Response to Serum 85
3.2.2.2 MKP-2 Induction Depends on Prior ERK Activation 89
3.2.3 Regulation of MAP Kinase Signalling by MKP-2 91
3.2.3.1 Effect of MKP-2 deletion on ERK and JNK phosphorylation 91
3.2.4 MKP-2 deficient MASMCs Exhibit a Reduction in Proliferative Capacity 97
3.2.4.1 MKP-2 Deletion Leads to a Decrease in MASMC Proliferation 97
3.2.4.2 MKP-2 Deficiency Leads to Increased Doubling Times in MASMCs 97
3.2.4.3 Accumulation of MKP-2 deficient MASMCs in G2/M Phase .. 100
3.2.4.4 MKP-2 Deficient MASMCs have no effect on G2/M Transition Proteins 100
3.2.5 MKP-2 Deletion Results in Cytokinesis Deficiency 105
3.2.5.1 MKP-$2^{-/-}$ MASMCs Exhibit a Delay in Cytokinesis 105
3.2.5.2 Optimising Conditions for G2/M Phase Arrest 109
3.2.5.3 MKP-2 is Essential for the Expression of Proteins Required for Cytokinesis ... 111
3.2.6 Over-Expression of MKP-2 Failed to Regain MKP-$2^{-/-}$ MASMCs Proliferative Deficiency 114

3.2.6.1 Adv.WT-MKP-2 Decreased Proliferation Rates in WT and KO MASMCs....114

3.2.6.2 Adv.WT-MKP-2 resulted in G1 Accumulation in WT and KO MASMC....115

3.2.6.3 Over-expression of Adv.WT-MKP-2 and Adv.CI-MKP-2 and the Differential Effect on ERK Signalling....119

3.2.7 Over-expression of CI-MKP-2 Suggests a Non-MAP Kinase Dependant Role for MKP-2 in MASMC Proliferation....121

3.2.7.1 Over-expression of Adv.CI-MKP-2 Decreased Proliferation Rates in WT and KO MASMCs....121

3.2.7.2 Over-expression of Adv.CI-MKP-2 Decreased Expression of Proteins Required for Cytokinesis in WT and KO MASMCs....126

3.3 Discussion....129

4.0 Effect of MKP-2 Over-Expression on Cellular Proliferation in HASMC....141

4.1 Introduction....141

4.2 Results....142

4.2.1 FCS-mediated Activation of ERK and c-Jun Signalling in HASMCs....142

4.2.2 PDGF-mediated Activation of ERK and c-Jun Signalling in HASMCs...143

4.2.3 Proliferation of HASMC in Comparison with MASMC....146

4.2.4 Over-expression of Adv.WT-MKP-2 in HASMCs....148

4.2.5 Over-expression of Adv.WT-MKP-2inhibits ERK Signalling in HASMCs....148

4.2.6 Over-expression of Adv-WT-MKP-2 Results in a Reduction in HASMC Proliferation....152

4.2.7 Over-expression of Adv.WT-MKP-2 Inhibits G1/S Progression of HASMCs....154

5.0 Discussion....156

5.0 General Discussion....162

6.0 References....170

Figures and Tables

Figure 1.1 Schematic of atherogenesis and an unstable atherosclerotic plaque .....

Figure 1.2 Example of post-stent neointima formation in the coronary artery .....

Figure 1.3 Schematic diagram depicting structural differences of artery and veins .....

Figure 1.4: Morphological differences between synthetic and contractile VSMC phenotype .....

Table 1.1 Rank order of potency of DNA synthesis by numerous activating agents.....

Figure 1.5: Schematic diagram of the cell cycle .....

Figure 1.6 Schematic diagram of mitosis .....

Figure 1.7: Schematic diagram of the chromosomal passenger complex required for abscission.....

Figure 1.8 MAP kinase signalling overview. .....

Figure 1.9 Arterial restenosis of smooth muscle cells driven by ERK signalling. .....

Figure 1.10: Classification, domain structure and phylogenetic analysis of the dual-specificity MAPK phosphatases .....

Table 1.2: Overview of the PTP family .....

Figure 2.1: Generation of mice lacking Dusp4/MKP-2 by targeted homologous recombination .....

Figure 2.2: MKP-2 tail tip DNA genotyping.....

Figure 2.3. Plate layout for adenoviral titration .....

Figure 2.4 Calculation for adenoviral titration .....

Figure 2.5: Analysis of GST-c-Jun purification and elution. .....

Figure 3.1: Histology of MKP-2 wild-type and knockout aorta .....

Figure 3.2: Smooth Muscle Actin staining in MASM culture from WT and MKP-2 KO mice .....

Figure 3.3: Expression of smooth muscle actin in response to PDGF .....

Figure 3.4: MKP-2 expression in response to FCS in MASMC.....

Figure 3.5: MKP-2 expression in response to FCS in MASMC .....

Figure 3.6 MKP-2 expression is dependent upon increasing FCS stimulation .....

Figure 3.7: Expression of MKP-2 is dependent on prior ERK activation in MASMCs ..

Figure 3.8: MAP kinase characterisation in WT and KO MASMCs in response to FCS..

Figure 3.9: MAP kinase characterisation in WT and KO MASMCs in response to PDGF.....

Figure 3.10: Effect of MKP-2 knockout on MASMC proliferation .....

Figure 3.11: Effect of MKP-2 knockout on doubling rate of MASMCs.....

Figure 3.12: Cell cycle G2/M accumulation in MASMC deficient in MKP-2.....

Figure 3.13: Expression of cyclin B and cdc-2 throughout the cell cycle.....

Figure 3.14: MASMCs lacking in MKP-2 exhibit a delay in mitosis. .....

Figure 3.15: MASMCs lacking MKP-2 exhibit a delay in abscission.....

Figure 3.16: MASMC lacking MKP-2 exhibit a reduced success rate in cytokinesis completion .....

Figure 3.17: Characterisation of nocodazole arrest treatment .....

Figure 3.18 MKP-2 is required for phosphorylation of cytokinetic proteins.....

Figure 3.19 Pfu curve of Adv. WT-MKP-2 in MASMCs.....

Figure 3.20 Effect of Adv.WT-MKP-2 on cell cycle in MASMCs .....

Figure 3.21: Effect of Adv. WT MKP-2 on proliferation .....

Figure 3.22: Adv. WT MKP-2 inhibits ERK signalling in MASMC .....

Figure 3.23 PFU curve of Adv.CI-MKP-2.....

Figure 3.24 Effect of Adv.CI-MKP-2 on MASMC Cell Cycle.....

Figure 3.25 Effect of Adv.CI-MKP-2 on MASMC Proliferation .....

Figure 3.26 Effect of Adv.CI-MKP-2 on MASMCs in proteins required for cytokinesis.

Figure 4.1: ERK signalling characterisation in HASMCs .....

Figure 4.2: JNK signalling characterisation in HASMCs.....

Figure 4.3 Proliferation of HASMC in comparison with MASMCs.....

Figure 4.4 PFU curve of Adv. WT-MKP-2 in HASMCs .....

Figure 4.5: Effect of Adv. WT MKP-2 on ERK signalling .....

Figure 4.6: Effect of Adv. WT MKP-2 on proliferation in HASMC.....

Figure 4.7 Effect of Adv.WT-MKP-2 on cell cycle progression in HASMCs.....

Chapter 1: Introduction

MKP-2 in smooth muscle cell function

1.0 Introduction

1.1 Vascular disease

Vascular disease is one of the major causes for death worldwide, particularly in many Western countries. Furthermore, vascular disease results in not only health implications but economical. Classification of vascular disease may be termed as a condition affecting blood vessels including coronary artery disease, stroke, hypertension, restenosis and diabetic vascular complication, where atherosclerosis is often primary underlying cause (Kearney et al., 2010; Gao et al., 2009).

1.1.1 Atherosclerosis

Atherosclerosis, the pathologic condition underlying myocardial infarction and other acute coronary syndromes, is the major cause of death in the Western world. Clinically apparent atherosclerosis takes decades to develop, beginning with cellular changes and intimal thickening, progressing to non-obstructive plaques over many years (Roger et al., 2012).

The genesis of vascular disease as a significant condition involves many societal features, investigated post World War II. The pivotal Framingham Heart study aimed to elucidate risk factors for vascular disease, where over 5000 men and women were recruited in 1948. Following recruitment the subjects underwent extensive physical examination and lifestyle interviews which would subsequently be analysed for common patterns with relation to cardiovascular disease development. The Framingham Heart study uncovered that risk of vascular disease amplified with increasing age, systolic blood pressure, smoking and cholesterol; data still supported in both animal and human subjects today. The prevalence of atherosclerosis has recently grown exponentially within the Western world; however this is not a novel condition as early episodes of the disease have been documented back thousands of years (Dawber et al., 1951).

1.1.1.1 History

Atherosclerosis was first noted within scientific literature in times of ancient Egypt, where Fallpoius described the transformation of artery into bone due as a factor of progressive aging (David et al., 2010). Among the first to describe atherosclerosis was Leonardo da Vinci (1452-1519), who stated that 'vessels in the elderly restrict the transit of blood through thickening of the tunics' (Davies et al., 1996). By the end of the 18th century, two theories dominated the discussion on the pathophysiology of atherosclerosis: the thrombogenic theory by Carl von Rokitansky and the inflammatory theory proposed by Rudolf Virchow. Rokitansky proposed that the deposits observed in the inner layer of the arterial wall were derived primarily from fibrin and other blood elements rather than being the result of a purulent process. Subsequently, the atheroma resulted from the degeneration of the fibrin and other blood proteins and finally these deposits were modified toward a pulpy mass containing cholesterol crystals and fatty globules. Virchow's description of the pathogenesis of atherosclerosis was based on an in-depth study of the histological characteristics of the atherosclerotic lesion in all its stages (Mayerl et al., 1996). Today, Virchow's concept of local intima injury as the initiating irritative stimulus is still accepted and has been extended to include other implications besides mechanical factors.

Recent work by Thompson et al., (2013) examined 137 mummies from populations of four disparate geographic regions by whole body CT scanning and compared calcification as an indicator of atherosclerosis with Common Era subjects. This study concludes that atherosclerosis was common in four preindustrial populations, and remains prevalent in contemporary human beings thus controversially suggesting that atherosclerosis is an inherent component of human ageing and not characteristic of any specific diet or lifestyle despite a number of study limitations.

1.1.1.2 Pathophysiology

Atherosclerosis is characterised by the presence of a complex fatty plaque which is a focal thickening originating from the intimal layer of a vessel. Numerous theories have been considered regarding atherogenesis, including the response to injury and lipid

hypotheses. However it is widely accepted that the initial step of atherosclerosis is damage to the endothelium; whether it be by hyperglycaemic conditions, hypertension, lipoproteins or mechanical stress (Freestone et al., 2010). The first response to endothelium insult increases lipoprotein permeability, leukocyte adhesion and enhance thrombic potential (Tritto and Ambrosio, 2004); cumulatively this insult requires a compensatory response from the endothelium which in turn alters the normal homeostatic properties of the intimal layer.

In the early atherogenic process arterial endothelial cells begin to express adhesion molecules (ICAM)-1 which binds various classes of leukocytes; whereas vascular cell adhesion molecule (VCAM)-1 binds monocytes and T-lymphocytes. After monocytes adhere to endothelial cells, they migrate to localize in the intima, transform into macrophages after stimulation by chemokines, and avidly engulf oxidized lipoprotein especially oxidized LDL (Schoen et al., 2005). When LDL particles become trapped in the vessel wall, they undergo progressive oxidation and become internalised by macrophages through scavenger receptors on the surface of the cells, leading to the formation of lipid peroxides, facilitating the accumulation of cholesterol esters, resulting in the formation of foam cells (Griendhing and Alexander., 1993).

Plaque formation consists of a core region packed with foam cells and lipid droplets, surrounded by VSMC and endothelial cells (Subramanian et al., 2010). The injury also induces endothelial cells to have procoagulant instead of anticoagulant properties and release vasoactive substances, the cytokines, and growth factors. The inflammatory response stimulates migration and proliferation of VSMC that become intermixed with the area of inflammation to form an intermediate lesion; consequentially producing extracellular matrix, converting a fatty streak into a mature atheroma and leading to further enlargement and restructuring of the lesion.

As the lesion advances, a fibrous cap which encloses the lesion from the lumen forms: composed of a mixture of the aforementioned components; leukocytes, lipids and debris which form a necrotic core (Ross, 1999). Atherosclerosis plaque ruptures are associated with increased infiltration of the fibrous cap by macrophages, and T-lymphocytes with reduced number of VSMC fibrous cap that make the thinning of VSMC-rich fibrous cap overlying the core, as depicted in Figure 1.1 (Wang et al.,

2012). Erosion or uneven thinning of the fibrous cap results in the expulsion of necrotic content into the bloodstream, releasing thrombogenic material such as phospholipids, tissue factor and platelet adhesion matrix molecules (McAlpine & Werstuck, 2008). This expulsion may result in coagulation and likely thrombus formation; the most frequent cause for myocardial infarction (Wang & Bennett, 2012).

1.1.2 Restenosis

Current therapeutic approaches to restore blood flow in stenotic blood vessels involve the use of percutaneous devices and coronary bypass surgery. These procedures disrupt normal integrity of the blood vessel, increasing the vessel luminal narrowing, a process termed restenosis; defined by narrowing of vessel diameter of 50% compared with the reference vessel. Restenosis is modulated by genetic background and conditions which affect the vascular system, including diabetes, hypertension, and hypercholesterolemia. In the 1970s, Andreas Gruntzig pioneered the use of transluminal dilatation of coronary arteries for symptomatic coronary artery disease and reported a 19% rate of restenosis. (Clowes et al., 1983; Ip et al., 1991) Subsequent studies demonstrated a restenosis rate of approximately 33% (Braun-Dullaeus et al., 1998). More than 25 years later, despite pharmacological and mechanical approaches to reduce the incidence of restenosis, it remains a significant problem.

1.1.2.1 Pathophysiology

A normal functioning endothelium is very important because it promotes vasodilatation and suppresses intimal hyperplasia by inhibiting thrombus formation, inflammation, and smooth muscle proliferation and migration. The endothelium provides a selectively permeable barrier that protects against circulating growth factor (Costa et al., 2005). Endothelial denudation and medial wall injury are the initial effects of balloon- and/or stent-induced injury and are important triggers of the wound “healing” program. Studies have shown that proper endothelial cell re-growth is essential for function (Abdullah et al., 2012)

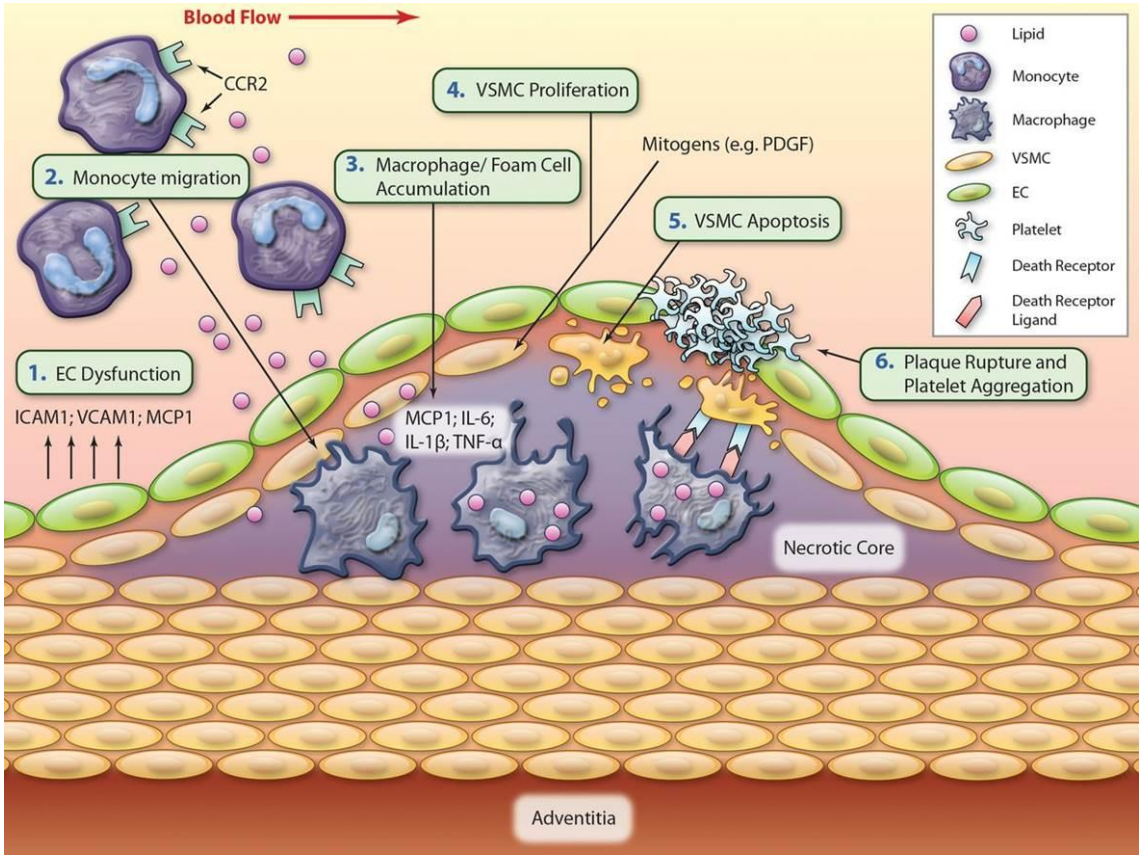

Figure 1.1 Schematic of atherogenesis and an unstable atherosclerotic plaque.

The advanced atherosclerotic plaque consists of a fibrous cap rich in VSMCs and collagen, surrounding a "necrotic" core comprising lipids, foam cells, and debris. Plaque formation involves a series of events initiated from (1) EC dysfunction and activation with increased surface adhesion molecules on ECs, including ICAM-1 and VCAM-1, and augmented vascular permeability promoting the (2) attachment and infiltration of lipid and inflammatory cells into the subendothelial space. (3) Monocytes differentiate into macrophages, engulf lipid to form foam cells and release proinflammatory cytokines to create an inflammatory environment. (4) In early lesions, VSMCs proliferate in response to mitogens such as PDGF and synthesise collagen to form the fibrous cap that encloses the growing lipid core. At later stages, VSMCs become activated and release inflammatory mediators which may promote further proliferation or apoptosis. (5) The gradual loss of VSMCs by apoptosis, in part mediated by engagement of death receptors on VSMCs with death ligands on macrophages and T lymphocytes, (6) plaque rupture, with subsequent platelet attachment and thrombosis. Figure adapted from Wang & Bennett, 2012.

Vascular smooth muscle cells retain remarkable plasticity during development and can undergo differentiation to a synthetic phenotype (Schwartz et al., 1986). This represents an advantage as it enables the efficient repair of the vasculature after injury. As in many evolutionarily conserved processes however, these properties can be disadvantageous and can predispose to abnormal responses after injury, contributing to restenosis. Vascular smooth muscle progenitor cells have been identified in multiple sites including the bone marrow, in the circulation, the vessel wall, and in extravascular sites (Daniel and Sedding, 2011).

The normally quiescent smooth muscle cells within the medial layer of the vessel wall are activated to migrate and proliferate in response to increased stimulatory growth factors and cytokines (PDGF, interleukin-1, and interleukin-6) and reduced endothelium-derived inhibitory factors (nitric oxide, heparin sulfate proteoglycan) (Alexander and Griendling, 1996). Studies have challenged the concept that neointimal formation is dependent on the proliferation and migration of local endothelial and smooth muscle cells (Douglas, 2007). It has been proposed that in models of post-angioplasty restenosis, graft vasculopathy, and hyperlipidemia-induced atherosclerosis, smooth muscle progenitor cells are mobilized from the bone marrow and hone to sites of vascular injury, differentiating into smooth muscle cells (Sata et al., 2002). In these studies, a bone marrow or circulating cell marker has been found to co-localise with vascular smooth muscle cell markers in vascular lesions after arterial injury or atherosclerosis. Based on the species, type of injury, and the method of labelling, the percentage of bone marrow– derived cells within the neointima is between 20% and 66%. Although the selective control of vascular smooth muscle progenitors in the vessel wall may be an attractive therapeutic target, the concept is controversial, and more studies are required to define the role of progenitor cells in mediating vascular diseases (Zhang et al., 2012).

It can be seen that the understanding of smooth muscle cell function in the context of vascular disease is critically important in the elucidation of new therapeutic targets.

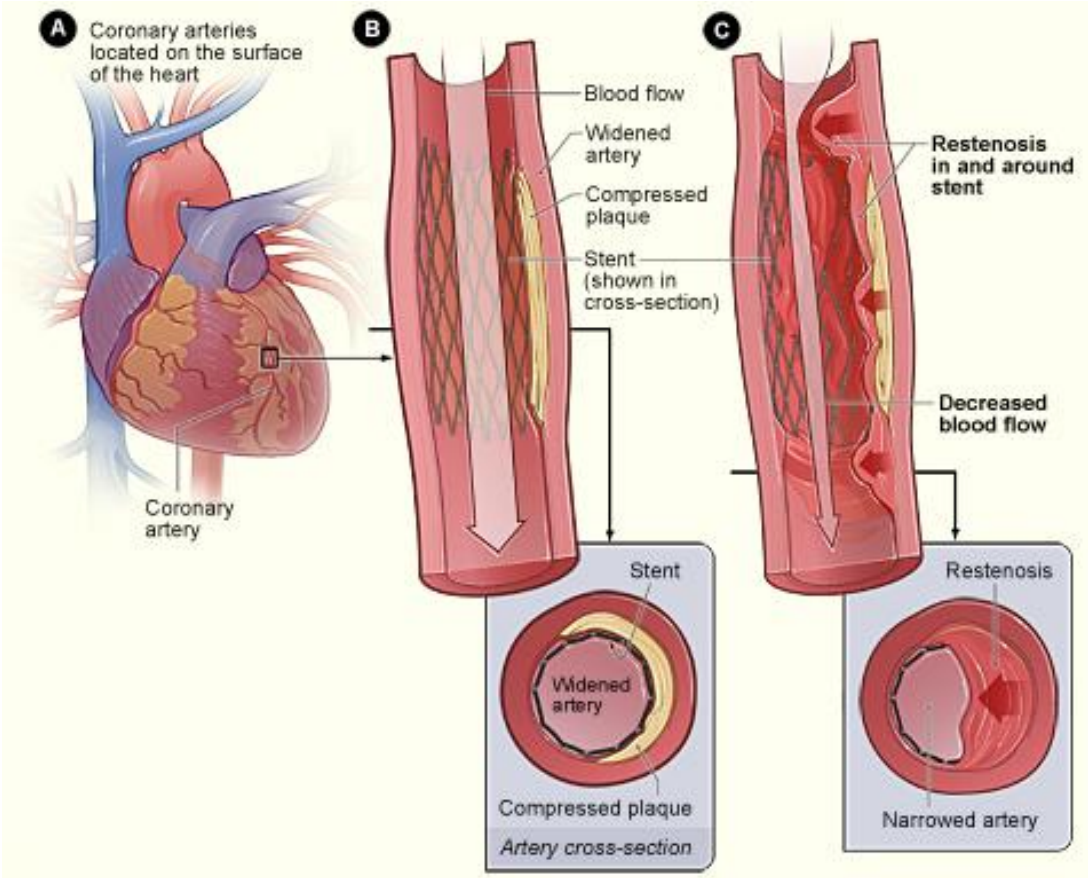

Figure 1.2 Example of post-stent neointima formation in the coronary artery.

Figure A shows the coronary arteries located on the surface of the heart. Figure B shows a stent-widened artery with normal blood flow. The inset image shows a cross-section of the stent-widened artery. In figure C, tissue grows through and around the stent over time. This causes a partial blockage of the artery and abnormal blood flow. The inset image shows a cross-section of the tissue growth around the stent. Adapted from the National Institute of Health.

1.2 Physiological Structure of Blood Vessels

1.2.1Blood Vessel Composition

Blood vessels are critical players in the circulatory system of every living mammal constituting of three main components; arteries, veins and capillaries. Blood vessels are subject to structural characterisation composing of three layers; adventitia, media and intima (Weinberg and Bell, 1985). The tunica intima is the innermost, single layer of simple squamous endothelial cells, surrounded by a thin layer of subendothelial connective tissue forming an interface between circulating blood in the lumen and the rest of the vessel wall. One of the key roles of the vascular endothelium is the delivery of oxygen and essential nutrients to surrounding tissues, relying upon the smooth endothelial layer to reduce pressure from blood flow (Michel et al., 2007). The tunica media constitutes of connective tissue and elastic fibre, rich in vascular smooth muscle cells (VSMC) required to control the calibre of the vessel. VSMCs produce extracellular matrix (ECM) during development, providing the arterial wall with the capacity to withstand the high pressure of circulating blood (Lacolley et al., 2011). The media is accessible to soluble plasma components, which are outwardly convected from the circulating blood through the vascular wall (Michel et al., 2007). The third, outermost layer is the tunica adventitia, composed of fibroblasts and connective tissue which provides structural support for the vessel and minimising tear during movement. The role of the adventitia has long been considered mostly limited to its structural and mechanical functions, with some involvement of the perivascular innervation in overall vascular responses; however there is emerging evidence proposing that the adventitia is involved in myofibroblast migration in the pathogenesis of atherosclerosis (Auger et al., 2007).

The three layer composition of the intima, media and adventitia may be evident in both veins and arteries; however they possess a number of physiological differences. Primarily, veins carry deoxygenated blood towards the heart whereas arteries carry oxygenated blood away from the heart, accounting for an increased thickness in the medial layer to compensate for the high blood flow. Another key factor in the difference in blood vessels is the presence of venous valves to prevent the backflow of blood (Figure1.1). The bicuspid valves are essential not only because of the low

pressure within the vein, but also due to the varying flow of blood and collapsible nature of the vessel. (Cox, 1979).

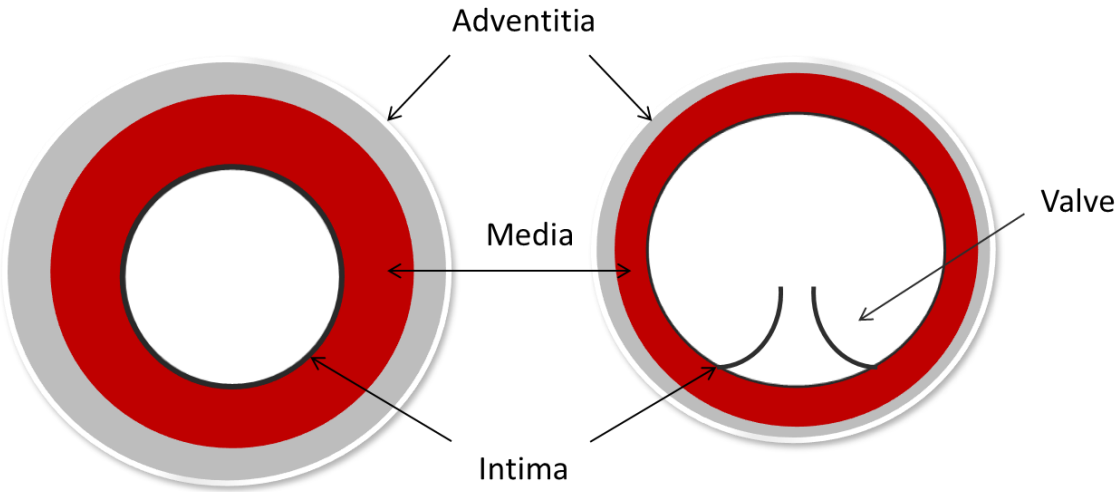

Artery	Vein
Delivers blood from the heart.	Delivers blood to the heart.
Thick smooth muscle cell medial layer to tolerate high blood flow.	Thin smooth muscle layer with semilunar valves that prevent the blood from flowing in the opposite direction.

Figure 1.3 Schematic diagram depicting structural differences of artery and veins.

As described above, arteries are primarily responsible for the delivery of blood away from the heart, whereas veins are predominantly responsible for the delivery of blood to the heart. Arteries have a narrower lumen area for blood flow when compared vein, this is due the a thicker composition of smooth muscle cells in the medial layer to tolerate high blood flow, as well as connective tissue in the adventitial layer.

1.2.2 Vascular Smooth Muscle Cells

Vascular smooth muscle cells are highly specialised cells located in the medial layer of arteries and veins whose principal function is contraction and relaxation. Thus they control of blood vessel tone, blood pressure, and blood flow. Smooth muscle has been shown to express a unique repertoire of contractile proteins, ion channels, and signalling molecules required for the cells physiological functions which is clearly unique compared with any other cell type (Owens, 1995).

The VSMCs, as stromal cells of the vascular wall, control the physiological environments but are also the targets of pathological changes. VSMCs residing in the healthy medial layer of blood vessels exist in a quiescent phenotype with a low proliferative index, but can however adapt to multiple functions in response to specific stimulus (Davis-Dusenbery et al., 2011). This ability of VSMCs to adapt is related to the high plasticity of these cells to reprogramme their expression pattern in response to both chronic and acute stimuli, mainly mediated by ligand–receptor interactions (Albinsson et al., 2010).

1.2.2.1 Contractility of Vascular Smooth Muscle Cells

The regulation of blood pressure has been largely attributed to VSMCs residing in the medial layer of the vessels, controlling both blood vessel constriction and relaxation. Vasoconstriction is activated by vasoactive molecules such as angiotensin II, inducing vascular smooth muscle cell contraction and subsequently reducing lumen area for blood flow, increasing blood pressure. However the counterbalance between vasoconstriction and vasodilation is essential for healthy regulation of blood flow. Vasodilation is regulated by endothelial derived relaxing factors (EDRF) such as nitric oxide which migrates to the medial layer of smooth muscle inducing relaxation, integral for permitting blood flow (Lacolley et al., 2011).

Smooth muscle contraction is required for control of blood flow and is dependent on the interaction of myosin with actin filaments (Gabella, 1984). Smooth muscle contraction is regulated by phosphorylation of the 20 kDa myosin light chain subunits

of myosin (MLC20) (Somlyo et al., 2003). This can occur by the Ca^{2+}/ calmodulin-dependent actions of myosin light chain kinase (MLCK) (Taylor et al., 1988) or by the Ca^{2+}-independent actions of several additional kinases, including Rho-kinase, integrin-linked kinase (ILK) and zipper-interacting protein kinase (ZIPK) (Niiro et al., 2001; Ihara et al., 2007). Contraction is initiated primarily by activation of MLCK under physiological conditions, and thus increased cytoplasmic Ca^{2+} $[Ca2+]_i$ is the primary driving force for contraction, as in other muscles (Ito et al., 2004). MLC phosphorylation can be stimulated by a variety of vasoactive hormones and signalling pathways, including the Ca^{2+}-dependent ERK pathway (see section 1.4.1). Alteration of either the synthesis or the phosphorylation state of the contractile proteins may influence myogenic tone, and finally blood pressure. During phenotypic modulation, a decrease in ERK1/2-mediated phosphorylation impedes VSMC contraction (Carrillo-Sepulveda et al., 2010).

1.2.2.2 Vascular Smooth Muscle Cell Phenotype

Since the earliest ultrastructural studies of smooth muscle tissue, it has been apparent that VSMCs exhibit a substantial phenotypic variation (Fritz et al., 1970). In fact, this diversity was considered for many years to be evidence of not one but two different cell types in the tunica media of artery walls, one for contraction and another for synthesis of extracellular matrix proteins (Wissler, 1968). Dedifferentiated VSMCs adapted to growth in cell culture, exhibiting a synthetic phenotype which is characterised by an increased proliferative rate, in alongside a morphological change. Synthetic-state cells have a fibroblast-like appearance, and their main functions are to proliferate and to produce extracellular matrix components. They are found in the embryo and the young growing organism, where they take part in the formation of the vessel wall (Hirose et al., 1999). Fully differentiated VSMCs in mature adult vessels, however display a contractile phenotype, in which the cells proliferate at a very discrete level and retain their hill-and-valley morphology. Contractile-state cells have a muscle-like appearance and contract in response to chemical and mechanical stimuli. They predominate in the vessels of adults and are primarily involved in the control of blood pressure and flow. However, these cells are able to return to a synthetic phenotype, and this appears to be

an important early event in atherogenesis. (Hirose et al., 1999). This variation was initially referred to as "VSMC phenotypic modulation" (Gomez et al., 2012). It has now believed that the contractile and synthetic phenotypes of the smooth muscle cells represent two ends of a spectrum. Recently however, Alexander and Owens (2012) suggest that the differentiation of VSMCs is not mutually exclusive with the proliferative capacity. The term VSMC "phenotypic switching" has come into common use to describe this reversible transition. It is important to understand that the two phenotypes share considerable overlap and that contractile cells can replicate and synthetic cells can possess contractile filaments (Gomez and Owens, 2012). The phenotypic switch, shown to drive vascular smooth muscle cell proliferation is consistent not only *in vitro* but in disease state. Studies have shown that the neointima formation in stenosed blood vessels is composed of smooth muscle cells in the synthetic phenotype and starkly contrasting from the normal medial layer which is predominantly composed of contractile, quiescent VSMCs (Shinohara et al., 2005).

Depending on the signals present in their local environment, contractile VSMCs can acquire distinct phenotypes, such as the ability to migrate and proliferate and to promote ECM production and inflammatory signals, such as IL-1β, IL-6 and MCP-1 (Wang & Bennett, 2012). The phenotypic modulation of VSMCs is determined by environmental signals, such as mechanical forces, endocytosis of specific molecules, and growth factors which influence expression of a panel of VSMC-specific genes (Curcio et al., 2011). Platelet-derived growth factor-BB (PDGF-BB) and transforming growth factor-β (TGF-β) are the key mediators of VSMC phenotypic switching; where PDGF-BB promotes cells into the synthetic phenotype, conversely TGF-β does so for the contractile phenotype (Owens et al.,2004). This phenomena is consistent in crossing from *in vitro* to *in vivo* studies as Owens et al., (2004) have shown that phenotypic modulation of VSMCs *in vivo* is mediated, at least in part, by transcription repression. The activity of these transcription factors and cofactors is regulated by a wide range of signalling pathways, including extracellular signal-regulated kinase (ERK), c-Jun-N-terminal kinase (JNK), p38 mitogen-activated protein kinases, Akt, Rho/Rho-kinase, and calcineurin/ calmodulin kinases (Rodriguez & Crespo, 2011).

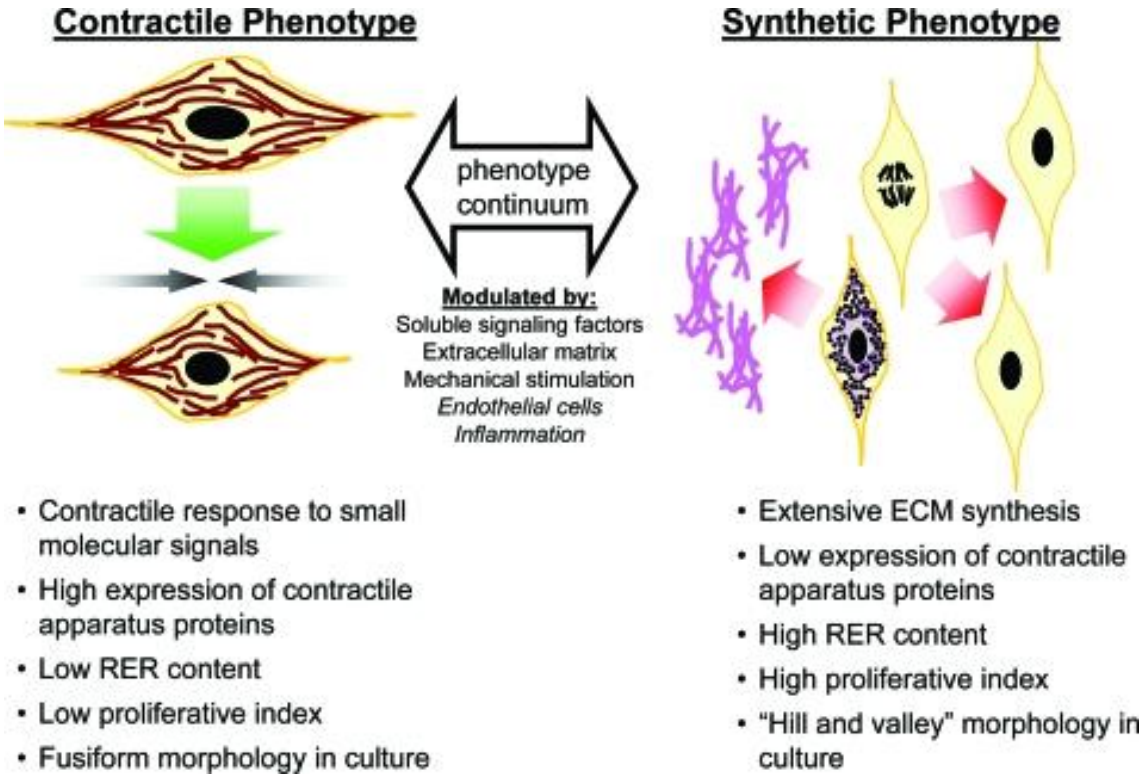

Figure 1.4: Morphological differences between synthetic and contractile VSMC phenotype.

Summary of characteristics of SMC phenotypes, which vary along a continuum from synthetic and proliferative to contractile and quiescent. The position along this continuum is modulated by a variety of extracellular signals. Adapted from Beamish et al., 2010.

1.2.2.3 Vascular Smooth Muscle Cell Proliferation

Like most other nontransformed cells, smooth muscle cells do not normally multiply in culture in the absence of serum (Thyburg et al., 1990). The proliferation of vascular smooth muscle cells can be stimulated by many growth factors and cytokines, both *in vitro* and *in vivo;* examples include platelet-derived growth factor (PDGF), tumour necrosis factor-alpha (TNF-α), interleukin-1 (IL-1), endothelin-1(ET-1), and angiotensin II (Curcio et al., 2011).

Vascular smooth muscle cells were among the first cell types shown to have specific receptors for PDGF and utilising a number of different approaches the significance and mechanism of PDGF signalling in VSMC proliferation was assessed, where this response could be inhibited by neutralising antibodies specific for the PDGF receptor (Heldin et al., 1981). Zhao et al., (2011) describe the mechanism of PDGF-β action in smooth muscle cells acting through phosphorylation of extracellular-regulated kinase 1/2 (ERK1/2) and Akt signalling. Interestingly, early studies had suggested an interaction between PDGF and insulin-like growth factor-l (IGF-I) in stimulating smooth muscle cell replication, (Clemmons, 1984; Pfiefle et al., 1987) and cells stimulated with PDGF were found to produce IGF-I (Hosang and Rouge., 1989). However, IGF-I alone appears in most cases to be but a weak mitogen for vascular smooth muscle cells (Clemmons, 1984). Furthermore, Thyberg et al., (1990) assessed the induction of DNA upon stimulation of an array of rat aortic smooth muscle cell activating agents; the rank order of potency obtained from this analysis is displayed below in Table 1.1.

Agent	Fold Stimulation
PDGF	10-15
FGF	5-10
EGF	3-8
IGF	1-3
IL-1	1-2
TGF	1-4

Table 1.1 Rank order of potency of DNA synthesis by numerous activating agents. Adult rat aortic smooth muscle cells (freshly isolated) were seeded on a substrate of fibronectin, were incubated in serum-free medium for 5 days, and were exposed to the indicate human recombinant polypeptide mitogens at different concentrations and for different times in the presence of tritiated thymidine. The results are presented as the approximate means of a series of experiments**.** Data obtained from Thyberg et al., 1990.

1.7 Cell Cycle

Whilst it is accepted that smooth muscle cells proliferate and generate key early signals, nonetheless very little has been conducted into the study of SMC in the cell cycle. The cell cycle is a complex regulatory network responsible for cell division, tightly coordinated by the synthesis, assembly and degradation of numerous macromolecules. Since the 1900s it had been known that cells multiply via cell division but the molecular mechanisms of the process were not elucidated until 1970 by Leland Hartwell while investigating the genetic background of *Saccharomyces Cerevisae*. Hartwell's work was advanced by the discovery of two major subtypes of cell cycle progression proteins, CDKs and cyclins by Paul Nurse and Tim Hunt, respectively (Hartwell et al., 1970; Hartwell et al., 1974; Nurse 2002). All three pioneers of this work were jointly commended for their fundamental discoveries of key regulators and processes controlling the cell cycle by being awarded the Nobel Prize in Medicine or Physiology in 2001 (Zetterberg et al., 2001). Dysregulation of the cell cycle has been well documented in the pathogenesis of numerous chronic disorders including cancer, Alzheimer's disease and Down's syndrome, and therefore has been the target of an array of therapeutic investigations (Holis et al., 2013; Kim et al., 2010). Currently, the regulation of smooth muscle cells in the cell cycle is fairly well-established in disease states such as restenosis and atherosclerosis, however much prominent work relying upon cancer cells; where their high proliferative rate makes for them to be an ideal model in cell cycle analysis (Chen et al., 2013).

The cell cycle can be divided into two main processes in relation to interphase and mitosis, where interphase can be further segmented into four stage; G0, G1, S, G2. The transition of cells between adjacent phases is aided by the activity of specific cyclin-CDK complexes. In this section, the progression between each phase of the cell cycle will be discussed, describing the requirement of protein equilibrium regarding the activation and degradation required for efficient cell proliferation.

1.3.1 G0/G1 Transition

Under normal physiological conditions, VSMCs reside in the G0 phase of the cell cycle in their quiescent and contractile phenotype (Kottke-Marchant et al., 2010), however the phenotypic switch is activated upon entry to the G1 phase of the cell cycle. As previously mentioned, PDGF activation is required for the conversion to the synthetic, proliferative phenotype of VSMCs; this acts via the ERK signalling pathway shown to be required to promote cells out of G0 phase (Chien et al., 2008) (discussed in section 1.4.1). Promotion of cells into G1 phase is reliant upon the interaction between cyclin dependant kinase (CDK)4/6 and cyclin D, to form a G1 promoting complex. The formation of this complex is induced by mitogenic factors (Detjen et al., 2003) and hormones such as follicle stimulating hormone (FSH) (Han et al., 2013). Furthermore, activating agents noted above such as PDGF, activate multiple kinase signalling pathways, notably the MAP kinase cascade which subsequently activates protooncogenes, *c-fos* and *c-myc* to directly promote the CDK4/6-cyclinD complex (Arellano et al., 1997). Multiple factors have been shown to inhibit the CDK4/6-cyclinD complex in order to act as checkpoints to restrict cellular proliferation in response to damage; inhibitory proteins p21 and p15 (Charron et al., 2006). P15 has shown the ability to inhibit this complex and is stimulated by transforming growth factor-beta (TGF-β). TGF-β not only stimulates p15 but similarly p21, which also acts to inhibit the CDK4/6-cyclinD complex. The inhibitory action of TGF-β in proliferation is supported in VSMCs, as previously mentioned TGF-β is responsible for the conversion of smooth muscle cells from their synthetic phenotype to the non-proliferative contractile phenotype. P21 is induced by growth arrest-specific homeobox (GAX) and therefore inhibits the G1 transition at high levels but has also been shown to aid the progression to G1 phase at low concentrations. (Gorski et al., 1993). Weir et al., (1995) detected levels of GAX mRNA in uninjured arteries however, upon injury and trigger of VSMC hyperproliferation GAX mRNA is significantly downregulated, correlated with an increase in *c-fos* and *c-myc*.

1.3.2 G1/S Transition

Whilst in G1 phase, VSMCs assemble vital factors for DNA replication prior to S phase transition. The associated regulatory protein complex for the G1/S transition is CDK2-cyclinE, which alike to G1 promotion has shown to be directly stimulated by protooncogenes *c-fos* and *c-myc* (Arellano et al., 1997). As cells approach S phase, they reach a checkpoint known as the "restriction point" to which cells are committed to DNA replication if surpassed. Considerable efforts in the cell cycle have been devoted to explain the restriction point switch in molecular terms, mainly focusing on the retinoblastoma protein (pRb) pathway as a candidate mechanism operating in G1 (Bartek et al., 2001). Phosphorylation of the retinoblastoma protein (pRb) plays an important role in cell cycle regulation, where hypophosphorylated pRb binds to the E2F-1 molecule. E2F-1 has been shown to upregulate the expression of cyclin E, with increasing concentrations have resulted in the hyperphosphorylated state of pRb and consequentially led to the progression of cells through the G1/S phase (Montagnoli et al., 1999).

Early work to address the role of *c-myc* in promoting cell cycle progression, construction of a mutant known as MadMyc capable of actively repressing *c-myc* target genes was developed (Berns, 1997). This mutant allowed examination of cellular effects upon both short-term and long-term silencing of endogenous *myc* (Santoni-Rugiu et al., 2000). Transient expression of MadMyc resulted in G1 arrest independent of functional pRb, yet mitogen-stimulated cells exposed to MadMyc in long-term experiments eventually entered S phase despite the lack of myc-mediated transcription (Leone et al., 1997). This would therefore suggest that multiple mechanisms are involved in G1/S progression through the cell cycle, independent of *c-myc*.

Within G1 phase the cyclin inhibitory proteins, p53, p21 and p27 counteract the activity of the CDK2-cyclinE complex and consequentially halt G1/S transition. This allows for a delay in cell cycle progression trigged when genetic material is damaged, to facilitate DNA repair. The p53 protein is a transcription factor which becomes stabilised and active upon DNA damage, and in turn regulates transcription of a large

number of genes, among them is p21, capable of silencing CDK2 which is essential for S phase entry (Agarwal et al., 1998).

Collectively, data generated regarding control of the G1/S border control has suggested a two-wave checkpoint response; both a transient and sustained effect. The initial response to damage is very rapid leading to the inhibition of CDK2 within around 30 minutes and lasting for several hours (Nitta et al., 1997). This early response is believed to act independently of p53 but instead depicts the action of Cdc25A as an inhibitory phosphatase to silence CDK2 and ultimately halt cells at the G1/S boundary (Ussar & Voss, 2004). This pattern of response fits well with the purpose of providing more time for DNA repair. The second method of G1/S arrest is a longer, more sustained response induced by p53 and p21. Due to the multiple protein alterations that p53 must undertake such as modification, accumulation, activation and most of all transcriptional induction of effectors such as p21, it is no surprise that this wave of response requires several hours (Hengst et al., 1998). It is believed that the p53/p21 process is activated in response to cells with severe DNA damage which are most likely to undergo apoptosis to efficiently remove these genetically damaged cells from the rest of the population (Agarwal, 1998). Therefore the G1/S transition is essential in ensuring only non-damaged cells, progress to complete mitosis.

1.3.3 S/G2 Transition

Once cells have undergone DNA replication, they enter the G2 phase at which point cells synthesise apparatus required for mitosis. Cells move into the G2 phase upon promotion by CDK2-cyclinA complex stimulated by the aforementioned, proto-oncogenes c-*fos* and c-*myc* which are activated by kinase signalling, where examples include ERK and JNK (which will be discussed in section 1.4). There has been little data identified about the regulation of such transition and as yet, no inhibitory proteins have been identified to directly counteract the action of the CDK2-cyclinA complex. It could therefore be deduced that as cells are able to independently pass through the cycle as they have surpassed the “restriction point” (Charron et al., 2006).

1.3.4 G2/M Transition

The G2/M checkpoint is an evolutionary conserved tightly regulated network. Similar to the other cell cycle transitions, the G2/M phase is aided by the presence of a CDK/cyclin complex; in such phase it is denoted as the mitosis promoting factor (MPF) consisting of CDK1 (otherwise known as cdc2 in mammalian cell types) and cyclin B (Wang et al., 2013). Cells prepare to enter mitosis by the dephosphorylation of cdc2 by the mitotic phosphatase cdc25C; from this point dephosphorylated cdc2 is in its active conformation and binds to cyclin B forming the MPF (Wang et al., 2013). It has shown to be clear that the MPF is required to be active for cells in mitosis until metaphase, where cyclin B is degraded as it marked by the ubiquitin pathway which flags it for destruction by proteasomes (Vagnarelli, 2012). The removal of cdc2 is regulated by phosphorylation of its tyrosine-15 residue by the kinase wee1. Phosphorylation of tyrosine-15 inhibits cdc2 activity allowing completion of mitosis (Touny &Banerjee, 2006)

Cells may exit G2 phase prematurely, after DNA synthesis and before mitosis (reviewed in Gelfant, 1977), interestingly however this phenomena is rarely mentioned. As with quiescence in G0, these cells can remain in $G2_0$ for prolonged periods before being stimulated by various environmental or hormonal cues to re-enter the cycle. $G2_0$ cells are commonly found in epithelia, sometimes in high numbers (Kaneko et al. 1984), where they must rapidly increase in number, whether found in the gut of hibernating animals as they wake (Kruman et al. 1988) or during wound healing (Gordon and Lane 1980). The mechanism of G2 cellular exiting, and the return to G2, remains to be defined and provides an interesting prospect for future work.

1.3.5 Mitosis

The final stage of proliferation is of course, mitosis. Walter Flemming originally coined the term mitosis in the early 1880s from the Greek word for thread, reflecting the shape of mitotic chromosomes (Flemming, 1882). The process of mitosis is dynamic and highly complex, resulting in duplication of a parent cell to two identical

daughter cells. Mitosis can be subcategorised into 5 phases; prophase, prometaphase, metaphase, anaphase and telophase.

The first phase of mitosis, namely prophase follows G2, the final step of interphase. Many studies carried out over the past 10-15 years have detailed the need for chromosomes to be organised into distinct spatial territories when entering mitosis (Cremer et al., 2001). A cell entering mitosis manifests a number of chromosomal changes; among these are condensation, or thickening of chromosomes. Condensin-mediated chromosome condensation is essential for resolution of sister chromatids and for the correct apposition of sister kinetochores towards opposite poles (Moore et al., 2005). Duplicated centrosomes, which are the organising centre of microtubules, begin to separate towards opposing poles of the cell.

The network of cytoskeletal components begins to break down, triggering the formation of the mitotic spindle, which is an arrangement of microtubules that is responsible for aligning duplicated chromosomes in later phases of mitosis. Whilst in prophase, the chromosomes are still enclosed within the nuclear envelope; however upon entry into prometaphase the nuclear envelope breaks down losing the nucleuo-cytoplasmic compartmentalisation (Burke and Ellengberg, 2002). Nuclear pore complex disassembly is vital for early stages of nuclear envelope breakdown, for example regulatory proteins such as cdc-2 and cyclin B require access to numerous downstream targets to ensure correct mitotic regulation (Hatzner et al., 2010). At the latter stages of prometaphase, the centrosomes have aligned at opposing poles of the cells and chromosomes are being moved towards the centre of the cell.

The distinctive feature of metaphase is the evident alignment of chromosomes at the centre of the cell, with movement being driven by kinetochore microtubules to form the metaphase plate (Vagnarelli et al., 2012). Cells may occupy a large proportion of their mitotic duration in metaphase, as the cell alignment acts as a checkpoint and cyclin B must be degraded before progressing to the next phase, anaphase (Fisher et al., 2012). Cyclin B undergoes destruction by proteasomes. Once the degradation of cyclin B has been completed, the anaphase promoting complex targets the inhibitory chaperone, securing for destruction to aid mitotic progression. Separase is released vital for breaking down cohesion, a protein responsible for the connection of sister chromatids

(McAlenan et al., 2013). Subsequently, the centromeres split and new daughter chromosomes are pulled poleward. Telophase is generally regarded as the final stage of mitosis, derived from the Latin *telos* which means end. It is during this time small nuclear vesicles in the cells begin to reform around the distinct group of chromosomes (Vagnarelli & Earnshaw, 2012). As the nuclear envelope reforms, two nuclei are created and chromosomes undergo the process of decondensation. With the formation of two distinct nuclei, the cells are required to complete cytokinesis to fully differentiate into two daughter cells.

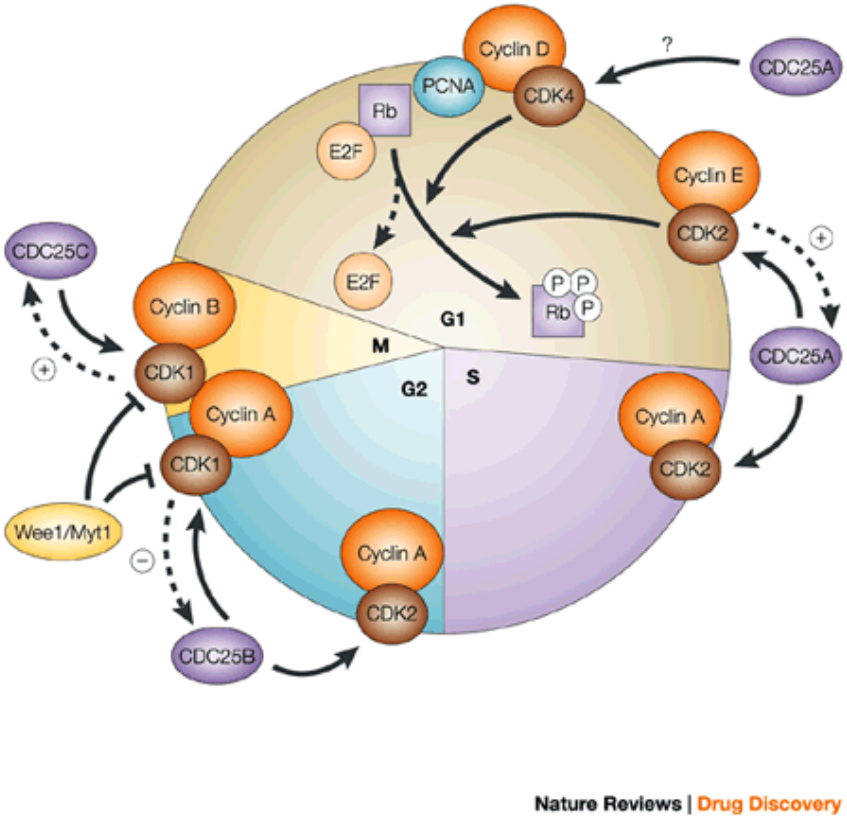

Figure 1.5: Schematic diagram of the cell cycle

As shown above in Figure 1.5, the progression of cell cycle depends on the specific CDK-cyclin interaction. CDK4 and Cyclin D are required to promote quiescent cells into G1 phase, CDK2/Cyclin E is required for G1/S promotion, similarly CDK2/Cyclin A is required for S/G2 transition and finally, CDK1/Cyclin B complex is essential for entry of cells into the G2/M phase of the cell cycle. This simplified schematic representation of the cell cycle includes cell-division cycle 25 (CDC25)-mediated cell-cycle progression. Dotted arrows represent known feedback loops, either positive (+) or negative (–), as indicated. It is unclear whether cyclin D–cyclin-dependent kinase 4 (CDK4) is a bona fide substrate of CDC25A. E2F is a transcription factor that was originally identified through its role in transcriptional activation of the adenovirus E2 promoter. P, phosphate; PCNA, proliferating-cell nuclear antigen; Rb, retinoblastoma protein. Adapted from Lyon et al., 2002.

1.3.6 Cytokinesis

Cytokinesis is the latter part of mitosis where two daughter cells separate into individual full cells. This process is initiated during anaphase, when the mitotic spindle reorganises to form a dense array of antiparallel microtubules between the two centrosomal asters — the central spindle. Together with microtubules from the spindle asters, the central spindle defines the position of the division plane between the segregated chromosomes. A pathway involving the small GTPase RhoA, leads to the assembly of an actomyosin ring at the cell cortex (Balasubramanian et al., 2013). Contraction of the actomyosin ring results in ingression of the attached plasma membrane to form a cytokinetic furrow, which partitions the cytoplasm into two domains. At this stage, sister cells remain connected by a narrow intercellular bridge containing dense antiparallel bundles of microtubules that overlap at a central region termed the midbody. Physical separation of the emerging sister cells is finally accomplished by plasma membrane fission at the intercellular bridge, a process known as abscission (Skop et al., 2004).

Successful cytokinetic completion requires tight temporal coordination with chromosome segregation. This is achieved by the activation of the E3 ubiquitin ligase anaphase promoting complex (APC), which initiates both chromosome segregation and cytokinetic furrow ingression (Pines, 2006). Simultaneous targeting of cyclin B for degradation leads to cdc2 inactivation, resulting in dephosphorylation of many cdc2 substrates promoting cytokinetic furrow ingression and mitotic exit. Finally, abscission is temporally coordinated with completion of chromosome segregation by a signalling pathway involving the Aurora B mitotic kinase (Steigemann et al. 2009. Norden et al. 2006).

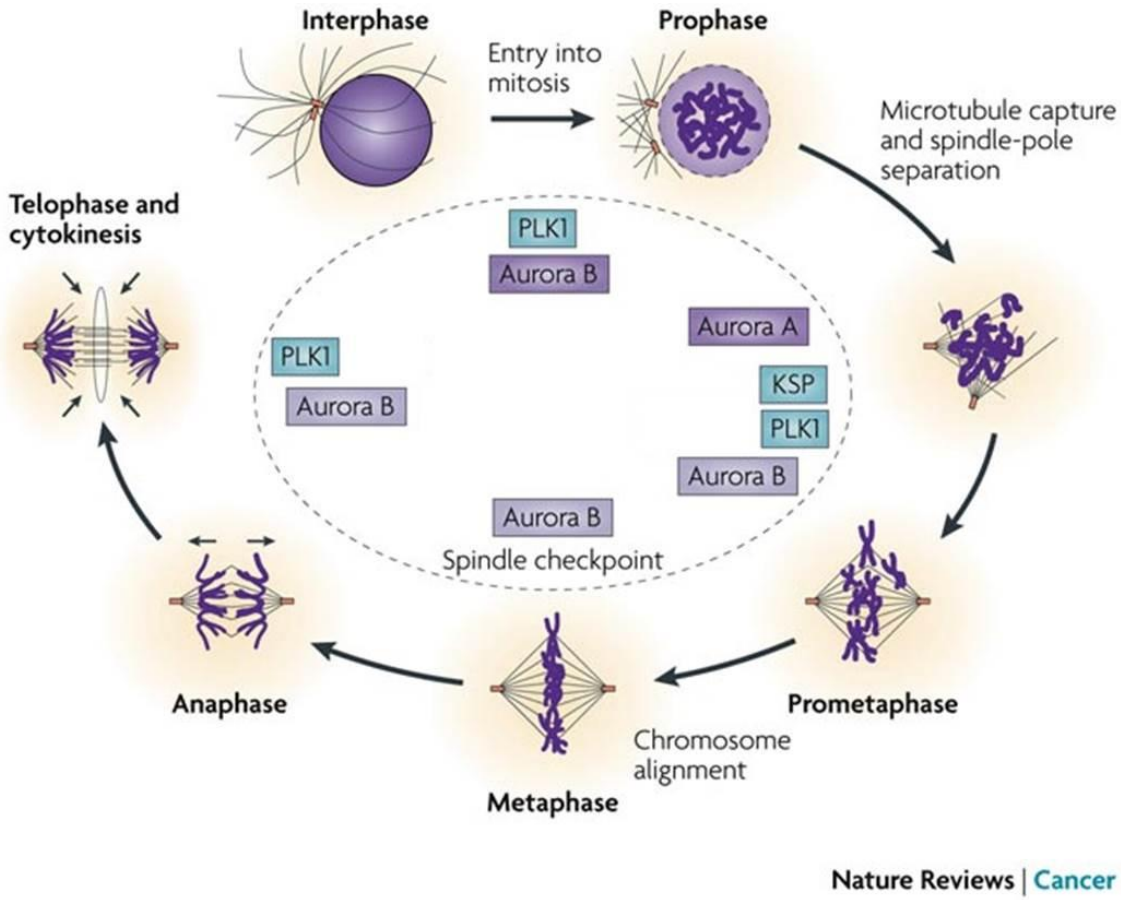

Figure 1.6 Schematic diagram of mitosis

Aurora B is a member of the chromosomal passenger complex (CPC) and is involved in histone H3 phosphorylation, chromosomal condensation, chromosomal alignment on the metaphase plate, bi-polar centromere-microtubule attachments, spindle checkpoint and cytokinesis. During mitosis, Polo-like kinase 1 (PLK1) is involved in centrosome maturation and formation of the mitotic spindle. PLK1 is also required for exit from mitosis and the separation of sister chromatids during anaphase. PLK1 might also have a role in cytokinesis through the phosphorylation of the kinesin-like motor protein MKLP1. Figure adapted from Jackson et al., 2007.

1.3.7 Abscission

In the final stages of cytokinesis, most animal cell types then remain connected by an intercellular bridge for around an hour until they are split by an actin-independent process termed abscission (Guizetti & Gerlich, 2010; Steigemann et al., 2009). Abscission proceeds by removal of cytoskeletal structures from the intercellular bridge, constriction of the cell cortex, and plasma membrane fission. It does so via two distinct mechanisms of membrane trafficking and intracellular signalling.

The intercellular bridge is filled with dense bundles of antiparallel microtubules that derive from the central spindle. These microtubules overlap at the midbody. More than 100 different proteins localise at the intercellular bridge (Skop et al., 2004), but the specific function of many components still remains unclear. However the midbody is generally regarded as a targeting platform for the abscission machinery.

Shortly upon cytokinetic furrow ingression completion, Golgi and endosome-derived vesicles accumulate at regions adjacent to the midbody (Gromley et al., 2005). Vesicles in the intercellular bridge fuse with the plasma membrane before abscission, and several vesicle-targeting and tethering factors, including centriolin and the exocyst complex (Gromley et al., 2005), Rab35, Rab11 (Fielding et al., 2005) and BRUCE (Pohl & Jentsch, 2008), are required for efficient abscission. These observations are consistent with a compound vesicle fusion model of abscission, which assumes that a separating membrane gathers inside the intercellular bridge, comparable to cytokinesis in plant cells (Baluska et al., 2006).

Extensive studies divulging the molecular mechanisms driving abscission have focussed on the ESCRT complex, largely because of the in vitro studies from the Hurley laboratory (Hurley, J. H. & Hanson, 2010). The endosomal sorting complex required for transport (ESCRT)-III is an essential abscission factor (Carlton & Martin-Serrano, 2007) that mediates membrane deformation and scission from the cytosolic face in a variety of biological processes, including virus budding, intraluminal vesicle budding and autophagy (Hurley & Hanson, 2010). ESCRT-III accumulates at regions adjacent to the midbody during late telophase (Elia et al., 2010). This is regulated by the centrosomal protein Cep55, which binds to the midbody component MKLP1 after

removal of an inhibitory phosphate on PLK1, once PLK1 is degraded by the APC (Bastos et al., 2010). Cep55 then recruits the ESCRT-III targeting factor ALIX to the midbody.

Disassembly of microtubule bundles inside the intercellular bridge depends on the microtubule severing protein spastin (Connell et al., 2009), which binds to midbody-localized ESCRT-III-associated protein CHMP1B (Yang et al., 2008). Lacroix et al., (2010) suggested spastin may be targeted to the abscission site by high levels of tubulin polyglutamylation within the intercellular bridge.

Despite the understanding of regulation of individual factors in abscission, the overall temporal control of abscission is still poorly understood. Abscission occurs only after removal of all chromatin from the division site, as the abscission machinery may otherwise damage unsegregated chromosomes, or fail due to mechanical hindrance. A tight temporal coordination between chromosome segregation and cytokinesis is ensured by the Aurora B kinase, which is kept active by unsegregated chromatin at the division plane to inhibit abscission until the division plane is cleared of chromatin. A recent study further indicates that abscission is temporally coordinated with postmitotic nuclear envelope reassembly (Mackay et al., 2010).

Studies investigating the mechanisms of abscission have uncovered that multiple components involved in cytokinesis are also required for accurate chromosome segregation. Examples include PLK1 and the chromosome passenger complex, which consists of Aurora B, INCENP, survivin, and borealin (Skop et al., 2004). Therefore, interference with the expression or regulation of these components may lead to both chromosome missegregation and failure of cytokinesis. Nonetheless, we must discuss the process which triggers proliferation and ultimately promotes cytokinetic completion, MAP kinase signalling.

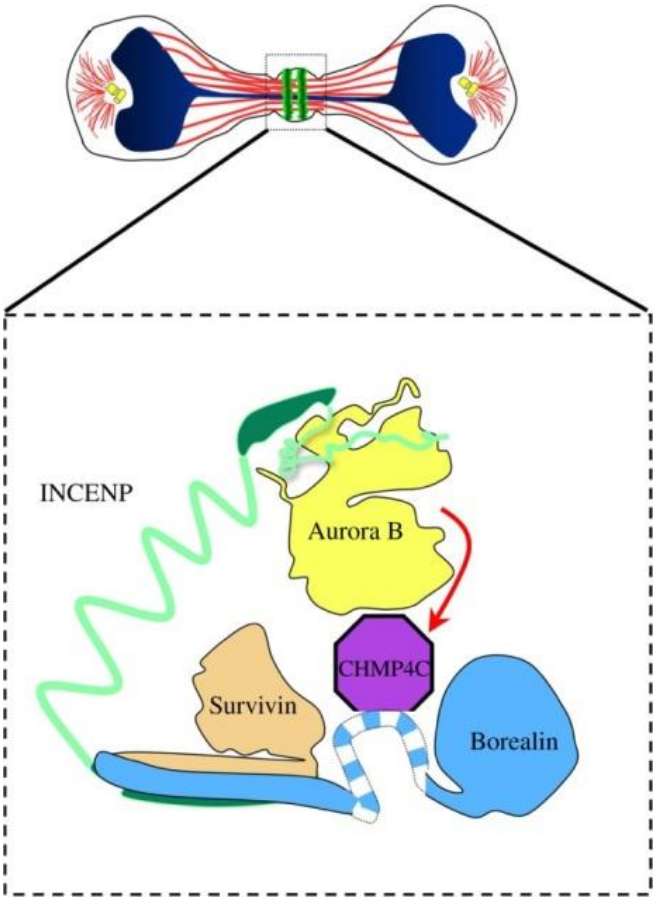

Figure 1.7: Schematic diagram of the chromosomal passenger complex required for abscission

The chromosomal passenger complex (CPC) is required for the completion of cytokinesis, located within the midbody of dividing cells. In the presence of a chromosome bridge, the CPC delays the timing of abscission through regulation of ESCRT-III. Borealin may have evolved to play a dual role in this process: first, by bringing Aurora B into contact with its substrate CHMP4C (red arrow); second, by directly interacting with CHMP4C through its central domain (blue and white striped segment) and interrupting ESCRT-III filament formation. Figure adapted from Carmena et al., (2012)

1.7 MAP Kinase Signalling

Building upon evidence that insulin and mitogens acted through novel, possibly convergent mechanisms to promote intracellular protein phosphorylation (Avruch et al., 1982; Blackshear et al., 1983) through the activation of protein (Ser/Thr) kinases (Cobb et al., 1983) Sturgill and Ray (1986) detected an insulin-activated protein (Ser/Thr) kinase activity in extracts of 3T3-L1 adipocytes, capable of phosphorylating a contaminating high molecular weight polypeptide identified as microtubule-associated protein-2 (MAP-2). Few bona fide regulatory tyrosine phosphorylations had as yet been identified, apart from those on various receptor and non-receptor tyrosine kinases themselves (Hunter and Cooper, 1985). The possibility that this MAP-2 kinase might be a ubiquitous effector of mitogenic stimuli was reinforced by the finding that the MAP-2 kinase polypeptide was identical to the 41−43kDa polypeptides (Rossomondo et al., 1985) characterised previously whose tyrosine phosphorylation was stimulated by many polypeptide growth factors (Nakamura et al., 1983; Cooper et al., 1984) and by active phorbol esters (Kohno et al., 1985; Gilbert et al., 1983). This realisation prompted the redesignation of acronym "MAP" from "microtubule-associated protein" to "mitogen-activated protein", and thus the MAP kinase family cascade as it is now known.

The emergence of the novel MAP kinase pathway prompted a surge of investigation to elucidate a physiological function for these novel substrates (Reviewed by Avruch et al., 2007). To date, the MAP kinase families have shown to regulate numerous critical cellular events such as proliferation, migration and differentiation, by stimulatory signals from the extracellular environment, growth factors, extracellular matrix proteins and adhesion molecules presented on the surface of neighbouring cells (Bennett et al., 2004). These extracellular cues are converted to a cellular response through their binding to specific receptors present at the surface of the recipient cell. Many growth factors bind and activate proteins of the receptor tyrosine kinase family (Yarden, 1988). Receptor tyrosine kinases (RTK) contain an extracellular ligand binding domain, a single transmembrane domain, and an intracellular region containing a tyrosine kinase domain and several regulatory tyrosines, which are modified via auto- or trans-phosphorylation (Katz et al., 2007). Upon binding to specific receptors, growth factors

drive the formation of receptor dimers, leading to the activation of the intrinsic tyrosine kinase domain. Subsequent phosphorylation of specific tyrosines enables the recruitment of various signalling adaptor proteins, triggering a number of kinase cascades, including MAP kinase cascade.

MAP kinase pathways target proteins throughout the cell, and as many substrates are nuclear they possess the ability to regulate changes in gene expression. The MAP kinase pathway is a triple kinase module, evolutionary conserved within eukaryotes, where MAP kinase elements are activated upon tyrosine and threonine phosphorylation within a conserved Thr-XXX-Tyr motif in the activation loop of the kinase domain. The phosphorylation of proteins by MAP kinases can affect many aspects of their function including DNA binding, protein stability, cellular localisation, and protein-protein interactions, as well as regulating other post-translational modifications (Yang et al., 2007). It is also worth noting that MAP kinases have recently exhibited properties outwith their prototypic role; where components have also functioned non-enzymatically to regulate transcription (Krishna and Narang, 2008).

There are four major MAP kinase signalling pathways identified in eukaryotes; the extracellular signal-regulated kinase (ERK), extracellular signal-regulated kinase 5 (ERK5), c-Jun N-terminal kinase (JNK) and p38 MAP kinase pathways (Wang and Tournier, 2006). Multiple activators of these pathways has been well documented, where the ERK pathway is activated predominantly by growth factors, whereas JNK and p38 pathways respond to a variety of extracellular stress signals. Additional complexity of the pathways comes from the presence of multiple subtypes for each family member (ERK1 and ERK2; JNK1, JNK2, JNK3; p38α, p38β, p38γ, p38δ) and the generation of further isoforms by differential splicing of these genes products (Krishna and Narang, 2008).

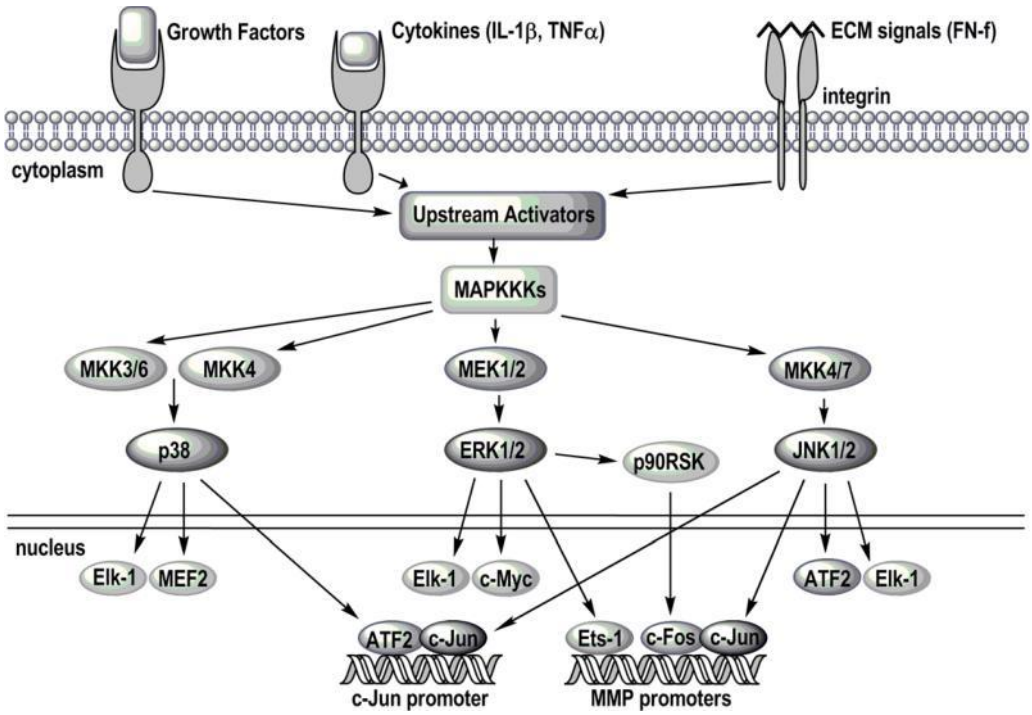

Figure 1.8 MAP kinase signalling overview.

A diverse array of receptors, including growth factor, cytokine, and integrin receptors, activate signalling pathways which lead to the activation of the MAP kinase pathways. MAP kinase kinase kinases (MAPKKKs) activate MAP kinase kinases (MKKs; MAP and ERK kinase or MEK), which in turn activate the MAP kinases (p38, ERK1/2, and JNK). The MAP kinases activate other kinases, such as p90RSK, and transcription factors that regulate gene transcription including Elk-1, MEF2, ATF2, c-Myc, Ets-1, and c-Jun. Figure adapted from Loeser et al., 2008.

1.4.1Extracellular signal regulated kinase signalling

1.4.1.1 Architectural features of ERK signalling

Signal transduction of the ERK pathway is initiated by the phosphorylation of the tyrosine kinase receptor upon binding of an agonist. In doing so, docking sites for adaptor proteins become exposed to where Grb2 binds to the receptor through an SH2 domain-phosphotyrosine interaction. Grb2 interacts with the guanine nucleotide exchange factor, SoS which is subsequently recruited to the plasma membrane promoting the conversion of G protein ras from a GDP-bound state to an active GTP-bound state. Ras-GTP acts upon the Raf molecule which induces the phosphorylation of serine residue in the activation loop of MEK (Kyriakis et al., 2012). Furthermore, ERK becomes phosphorylated by MEK on threonine and tyrosine residues at the activation loop. The activation of ERK results in translocation to the nucleus where ERK phosphorylates and activates various transcription factors such as E2F-1, Elk-1, AP-1 and *myc* which, as previously mentioned, play a role in promoting CDK-cyclin complexes and ultimately cellular proliferation. The physiological response induced by ERK depends on cell surface receptor density, the amount of ligand, the duration of the signal and the cell type under consideration and subcellular distribution of ERK itself (McKay and Morrison, 2007).

An increasing body of evidence has noted ERK acting on a number of different sites of cell cycle machinery. ERK is present in cytoplasmic regions during interphase (Cyert, 2001), however translocates to the nucleus upon mitogenic stimulation. Brunet *et al*., (1999) shows the translocation of ERK is necessary for G1/S progression. Furthermore, studies have shown a role for ERK in mitotic chromosome condensation; where ERK is known to phosphorylate MSK1 which in turn, phosphorylates histone H3 on residues vital for function. From data by Liu et al., (2004) it could be eluded that ERK1 alone is responsible for this function and may be required for progression into mitosis. The study noted a reduction in ERK1 in cells but not ERK2, therefore suggesting ERK1 must be essential for the synthesis of proteins required for mitosis.

During mitosis, ERK has shown present in spindle asters, centrosomes and kinetochores (Sharpiro et al., 1998; Zecevic et al., 1998). The ERK function in the

aforementioned mitotic apparatus is still unknown, however Gachet et al., (2001) describe the presence of an ERK-dependent spindle assembly checkpoint in *Schizosaccharomyces pombe.* Direct investigation into presence of an ERK spindle assembly point in mammalian cells has yet to be conducted, although in *Xenopus laevis* ERK has been shown to phosphorylate Cdc20, a protein located at mammalian centromeres thus suggesting a role for ERK in mitosis (Chung et al., 2003).

1.4.1.2 ERK in hyperproliferative disease

The ERK pathway has been intensely studied with regards to its role in hyperproliferative disease; largely cancer where numerous cases of mutations in the ERK signalling cascade have been reported. Notably, constitutively active $p21^{ras}$ and B-raf (Boutros et al., 2008) have been well studied in a hyperproliferative disease state. Schubbert et al., (2007) detail specificities of ras subtypes, where K-ras mutations are known to contribute to numerous human cancers, including lung and colon, where mutation is present in ~50% of colon cancers. B-raf mutations, however, were shown to be present in around 66% of all malignant melanomas (Halilovic and Solit, 2008), with an amino acid substitution of glutamate for valine; resulting in the constitutive activation of the ERK pathway, and thus the hyperproliferative cellular state associated with the pathogenesis and progression of cancer (Marshall and Vousden, 2011).

1.4.2 c-Jun N-terminal kinase signalling

1.4.2.1 Architectural features of JNK signalling

The c-Jun N-terminal kinase (JNK), also recognised as the stress-activated protein kinase (SAPK) is activated primarily under stress conditions including UV radiation, DNA damage and inflammatory cytokines. Nevertheless, activation via growth factors has also been described although at somewhat a less efficient activation (Kyriakis et al., 2012). Similar to ERK, JNK is activated by phosphorylation on tyrosine and threonine residues, however is catalysed by MKK4 and MKK7 which are phosphorylated and activated by several proteins namely, MEKK1-4, MLK1-3 and Tak1 (Han et al., 1998).

Once activated, JNK translocates to the nucleus and mitochondria where pools of active JNK accumulate. Activation of the JNK pathway results in the phosphorylation and activation of transcription factors in the nucleus, namely c-Jun, JunA, ATF2 and Elk1. Crosstalk between MAP kinase pathways has been described via the small G protein rac which induces the activation of both MEKK1-4 of the JNK pathway, and raf of the ERK pathway.

It is widely established that programmed cell death is linked to the JNK pathway (Dhanasekaran and Reddy, 2008). However, interesting results from studies by Chang et al., (2006) and Ventura et al., (2006) provide insight into the complexity of JNK signalling, demonstrating that early transient JNK activation promotes cell survival and proliferation, however, prolonged JNK activation mediates apoptosis and ultimately cell death.

As with ERK, JNK has also been implicated in the cell cycle. A recent study by Guitterez et al., (2010) details the impact of JNK in the G2/M phase transition. JNK is required to phosphorylate Cdc25C during mitosis which dephosphorylates and inactivates cdc2 and allowing entrance to mitosis. The development of JNK inhibitor SP600125 in 2001, allowed for further insight into the role of JNK in mitosis. In the presence of the inhibitor, multinucleate mammalian cells with 4N DNA content were shown to accumulate in the G2/M phase of the cell cycle. MacCorkle and Tan (2004) propose this to be a result of defective spindle formation and also possibly a dysfunction in chromosome segregation at anaphase in mitosis and thus JNK is required for full mitotic completion.

1.4.2.2 JNK in hyperproliferative disease

JNK has been shown to exhibit differential cellular effects, probably evident most so in cancer where for example, JNK1, but not JNK2, deficiency significantly decreased HCC (hepatocelluar carcinoma) in the DEN (diethylnitrosamine)-induced HCC mouse model (Hui et al., 2008). Combining this evidence with work from Chen et al., (2001) it could be suggested that JNK1 performs with a role as a tumour suppressor, whereas JNK2 exhibits function as a tumour promoter aiding hyperproliferation. Chen et al.,

(2002) examined mouse embryonic fibroblasts, under both basal and PMA stimulation, demonstrating that the loss of JNK1 enhanced the expression of antiapoptotic genes, whereas cells lacking JNK2 displayed increased expression of genes related to tumour suppression and induction of cell differentiation, or cell proliferation. Thus JNK has differential roles in proliferation and apoptosis of cancer disease progression.

1.4.3 p38 MAP kinase signalling

1.4.3.1 Architectural features of p38 MAP kinase signalling

The p38 pathway consists of four isoenzymes; α, β, γ and δ, where p38α has been the greatest explored within the scientific literature. Similar to JNK, p38 MAP kinase is also activated by stress and cytokines and plays a critical role in immune response. However, in analogy to the JNK cascade, the p38-MAP kinase route is predominately activated by stress conditions and inflammatory cytokines but seems almost insensitive to growth factor stimuli. Due to the importance of p38 with immunological responses, it has been directly linked with asthma and autoimmune diseases, rheumatoid arthritis (Senolt *et al.*, 2009).

Upon activation of the p38 MAP kinase pathway, TAK1 becomes phosphorylated to MKK6 then to p38 MAP kinase. However, with the p38α isoform, p38 is activated by TAB1, which is controversially not an MKK but an adaptor protein with no present catalytic activity. From this recent breakthrough, questions have been raised over the increasingly important regulatory roles of adaptor proteins within the MAPK pathways (Sakurai et al.,2000).

1.4.3.2 p38 MAP kinase in hyperproliferative disease

Furthermore, p38 MAP kinase has been implicated in hyperproliferative diseases other than neointimal hyperplasia, where Iwasa et al., (2003) displayed an increased proliferative capacity of mouse embryonic fibroblasts which had been pharmacologically treated with p38 MAP kinase inhibitors. The suppressive function

of p38 MAP kinase has been evident in many cellular systems; hematopoietic cells derived from p38α$^{-/-}$ fetal livers proliferated faster and formed more myeloid colonies *in vitro* where erythroid cells deficient in p38α exhibited significantly enhanced doubling ability rates (Hui et al., 2007).

1.4.4 MAP Kinase Signalling in Atherosclerosis

MAP kinase signalling has been well-characterised in vascular smooth muscle cells; with distinct roles in proliferation, migration, differentiation and apoptosis (Katz et al., 2007; Kim and Choi, 2012). In addition, an advanced body of data has emerged in the last decade detailing distinct roles for MAP kinase signalling in vascular diseases (Reviewed in Yu et al., 2007); with a focus upon atherosclerosis and restenosis.

Due to the multifactorial aetiology of atherosclerosis, studies investigating the role of MAP kinases have included numerous cell types involved with the disease. Treatment of macrophages with the JNK pathway inhibitor SP600125 blocked oxLDL-induced foam cell formation, but macrophages with the ERK pathway inhibitor U1026 displayed no effect (Rahaman et al., 2006). The redundant role for ERK in foam cell production was supported by Zhao et al., (2002) who state an oxLDL-induced foam cell formation in the J774 macrophage cell line was found to be inhibited by administration of the p38 MAPK inhibitor SB203580, but was not blocked by administration of the ERK pathway inhibitor PD98059. Collectively these data suggest stress-activated MAP kinases, JNK and p38 MAP kinase play are role in the formation of foam cells with an atherosclerotic lesion.

To determine the specific role of JNK1 and JNK2 in the development of atherosclerosis, disease model ApoE null mice were bred with either JNK1$^{-/-}$ or JNK2$^{-/-}$ mice and placed on a high fat diet (Ricci et al., 2004). Interestingly, JNK2$^{-/-}$ ApoE$^{-/-}$ displayed an increased resistance to atherosclerotic lesion formation when compared with JNK1$^{-/-}$ ApoE$^{-/-}$. The authors stated that the lesions present in JNK2 knockouts did not have altered cellular composition, but were simply smaller in absolute size. This therefore established the proposed mechanism regarding the differential role of JNK isoforms in cancer; an effect mirrored in atherosclerosis.

Further exploration of the role of MAP kinases in atherosclerotic lesion development was provided by the analysis of $Grb2^{+/-}$ $ApoE^{-/-}$ mice fed a high fat diet for two months. Proctor et al., (2007) described a reduction in atherosclerotic lesion of $Grb2^{+/-}$ $ApoE^{-/-}$ mice in comparison with $ApoE^{-/-}$ mice suggesting a role for ERK in the development of atherosclerosis contrary to the work of Rahaman et al., (2006). Nevertheless, this discrepancy may be explained by the limitations of different tools; delivery of ERK inhibitor versus genetic modification of Grb2 levels.

1.4.5 MAP Kinase Signalling in Restenosis

Atherosclerotic vascular disease is often treated by percutaneous transluminal balloon angioplasty and/or by arterial stenting. Unfortunately, in many cases, neointima formation occurs a short time after balloon angioplasty or stenting thereby resulting in arterial restenosis. Neointima formation is primarily a disorder of smooth muscle cells where migration and proliferation of these cells, in addition with extracellular matrix deposition in the intima are regarded as important features of this disorder (Koyama et al., 1998; Yu et al., 2007). Although, the incidence of restenosis is markedly reduced when drug eluting stents are employed, the incidence of restenosis is still markedly high. Both physiologically and pharmacologically, more information about neointima formation would be clinically useful.

Neointima formation may be triggered by the local release of growth factors, cytokines and ligands in response to mechanical injury by balloon angioplasty or stent placement. The release of bioactive factors at the site of vascular intervention is thought to be a consequence of endothelial cell injury, binding to receptors on the surface of smooth muscle cells promoting the activation of intracellular signalling cascades and leading to cell migration and proliferation. Balloon injury of the rat carotid artery results in the rapid activation of ERK1/2, p38 MAP kinase and JNK1/2 (Tanaka et al., 1998; Sirois et al., 1997).

To further investigate the role of MAP kinase signalling in restenosis, the ras protein has been targeted as key transducers of mitogenic signals from the plasma membrane to the nucleus. The role of ras proteins in response to arterial injury *in vivo* was assessed

in balloon injured rats by inactivated cellular ras by a dominant negative mutant (Indolfi et al., 1995). The N17H ras mutant resulted in a significant reduction (of around 55%) of neointima formation when compared with animals treated with LacZ control. Even from early studies, PDGF-induced ERK signalling has been believed to regulate to VSMC proliferation and by the use of neutralising antibodies was shown to inhibit neointimal smooth muscle cell accumulation after angioplasty (Ferns *et al*., 1991). The promotion of proliferation was further supported by Sirois *et al*., (1997) who have shown inhibition of PDGF-β receptor subunit expression by antisense oligonucleotides and noted a corresponding suppression of neointimal thickening, whereas the over-expression of PDGF-β receptor promoted remodelling in a porcine model.

To address the role of the ERK cascade in neointima formation, $Grb2^{-/-}$ mice were subject to carotid injury by use of a beaded probe method. Three weeks after injury, carotid arteries were examined for hyperproliferation in neointima formation and signalling pathway activation. $Grb2^{-/-}$ mice were resistant to carotid injury-induced neointima formation with a dramatically reduced number of intimal smooth muscle cells. In addition, Grb2 haplo-insufficient mice exhibited reduced ERK, JNK and p38 MAPK activation in carotid artery extracts post-injury (Zhang et al., 2003). To examine the role of ras activation in ERK dependant neointima formation, mice with smooth muscle cell-specific targeted disruption of the Nf1 gene that encodes neurofibromin, a GTPase that deactivates ras, were examined (Xu et al., 2007). Mice with smooth muscle cell-specific Nf1 knockout were subjected to carotid artery injury by external ligation. After 28 days and completion of the study, arteries were examined and Nf1smKO mice were found to develop exaggerated neointima formation with a dramatically increased intima-to-media ratio. Cellular proliferation rates were increased, as was ERK1/2 activation in the neointima in Nf1smKO mice when compared to control animals.

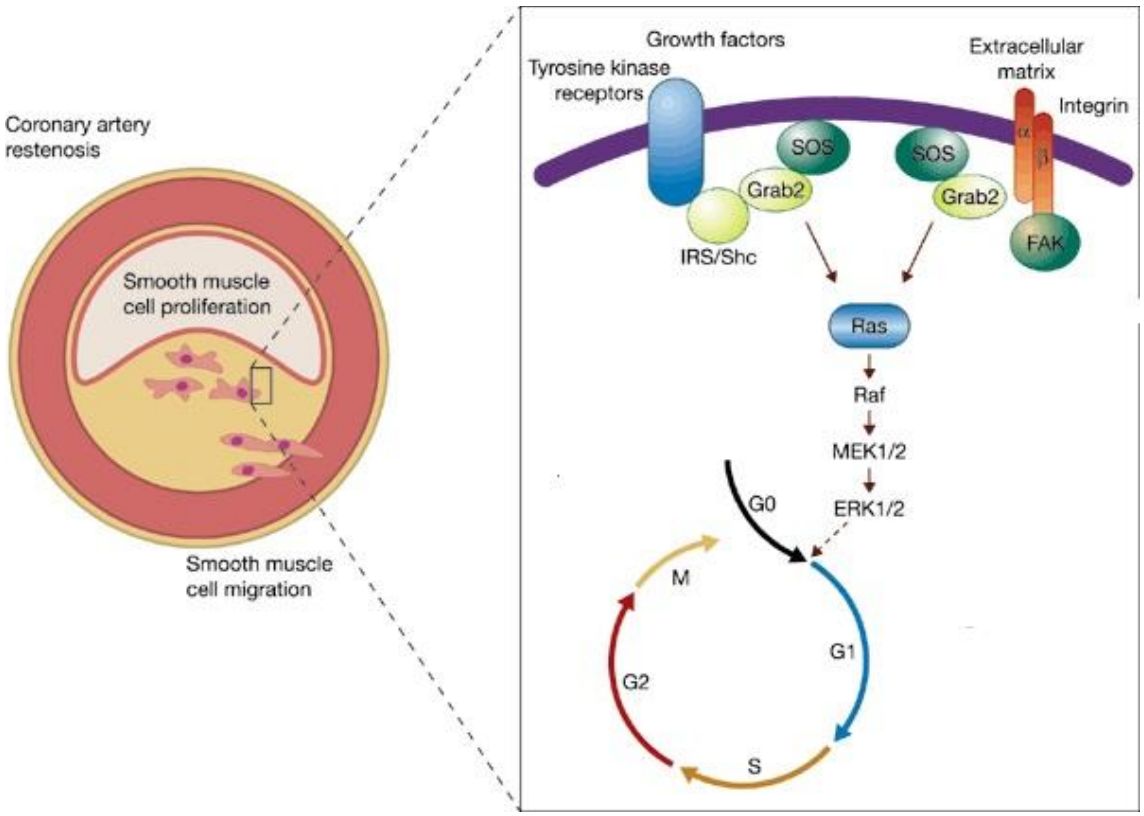

Figure 1.9 Arterial restenosis of smooth muscle cells driven by ERK signalling. Arterial restenosis of smooth muscle cells driven by ERK signalling and subsequently activating G0/G1 progression in the cell cycle. Figure adapted from Chien et al., 2004

Moreover, JNK has been implicated in neointimal hyperplasia, interestingly it has been shown that the AP-1 member c-Jun is required for both platelet-derived growth factor (PDGF)-induced VSMC migration and proliferation (Zhan et al., 2002). VSMCs infected with recombinant dominant-negative adenovirus for c-Jun lacking the transactivation domain of wild c-Jun (Ad-DN-c-Jun). Ad-DN-c-Jun, which specifically blocked AP-1 transcriptional activity, significantly inhibited PDGF-BB–induced increases in proliferation. Further analysis exhibited an arrest of Ad-DN-c-Jun treated cells in PDGF-BB–induced entrance of SMCs into S phase. Moreover, inhibition of JNK activity using recombinant adenovirus containing a dominant-negative mutant of JNK attenuated PDGF-induced VSMC migration and proliferation *in vitro* (Zhan et al., 2003).

In order to examine the role of p38 MAP kinase in the pathogenesis of neointima formation, transgenic mice with smooth muscle cell-specific inducible expression of dominant negative p38α were produced (Muslin, 2009). In these mice, tetracycline administration resulted in the expression of dominant negative p38α in the smooth muscle cells of the aorta and carotid arteries. Mice expressing DN-p38α in SMCs were resistant to neointima formation after carotid injury when compared to control animals. To address the mechanism by which p38α promotes the proliferation of smooth muscle cells, PDGF stimulation was demonstrated to result in the p38α-dependent phosphorylation of the retinoblastoma protein (Rb), a master regulator of cell cycle progression. Furthermore, PDGF stimulation of cultured smooth muscle cells promoted the p38α-dependent expression of minichromosome maintenance protein 6 (MCM6), a protein required for DNA synthesis in the S phase of the cell cycle (Muslin, 2009).

Collectively, it is clear that there is an abundance of evidence to link MAP kinase signalling in a major role regarding the pathological progression of both atherosclerosis and restenosis. Therefore the possibility remains to target endogenous regulators of MAP kinase signalling with an aim to alter their expression and function. With the emerging recognition of protein phosphatases, we discuss the possibility of examining a role for MAP kinase phosphatases in vascular disease.

1.5 Regulation of MAP Kinase Signalling Pathways by Protein Phosphatases

Over the past decades, much of the interest of the scientific community has been directed towards protein kinases, with protein phosphatases being considered less interesting, regarded as regulatory enzymes playing a nonspecific role in modulating phosphoprotein homeostasis. Recent findings, however, have led to the emerging recognition that protein phosphatases play key roles in establishing the levels of phosphorylation in cells, and therefore participating in the regulation of many physiological processes, including cell growth, tissue differentiation and cellular communication (Tonks, 2006). Many phosphatases are devoted to dephosphorylating MAP kinase activity in order to control the strength and duration of the intrinsic MAP kinase activity within the cell (Keyse, 2008).

1.5.1 The Protein Tyrosine Phosphatase Family (PTPs)

The protein tyrosine phosphatases (PTPs) gene superfamily consists of 107 genes in the human genome, sharing a canonical C(X)5R motif in their active sites (Alonso et al., 2004). This family is comprised of four main groups based on their amino acid sequence in the phosphatase catalytic domains, with Class I cysteine based PTPs by far the largest. These can be further divided into the classical PTPs, including the receptor PTPs (RPTPs) and non-receptor PTPs (NRPTPs), and the dual specificity phosphatases (DUSPs), which can dephosphorylate serine and threonine in addition to tyrosine residues (Tigalis and Bennet, 2007) (as shown in Table.2). Phosphatases use three main strategies to physically target their substrates; targeting domains that are covalently linked to the catalytic domains, exploiting a complementary strategy by Small Linear Motifs to dock into a substrate binding pocket or binding non-covalently to regulatory subunits or scaffold proteins that mediate substrate docking (Sacco et al., 2012). The three mechanisms contribute to phosphatase substrate recognition, although the relative importance of the three in different phosphatase families remains to be established.

Over time, using an array of genetic and biochemical techniques, many substrates that these enzymes dephosphorylate were identified; where the class I PTP family of MAP

kinase phosphatases (MKPs) was found to dephosphorylate major homologs of the MAP kinases on both tyrosine and threonine residues within the TXY activation motif of the kinase. This MKP family was shown to exhibit different specificities towards MAP kinase member and thus essential regulators of MAP kinase-mediates signalling within a wide range of biological processes.

1.6 MAP Kinase Phosphatases

1.6.1 MAP Kinase Phosphatase Structure

The MKPs share a strong sequence homology of between 37-50% in the catalytic domain; using the example of MKP-3 and MKP-X, Keyse and Emslie (1992) describe a shared homology of up to 75%. The catalytic domain comprises of a highly conserved consensus sequence **D**X_{26}(V/L)X(V/I)H**C**XAG(I/V)-S**R**SXT(I/V)X XAY(L/I)M, in the single letter code where X represents any amino acid and the letters in bold denote amino acids essential for catalysis. To date, at least ten MKP homologues have been identified in mammalian tissue, along with several truncated atypical isoforms, with each comprising of two domains; the MAP kinase binding domain (MKB) at the N-terminal and the DSP domain in the C-terminal. The C-terminal DSP domain is homologous to the prototypic DUSP VH-1, and the N-terminal MKB domain is homologous to the rhodanese family with sequence homology to catalytic domain of the cdc25 phosphatase (Keyse and Ginsburg, 1993). The MKB domain contains a cluster of positively charged amino acids, whose role it is to determine the binding specificity of MKPs towards MAP kinases (Tanoue et al., 2001). Numerous studies have demonstrated the catalytic activation of several MKPs by substrate binding to the MKB (Camps et al., 2000; Chen et al., 2001; Zhang et al., 2005). Upon binding of phosphorylated MAP kinase to the MKB domain, a conformational change occurs and consequentially increases the catalytic activity of the phosphatase (Farooq & Zhou, 2004).

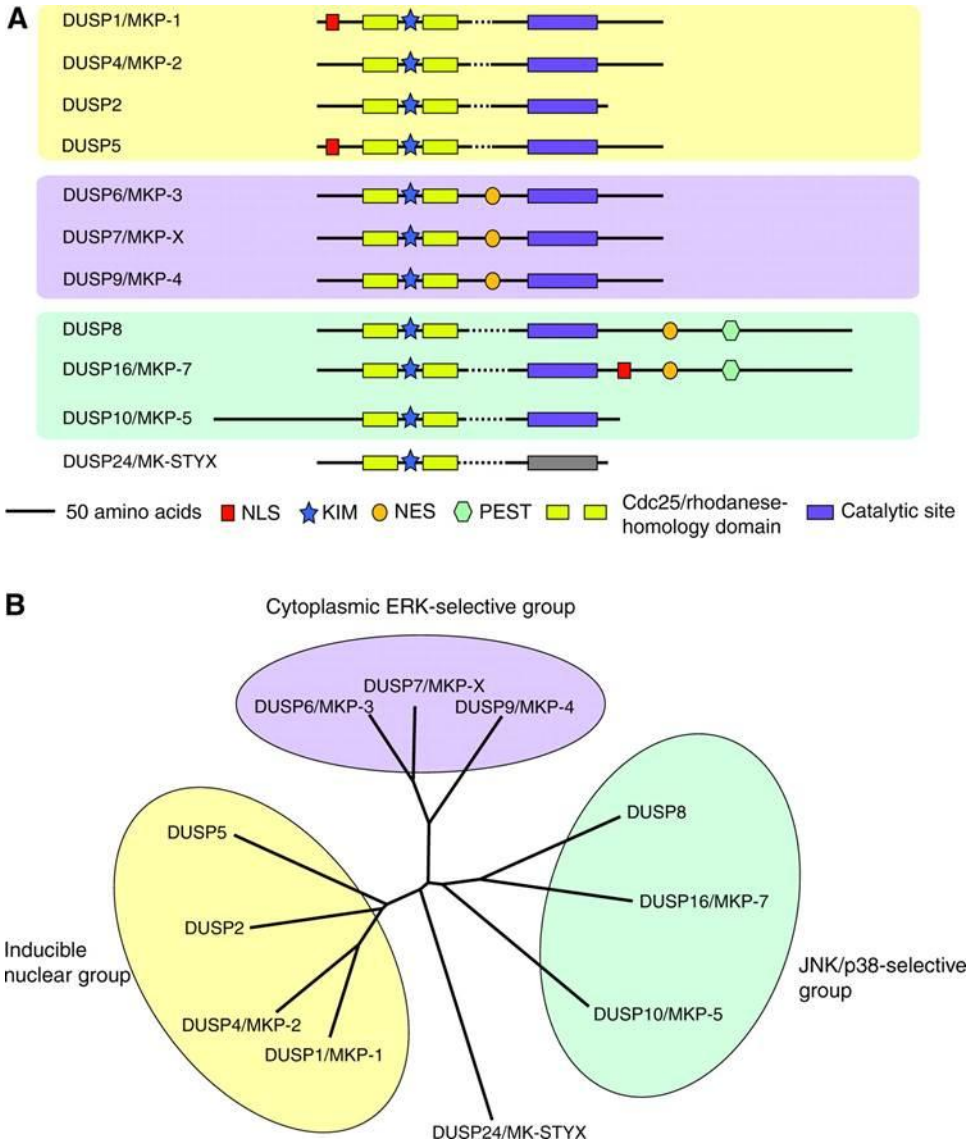

Figure 1.10: Classification, domain structure and phylogenetic analysis of the dual-specificity MAPK phosphatases.

(A) Domain structures of the ten catalytically active DUSP proteins and MK-STYX. In addition to the N-terminal non-catalytic domain containing the Cdc25/rhodanese-homology region and the catalytic site, the positions of the conserved kinase-interaction motif (KIM), nuclear localisation signals (NLS), nuclear export signals (NES) and PEST sequences are indicated. The three subgroups revealed by the phylogenetic analysis are indicated by the background colour. (B) DUSP sequence analysis. Human DUSP amino acid sequences were aligned using CLUSTALW (http://align.genome.jp/) and a phylogenetic tree was generated. Adapted from Dickson & Keyse, 2006.

1.6.2 Classification of MKPs

Characterisation of MKPs has largely been based on four main attributes: tissue distribution, substrate specificity, regulation of cellular expression and activity in response to extracellular stimuli and, in particular, subcellular distribution. This characterisation allows for each phosphatase to be subdivided into three main families; Type I, II and II (Patterson et al., 2009). The first group encompasses the type 1 nuclear inducible phosphatases MKP-1, PAC-1, MKP-2 and VH-1 which express an NLS (nuclear localization sequence) within the C-terminus. The second type II group of MKPs, including MKP-3, MKPx and MKP-4, are strictly cytoplasmic, due to the presence of NESs (nuclear export sequences). The type III group comprising VH-5, MKP- 5 and MKP-7 are localised in either the nucleus or cytosolic compartments (Lawan et al., 2012).

Other distinctive features of DUSP regulation vary across the groupings and can be exemplified by a number of key studies; the prototypical MKP-1 is induced in response to a variety of stimuli primarily believed to be via an ERK-dependent pathway as part of a negative feedback loop. Binding of MKP-1 to ERK via the MKB followed by catalytic activation enhances phosphatase activity (Slack et al., 2001). It should be noted that ERK-induced phosphorylation also promotes resistance to proteasome mediated degradation (Brondello et al., 2009). Many of the type I DUSPs, including MKP-1, dephosphorylate more than one MAP kinases *in vitro*, although substrate profiles have previously been shown to be cell-type specific (Alessi et al., 1993). Type II DUSPs are exemplified by MKP-3, which can be expressed constitutively in a number of cell types. Comparable to MKP-1, Camps et al., (1998) found that binding of ERK to the MKB of MKP-3 increases phosphatase activity. The type III DUSP MKP-7, requires C-terminal Ser466 phosphorylation by ERK to suppress proteasomal degradation and maintain functional integrity, however has a greater affinity for JNK and p38 over ERK (Masuda et al., 2001). Based on structural similarity between the MAP kinase-binding domain of MKP-5 and MKP-7, the authors suggest that this mechanism may be a conserved feature of the p38 and JNK-specific phosphatases MKP-5, DUSP8 and MKP- 7 and may underpin their ability to interact specifically with these kinases rather than with ERK (Zhang et al., 2011). This is certainly a

possibility, but it should be remembered that in the nuclear phosphatase MKP-1, which can interact with ERK, JNK and p38, the KIM is only required for interaction with ERK and p38 and thus more information is required regarding the binding of the MKPs to their MAP kinase substrates.

PTP Family	Members (N)	Substrate Specificity
Class I	Receptor PTPs (21)	pTyr,
	Non-receptor PTPs (17)	pTyr
	MKPs (11)	pTyr, pThr
	Atypical DUSPs (19)	pTyr, pThr
	Slingshots (3)	pSer
	PRLs (3)	pTyr
	Cdc14 (4)	pThr, pSer
	PTEN (5)	D3-phosphoinositides
	Myotubularin (16)	D3-phosphoinositides
Class II	LMWPTPs (1)	pTyr
Class III	Cdc25 (3)	pTyr, pThr
Class IV	Eya (4)	pTyr, pSer

Table 1.2: **Overview of the PTP family**, which is subdivided in 4 classes. PTP: protein tyrosine phosphatase; MKP: mitogen-activated protein kinases phosphatase; DUSP: dual-specificity phosphatase; PRL: phosphatase of regenerating the liver; CDC: cell division cycle; PTEN: phosphatase and tensin homolog; LMWPTP: low molecular weight protein tyrosine phosphatase; Eya: Eyes absent homolog. Based on Alonso et al.,(2004).

1.6.3 Physiological Role of MKPs

1.6.3.1.MKP-1

MAP kinase phosphatase-1 is the archetypal member of the MKP family, where it was identified as an immediate-early response gene in 1992 by Keyse and Emslie. MKP-1 is expressed in a wide variety of tissues with the most notable levels observed in the heart, lungs and liver (Charles et al., 1992; Noguchi et al., 1993). By use of immunofluorescent microscopy and cellular fractionation, MKP-1 was shown to be located primarily within the nucleus. This is actioned by the presence of a NH_2-terminus LXXLL motif (Wu et al., 2005). However it has been reported that pools of MKP-1 are also present in mitochondria (Rosini et al., 2004).

The catalytic activity of MKP-1 is regulated by its interaction with MAP kinases, where direct binding of ERK, JNK or p38 MAP kinase potentiates the catalytic activity of MKP-1 (Hutter et al., 2000; Slack et al., 2002). Hutter et al., (2000) described the interaction of MKP-1 with MAP kinases to interact via the MAP kinase binding domain, or otherwise known as the kinase interaction motif (KIM). Early studies suggested that MKP-1 possessed the ability to dephosphorylate and inactivate only ERK (Sun et al., 1993; Duff et al., 1995), nevertheless it is now widely accepted that MKP-1 dephosphorylates p38 MAP kinase, JNK and to a lesser extend ERK, shown in both *in vitro* and *in vivo* studies (Wu and Bennett, 2005).

The expression of MKP-1 is subject to regulation by extracellular stimuli, where the basal expression of MKP-1 is relatively low in most cell types. However, in response to mitogens, growth or stress factors, MKP-1 is rapidly induced as an early-immediate response gene (Tucsek et al., 2011). Interestingly, MAP kinases themselves have shown to be good inducers of MKP-1, acting by a negative feedback loop between MAP kinases and MKP-1 (Lawan et al., 2013). MKP-1 has also been recognised for its involvement in protein stability. Brondello et al., (1999) detail that MKP-1 expression is enhanced upon ERK phosphorylation on two key residues of MKP-1: serine 359 and serine 364. It is clear that ERK phosphorylates MKP-1 at multiple residues; however the physiological impact or significance of this negative-feedback action is yet to be fully elucidated.

1.6.3.1.1 MKP-1 in Disease

The function of MKP-1 has been extensively studied using a number of techniques including siRNA and adenoviral over-expression; currently however, the most extensively utilised tool is the generation MKP-1 knockout mice (Wu et al., 2006). While reproduction and growth in MKP-1 deficient mice does not differ largely from wild-type animals, the MKP-$1^{-/-}$ mice exhibit an abundance of physiological modifications and distinct disease phenotypes (Dorfman et al., 1996; Wancket et al., 2012). MKP-1 has been implicated in conditions including cancer, metabolic disorders, immune dysregulation and asthma (Wancket et al., 2012; Lawan et al., 2013).

1.6.3.1.1.1 MKP-1 in Cancer

MAP kinases are crucial regulators of cell fate, including proliferation and apoptosis. Given the role of MKP-1 in inhibiting MAP kinase activation, it is not surprising that MKP-1 has emerged as a crucial feedback control regulator. However, there is conflicting evidence for MKP-1 playing a role in cancer, as both a tumour suppressor and an oncogene (Reviewed in Keyse et al., 2008). Elevated MKP-1 expression was reported advanced breast carcinoma, pancreatic cancer and non-small long carcinoma (Rojo et al., 2009; Liao et al., 2003). In contrast however, there are multiple examples of cancers where MKP-1 expression decreased such as prostate cancer (Rauhala et al., 2005) and colon tumours (Loda et al., 1996). It is currently unclear what factors lead to altered MKP-1 expression in multiple cancers, however multiple hypotheses have been proposed. It believed that MKP-1 oncogenic mutations of the MAP kinase pathways may have an impact on downstream MKP-1 activity (Harris and McCormick 2010). Furthermore, tumour suppressor p53 regulates MKP-1 expression and is often mutated or deleted in human cancers and therefore, loss of p53 may alter MKP-1 activity (Yang and Wu, 2004). However, to date there are no such reports demonstrating that MKP-$1^{-/-}$ mice display any signs of increased tumorigenesis. Despite the speculation of this mechanism, it is well established that the role of MKP-1 to inhibit MAP kinase signalling has a profound effect on cell proliferation and apoptosis within tumours (Wancket et al., 2012).

1.6.3.1.1.2 MKP-1 in Cardiovascular Disease

With the discovery of the prototypic MKP-1 and the advancement of disease models, Reddy et al., (2004) utilised two atherosclerotic models; low-density lipoprotein receptor (LDLR) $^{(-/-)}$ mice on a Western diet, and 10-week or ApoE $^{(-/-)}$ mice on a chow diet. The group state that there is elevated MKP-1 mRNA expression in correlation with the atherosclerotic disease phenotype, suggesting MKP-1 expression is associated with hypercholesterolemia and atherosclerosis.

Imaizuma et al., (2010) backcrossed MKP-$1^{-/-}$ mice with $ApoE^{-/-}$ mice, describing that the atherosclerotic and *en face* lesions along the aorta were significantly smaller than lesions found in $ApoE^{-/-}$ mice. This group further investigated lesion composition, where there was a reduction in lipid formation within the lesions in MKP-$1^{-/-}ApoE^{-/-}$ mice in comparison with ApoE¯alone. This therefore suggests that MKP-1 may serve as a therapeutic target in reducing atherosclerotic lesion development.

1.6.3.2 MKP-2

MAP kinase phosphatase-2 was first isolated in PC12 cells from the Dusp4 gene by Misra-Press et al., (1995). The gene was found to encode a protein of 394 amino acids with a predicted molecular weight of 43kDa and a shared sequence homology of around 60% with MKP-1. Further investigation detailed the presence of MKP-2 mRNA in a number of tissue including brain, spleen and testes, with the highest expression exhibited in heart and lung samples (Keyse, 2008). There is a difference in tissue distribution when compared with MKP-1, suggesting a role for MKP-2 distinct of that from the prototypic MKP-1. By use of fluorescent microscopy, MKP-2 was located within the nucleus and thus was categorised in the type I family DUSPs (Sloss et al., 2005). Nuclear localization is thought to be regulated by the triple arginine sequence within the MAP kinase binding domain which functions as an NLS (Chen et al., 2001); however, an additional more distal sequence has also been reported (Sloss et al., 2005). MKP-2 is an inducible phosphatase, where activation of ERK is required for MKP-2 expression. Tresini et al., (2007) reported that the knock-down of MKP-2 expression by MKP-2 specific short hairpin RNA or expression of the phosphatase

resistant ERK2 (D319N) mutant, ablates the effect of endogenous MKP-2 levels and subsequently senescence is delayed. The induction of MKP-2 is activated by an array of stimulus, including serum, growth factors, phorbol esters and hormones (Reviewed Lawan et al., 2012). Initial studies regarding activation of MKP-2, describe the dephosphorylation of specific MAP kinase substrates: ERK and JNK *in vitro,* and how interaction of ERK and JNK enhances its catalytic activity (Chen et al., 2001). MKP-2 can also bind strongly to p38 MAP kinase, but does not readily dephosphorylate this substrate *in vitro*, although one study has indicated the potential regulation of p38 in hepatocytes (Berasi et al., 2006).

An accumulating body of evidence is emerging regarding the presence of splice variants among some members of the dual-specific phosphatase family. MKP-2 was reported to possess a novel splice variant which does not possess the ability to bind to ERK and therefore may be important in the dysfunction of MAP kinase signalling in disease states, with particular note to cancers (Cadalbert et al., 2010). Overall, cellular signalling regulated by MKP-2 may be crucial in an array of pathologies.

1.6.3.2.1 MKP-2 in disease

Since the discovery of the DUSPs, little exploration into MKP-2 and its physiological function has been conducted with most research favouring the prototypic DUSP, MKP-1. Emerging studies have implicated MKP-2 in numerous cellular functions and diseases, where examples include apoptosis, proliferation and consequentially cancer (Sieben et al., 2005; Barry et al., 2001).

1.6.3.2.2 MKP-2 in Cancer

MKP-2 has proved to play an interesting role in cancer, acting as both an onco-protein and a tumour suppressor. Indirect evidence links MKP-2 as a tumour promoter in the development of ovarian cancers (Sieben et al., 2005), oesophagogastric rib metastasis (Barry et al., 2001) and pancreatic tumours. Indeed, MKP-2 expression is also dramatically increased in liver carcinoma (Hasegawa et al., 2008) and by the homeobox

gene of the HoxA10 family, which is linked to acute myeloid leukaemia (Wang et al., 2007). Contrastingly, the *DUSP4* gene is also considered to be a candidate tumour-suppressor gene, with its deletion implicated in breast cancer (Venter, 2005). MKP-2 has been mapped to the 8p11-p12 gene locus (Smith et al., 2007); significantly, this locus is lost in several prostatic neoplasms (Emmet-Buck et al., 1995), and allelic loss within the short arm of chromosome 8 is a frequent event in prostate cancer (Issacs, 1995). Consistent with these data is a recent genomic screen which correlates *DUSP4* deletion with EGFR-mutant tumours in lung cancer within the 8p locus (Chitale et al., 2009), and a study showing hypermethylation of the *DUSP4* promoter in gliomas (Waha et al., 2010).

1.6.3.2.3 MKP-2 in Cellular Studies

The physiological understanding of MKP-2 has been greatly advanced with the development of Dusp4 knockout mice models. Al Mutairi et al., (2010) utilised one such model, showing systemic infection of the pathogen *Leishmania Mexicana* is enhanced due to enhanced uptake of the parasite and reduced Th1 responses, facilitated by high levels of macrophage arginase-1 and low levels of NO production. Further immunological studies have shown MKP-2 to have a positive role in sepsis (Cornell et al., 2010), contrary to the effect shown in MKP-1 (Salojin et al., 2006).

Furthermore, a novel effect of MKP-2 on the cell cycle was elucidated by Lawan et al., (2011). Mouse embryonic fibroblasts cultured from Dusp4 deficient mice show decreased proliferation rates and enhanced apoptosis associated with a minor up-regulation of ERK activation (Lawan et al., 2011). In addition, a G2/M-phase arrest in cell cycle was evident with a proportion of cells with enhanced cyclin B1 expression. This finding is consistent with a recent study in mice mammary tumour cells *in vitro* using Dusp4 siRNA (Hasegawa et al., 2007); however, in these cells the G2/M-phase arrest is associated with a loss of cyclin B1. This effect within a late stage of the cycle is a potentially important novel feature of MKP-2 function and again distinct from that observed for MKP-1, which is usually associated with cell-cycle entry. As a result,

MKP-2 dependant alterations in proliferation and cell cycle progression may impact on proliferative pathologic conditions such as cancer and vascular disease.

1.6.3.3 MKP-3

MAP kinase phosphatase-3 was cloned from a superior cervical ganglion cDNA library (Muda et al., 1996). MKP-3 is a type II cytoplasmic phosphatase, due to presence of a leucine-rich nuclear export sequence (NES). The MKP-3 tissue expression remains varied partially overlapping with previously mentioned DUSPs MKP-1 and MKP-2; MKP-3 is present in lungs, heart, brain, spleen and kidney. However, studies by Muda et al., (1996) do not to find expression of MKP-3 in skeletal muscle and testis.

During subsequent characterisation of the cytoplasmic phosphatase MKP-3, it was quickly realised that this enzyme could bind specifically to the classical ERK1/2 MAP kinases *in vitro*, and that this binding defined its ability to specifically dephosphorylate and inactivate these MAP kinases *in vivo* (Keyse et al., 1996; Muda et al., 1996).

Alike to previously mentioned DUSPs, MKP-3 requires ERK to induce the activity of the phosphatase. The binding of MKP-3 to ERK2 is associated with catalytic activation of the bound phosphatase *in vitro* (Stewart et al., 1999). Structural and biochemical studies demonstrated activation of MKP-3 resulted from a conformational change within the catalytic domain of the protein and, primarily, the movement of a loop containing a conserved Asp residue, which acts as a general acid during catalysis such that this residue is positioned optimally to perform its function (Rigas et al., 2001; Zhou et al., 1999). It was quickly realised that binding and catalytic activation were largely predictive of substrate selectivity for a number of MKPs.

Within the current literature, there are implications for MKP-3 in certain conditions such as cancer. Similarly to MKP-2, there are disputed roles for MKP-3 in numerous cancers where it has been shown to enhance 17β-estrodial-induced cell growth in endometrial adenocarcinoma cell (Zhang et al., 2013). This study was controversial as earlier work has labelled MKP-3 as a tumour suppressor as its activation is often linked with pancreatic cancers mediated by promoter hypermethylation or chromosomal loss (Furukawa et al., 2004).

1.6.3.4 MKP-5

MAP kinase phosphatase-5 is a type III family member which was cloned to p38 MAP kinase in a yeast two-hybrid experiment. MKP-5, alike to the other members of the type III family was located in both the nucleus and the cytoplasm. DUSP10, the gene which encodes for MKP-5 is well conserved in mammals and its expression was found in the heart, lung, liver and skeletal muscle (Tanoue et al., 1999). Contrary to previously mentioned MKPs, MKP-5 does not require the binding of a substrate for an active site conformation change, it itself exists in a ready active conformation. MKP-5 possesses an *in vitro* substrate specificity for p38 MAP kinase and JNK, but not ERK (Caunt and Keyse, 2013) and is thereby induced in response to stress activators such as TNF-α, anisomycin and osmotic stress (Jeong et al., 2006; Masuda et al., 2000).

Recent emerging literature is linking MKP-5 to immune function, utilising a DUSP10 knockout mouse models macrophages cultured from such mice generate more pro-inflammatory cytokines when exposed to lipopolysaccharide (LPS). In addition, MKP-5 deficient mice present increased resistance to experimental autoimmune encephalitis but show little difference in the primary response to infection with lymphocytic choriomeningitis virus (LCV) when compared with wild-type animals (Zhang et al., 2004). Further immunological responses were analysed in MKP-$5^{-/-}$ mice which displayed severe lung tissue damage following LPS challenge, characterised by increased neutrophil infiltration and oedema compared with wild-type controls. In response to LPS, MKP-5-deficient macrophages produced significantly more inflammatory factors including inflammatory cytokines, nitric oxide, and superoxide (Qian et al., 2012). Taken together, these results suggest that MKP-5 is vital in the homeostatic regulation of MAP kinase activation in inflammatory responses.

MKP-5 negatively regulates muscle stem cell function in mice. MKP-5 controlled JNK to coordinate muscle stem cell proliferation and p38 MAPK to control differentiation. The authors identify MKP-5 as an essential negative regulator of the promyogenic actions of the MAP kinases and suggest that MKP-5 may serve as a target to promote muscle stem cell function in the treatment of degenerative skeletal muscle diseases (Shi et al., 2013).

1.7 Aims and Objectives

Given the lack of information on MKP-2 in vascular smooth muscle function and disease, this thesis proposes to characterise the cellular functions of MKP-2 and MAP kinase mediated signalling in mouse aortic smooth muscle (MASMCs), isolated from novel Dusp4 deletion mouse.

It also aims to examine whether WT-MKP-2 over-expression using adenoviral vectors can regain wild-type function. Further elucidation of a role for MKP-2 in smooth muscle cell function will utilise a catalytically-inactive MKP-2 over-expression system using adenoviral vectors to assess the potential gain of wild-type function independent of phosphatase activity.
From the results obtained in the mouse model, this thesis aims to provide an insight into a proliferative role for MKP-2 in human aortic smooth muscle cells by the use of adenoviral over-expression.

It is hypothesised that cells derived from the Dusp4 knockout mouse will display both an increased expression in MAP kinase phosphorylation and a reduction in cellular proliferation. From previous work within the literature, it could be proposed that Dusp4 deficient MASMCs will exhibit an accumulation in G2/M phase of the cell cycle.

Utilising the MKP-2 adenoviral over-expression system in human aortic smooth muscle cells, it is hypothesised that a reduction in MAP kinase signalling will be observed with a subsequent reduction in proliferation.

2.0 Materials and Methods

2.1 General reagents

All materials used were of highest grade available and were purchased from Sigma-Aldrich Co Ltd. (Poole, Dorset, U.K.) unless otherwise stated.

2.1.1 General Reagents

Pre-stained SDS-PAGE molecular weight markers: Biorad Laboratories (Hertfordshire, U.K.)

Bovine serum albumin: Gibco BRL (Paisley, UK)

DTT: Boehringer Mannheim Ltd (East Sussex, UK)

Ethanol: VWR (Leicestershire, UK)

Hydrochloric acid: Fisher Scientific (Leicestershire, UK)

Methanol: VWR (Leicestershire, UK)

Nitrocellulose membrane (Protran): Schleicher & Schuell (Surrey, UK)

ECL Detection Reagents: Amersham International PLC (Aylesbury Buckinghamshire, U.K)

3MM paper: Whatman (Kent, U.K.)

Acrylamide: Carl Roth (Karlsruhe, Germany)

2.1.2 Reagents for cell culture and transfection

Corning B.V. (Netherlands)

Cell Culture plasticware

GIBCO BRL. (Paisley, U.K.)

Antibiotics (Penicillin streptomycin), Foetal calf serum (FCS), L-glutamine, Dulbecco's Modified Eagles Medium (DMEM) HBSS, Fungizone.

2.1.3 Antibodies

Santa Cruz Biotechnology Inc (CA, USA)

Anti-ERK1/2 (Rabbit monoclonal, C-14) (1:15000)

Anti-phospho-ERK (Mouse monoclonal, E-4) (1:10000)

Anti-JNK-1 (Rabbit polyclonal, FL) (1:10000)

Anti-pHistone H3 (Ser10) (1:5000)

Anti-Cyclin B1 (1:5000)

Anti-MKP-2 (1:3000)

Amersham International Plc, (Aylesbury, Buckinghamshire, U.K.)

Horseradish peroxidase (HRP)-conjugated sheep anti-mouse IgG, (1:10000)

HRP-conjugated donkey anti-rabbit IgG (1:10000)

Cell Signalling (Massachusetts, USA)

Anti-p-Aurora A/B/C (1:5000)

Anti-GAPDH (1:30000)

Anti-p-cdc2 (1:5000)

Anti-Histone H3(1:15000)

2.1.4 Plasmids

The following constructs were kindly provided by

J.R Woodgett (Ontario Cancer Institute, Princess Margaret Hospital, Toronto, Canada).

GST tagged truncated N-terminus of c-Jun 5-89

2.1.5 Radiochemicals : PerkinElmer life sciences, Cambridge, UK

γ [^{32}P]-ATP (3000 Ci/mmol^{-1})

2.2 Cell Culture

All cell culture was performed in a class II cell culture fume hood, under sterile conditions.

2.2.1 Mouse aortic smooth muscle cells (MASMCs)

MASMCs were maintained in DMEM media supplemented with 10% FCS, L-glutamine (27µg/ml), penicillin (250 units/ml) and streptomycin (25mg/ml). Cells were incubated at 37^0C in humidified air with 5% carbon dioxide. Once the cells had reached 90-100% confluency the media was removed via aspiration and the cells washed once in 1ml trypsin. The trypsin was aspirated off and replaced and the cells incubated at 37^0C. Once some of the cells had started to lift off the culture flask the trypsin was removed and the cells washed off the culture flask with 10mls DMEM media. The cells were diluted as required in DMEM and seeded into new T75cm^2 cell culture flasks to maintain stock flasks, or into well plates for experiments. Cells were washed and quiesced in serum free media for 24h prior to stimulation.

2.2.1.2 Culturing of mouse aortic smooth muscle cells (MASMCs)

Wild-type and Dusp4 knockout mice were sacrificed between 4 and 8 weeks of age by carbon dioxide asphyxiation. The thorax was rinsed in 70% ethanol and skin removed from thorax and abdomen. The aorta was removed from left subclavian origin to diaphragmatic insertion. The aorta was transferred to sterile HBSS (1xHBSS, 1% Penicillin/Streptomycin, 0.1% Fungizone) in a sterile dish. Under dissection microscope, all fat and connective was gently removed using Dumont #5 forceps. Collagenase Type II (175U/ml) was added to 1ml HBSS, aorta was added to this volume and placed in 37ºC incubator for 3-5 min at which point the adventitia was removed. The aorta was cut longitudinally exposing the endothelium which was gently brushed off and dissected further in pieces approximately 1-2 mm in size. The dissected fragments were placed into 6-well plates incubated overnight in MASMC media.

The following morning, dissected aorta was placed in an enzyme solution (100µl of 7.5µg Collagenase II in 5.5ml HBSS) wrapped in Nescofilm for 4 to 6h at 37 ºC. Media was added to the tube and centrifuged for 5 min at 300g and supernatant aspirated. The pellet was resuspended in 2ml media, placed into a 6-well plate and incubated at 37 ºC and 5% CO_2 until confluent.

2.2.2 Human Embryonic Kidney (HEK) 293

HEK293 cells were maintained in modified eagle's medium (MEM) supplemented with penicillin (250units/ml), streptomycin (100ug/ml), L-glutamine (27mg/ml) and 10% (v/v) foetal calf serum. Medium was changed every 2 days thereafter. Cells were passaged using 1 x SSC solution (150mM of NaCl and 4.41g of sodium acetate dissolved in 1 litre of water then pH adjusted to 7.0 with a few drops of sterile NaOH).

2.2.3 Human aortic smooth muscle cells (HASMCs)

Cryopreserved Primary HASMCs (approx. 500,000 cells/vial) were purchased from Cascade Biologics. HASMCs were maintained in10% FCS, L-glutamine (27µg/ml), penicillin (250 units/ml), streptomycin (25mg/ml). Cells were incubated at 37^0C in humidified air with 5% carbon dioxide. Once the cells had reached 90-100% confluency the media was removed via aspiration and the cells washed once in 1ml trypsin. The trypsin was aspirated off and replaced and the cells incubated at 37^0C. Once some of the cells had started to lift off the culture flask the trypsin was removed and the cells washed off the culture flask with 10mls DMEM media. The cells were diluted as required in DMEM and seeded into new T75cm^2 cell culture flasks to maintain stock flasks, or into well plates for experiments. Cells were washed and quiesced in serum free media for 24h prior to stimulation. Medium was changed every 2 days thereafter until the cell were utilised.

2.3 Generation of MKP-2 deficient mice

The deletion of the MKP-2 (Dusp4) gene was performed by Genoway, Lyon, France using standard procedures (as outlined in Al-Mutairi et al., 2010). Briefly, the short

arm and the long arm flanking both side of the cluster of exon 204 of the mouse MKP-2 gene was obtained by PCR using the following primers for the small homology arm:

5'-GTGCCTGGTTCTGTGTGTGTCTGTTCTCC-3' forward primer

5'-TCTTACAGCCCTCTTTCCTCACGGTCG-3' for the reverse primer.

For the long homology arm:

5'-CTTTAGGAGCGACGGCCAGGAACACAGG-3' forward primer

5'-ACCCTGCCACACAGGTTGGAGCAAGG-3' for the reverse primer.

Selected clones obtained from these PCR amplifications were sequenced to minimise the number of point mutations carried through. Both arms were introduced into a pBS vector in either side of the neomycin cassette. The final vector was transfected into 129Sv mouse embryonic stem cells (ES). Only the clones that had homologous recombination events were selected for first by PCR then using Southern Blotting for the short and long arm on the construct. The screening for the short arm was further used to screen the animal carrying the construct. Four different ES clones were injected into C56Bl/6 blastocytes and re-introduced into OF1 pseudo-pregnant females. Fourteen different male chimeras were obtained and crossed with C57Bl/6 females to obtain an F1 generation. The F1 generation was screened for germ line transmission of the mutation. Three males and two females from the F1 generation were heterozygotes for the mutation and were subsequently used for breeding purposes.

2.3.1 Ethical approval

Ethical approval for the use of human tissues was obtained from the West of Scotland Ethics Committee and Strathclyde University Ethics Committee. Written informed consent was obtained from each subject to utilise excess tissue for research. Ethical approval for the use of animals in this study was obtained from the Home Office, as well as Strathclyde University Ethics Committee. All *in vivo* work was carried out according to the Animals (Scientific Procedures) act 1986.

2.4 DNA Preparation for Mouse Genotyping

2.4.1 DNA extraction

A section of mouse tail (~4mm) was removed using sterile scissors and placed in Eppendorf tubes containing 0.5ml of lysis buffer. The samples were incubated at 65ºC overnight on a shaker. Samples were spun at 11000rpm for 20 min to remove insoluble material. The supernatant were transferred into new Eppendorf tubes. NaAc pH5.5 3M, isopropanol was added and tubes were inverted several times. Samples were centrifuged for 2 min at 13000rpm, the supernatant was discarded before the addition of 0.5ml of ice cold 70% ethanol. Samples were centrifuged once more before supernatant was discarded, the pellets were then air dried at room temperature for 30 min. The addition of 100ul of sterile water to the samples was followed by heating for 30 min at 65ºC. Samples were there forward stored at -20ºC until required for PCR.

2.4.2 Polymerase chain reaction (PCR) amplification

The extracted DNA was used directly for PCR using MKP-2 primers P7-P8 (WT) and PE1-PF2 (KO). The PCR amplifications were in a volume of 50µl containing 49µl of PCR master mix performed with Taq DNA polymerase (Promega USA). MKP-2 primers: WT forward primer; 5-CTTCAGACTGTCCCAATCAC-3' and WT reverse primer 5'-GACTCTGGATTTGGGGTCC-3 KO forward primer; 5-TGACTAGGGGAGGAGTAGAAGGTGGC- 3 and KO reverse primer 5-ATAGTGACGCAATGGCATCTCCAGG- 3. PCR conditions for MKP-2: denaturation 95ºC 2 min; 35 cycles and each cycle have denaturation 95ºC 30 s, annealing 58ºC 30 s, extension 2ºC 5 min and final extension 72ºC 5 min. The PCR products were separated by agarose gel electrophoresis.

2.4.3 DNA detection

The amplified PCR products were separated and detected by using agarose gel (1%) electrophoresis. One gram of agarose and the electrophoresis buffer 1X TAE (consisting of Tris 40 mM, EDTA 1 mM and acetic acid 1.1%) were mixed and heated for 3-4 min in a standard microwave until the agarose was dissolved. The resulting

solution was transferred into the gel cast to allow for solidification, this was then transferred to the electrophoresis chamber containing 1X TAE buffer. Gels were run at 90-120 volts for 45-90 min. Ethidium bromide was directly added to the agarose gel solution. For sample loading 10 µl was used. Bands were detected under UV-light (nm) on an image station (Genesnap from Syngene).

2.4.4 Dusp4 knockout mouse characterisation

2.4.41 MKP-2 knockout generation

The deletion of the Dusp4 gene was performed by Genoway, Lyon, France under instruction by Dr. Laurence Cadalbert (The Beatson Institute for Cancer Research, Switchback Road, Bearsden Glasgow G61 1BD) who devised the deletion strategy. Such strategy involved the deletion of exon 2-4 and thus replacing the selected region with a Neomycin resistant cassette from the mouse MKP-2 gene (gene sequence available from Ensemble database: ENSMUSG000000120875). Therefore most of the reading frame (starting in exon-1) and also the 3'UTR region of the MKP-2 mRNA (present in exon-4) was deleted (see Figure 3.1). Details of the construct can be found in Materials and Methods section. Dusp4 mice were routinely genotyped by PCR of tail tip DNA to confirm the genotype of each mouse subset (see Figure 3.2).

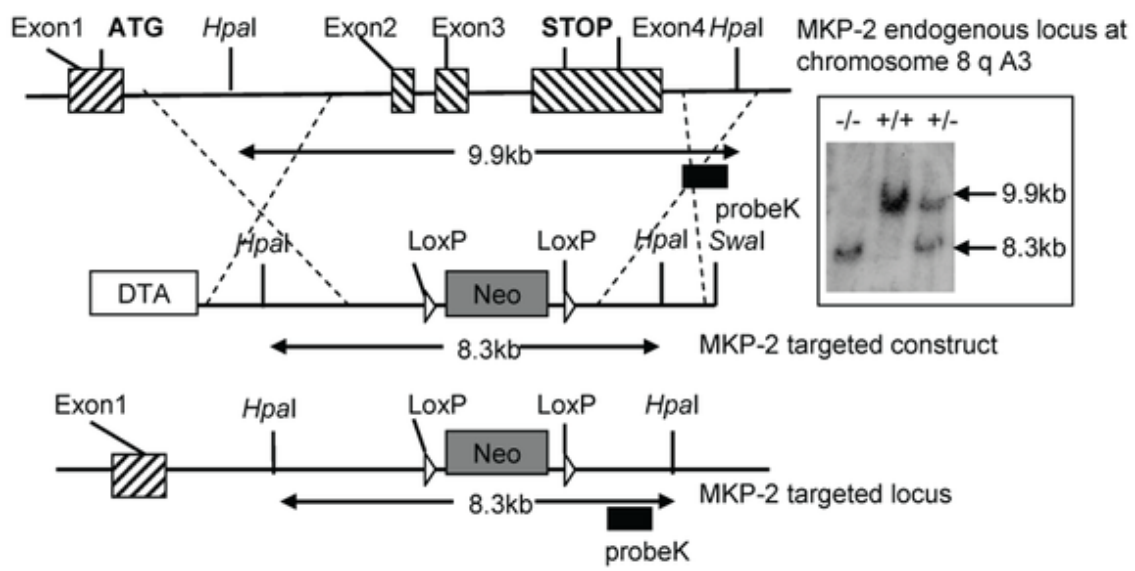

Figure 2.1: Generation of mice lacking Dusp4/MKP-2 by targeted homologous recombination.

Schematic showing the Dusp4/MKP-2 gene locus, the targeted construct and the resulting targeted allele. Recombination events are indicated by dashed lines and show the replacement of a 8.3kb SwaI Dusp4/MKP-2 genomic fragment containing exon 2-4 by the PGK-Neo cassette. SwaI and HpaI described the restriction sites for the respective enzymes. The Pgk Neo cassette is flanked by LoxP sites. DTA represents the negative selection cassette. Derived from Al-Mutairi et al., 2010.

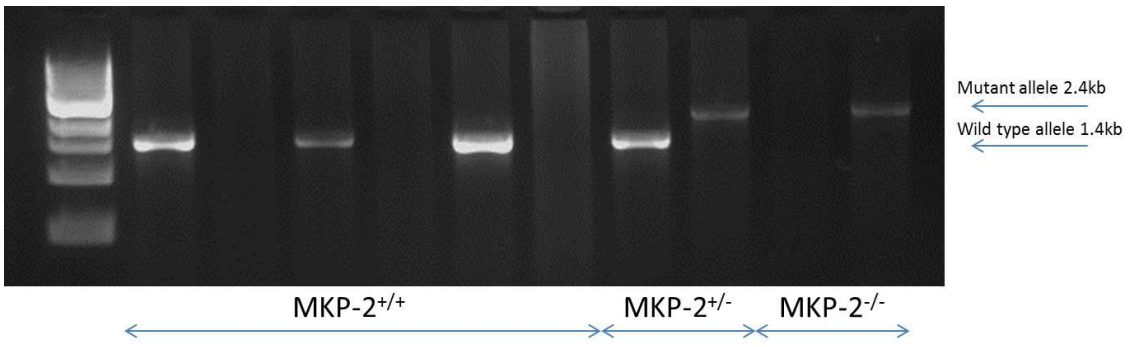

Figure 2.2: MKP-2 tail tip DNA genotyping

The PCR screening for MKP-2 mice genotype. The arrows illustrate the mutated allele 2.4 kb and wild type allele 1.4 kb localization. Digestion products were analysed on 1% agarose gel.

2.5 Preparation of recombinant adenoviruses

2.5.1 Adenoviral crude lysates

Crude lysates of wild-type mitogen-activated protein kinase phosphatase-2 (WT-MKP-2) adenovirus were generated in HEK293 cells by infecting a 75cm^2 flask with 0.75µl of original stock virus. Flasks were incubated at 37ºC, 5% CO_2, 95% air for 4-7 days until a cytopathic effect is evident and cells begin to lose adherence and detach from the flask surface. Cells were removed by washing in media, collected and subjected to centrifugation (1500g for 5min). The supernatant was removed and pellet washed twice in PBS and centrifuged further again at 1500g for 5min. The pellet collected was resuspended in 1ml of HE buffer (10mM HEPES pH7.5, 1mM EDTA). The pellet underwent a freeze-thaw process in triplicate using liquid nitrogen to freeze and 37 ºC water bath to thaw. Once the process was completed three times, cells were centrifuged at 1500g for 5 min in order to pellet the debris. The supernatant, which constitutes the crude adenoviral lysate, was collected in a sterile tube and stored at -80 ºC until required.

2.5.2 Generation and purification of high-titre adenoviral stocks

The high-titre stock of adenovirus was generated by large scale amplification of the crude adenoviral lysates as described in section 2.5.1. Twenty-one 150cm^2 flasks of HEK293 cells were grown to approximately 70-80% confluency. While keeping one flask as a negative control, 20 flasks was medium changed to 2% FCS (19ml) while an additional 1ml was added of diluted adenovirus (100µl crude lysate added to 20mls of HEK293 medium). These flasks were incubated at 37 ºC, 5% CO_2 until cytopathic effects were evident and cells began to detach from the flask. The cells were washed with medium and pooled together and transferred to 50ml tubes for centrifugation (1500g for 5min). Majority of supernatant was removed and stored in -80 ºC for up to one week until desired.

Similar to crude lysate, the pellet underwent the freeze-thaw process in triplicate where freezing took place in liquid nitrogen and thawing in 37 ºC water bath. Following the

third cycle, cells were pelleted by centrifugation at 1500g for 5 min and supernatant collected with the pellet discarded. Using a BD Adeno-X virus purification kit form Clontech Laboratories was then used for adenoviral purification. The supernatant was subject to filtering and incubation with benzonase (25units/µl) (50mM Tris-HCl pH8.0, 20mM NaCl, 2mM $MgCl_2$, 50% glycerol) at 37 ºC for 30 min. Meanwhile, 1x dilution buffer and 1 x washing buffer were prepared according to manufacturer's instructions. The benzonase treated filtrate was mixed with an equal volume of 1 x dilution buffer and passed through a BD Adeno-X syringe with the filter attached, followed by washing with 1 x washing buffer. Adenovirus was later eluted from the filter using elution buffer and the elutate collected in sterile Eppendorf tubes and aliquots stored at -80 ºC prior to titration.

2.5.3 Adenoviral titration

Titration of the end-point dilution method to quantify virus production was previously described by Nicklin and Baker (1999). Serial dilutions of adenovirus were applied to a 96-well plate of HEK293 cells at around 60% confluency. The plate was incubated at 37ºC, 5% CO_2 for 24h, after which time the media was changed to HEK media containing 2% FCS. After an incubation of around 8-10 days at 37 ºC and 5% CO_2 cytopathic effect would be apparent. Wells which contained plaques were counted numerically and the titre was calculated as shown below.

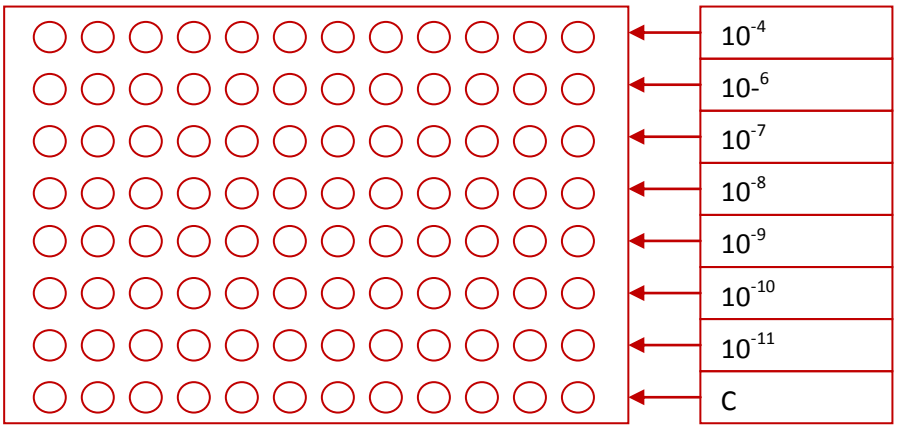

Figure 2.3. Plate layout for adenoviral titration. Serial dilutions of adenovirus were added to each row of HEK293 cells. At a day between 8-10 day incubation, cells displaying cytopathic effect were counted for further calculation.

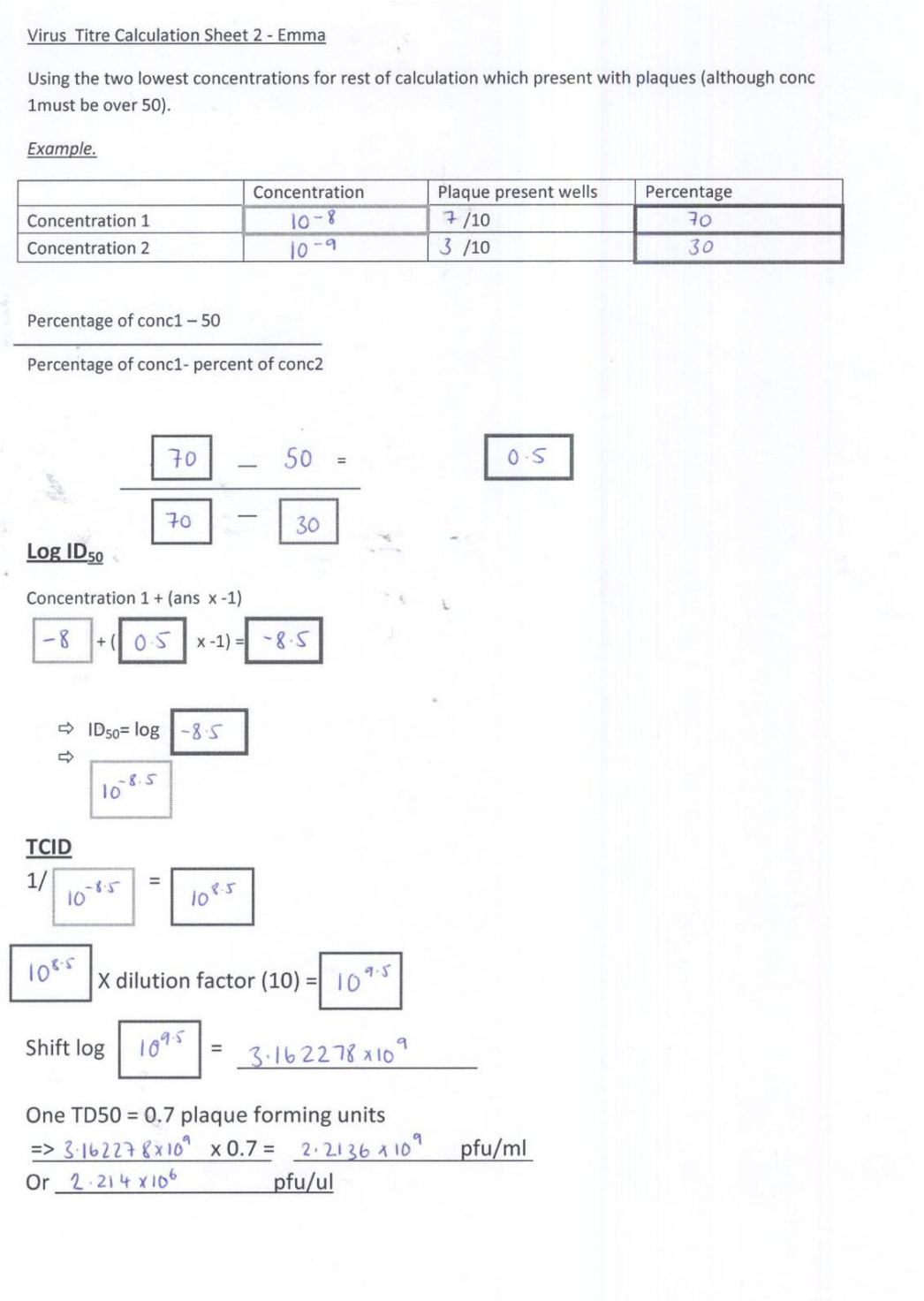

Virus Titre Calculation Sheet 2 - Emma

Using the two lowest concentrations for rest of calculation which present with plaques (although conc 1must be over 50).

Example.

	Concentration	Plaque present wells	Percentage
Concentration 1	10^{-8}	7 /10	70
Concentration 2	10^{-9}	3 /10	30

Percentage of conc1 – 50

Percentage of conc1- percent of conc2

$$\frac{70 - 50}{70 - 30} = 0.5$$

Log ID_{50}

Concentration 1 + (ans x -1)

$-8 + (0.5 \times -1) = -8.5$

⇨ $ID_{50} = \log -8.5$

⇨ $10^{-8.5}$

TCID

$1/10^{-8.5} = 10^{8.5}$

$10^{8.5}$ X dilution factor (10) = $10^{9.5}$

Shift log $10^{9.5}$ = 3.162278×10^{9}

One TD50 = 0.7 plaque forming units

=> 3.162278×10^{9} x 0.7 = 2.2136×10^{9} pfu/ml

Or 2.214×10^{6} pfu/ul

Figure 2.4 Calculation for adenoviral titration. Serial dilutions of adenovirus were added to each row of HEK293 cells. At a day between 8-10 day incubation, cells displaying cytopathic effect were assessed. This was adapted from Nicklin and Baker (1999).

2.5.4 Infecting SMCs with adenovirus

To establish the appropriate volume of adenovirus to add to cells in order to give a sufficient multiplicity of infection (MOI), cells were grown to approx. 50-60% confluency in 12 or 6-well plates. The cell number in 10µl was assessed by using a haemocytometer and the cell number was determined by the formula:

Total amount of cells (10µl) x 10^3 / 4

The amount of adenovirus applied to the cells was determined by another formula:

PFU x total number of cells / titre of the adenovirus

An appropriate MOI of adenovirus (50-500 pfu/cell) was added to the cells and incubated for 24h in quiescent growth medium before stimulation. After this period cells were exposed to selected agonists (FCS, PDGF) for selected timepoints.

2.6 Detection and analysis of proteins (Western Blotting)

2.6.1 Preparation of samples for SDS-PAGE and immunoblotting

Cells were grown to confluency in 12-well plates (unless otherwise stated) then rendered quiescent (24hrs) and stimulated for required time points before being rinsed once in ice cold PBS and lysed by the addition of hot (~85°C) Laemmli sodium dodecyl sulphate (SDS) sample buffer (63mM Tris HCl (pH 6.8), 2mM $Na_4P_2O_7$, 5mM EDTA. 10% Glycerol (v/v), 2% SDS (w/v) and 0.007% (w/v) bromophenol blue to which was added 50 mM dithiothreitol (DTT) immediately before use). Cells were scraped from wells on ice and lysates drawn repeatedly through a 16-gauge needle

attached to a 1ml syringe to shear chromosomal DNA. Samples were transferred to a microfuge tube, the lid pierced and boiled for 5 min at 95^0C to denature proteins and stored at -20°C until required for SDS-polyacrylamide gel electrophoresis.

2.6.2 SDS-polyacrylamide Gel Electrophoresis

Gel kit apparatus was first cleaned in 70% ethanol before assembly, then distilled water added to check the glass plates were flush and not leaking. Resolving was prepared using required amount of acrylamide: [N, N'-methylenebis-acrylamide (37.5:1), 0.375M Tris (pH8.8), 0.1% (w/v) SDS and 0.05% (w/v) ammonium persulphate. Polymerisation of the resolving gel was initiated by the addition of 0.05% (v/v) N, N, N', N'-tetramethylethylenediamine (TEMED). The gel solution was poured into the assembled glass plates (Bio-Rad) until 2-3inches from the top. A thin layer of 0.1% SDS solution was added to the gel, to prevent drying, and to disperse bubbles. Once the gel was set, the 0.1% SDS was discarded and the appropriate teflon welled combs slotted into the glass plates, the stacking gel solution [5% (w/v) acrylamide, 125mM Tris-HCl (pH 6.8), 0.1% (w/v) SDS, 0.05% (w/v) ammonium persulphate, 0.1% (v/v) TEMED] was then made and added directly on top of the resolving gel. The gel was allowed to polymerise for 15 min before the comb was removed, the wells were then washed with sterile distilled water. Gels were placed in the specified western blot tank and this was filled with running buffer [24.8mM Tris, 191.8mM glycine, 0.1% SDS], samples were loaded in the appropriate wells, run concurrently with a pre-stained SDS protein marker of known molecular weights at 125V for approx 105 min.

The resolved proteins on the gel were then transferred to nitrocellulose membranes. The gel was placed on top of the nitrocellulose membrane and sandwiched between two Whatmann 3MM papers and two fibrous blotting pads (Bio-Rad). The cassette(s) were then placed in a Biorad mini trans-blot electrophoresis tank along with an ice pack. The tank was then filled with transfer buffer [25mM Tris, 192mM glycine, 20% (v/v) methanol] and was left to run for 2h at a constant current of 285mA.

After transfer of the proteins from the gel to the nitrocellulose membrane, the membrane was trimmed to the size of the gel. The membrane was then blocked in a 2% BSA/Natt solution [150mM NaCl, 20mM Tris-HCl (pH 7.4), 0.2% Tween 20] for 2h, followed by incubation overnight with a primary antibody of choice at an appropriate concentration in 0.2% BSA/Natt solution. The following morning, the membrane was washed with Natt buffer for 75min, changing the wash every 15min, the membrane was then probed with the appropriate horse-radish peroxidase conjugated secondary antibody in 0.2% BSA/Natt for 90 min. The membrane was then washed again in Natt as previous, before proceeding to chemiluminescence (ECL) detection of proteins. The membrane was incubated in ECL solution for two min, then mounted in an exposure cassette and exposed to X-ray film (Kodak LS X-OMAT) for the required time and developed using the X-OMAT machine (KODAK M35-M X-OMAT processor).

2.7 Cell population synchronisation using nocodazole

Mouse aortic smooth muscle cells were synchronised using nocodazole arresting cells in prometaphase of mitosis. Nocodazole (50ng/ml) was applied for 16h to MASMCs plated in 6-well plates incubated in full media at 37ºC. Once timepoint has been reached, cells were washed in duplicate in PBS and returned to full media for the appropriate timepoint. Cells were placed on ice to terminate the reaction and either harvested for flow cytometry or lysed for western blotting.

2.8 Proliferation rate of smooth muscle cells

Confluent SMCs were detached with trypsin-EDTA, seeded 10,000 cells/well in 10% FCS-DMEM, and allowed to attach for 24 h at 37°C, 5% CO_2. Cells were starved in serum free media for 24 h and then stimulated for either 24 or 48 h. At the noted timepoint, cells were trypsinised and counted using a haemocytomer as described above in section 2.5.4.

2.9 Doubling time of smooth muscle cells

Confluent smooth muscle cells were trypsinised and seeded in 6-well plates at 2 x 10^4 cells per well. Cell doubling time protocol was an adaptation of culture of animal cells technique described previously (Freshney, 1994). Cells were incubated for 24 h at 37°C, 5% CO_2. After 24 h cells in 2 wells were trypsinised and counted with haemocytometer as previously described in section 2.5.4. The procedure was repeated after 48 h.

2.10 Cell Cycle Analysis

Intracellular DNA was stained with propidium iodide and analysed for cell cycle profiles. HASMCs were grown to 70% confluency in a 6-well plate and quiesced in 1% FCS and released in growth media for a further 24h. Cells were harvested with TrypLE Xpress or trypsin and washed with PBS in Eppendorf tubes. Cell fixation was conducted by drop wise addition of ice-cold 70% ethanol and incubated at 4^{o}C overnight. HASMCs were washed in PBS and centrifuged for 10 min at 2000rpm followed by the addition of RNase A (50ug/ml) and incubation for 1 h at 37^{o}C in order to ensure only DNA staining. Samples were then stained with propidium iodide (PI) at 50µg/ml. Using the FACScan flow cytometer, the FACScan Diva software (Becton Dickinson, Oxford, UK) was used to analyse cell cycle parameters gated to 10,000 events

2.11 Histological sectioning and staining of vascular tissues

2.11.1 Fixation, wax embedding and cutting of tissues

Vessel segments were fixed in 10% paraformaldehyde for a minimum of 24h prior to processing. Tissues were then processed in a Citadel 1000 (Thermo Shandon, UK) processor overnight in the following conditions: 70% Ethanol: 3h, 90% Ethanol: 3.5h, 100% Ethanol: 2h, 100% Ethanol: 1h, 1:1 (v/v) of Ethanol: Histo-clear: 1h, 100% Histoclear: 1h, 100% Histoclear: 1h, Paraffin Wax: 2h, Paraffin Wax: 2h.

Thereafter tissues were embedded in paraffin wax using a Leica EG1140H (Leica Microsystems, UK) embedder and 5μm sections cut using a Leica RM2125RTF (Leica Microsystems, UK) microtome. Tissue sections were floated onto silanised slides using a water bath at 60°C. Slides were silanated by: acetone wash: 10 min, submersed in 3-aminopropyltriethoxysilane (APES) solution (0.1% APES in acetone): 10 min, running tap water: 10 min, covered and air dried for 48h.

Once wax embedded sections were mounted on the silinated slides they were placed in an oven set between 60-65°C for 30 min. On their day of use, the slides were placed again in an oven at 60-65°C for 15 min.

2.11.2 Rehydration and dehydration of tissue slides

Prior to histological staining or immunohistochemistry, tissue sections were rehydrated using a Varistain 24-4 auto strainer (Thermo Shanodon, UK) in the following solutions: Histoclear: 10 min, Histoclear: 10 min, Histoclear: 10 min, 100% Ethanol: 5 min, 100% Ethanol: 5 min, 100% dH_2O: 5 min.

At the end of staining, the slides were dehydrated using the following protocol: 100% Ethanol: 10 min, 100% Ethanol: 10 min, 100% Ethanol: 10 min, Histoclear: 5 min, Histoclear: 5 min, Histoclear: 5 min.

2.11.3 Haematoxylin and eosin

The tissue slides were rehydrated as stated in section 2.2.4.2, and placed into metal racks for staining using the following procedure: Haematoxylin: 6 min, dH_2O: 1 min, Acid alcohol (1%): 3 sec, dH2O: 1 min, Scots tap water substitute: 2 min, dH2O: 1 min, Eosin: 1 min, dH2O: 1 min. Thereafter slides were dehydrated and mounted using histomount and 24x50mm coverslips. Slides were left to dry overnight before analysis.

2.12 Immunofluorescence Microscopy

Smooth muscle cells were grown on plain cover slips and fixed by aspirating the culture medium and applying 4% paraformaldehyde for 10 min. This was followed by a 10 min exposure to cold methanol. The slides were then washed with PBS (x3 washes) and exposed to 0.01% triton-x for 10min. Non-specific binding was blocked using 1% BSA in PBS for 1 h at room temperature and then primary antibody α-smooth muscle actin was added without washing at concentrations of 1:100, 1:250, 1:500 & 1: 1000 made in PBS containing 1% BSA and the cells were incubated overnight at 4°C. The α-smooth muscle actin primary antibody was raised in rabbit. The secondary antibody was mouse and was applied at a dilution of 1:200 in sterile PBS and followed by incubation at room temperature for 1h. After washing, cover slips were mounted using Vectashield® mounting medium containing DAPI (Vecta laboratory) and stored in the dark at 4°C until they were viewed and photographed. The DAPI in the mounting medium stained the cells' nucleus blue. Pictures were taken using Nikon Eclipes™ E600 Oil Immersion 67 microscope connected to a photometrics (CoolSnap™ Fx) digital camera managed by MetaMorph™ software (Universal Imaging Corporation, West Chester, PA).

2.13 Time Lapse Microscopy

For time-lapse microscopy, cells were grown to 60% confluency in 60mm dishes and 24 h later viewed using a 20× lens in a PH2-heated platform fitted with a TC-344B dual automatic temperature controller (Warner Instruments). Cells were imaged at 37°C on an inverted microscope (Zeiss Axiovert 200M). Time-lapse images (exposure 500 ms) were taken every 500 ms.

2.14 Determination of protein concentration using Bradford's reaction

Quantification of protein concentration was determined using the Bio-Rad protein assay kit based on the Bradford method. For each assay performed a standard curve was prepared using dilutions of BSA (5-20µg/ml) as a protein standard prepared in the appropriated buffer. 1µl of protein sample of unknown concentration was mixed with 199µl Bradford solution diluted 5 times in distilled water and incubated at room temperature for 15 min. The protein concentration of each sample was calculated from the standard curve.

2.15 Expression and purification of GST-c-jun construct

2.15.1 Growth of GST-c-jun

Recombinant GST-tagged constructs were grown at 37^{o}C in a 5ml culture of XYT broth (16g/L tryptone, 10g/L yeast extract, 5g/L NaCl), containing 100µg/ml ampicillin, and orbital shaken overnight. This was then transferred to a 500ml 2XYT broth, containing 100µg/ml ampicillin and incubated at 37^{o}C with orbital shaking until an A_{600} of 0.6-0.8 was obtained. Cultures were cooled to 30^{o}C and expression was induced by addition of 100µM isopropyl thio-β-D-galactopyranoside (IPTG) with incubation at 30^{o}C for 4h. Cells were harvested by centrifugation at 4^{o}C at 10,000 x g (400rpm x 15 min) in 250ml autoclaved centrifuge tubes and pellets placed in the -20^{o}C freezer overnight. All subsequent steps were carried out at 4^{o}C.

2.15.2 Purification of GST-Fusion proteins

Recovered pellets of bacterial cells were resuspended in 12.5ml of lysis buffer [30ml stock contains; 50mM Tris-HCl (pH8.0), 100mM NaCl, 1mM EDTA, on the day of the experiment the following were added; 1mM benzamidine, 1mM of β-mercaptoethanol, 2µg/ml leupeptin, 2µg/ml aprotonin, 2µg/ml pepstatin A, 200µM PMSF]. The resulting suspension was then frozen in a dry ice-methanol bath and left to thaw at room temperature. The bacterial suspension was further disrupted using a probe sonicator (3 x 15 seconds at 50% intensity followed by 3 x 10 seconds at 80% intensity). 1.25ml of triton X-100 detergent buffer (20% w/v) was then added to 25ml of bacterial

suspension (to a final concentration of 1% (w/v) Triton X-100) and the preparation placed on a rotary wheel for 60 min at 40C. The solubilised extract was centrifuged at 10,000 x g for 15 min and the supernatant added to a 1ml matrix of glutathione (GSH)-sepharose beads, which had been equilibrated by washing twice with 10ml of lysis buffer and centrifugation at 300rpm for 2 min in between, and incubated at 4^{o}C for 1h with gentle rotation. Following affinity purification the GSH sepharose matrix was centrifuged at 300 rpm for 2 min and the supernatant was discarded. The beads were then washed twice in 10 ml lysis detergent buffer (1% (w/v) Triton X-100) to remove any unbound protein and centrifuged at 300rpm for 2 min in between and collected beads were stored in lysis detergent buffer at 4^{o}C.

2.15.3 Elution of GST-Fusion proteins

To elute the GST-fusion proteins from the GSH sepharose matrix two approaches were undertaken. For small scale elution of the GST-fusion protein i.e. to estimate protein amounts immobilised on the beads, 20µl of the GSH sepharose matrix was removed and washed twice with 200µl elution buffer [50mM tri-HCl pH 8.0 containing 100mM NaCl, 0.1% Triton X-100, 10mM reduced glutathione, 10µg/ml leupeptin, 10µg/ml aprotonin, 10µg/ml pepstatin A] and incubated with gentle rotation at 4^{o}C for 30 min. Samples were then centrifuged at 13,000 x g for 1 minute and the supernatants obtained for the next step. Protein concentration of the supernatants containing eluted proteins was determined as described in section 2.22, this was used to determine the volume of bead slurry required to provide sufficient substrate per assay.

2.15.4 Electrophoretic analysis of GST-Fusion proteins

Purification of the proteins was confirmed by SDS-PAGE using samples taken at various stages during the purification procedure, followed by staining of the gel with Coomassie blue [80% (w/v) methanol, 20% (w/v) acetic acid, 0.1% (w/v) Coomassie blue], for 1h to allow visualisation of proteins. This was then washed with a destain solution [500ml dH_2O, 400ml methanol, 100ml glacial acetic acid] for approximately 4h, to remove non-specific background staining. The resultant gel was then sandwiched

between two cellophane sheets and dried **(Figure 2.3)** in the gel dryer (Hoefer Scientific Instruments, U.S.A).

2.15.5 JNK Solid Phase phosphorylation of Truncated GST-c-jun

JNK activity in solubilised extracts was assessed via measurement of incorporation of radiolabelled phosphate into recombinant GST-c-jun $_{(5\text{-}89)}$ bound to glutathione sepharose beads. Therefore increased phosphorylation is a measurement of increased kinase activity.

Cells were rendered quiescent and stimulated for the required time, the cells were then washed twice in ice cold PBS to terminate the stimulation before being lysed in JNK solubilisation buffer (20mM HEPES-NaOH pH 7.7, 50mM NaCl, 0.1mM EDTA, 1% (w/v) Triton X-100, 0.1mM Na_3VO_4, 0.2mM PMSF, 0.5mg/ml leupeptin, 0.5mg/ml aprotinin). The cells were removed using a cell scraper and placed in Eppendorf tubes, vortexed for 2 seconds and left on ice for 30 min. The samples were centrifuged at 13,000rpm at 4^{o}C to remove cell debris and the lysates mixed with GST-c-jun beads overnight at 4^{o}C.

The beads were then pelleted by centrifugation at 13,000rpm for 1 min and washed once in solubilisation buffer and once in kinase buffer (25mM HEPES –NaOH, 20mM $MgCl_2$, 5mM glycerophosphate, 0.1mM Na_3VO_4, 2mM DTT, pH7.5. The beads were resuspended in 25ul of kinase buffer and the reaction initiated via addition of 5ul of 150µm ATP and 1µCi [γ^{32}P]-ATP to a total volume of 30µl. The samples were agitated at 30^{o}C for 30 min, the reactions were terminated via the addition of 10ul of 4X Laemmli sample buffer. The samples were then boiled for five min and resolved by 11% SDS-PAGE. Gels were fixed for 30 min in a 40% methanol, 10% acetic acid solution, before being sandwiched between two cellophane sheets and dried in the gel dryer (Hoefer Scientific Instruments, U.S.A). The incorporation of [γ^{32}P] into the substrate was detected via autoradiography and quantified through scanning densitometry.

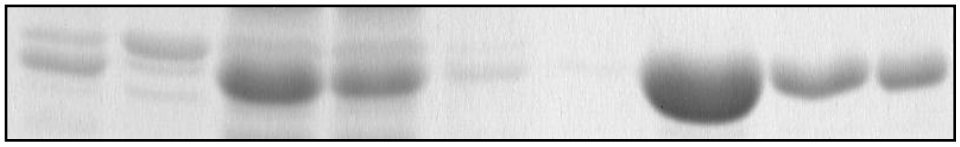

1 2 3 4 5 6 7 8 9

1 – Homogenate

2 - Pellet from post detergent sample

3 – Supernatant from post detergent sample

4 – Post binding supernatant

5 – Wash

6 – Wash 2

7 – Elution 1

8 – Elution 2

9 - Beads

Figure 2.5: Analysis of GST-c-Jun purification and elution.

Samples from each stage the purification process were collected and subjected to SDS-PAGE. Proteins were detected using coomassie blue stain as described previously. GST-c-Jun from elution 1 and 2 can be seen in lanes 7 and 8 respectively at approximately 36Kda. Lane 10 illustrates that GST-c-jun has bound to the sepharose beads. Annotation of each lane on the gel is shown above.

2.16 Scanning and Densitometry

Western blots were scanned on an Epson perfection 1640SU scanner using Adobe Photoshop 5.0.2 software. The scanned images were then normalised to a control and quantified using ImageJ.

2.17 Statistical Analysis

All data shown were expressed as mean ± SEM and were representative of at least three separate experiments. Whenever applicable statistical analysis was performed using one-way ANOVA with Dunnet's post-test or paired Student's t-test with Bonferoni's considerations. Differences were considered significant at $P<0.05$ and represented with *.

Chapter 3: Characterisation of cellular functions of MKP-2 in primary mouse aortic smooth muscle cells (MASMC).

3.1 Introduction

In this chapter, the consequence of MKP-2 deletion on the cellular function of mouse aortic smooth muscle cells was examined. Mitogen activated protein kinases are well recognised as key regulators of many cellular functions, such as proliferation, differentiation and gene expression. The process of activation is initiated by mitogen-receptor binding which subsequently leads to dual phosphorylation in the Thr-X-Tyr motif (Hutter et al., 2001). Vital intrinsic regulation of MAP kinase is mediated by the action of dual specific phosphatases (DUSPs), which possess to ability to dephosphorylate and inactivate MAP kinase. Specifically, the action of Dusp4 (also known as MKP-2) has been shown to dephosphorylate MAP kinases, ERK and JNK *in vitro.* However, much previous work within the literature on MKP-2 has been conducted using protein techniques such as siRNA which can limit interpretation due to rundown efficiency. Progressing from basic expression techniques, a Dusp4 deficient mouse model was developed in order to elucidate the functional properties of MKP-2 in numerous murine cell types. Previous studies utilising this model have focussed largely in an immunological setting, where studies from the laboratory have shown macrophages to exhibit changes in MAP kinase phosphorylation, as well as alteration in cytokine release (Al-Mutairi et al., 2010). Furthermore recently published work has shown MKP-2 to play a key role in the control of infection with *Toxoplasma gondii* by modulating iNOS and arginase-1 activities (Woods et al., 2013). One study has detailed how MKP-2 deletion in fibroblasts results in a reduction in proliferative capacity (Lawan et al., 2011). Despite this, there has been little investigation regarding the consequence of MKP-2 deletion on cell growth and proliferation.

Therefore within this chapter, the cellular characterisation of MKP-2 deletion in vascular smooth muscle cells has been examined. Firstly, the induction of MKP-2 was assessed in MASMCs. Moreover, the consequence of MKP-2 deletion on MAP kinase activation and cellular proliferation was examined. The expression of two adenoviral MKP-2, Adv.WT-MKP-2 and Adv.CI-MKP-2 were utilised to assess the effect and potential gain of function in MKP-$2^{-/-}$ MASMCs.

3.2 Results

3.2.1 Characterisation of MKP-2 knockout

3.2.1.1 Aorta dissected from MKP-$2^{+/+}$ and MKP-$2^{-/-}$ exhibit no significant differences

Previous work described young adult male MKP-$2^{+/+}$ and MKP-$2^{-/-}$mice demonstrated no apparent phenotypic defects, bred normally and had normal body weights similar to wild type littermates (Lawan et al., 2011). Knockout animals are fertile and display no evident behavioural, developmental or growth abnormalities. In order to characterise smooth muscle cells derived from the mouse aorta of the mice, firstly the aorta was assessed. Aortae was dissected from MKP-$2^{+/+}$ and MKP-$2^{-/-}$ mice and fixed in paraformaldehyde. Slices were obtained and stained with haematoxylin and eosin for an overview of any major structural changes between the aortae. However, as show in Figure 3.1 there are no significant structural differences between the aortae of wild-type and knockout mice. Furthermore, aortae exhibit comparable adventitial, medial and intimal layers, however further examination may be required to assess specific cellular composition of these vessel layers.

3.2.1.2 Characterisation of smooth muscle cells derived from mouse aorta

Smooth muscle cells were derived using a collagen digestion method. However, due to the multicellular triple layered structure of the aorta, it is important to qualitatively characterise the cells obtained from the vessel to ensure they are a pure smooth muscle cell population from the medial layer. MKP-$2^{+/+}$ and MKP-$2^{-/-}$ smooth muscle cells were grown on coverslips and fixed, following antibody staining with α- smooth muscle actin (SMA-α) and DAPI for the nucleus. With reference to Figure 3.2, MASMCs derived from both wild-type and knockout mice were positive for SMA-α confirming the purity of the cells cultured.

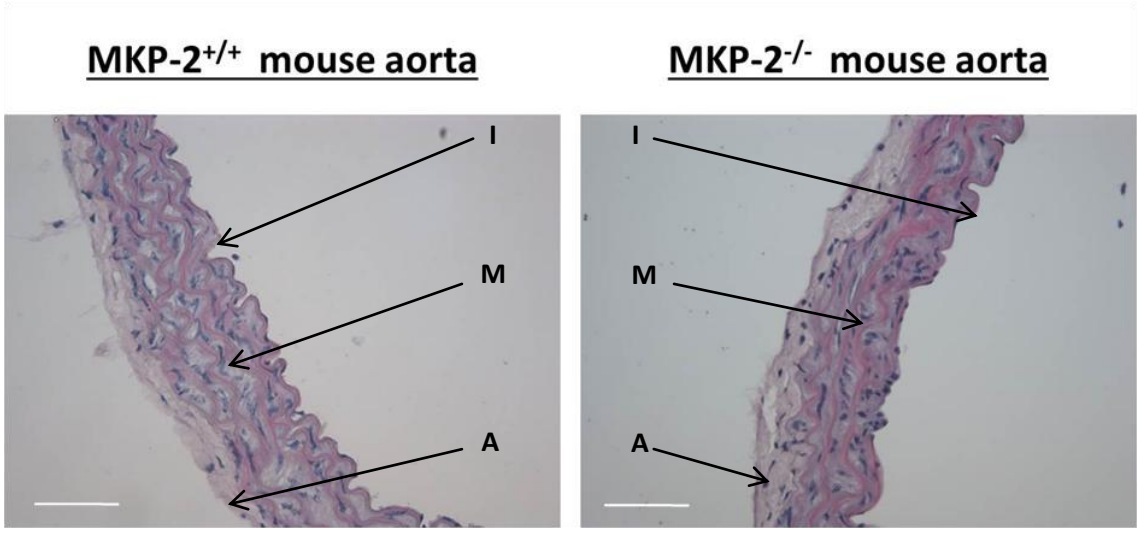

Figure 3.1: Histology of MKP-2 wild-type and knockout aorta

Aortae was dissected from MKP-$2^{+/+}$ and MKP-$2^{-/-}$ mice and fixed in paraformaldehyde as described in the Materials and Methods section. Slices were obtained and stained with haematoxylin and eosin for an overview of any major structural changes between the aortae. These images are representative of two independent experiments. Scale bar 100µm (Key: I, intima; M, media; A, adventitia).

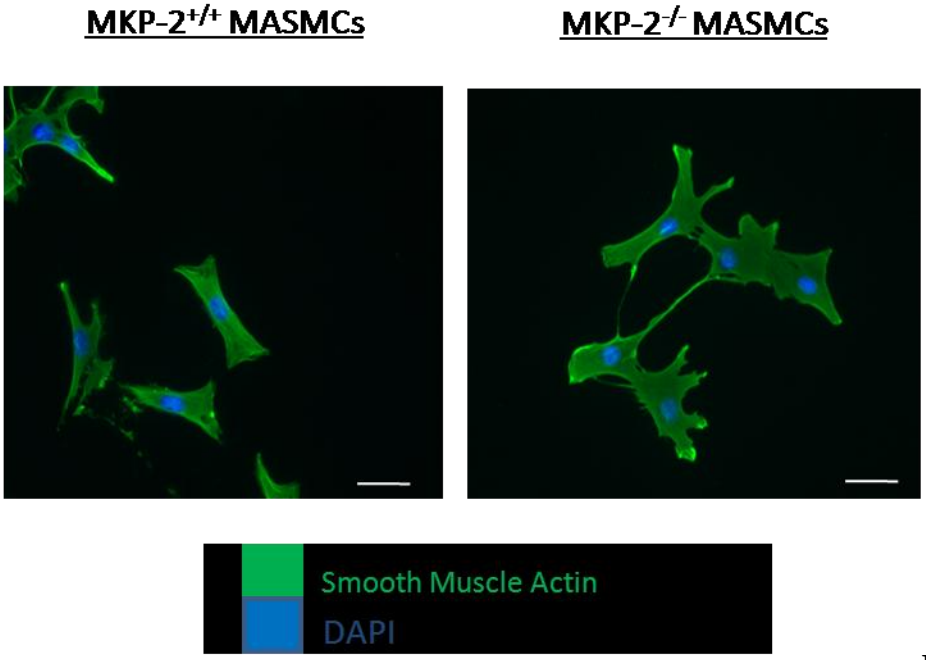

Figure 32Smooth Muscle Actin staining in MASM culture from WT and MKP-2 KO mice

The immunofluorescence image (x20), of smooth muscle cells both stained with α-smooth muscle actin, in panel A the localization of α-smooth muscle actin (green) was shown in cultured smooth muscle cells and nuclei stained with blue Dapi. Scale bar 50µm. The result is representative of two independent experiments.

3.2.1.3 Smooth muscle phenotype is comparable between wild-type and MKP-2 knockout cells

As described previously in the introduction, smooth muscle cells exist in two major phenotypes or as an intermediate between both, therefore it was important to determine whether the deletion of MKP-2 had any effect on the MASMC phenotype. Using SMA-α as a marker of smooth muscle cells in the contractile phenotype, cells were stimulated with PDGF for 48 h to promote cells into the synthetic phenotype, as detailed previously in the literature (Hunter et al., 2011). It can be observed in Figure 3.3 that upon stimulation with PDGF, both wild-type and knockout smooth muscle cells differentiate into the synthetic phenotype marked by a decrease in SMA-α expression; where no difference between wild-type and knockout MKP-2 cells were exhibited. The level of conversion of contractile to synthetic phenotype was comparable between MKP-$2^{+/+}$ and MKP-$2^{-/-}$ cells (WT 0.36±0.053 vs. KO 0.33±0.7; p=0.348; n=3). Furthermore, the baseline levels of SMA-α were non-significant (WT 1±0.067 vs. KO 0.97±0.082; p=0.667; n=3).

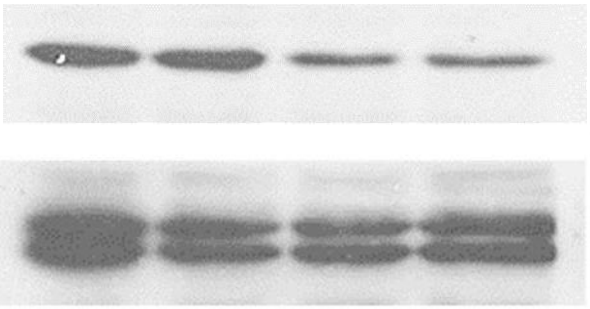

Time (hours)	0		48	
MKP-2	+	-	+	-
PDGF (10ng/ml)	-	-	+	+

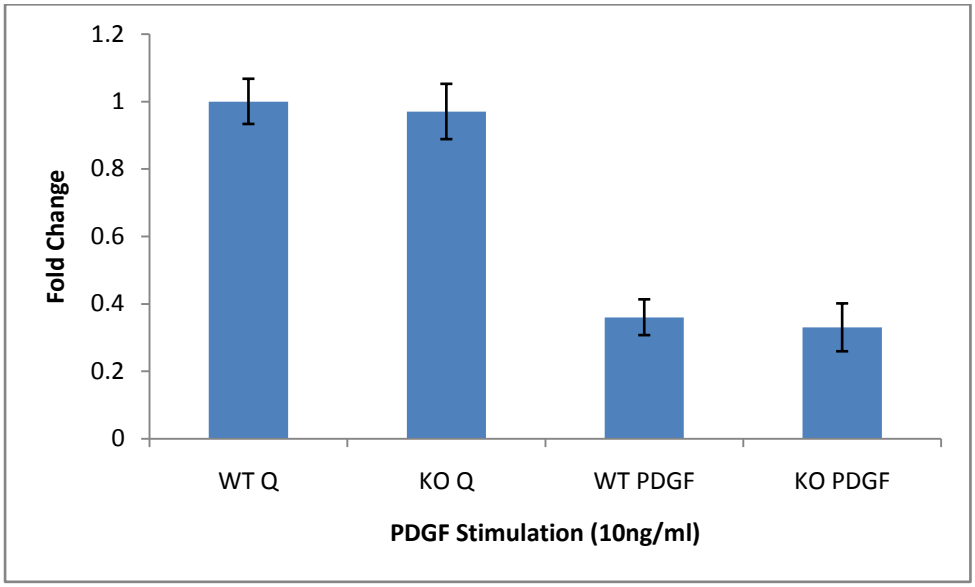

Figure 3.3: Expression of smooth muscle actin in response to PDGF

Subconfluent mouse aortic smooth muscle cells were rendered quiescent in 0.1% FCS for 24h prior to stimulation of PDGF (10ng/ml) for 48h. Whole cell lysates were prepared, separated by SDS PAGE and probed for SMA (42kDa) as described in the Materials and Methods section. Blots were stripped and reprobed for T-ERK which was used a loading control (42/44kDa). These results are representative of 3 independent experiments.

3.2.2 Induction of MKP-2

3.2.2.1 Induction of MKP-2 in response to Serum

Initially the kinetics of MKP-2 induction in response to FCS was examined over shorter (4-8h) and longer time courses (0-48 h). MASMCs were grown to confluency in 6-well plates and serum starved for 24h before incubation with 10% FCS. Whole cell lysates were analysed by Western blotting for MKP- 2 expression. The data presented in figure 3.6 shows that MKP-2 protein was induced after 4h in MKP-$2^{+/+}$ MASMCs and was sustained until 8h. However, no induction was observed in MKP-$2^{-/-}$ MASMCs. In MKP-$2^{+/+}$ MASMCs, (Figure 3.4) MKP-2 protein expression was induced after 24 h, and was sustained for up to 48 h. However, no induction was observed in MASMCs derived from MKP-$2^{-/-}$ mice ($p<0.01$). Total ERK levels were unchanged, indicating equal protein loading. This confirmed the complete absence of MKP-2 protein in MKP-2 $^{-/-}$ MASMCs and also established that serum is capable of activating endogenous MKP-2 expression in MKP-2 $^{+/+}$ MASMCs.

Having established the kinetics of MKP-2 induction, a concentration response curve to serum was established. Cells were serum starved for 24 h and incubated with increasing concentration of FCS (0.5, 1, 5 and 10%) for 4h. The results (shown in Figure 3.6) demonstrate that FCS induced a concentration dependent increase in MKP-2 protein expression with the evident induction beginning at 5% FCS (5.19±1.1 fold increase in SMA expression) with maximal induction attained with 10% FCS (36.32±4.2 fold increase in SMA expression). However, no expression was observed in MASMCs derived from MKP-$2^{-/-}$ mice. This again confirmed the absence of MKP-2 protein in MKP-$2^{-/-}$ MASMCs. Furthermore, since FCS exerts its maximal effect at the concentration of 10%, this concentration was used in the remaining experiments.

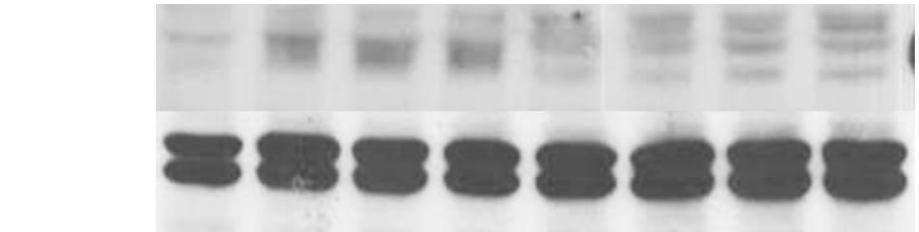

Time	0	4	6	8	0	4	6	8
MKP-2	+	+	+	+	-	-	-	-
FCS (10%)	-	+	+	+	-	+	+	+

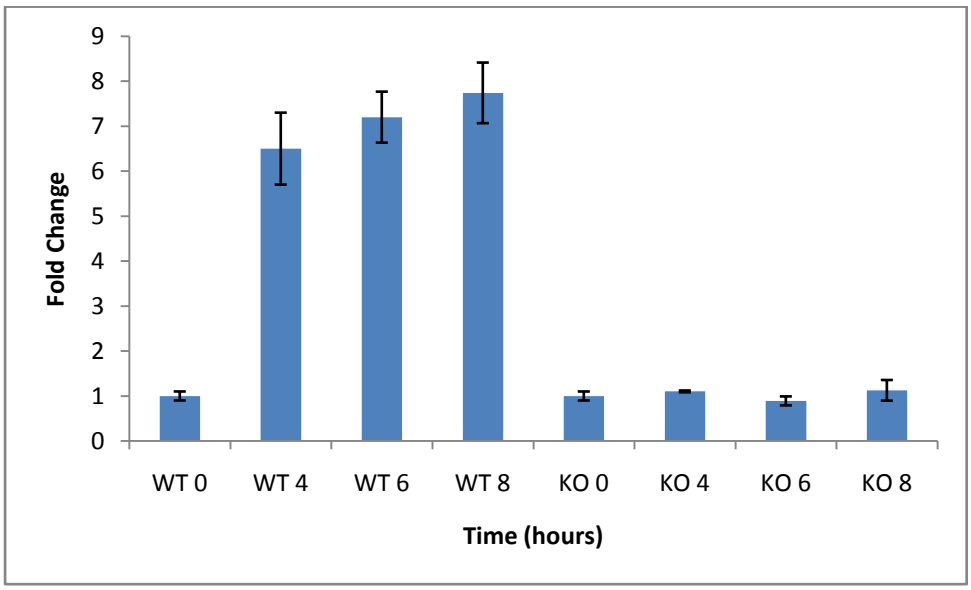

Figure 3.4: MKP-2 expression in response to FCS in MASMC

Confluent mouse aortic smooth muscle cells of both WT and MKP-2 KO were rendered quiescent in 0.1% FCS for 24h prior to stimulation of FCS (10%) for the times indicated. Whole cell lysates were prepared, separated by SDS PAGE and probed for MKP-2 (43kDa) as described in the Materials and Methods section. Blots were stripped and reprobed for T-ERK which was used a loading control These results are representative of 3 independent experiments. Each value represents mean±S.E.M. Gels were quantified by scanning densitometry.

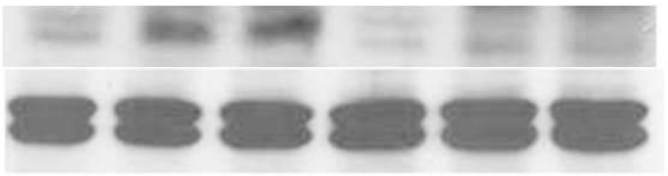

Time	0	24	48	0	24	48
MKP-2	+	+	+	-	-	-
PDGF (10ng/ml)	-	+	+	-	+	+

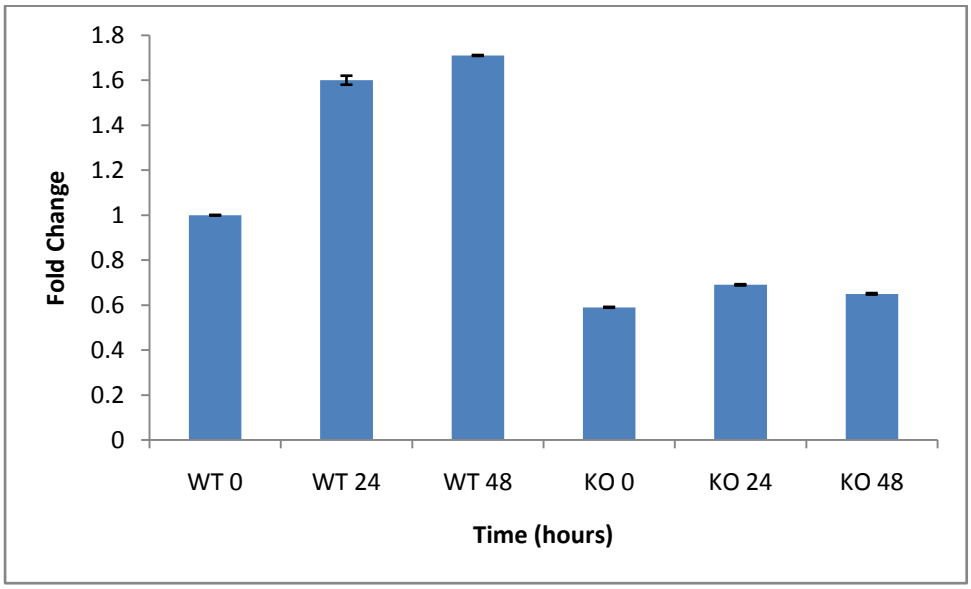

Figure 3.5: MKP-2 expression in response to FCS in MASMC

Confluent mouse aortic smooth muscle cells of both WT and MKP-2 KO were rendered quiescent in 0.1% FCS for 24h prior to stimulation of PDGF (10ng/ml) for the times indicated. Whole cell lysates were prepared, separated by SDS PAGE and probed for MKP-2 (43kDa) as described in the Materials and Methods section. Blots were stripped and reprobed for T-ERK which was used a loading control These results are representative of 3 independent experiments. Each value represents mean±S.E.M. Gels were quantified by scanning densitometry.

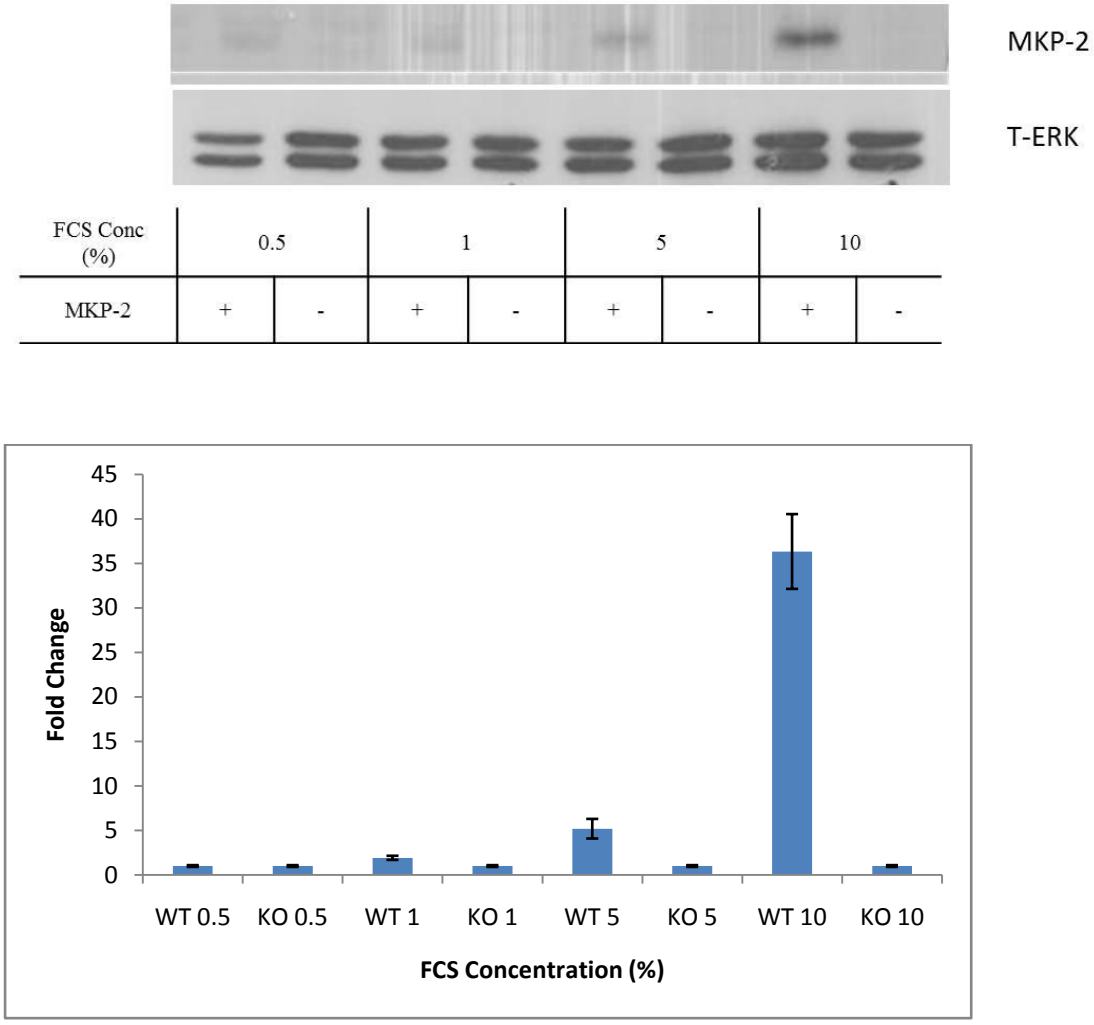

Figure 3.6 MKP-2 expression is dependent upon increasing FCS stimulation

Confluent mouse aortic smooth muscle cells of both WT and MKP-2 KO were rendered quiescent in 0.1% FCS for 24h prior to stimulation of FCS (0.5, 1, 5, and 10%) for the 4h. Whole cell lysates were prepared, separated by SDS PAGE and probed for p-ERK (44/42kDa) and MKP-2 (43kDa) as described in the Materials and Methods section. Blots were stripped and reprobed for T-ERK which was used a loading control These results are representative of 2 independent experiments. Each value represents mean±S.E.M. Gels were quantified by scanning densitometry.

3.2.2.2 MKP-2 induction depends on prior ERK activation

Studies have indicated that MAP kinases, in particular ERK, play a role in the induction of MKPs as part of a negative feedback loop which could potentially affect the dephosphorylation capacity of the phosphatase towards these kinases. Wild type MASMCs were pre-incubated with MEK inhibitor, U0126 (10 µM), JNK inhibitor, SP600125 (10 µM) or p38 MAP kinase inhibitor, SB203580 (10 µM) for 1 h prior to being stimulated with 10% FCS for 4h. Whole cell lysates were analysed by Western blotting for MKP-2 expression in the presence of these inhibitors. Figure 3.7 shows a representative Western blot demonstrating that pre-treatment of wild type MASMCs with the selective ERK inhibitor U0126 caused a significant, 68.3% inhibition of MKP-2 induction (Control 15.3±1.644, U0126 4.17±1.29; p= 0.008). In contrast, inhibition of JNK signalling using SP600125 had no significant inhibitory effect on MKP-2 induction (Control 15.3±1.644, SP600125 14.1±0.8). Interestingly, pre-treatment with the p38 MAP kinase inhibitor SB203580 resulted in a fairly modest but significant inhibition (28%) of MKP-2 expression (Control 15.3±1.644, SB203580 10.7±1.1; p=0.012). This data confirmed that activation of the ERK pathway predominately promotes the induction of MKP-2 in wild type MASMCs. However, it should also be noted that p38 MAP kinase may also possess the ability promote MKP-2 activation with a 28% inhibition upon treatment with SB203580. Nevertheless, this inhibition may be statistically significant but questions could be raised over the physiological significance of this result.

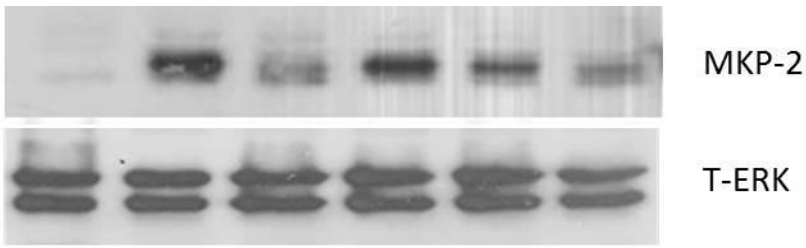

FCS (10%)	-	+	+	+	+	+
U0126 (10uM)	-	-	+	-	-	+
SP600125	-	-	-	+	-	+
SB203580	-	-	-	-	+	+

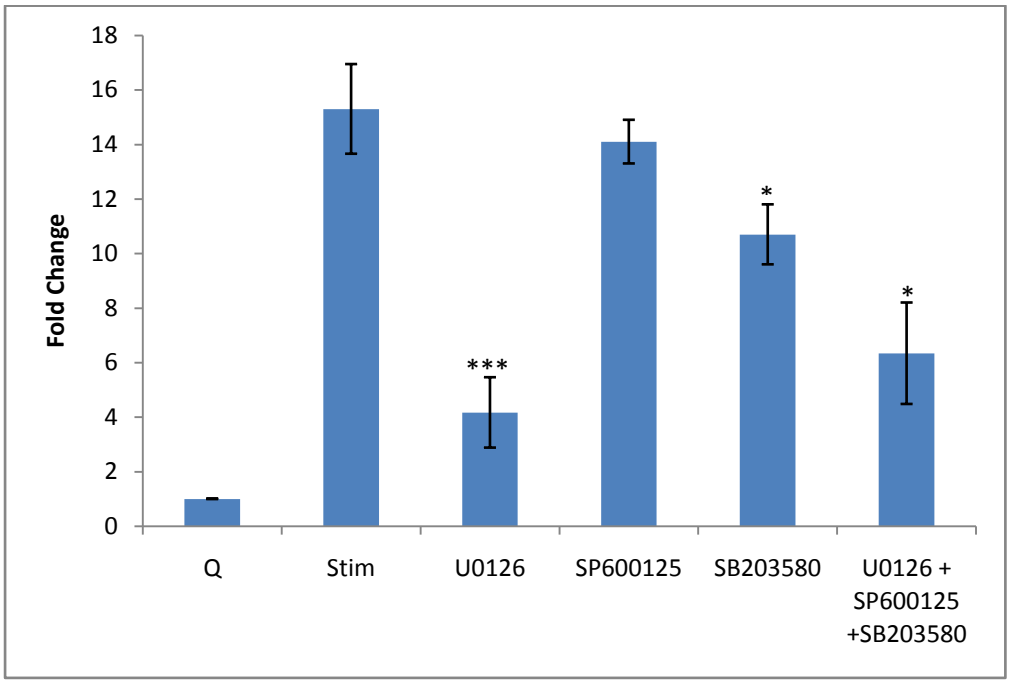

Figure 3.7: Expression of MKP-2 is dependent on prior ERK activation in MASMCs

MASMCs were grown to confluency on a 6-well plate and quiesced for 48 h in serum free media. Cells were pre-incubated with U0126 (10 uM) (p=0.008), SP600125 (10 uM) or SB203580 (10 uM) (p=0.012) for 1h prior to being stimulated with 10% FCS for the times indicated. Whole cell extracts were resolved by SDS-PAGE and examined by Western blotting for induction of MKP 2 (43kDa). Blots were stripped and reprobed

for T-ERK which was used a loading control These results are representative of 3. Gels were quantified by scanning densitometry.

3.2.3 Regulation of MAP kinase signalling by MKP-2

3.2.3.1 Effect of MKP-2 deletion on ERK and JNK phosphorylation

Given that MKP-2 is proposed to be a negative regulator of ERK and JNK signalling, initial experiments were conducted to investigate whether the deletion of this protein had any effect on the phosphorylation levels of ERK and JNK. MASMCs were grown to confluency in 6-well plates and serum starved for 24h. The expression of phosphorylated MAP kinases was measured by Western blotting with antibodies that specifically recognise both phospho-Tyr and phospho-Thr residues that are regarded to be necessary and sufficient for the activation of MAP kinases. Both ERK and JNK phosphorylation was examined over the indicated time course. Initially as depicted as quantified data in Figure 3.10, FCS caused a rapid increase in ERK phosphorylation which peaked at 4h and reduced in expression at 8h. However, there was no significant difference between MKP-$2^{+/+}$ and MKP-$2^{-/-}$ MASMCs in either magnitude or kinetics of phosphorylation (WT 3.21±0.121, KO 3±0.058; p=0.361). FCS also promoted a sustained increase in ERK phosphorylation (Figure 3.8) however, the loss of MKP-2 again did not alter the level of stimulation between the two cell types. This result suggested that serum was capable of inducing similar phosphorylation of ERK in both MKP-$2^{+/+}$ and MKP-$2^{-/-}$ MASMCs however no difference was exhibited in ERK phosphorylation between wild-type and knockout cells.

The effect of MKP-2 deletion on JNK phosphorylation was also examined over the indicated time course. Unfortunately due to difficulties with the specific phospho-JNK antibodies, the downstream transcription factor c-Jun was assessed as an indicator of JNK phosphorylation. As shown in Figure 3.8, FCS caused a minor increase in c-Jun phosphorylation which was nevertheless, significantly different from controls (WT p=0.001; KO p=0.027). Furthermore, there was no significant difference in the level of phosphorylation in MKP-$2^{-/-}$ MASMCs relative to MKP-$2^{+/+}$ MASMCs (WT 4.697±0.113 fold stimulation, KO 5.07±0.419 fold stimulation; p=0.055).

Similar to the experiment with serum, PDGF was used to examine the phosphorylation of ERK and c-Jun in wild type and MKP-$2^{-/-}$ MASMCs. Baseline levels of ERK were slightly elevated in MKP-2 knockout MASMCs (WT 1±0.00, KO 1.28 ±0.214; p=0.744). PDGF caused ERK phosphorylation within 2h and remained high up to 4h and reduced at 8h. (Figure 3.8) Nevertheless, in the absence of MKP- 2, ERK phosphorylation was not significantly altered (At 4h WT 3.19±0.02 fold stimulation, KO 3.39±0.07 fold stimulation; p=0.066). Similar to serum stimulation, PDGF generated a weak but significant increase in p-c-Jun over a time course which was not significantly affected by the loss of MKP-2. c-Jun phosphorylation was significantly upregulated (1±0.00, 1.61±0.236 fold stimulation; p=0.046) from control upon stimulation with PDGF. It should be noted that c-Jun baseline depicted in Figure 3.9 is high, however upon quantification of all experiments, this observation became negligible suggesting this could merely be an artefact. Similar to serum stimulation, there were no significant differences in p-c-Jun phosphorylation in MKP-2 deficient cells when compared with wild-type MASMCs (WT 1.4500±0.0473 fold stimulation, KO 1.3733±0.0581 fold stimulation; p=0.542). Collectively, it can be deduced that there are no significant differences in MAP kinase signalling between wild-type and MKP-2 deficient MASMCs.

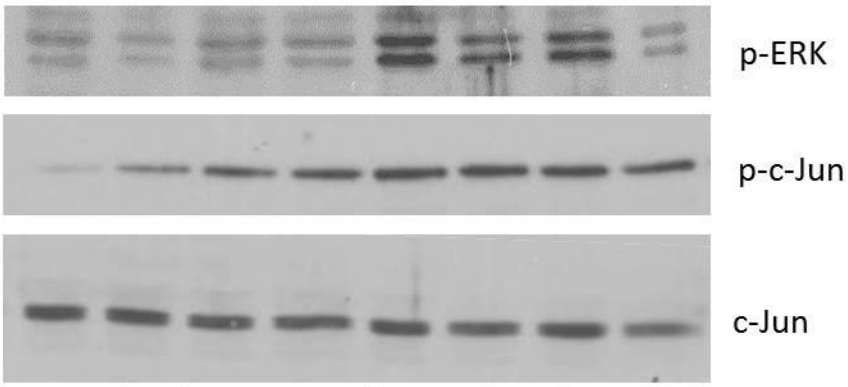

Time	0		2		4		8	
MKP-2	+	-	+	-	+	-	+	-
FCS (10%)	-	-	+	+	+	+	+	+

Figure 3.8: MAP kinase characterisation in WT and KO MASMCs in response to FCS

Confluent mouse aortic smooth muscle cells from both WT and MKP-2 KO were rendered quiescent in 0.1% FCS for 24h prior to stimulation of FCS (10%) for the times indicated. Whole cell lysates were prepared, separated by SDS PAGE and probed for p-c-Jun (48kDa) and p-ERK (44/42 kDa) as described in the Materials and Methods section. Blots were stripped and reprobed for c-Jun which was used a loading control These results are representative of 3 independent experiments. Each value represents mean±S.E.M. Gels were quantified by scanning densitometry.

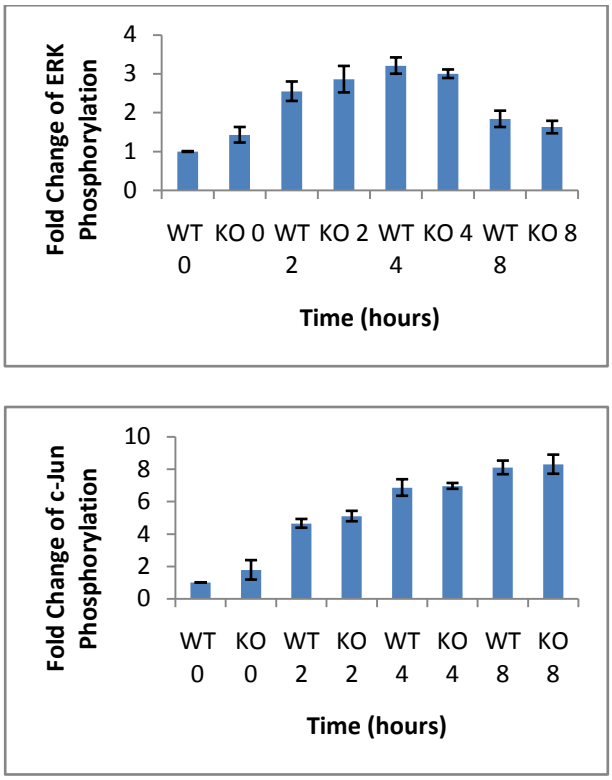

Figure 3.8 cont: MAP kinase characterisation in WT and KO MASMCs in response to FCS

Confluent mouse aortic smooth muscle cells from both WT and MKP-2 KO were rendered quiescent in 0.1% FCS for 24h prior to stimulation of FCS (10%) for the times indicated. Whole cell lysates were prepared, separated by SDS PAGE and probed for p-c-Jun (48kDa) and p-ERK (44/42 kDa) as described in the Materials and Methods section. Blots were stripped and reprobed for T-ERK which was used a loading control These results are representative of 3 independent experiments. Each value represents mean±S.E.M. Gels were quantified by scanning densitometry.

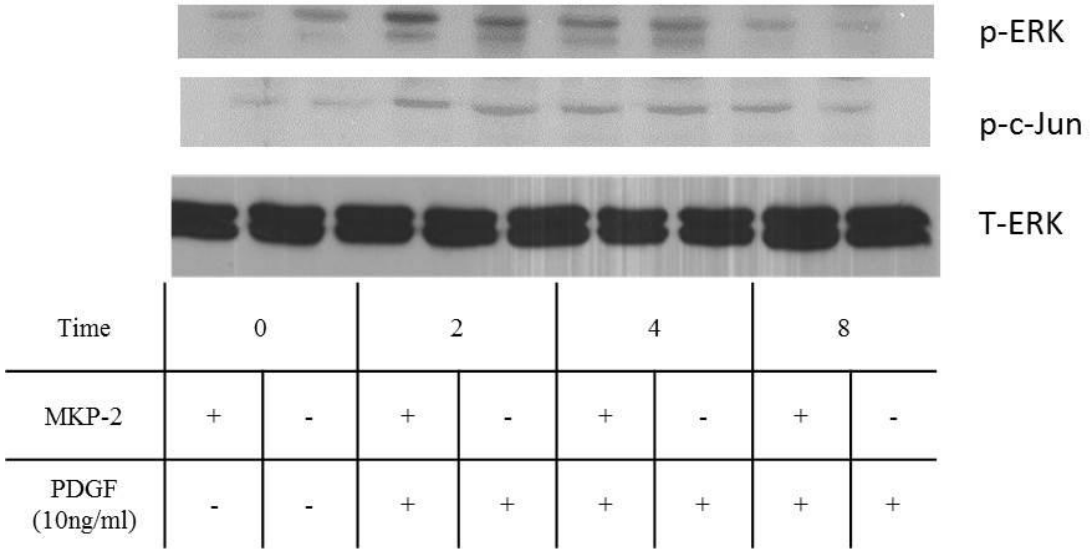

Figure 3.9: MAP kinase characterisation in WT and KO MASMCs in response to PDGF

Confluent mouse aortic smooth muscle cells from both WT and MKP-2 KO were rendered quiescent in 0.1% FCS for 24h prior to stimulation of FCS (10%) for the times indicated. Whole cell lysates were prepared, separated by SDS PAGE and probed for p-ERK (44/42kDa) and p-c-Jun (48kDa) as described in the Materials and Methods section. Blots were stripped and reprobed for T-ERK which was used a loading control These results are representative of 3 independent experiments. Each value represents mean±S.E.M. Gels were quantified by scanning densitometry.

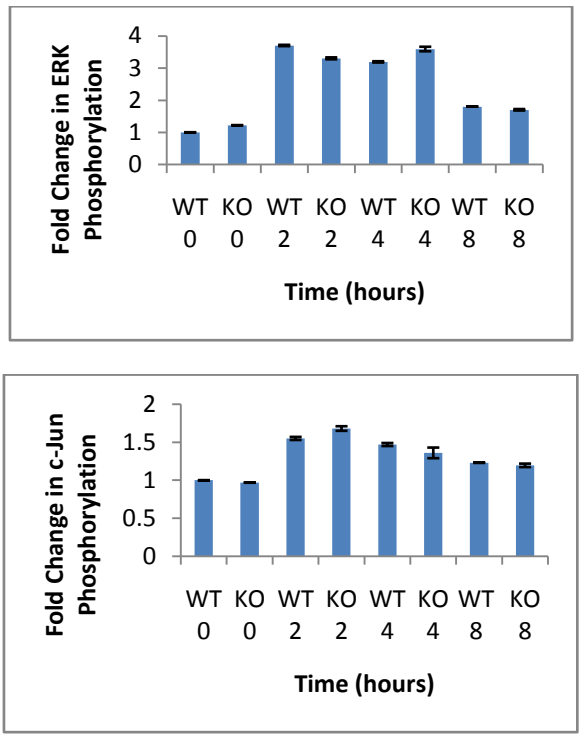

Figure 3.9 cont: MAP kinase characterisation in WT and KO MASMCs in response to PDGF

Confluent mouse aortic smooth muscle cells from both WT and MKP-2 KO were rendered quiescent in 0.1% FCS for 24h prior to stimulation of FCS (10%) for the times indicated. Whole cell lysates were prepared, separated by SDS PAGE and probed for p-ERK (44/42kDa) and p-c-Jun (48kDa) as described in the Materials and Methods section. Blots were stripped and reprobed for c-Jun which was used a loading control These results are representative of 3 independent experiments. Each value represents mean±S.E.M. Gels were quantified by scanning densitometry.

3.2.4 MKP-2 deficient MASMCs exhibit a reduction in proliferative capacity

3.2.4.1 MKP-2 deletion leads to a decrease in MASMC proliferation: Cell counting

Whilst the MAP kinase characterisation of MKP-2 deficient MASMCs proved to be largely inconclusive, these cells exhibited significant differences in their proliferative capacity. Experiments assessing mouse aortic smooth muscle proliferation by means of haemocytomer counting is a direct measurement of cell number at different time points (see Materials and Methods section). As depicted in Figure 3.10, serum-stimulated MKP-$2^{+/+}$ MASMCs over a 48h time period, resulted in a significant increase in cell number which was apparent as early as 24 h (0h 8.133±0.33 x10^4cell number, 24h 15.64±1.13 x10^4cell number; p=0.016). The trend in cell number increase was observed in these cultures was similar to that exhibited in MKP-$2^{+/+}$ MASMC (0h 8.190 ±0.186 x10^4cell number, 24h 12.88±0.35 x10^4cell number; p=0.006). There were no significant difference in cell number between wild-type and knockout MKP-2 MASMCs at the 0h time point which would suggest no marked adherence difference (8.133±0.33 x10^4cell number; 8.190 ±0.186 x10^4cell number; p= 0.916). Interestingly however, at the 24h time point, a marked but non-significant difference in MKP-$2^{+/+}$ and MKP-$2^{-/-}$ cell number was evident (WT 15.64±1.13 x10^4cell number, KO 12.88±0.35 x10^4cell number; p=0.196). At the later time point of 48h, a significant difference in cell number was evident between WT and KO MASMCs (WT 22.284±0.665 x10^4cell number, KO 16.510±0.90 x10^4cell number; p=0.04). This suggests MKP-2 is required for mouse aortic smooth muscle cell proliferation.

3.2.4.2 MKP-2 deficiency leads to increased doubling times in MASMCs

Given the prominent growth deficit observed in MKP-$2^{-/-}$ MASMCs these cells were further assessed detail by focussing on the cellular doubling rates. Cell doubling time protocol was an adaptation of culture of animal cells technique described previously (Freshney, 1994), (see Materials and Methods). The data presented in figure 3.11 demonstrated that smooth muscle cells derived from MKP-$2^{-/-}$ mice had markedly longer cell doubling time; 2 fold increase in comparison with wild type. It is good to note, considering the early time points, there was no evident increase in cell number

detected between both cell types. These results establish that MKP-2 deficient MASMCs are phenotypically different from wild type and these cells are likely to react differently in response to growth stimuli *in vitro.* A lengthy cell doubling time indicates a decrease in cell division rate and is thought to imply a low proliferative ability (Basegara, 1985).

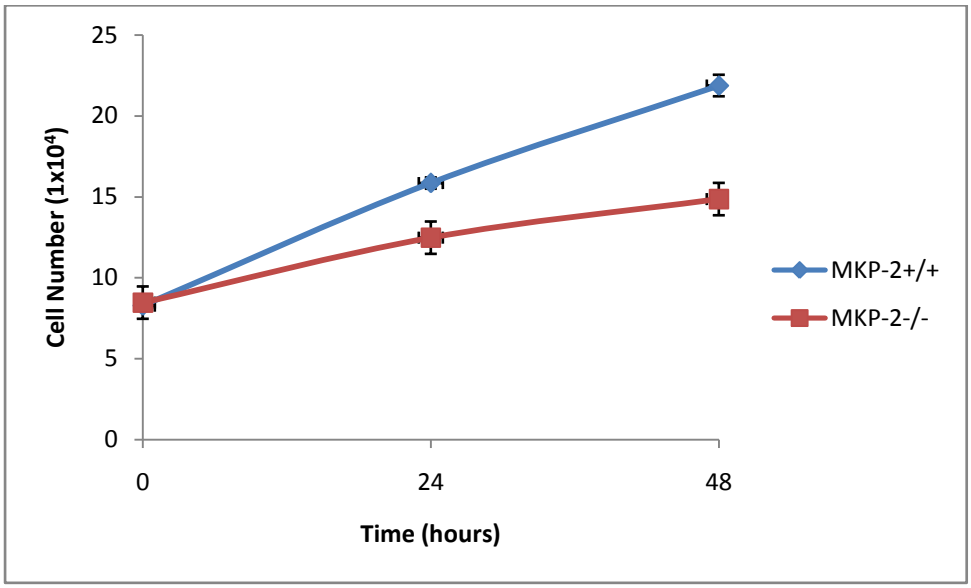

Figure 3.10: Effect of MKP-2 knockout on MASMC proliferation

Subconfluent mouse aortic smooth muscle cells were rendered quiescent in 0.1% FCS for 24h prior to stimulation, both MKP-$2^{+/+}$ and $^{-/-}$ were stimulated with 10% FCS for the times indicated. Proliferation was measured by cell counting at 24h intervals over a 48h time period. These results are representative of 4 independent experiments, mean ± S.E. *, $p < 0.05$ when compared with wild type MASMCs

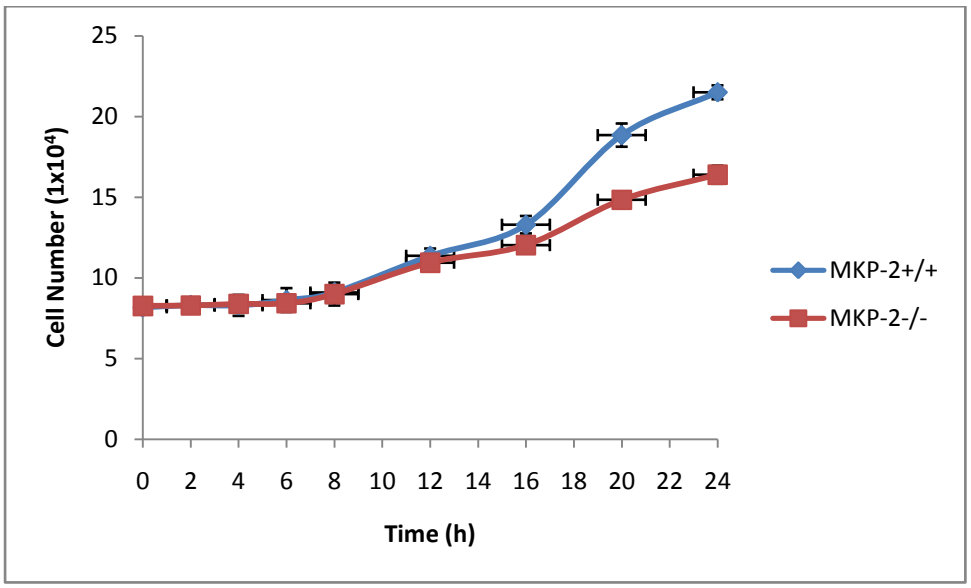

Figure 3.11: Effect of MKP-2 knockout on doubling rate of MASMCs

Subconfluent mouse aortic smooth muscle cells were rendered quiescent in 0.1% FCS for 24h prior to stimulation, both MKP-$2^{+/+}$ and $^{-/-}$ were stimulated with 10% FCS for the times indicated. Proliferation was measured by cell counting at intervals over a 24h time period. These results are representative of 3 independent experiments.

3.2.4.3 Accumulation of MKP-2 deficient MASMCs in G2/M phase

Following the observation that the deletion of MKP-2 significantly reduced smooth muscle cell proliferation, further experiments were conducted to elucidate the differences in growth characteristics by investigating cell cycle parameters. Flow cytometric analysis byDNA propidium iodide staining assesses each phase of the cell cycle. The results presented in Figure 3.12 demonstrates that MASMCs derived from the MKP-$2^{-/-}$ model exhibit a significant reduction in cells residing in G1 phase of the cell cycle (p=0.012) when compared with MKP-$2^{+/+}$ MASMCs. Interestingly, an evident increase in the DNA content of cells derived from MKP-$2^{-/-}$ in G2/M phase (77.4%) in comparison with cells from MKP-$2^{+/+}$ (51.2%) (P=0.001). These data suggests that MKP-2 deletion has resulted in the inhibition of normal progression of these cells through the cell cycle.

3.2.4.4 MKP-2 deficient MASMCs have no effect on G2/M transition proteins

In order to correlate these changes in cell cycle parameters with regulated proteins at specific phases of the cycle, cyclin B1 expression and cdc-2 phosphorylation were examined. These proteins are well recognised indicators of G2/M phase transition (Gutierez et al., 2010) (figure 3.13). Stimulation of quiescent MKP-$2^{+/+}$ MASMCs with serum induced an significant increase in cyclin B1 which was apparent by 8 h and increased further up to 24 h, a trend evident in both WT and KO MASMCs (WT-1.0167±0.0441 fold stimulation, 0.5200±0.0379 fold stimulation; p=0.016; KO 1.007±0.103, 0.473±0.023; p=0.023). Interestingly however, there were no significant differences between either basal (p=0.908) or stimulated cyclin B expression in MKP-2 deficient cells (p=0.625). This expression correlated with a decrease in cdc-2 phosphorylation, taken together this is to be expected, due to the established role of these proteins acting as mutual partners of a mitosis-promoting complex. Stimulation of quiescent MKP-$2^{+/+}$ MASMCs with serum induced an significant decrease in p-cdc-2 which was apparent by 8 h and sustained up to 24 h, a trend evident in both WT and KO MASMCs (WT 1.0333±0.033 fold stimulation, 2.5111±0.0768 fold stimulation; p=0.005 KO 1.0081±0.0520 fold stimulation, 2.5240±0.0692 fold stimulation;

p=0.004). Interestingly however, there were no significant differences between either basal (p=0.908) or stimulated cyclin B expression in MKP-2 deficient cells In MKP-$2^{-/-}$ MASMCs both cyclin B1 expression and cdc-2 phosphorylation were unchanged when compared with MKP-$2^{+/+}$ (p=0.932). This data was unexpected as G2/M phase cycle arrest is usually associated with an accumulation of cyclin B1 and an extended phosphorylation of cdc-2.

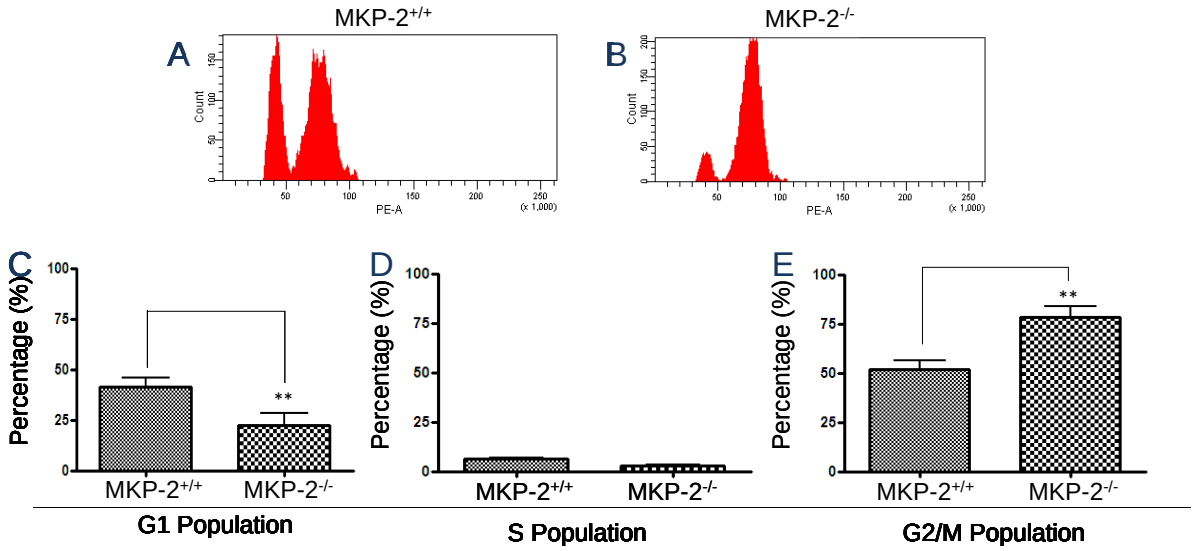

Figure 3.12: Cell cycle G2/M accumulation in MASMC deficient in MKP-2.

Subconfluent mouse aortic smooth muscle cells were rendered quiescent in 0.1% FCS for 24h prior to stimulation, both MKP-2+/+ and MKP-2−/− were stimulated with 10% FCS for 24h. Whole cells were harvested and fixed in 70% ethanol and stained with propidium iodide as outlined in the Materials and Methods section. A) Raw representative histogram of MKP-$2^{+/+}$ MASMCs in different phases of cell cycle. B) Raw representative histogram of MKP-$2^{-/-}$ MASMCs in different phases of the cell cycle. C) Comparison of MKP-$2^{+/+}$ and MKP-$2^{-/-}$ MASMCs in G1 phase of the cell cycle. D) Comparison of MKP-$2^{+/+}$ and MKP-$2^{-/-}$ MASMCs in S phase of the cell cycle. E) Comparison of MKP-$2^{+/+}$ and MKP-$2^{-/-}$ MASMCs in G2/M phase of the cell cycle.These results are representative of 4 independent experiments, mean ± S.E. **, $p < 0.01$ when compared with wild type MASMCs. Statistical analysis was corrected using Bonferoni's considerations.

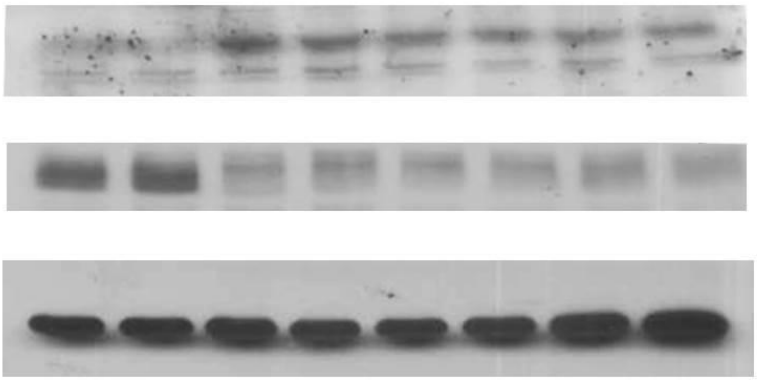

Time (mins)	0		8		16		24	
FCS (10%)	-	-	+	+	+	+	+	+
MKP-2	+	-	+	-	+	-	+	-

Figure 3.13: Expression of cyclin B and cdc-2 throughout the cell cycle

Confluent mouse aortic smooth muscle cells of both WT and MKP-2 KO were rendered quiescent in 0.1% FCS for 24h prior to stimulation of FCS (10%) for the times indicated. Whole cell lysates were prepared, separated by SDS PAGE and probed for cyclin B1 (58kDa) and p-cdc-2 (34kDa) as described in the Materials and Methods section. Blots were stripped and reprobed for GAPDH which was used a loading control These results are representative of 3 independent experiments. Each value represents mean±S.E.M. Gels were quantified by scanning densitometry.

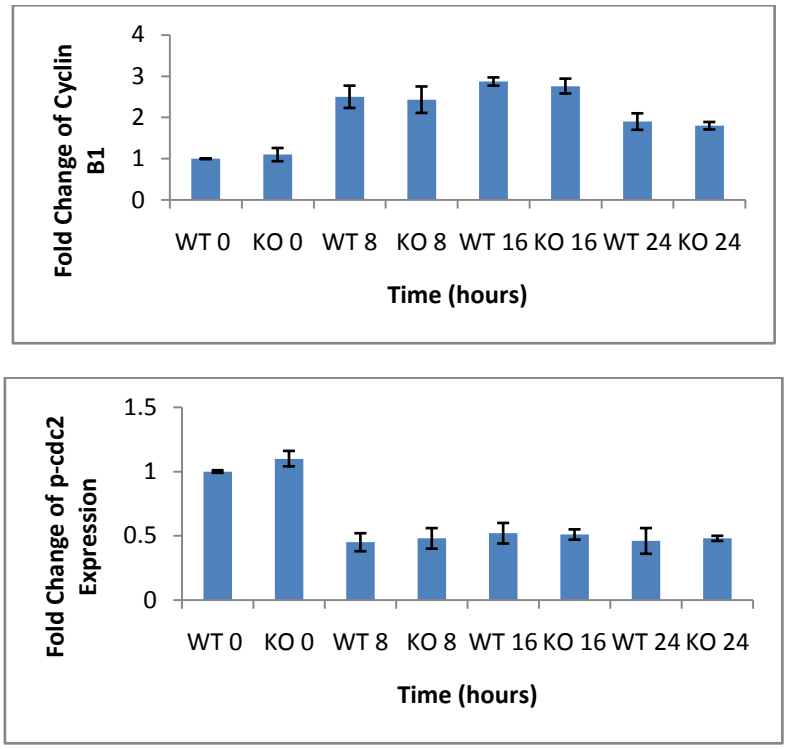

Figure 3.13: Expression of cyclin B and cdc-2 throughout the cell cycle

Confluent mouse aortic smooth muscle cells of both WT and MKP-2 KO were rendered quiescent in 0.1% FCS for 24h prior to stimulation of FCS (10%) for the times indicated. Whole cell lysates were prepared, separated by SDS PAGE and probed for cyclin B1 (58kDa) and p-cdc-2 (34kDa) as described in the Materials and Methods section. Blots were stripped and reprobed for GAPDH which was used a loading control These results are representative of 3 independent experiments. Each value represents mean±S.E.M. Gels were quantified by scanning densitometry.

3.2.5 MKP-2 deletion results in cytokinesis deficiency

3.2.5.1 MKP-$2^{-/-}$MASMCs exhibit a delay in cytokinesis

To further investigate the role for MKP-2 in MASMC cell cycle, and moving forward from the techniques which provide merely a snapshot in G2/M phase of the cell cycle, time lapse microscopy was utilised. Mouse aortic smooth muscle cells were grown in 60mm dishes enclosed in an environmental chamber at optimal condition (37ºC, 5% CO_2), and images were taken every 500 seconds to aid the visualisation of endogenous cellular proliferation. With reference to Figure 3.16, MKP-$2^{-/-}$ MASMCs display a delayed mitotic progression when compared with cells derived from wild-type mice. There is an evident delay in telophase and cytokinesis, with MKP-$2^{-/-}$ requiring 72min to reach cytokinesis from metaphase compared with 39min in MKP-$2^{+/+}$ smooth muscle cells. Further time points were assessed to ascertain a difference in cytokinesis between wild-type and knockout MKP-2 MASMCs. As depicted in Figure 3.17 the intercellular bridges between MKP-2 deficient cells display a difficulty in separating into two daughter cells; resulting in an increased cytokinetic failure in these cells. Overall, quantification reveals 78% of wild-type MASMCs successfully completed cytokinesis throughout the duration of each movie, compared with 42% of MKP-2 deficient cells successfully completing cytokinesis. Additional analysis reveals a marked increase in time for cells completing cytokinesis (WT 9 min, KO 19 min) (Figure 3.16). Collectively these data reveal that MKP-2 deficient smooth muscle cells have a delay in cytokinesis with a marked reduction in the overall cytokinetic success rate, with some cells never fully completing cytokinesis throughout the duration of the experiment. Taken together, these data suggest an essential role for MKP-2 in cytokinesis.

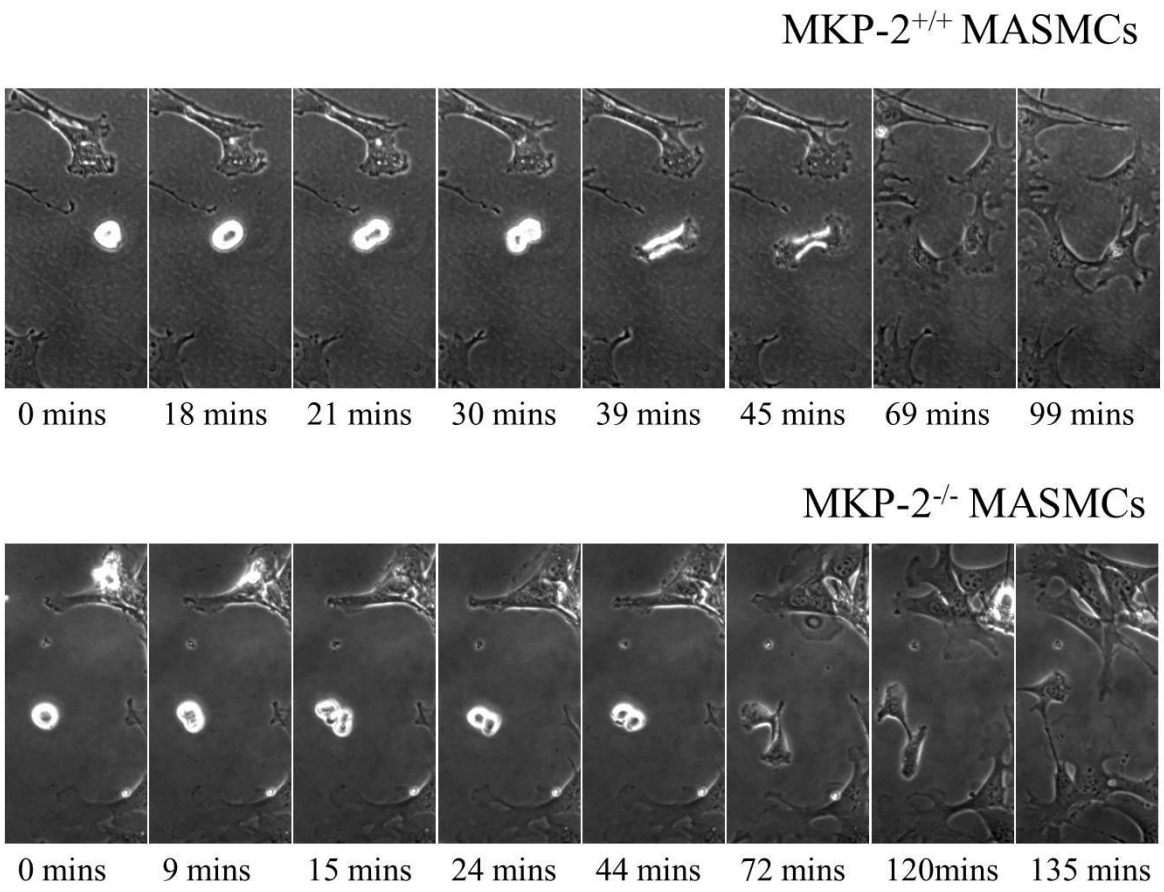

Figure 3.14: MASMCs lacking in MKP-2 exhibit a delay in mitosis.

Subconfluent mouse aortic smooth muscle cells of both MKP-2+/+ and MKP-2−/− grown in full media (10% FCS) and analysed using Zeiss microscope. Images were taken every 3min for the duration of the experiment. These results are representative of 3 independent experiments.

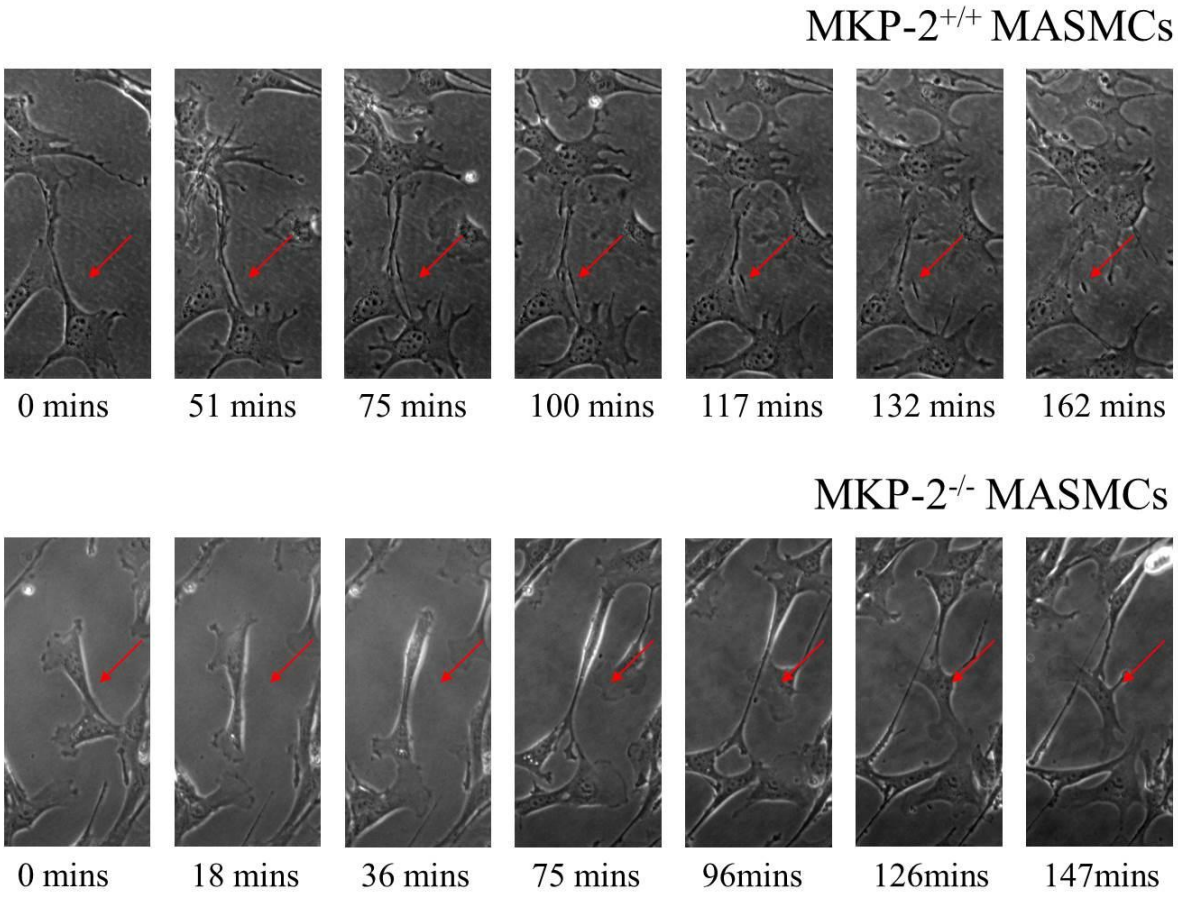

Figure 3.15: MASMCs lacking MKP-2 exhibit a delay in abscission.

Subconfluent mouse aortic smooth muscle cells of both MKP-$2^{+/+}$ and $^{-/-}$ grown in full media (10% FCS) and analysed using Zeiss microscope. Images were taken every 3 min for the duration of the experiment. These results are representative of 3 independent experiments.

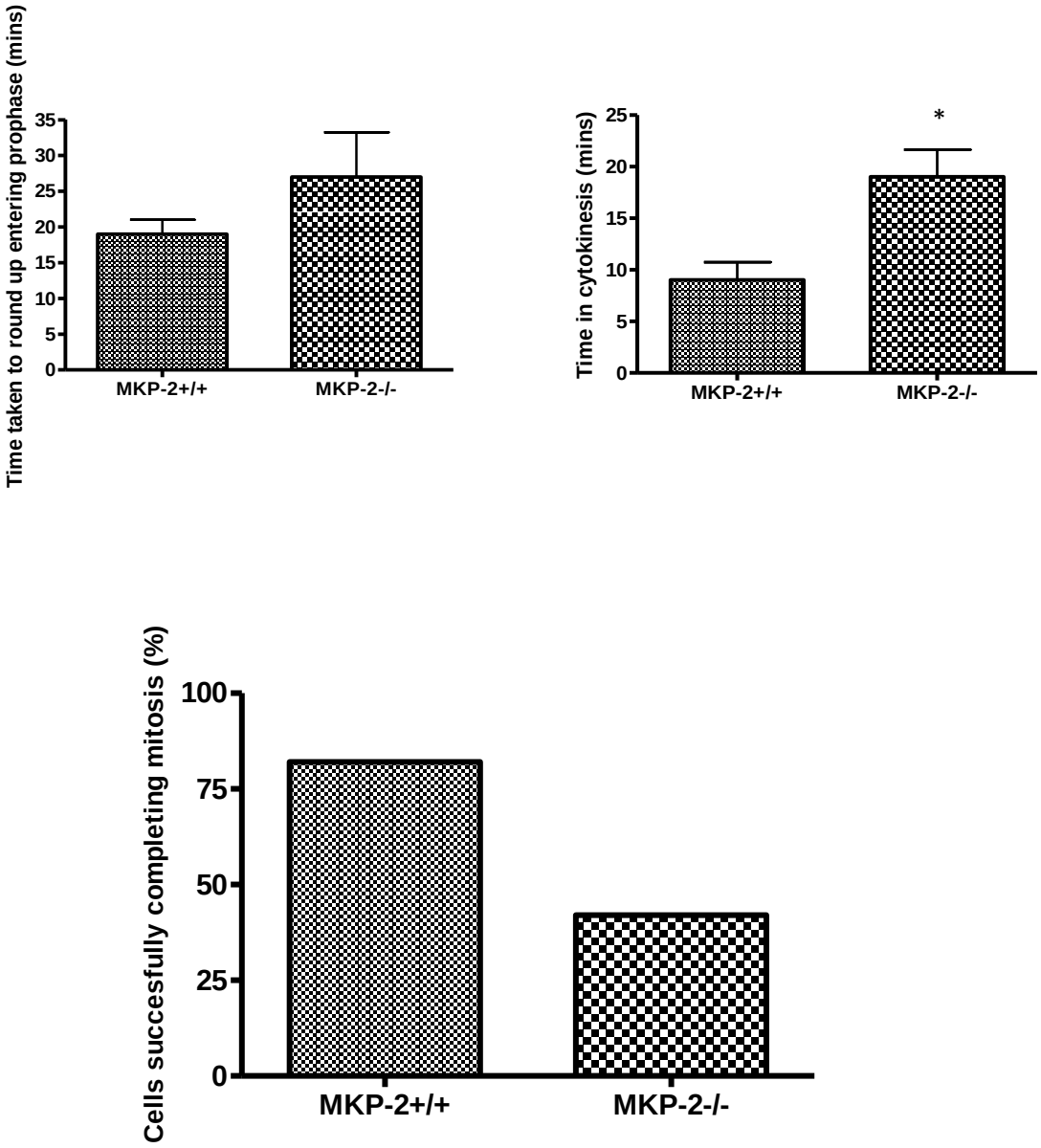

Figure 3.16: MASMC lacking MKP-2 exhibit a reduced success rate in cytokinesis completion

Subconfluent mouse aortic smooth muscle cells of both MKP-$2^{+/+}$ and $^{-/-}$ grown in full media (10% FCS) and analysed using Zeiss microscope. Images were taken every 3 min for the duration of the experiment. Cells were tracked over still TIF images and quantified accordingly. *$P<0.05$ mean ± SEM.

3.2.5.2 Optimising conditions for G2/M phase arrest

Since the emergence of mitotic inhibitors, they have been utilised as synchronisation tools to aid in the analysis of mitotic proteins which are rapidly turned over (Sentein, 1977). The inhibitor of choice in this case is nocodazole, which acts as an anti-microtubule polymerisation agent; the absence of microtubule attachment to kinetochores activates the spindle assembly checkpoint, causing the cell to arrest in prometaphase (Xu et al., 2002). MASMCs were treated with varying concentrations (10ng/ml – 100ng/ml) of nocodazole to ascertain optimal treatment conditions, not only with a high percentage of cells accumulating in the G2/M phase but also the ability of the cells to regain microtubule attachment and complete cycling post-treatment (Figure 3.17). Low concentrations of nocodazole (10ng/ml and 20ng/ml) had little or no effect on prometaphase arrest when analysed by flow cytometry, with a G2/M accumulation of 33.4% and 35.1%, respectively. However, both 50ng/ml and 100ng/ml displayed a significant accumulation of cells in G2/M phase of the cell cycle with 81.9% and 74.2%, accordingly. Critically however, at the top nocodazole concentration of 100ng/ml cells were unable to cycle again, rendering this condition unsuitable. Deduced from these results, the nocodazole concentration of 50ng/ml will be used here forth in order to synchronise cells in order to assess mitotic and cytokinetic proteins.

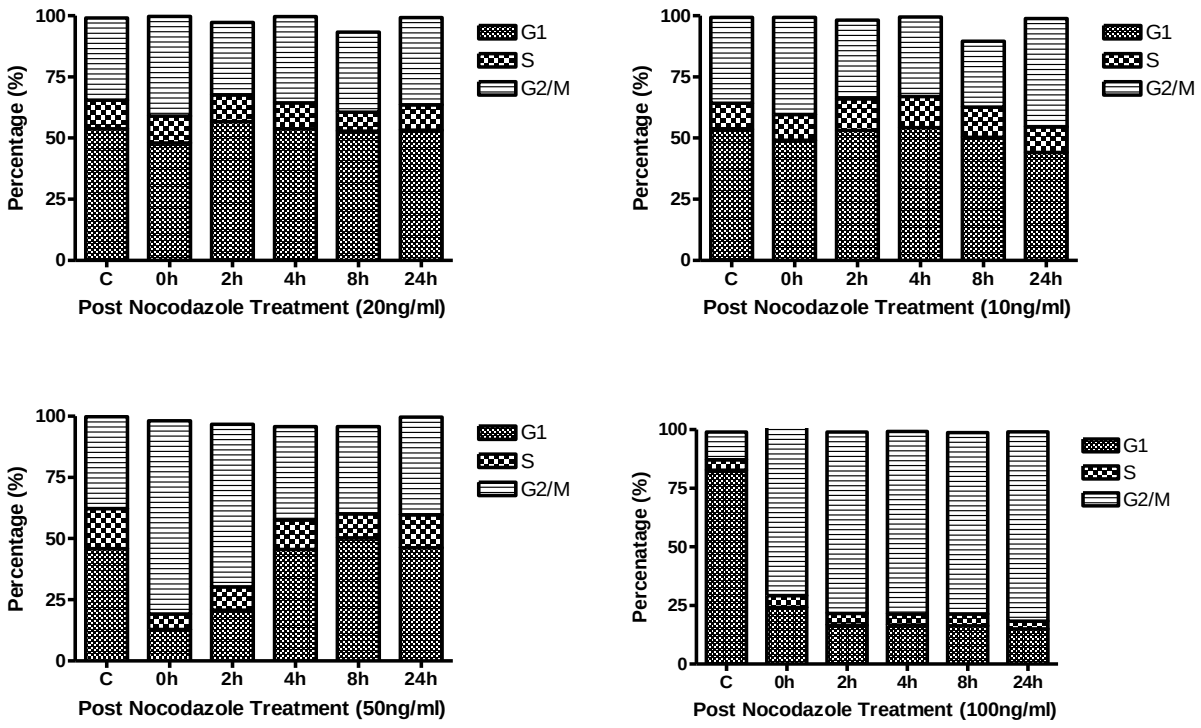

Figure 3.17: Characterisation of nocodazole arrest treatment

Subconfluent mouse aortic smooth muscle cells were treated with increasing concentrations of nocodazole for 16h. Cells were washed twice in PBS and stimulated with 10% FCS for the noted timepoint. Whole cells were harvested and fixed in 70% ethanol and stained with propidium iodide as outlined in the Materials and Methods section. These results are representative of 2 independent experiments.

3.2.5.3 MKP-2 is essential for the expression of proteins required for cytokinesis

In order to correlate the difference in cytokinetic parameters between MKP-2 wild-type and knockout smooth muscle cells, they were synchronised by nocodazole to arrest in prometaphase of mitosis and subsequently released back into the cell cycle. Timepoints were determined from previous time-lapse microscopy data in order to convey approximate phases of prometaphase (0h), telophase (1h) and cytokinesis (2h) respectively. At such times post-release, cells were lysed and assessed using SDS-PAGE. Cytokinesis is a complex, well-regulated process and proteins of interest known to be essential in the progression of cytokinesis, include Aurora B, VRK1 and their shared downstream target Histone H3 (Jeong et al., 2013). A significant reduction in aurora B phosphorylation was evident in both asynchronous (WT 1±00 fold stimulation, KO 0.31±0.14 fold stimulation; p=0.0126) and nocodazole treated MKP-$2^{-/-}$ cells (WT 1.37±0.14 fold stimulation, KO 0.81±0.04 fold stimulation; p=0.039) in comparison with wild-type cells (Figure 3.18). This trend is also noted in VRK1 expression, however to a lesser extent than aurora B. Further analysis to investigate the effect of the reduction in expression of the noted mitotic kinases, Aurora B and VRK1, focussed upon their shared downstream target Histone H3 on the Ser10 residue. Interestingly, there is no difference in Histone H3 phosphorylation between MKP-$2^{+/+}$ and MKP-$2^{-/-}$ asynchronous cells (p=0.08), however upon prometaphase arrest there is a marked reduction in histone H3 phosphorylation at the 0h, 1h and 2h time points (p=0.00, 0.03, 0.006, respectively). The noted reduction of mitotic protein expression supports previous data described regarding the phenotype associated with MKP-$2^{-/-}$ smooth muscle cells and the deficiency in cytokinesis progression.

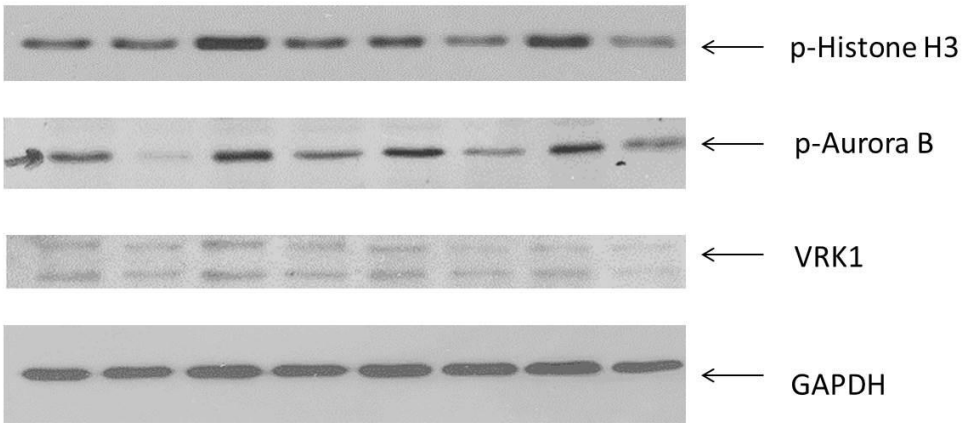

Time (hours)			0		1		2	
Nocodazole (50ng/ml)	-	-	+	+	+	+	+	+
FCS (10%)	+	+	+	+	+	+	+	+
MKP-2	+	-	+	-	+	-	+	-

Figure 3.18 MKP-2 is required for phosphorylation of cytokinetic proteins

Subconfluent mouse aortic smooth muscle cells were treated with nocodazole (50ng/ml) for 16h. Cells were washed twice in PBS and stimulated with 10% FCS for the noted timepoint. Whole cell lysates were prepared, separated by SDS PAGE and probed for p-Histone H3 (ser10) (17kDa), VRK1 (48kDa), p-Aurora B (40 kDa) and GAPDH (37kDa) as described in the Materials and Methods section. Blots were stripped and reprobed for GAPDH which was used a loading control. These results are representative of 3 independent experiments.

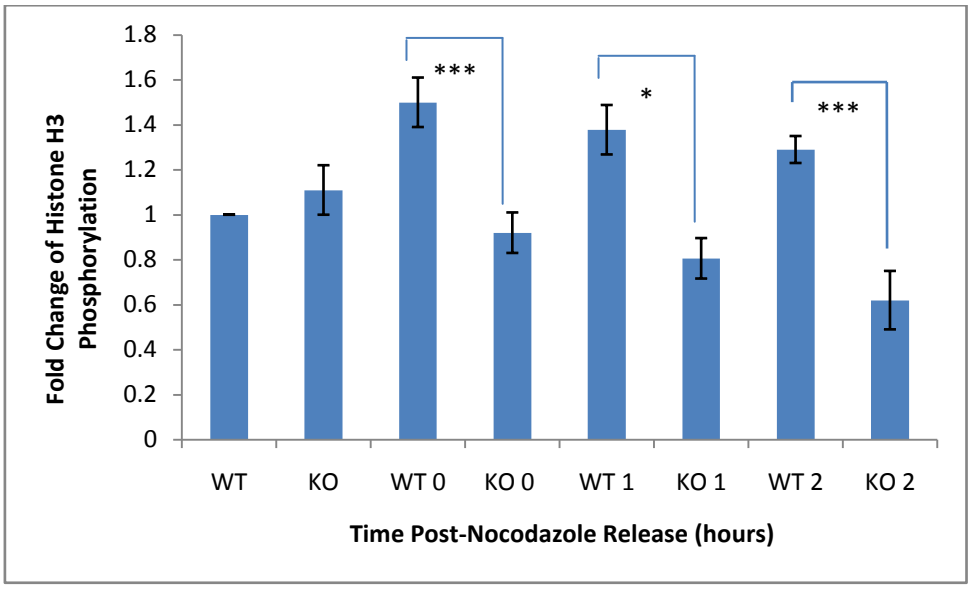

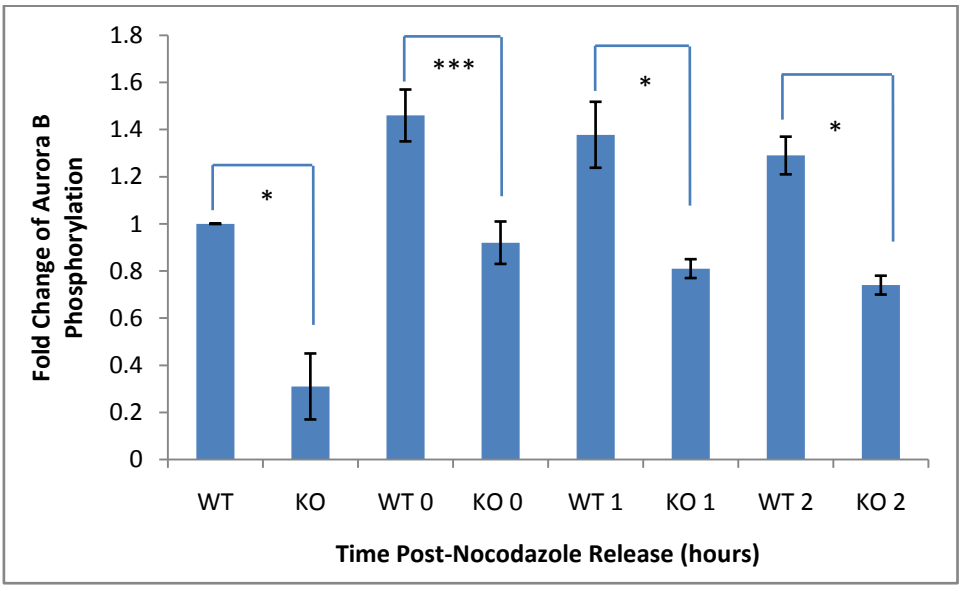

Figure 3.18 cont. Effect of MKP-2 proteins required for cytokinesis

Subconfluent mouse aortic smooth muscle cells were treated with nocodazole (50ng/ml) for 16h. Cells were washed twice in PBS and stimulated with 10% FCS for the noted timepoint. Whole cell lysates were prepared, separated by SDS PAGE and probed for p-Histone H3 (ser10) (17kDa), p-Aurora B (40kDa) and GAPDH (37kDa) as described in the Materials and Methods section. These results are representative of 3 independent experiments. . *P<0.05 ***P<0.01 mean ± SEM

3.2.6 Over-expression of MKP-2 failed to regain MKP-2$^{-/-}$ MASMCs proliferative deficiency

3.2.6.1 Over-expression of Adenoviral WT-MKP-2 decreased proliferation rates in both wild-type and MKP-2 deficient MASMCs

Having established from previous experiments that MKP-2 deletion significantly inhibited proliferation in MKP-2 deficient MASMCs, a gain of function study was conducted to determine whether over-expression of Adv. MKP-2 could reverse this deficit in cell growth. For this purpose MASMCs were infected with increasing concentrations of Adv. MKP-2 (200-500pfu) and assessed for MKP-2 expression by Western blotting (see figure 3.19). Maximum expression was achieved between 300 and 500pfu. Based on this result the cells derived from MKP-2$^{-/-}$ were infected with Adv.MKP-2 at 300pfu and cellular proliferation assessed at this concentration. In accordance with earlier data, cellular proliferation was reduced in the absence of MKP-2 at all time points assessed. Interestingly, cellular proliferation was not regained following Adv. MKP-2 over-expression in MKP-2$^{-/-}$ MASMCs as shown in Figure 3.23 (KO 14.859± 0.907x10^4 cell number, KO + Adv.WT-MKP-2 15.9± 0.907x10^4 cell number; p=0.067). In fact, addition of Adv. WT-MKP-2 cells derived from MKP-2 wild-type, displayed a decrease in proliferation rate likewise. (WT 21.87±0.665 x10^4 cell number, WT + Adv.WT-MKP-2 17.39±1.63 x10^4 cell number; p=0.03). These results demonstrate that Adv. WT-MKP-2 over-expression did not possess the ability to reverse the proliferative deficiency of these cells and suggest that MKP-2 overexpression is responsible for the decrease in cell growth observed in these cells. Taken together, it could be noted that MKP-2 plays a significant role in proliferation in mouse aortic smooth cells.

3.2.6.2 Over-expression of Adenoviral WT-MKP-2 resulted in G1 accumulation in both wild-type and MKP-2 deficient MASMCs

In order to further elucidate how the over-expression of Adv. WT-MKP-2 resulted in a significant reduction in proliferation of both wild-type and knockout smooth muscle cells, analysis of the cell cycle profiles were assessed using flow cytometry. It can be observed that over-expression of MKP-2 results in an accumulation of cells in G1 phase of the cell cycle in both MKP-$2^{+/+}$ (WT 74.1% vs. 92.3% with Adv.WT-MKP-2) and MKP-$2^{-/-}$ smooth muscle cells (KO 62.5% vs. 88.1% with Adv.WT-MKP-2) (depicted in Figure 3.20). Consistent with previous data displayed in Figure 3.14, MASMCs derived from the MKP-2 knockout mouse exhibited a greater G2/M accumulation (WT 26% vs. KO 38%). This result supports data described in section 3.2.6 where Adv.WT- MKP-2 over-expression did not possess the ability to reverse the proliferative deficiency of these cells; suggesting that alteration of MKP-2 expression is responsible for the decrease in cell growth observed in these cells.

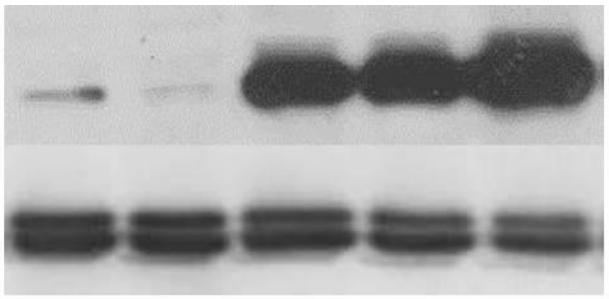

PFU	-	-	200	300	500
LacZ	-	+	-	-	-
Adv.WT-MKP-2	-	-	+	+	+
FCS	+	+	+	+	+

Figure 3.19 Pfu curve of Adv. WT-MKP-2 in MASMCs

Confluent mouse aortic smooth muscle cells were infected with Adv.WT-MKP-2 in concentrations varying from 200-500 pfu in 0.1% media. Cells were stimulated in 10% FCS, prepared, separated by SDS PAGE and probed for MKP-2 (43kDa). Blots were stripped and reprobed for T-ERK which was used a loading control These results are representative of 3 independent experiments.

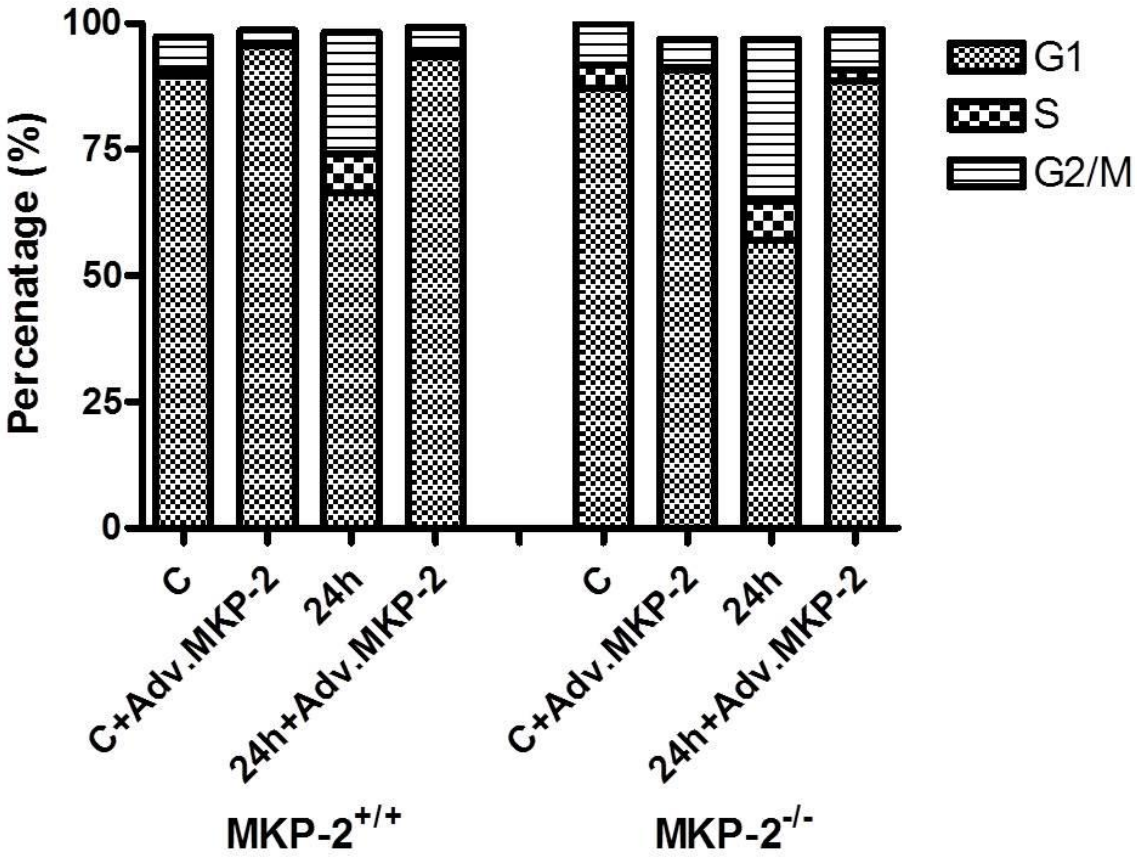

Figure 3.20 Effect of Adv.WT-MKP-2 on cell cycle in MASMCs

Subconfluent mouse aortic smooth muscle cells were infected with Adv.WT-MKP-2 (300pfu) rendered quiescent in 0.1% FCS for 24h prior to stimulation, both MKP-$2^{+/+}$ and $^{-/-}$ were stimulated with 10% FCS for 24h. Whole cells were harvested and fixed in 70% ethanol) and stained with propidium iodide as outlined in the Materials and Methods section. These results are representative of 2 independent experiments.

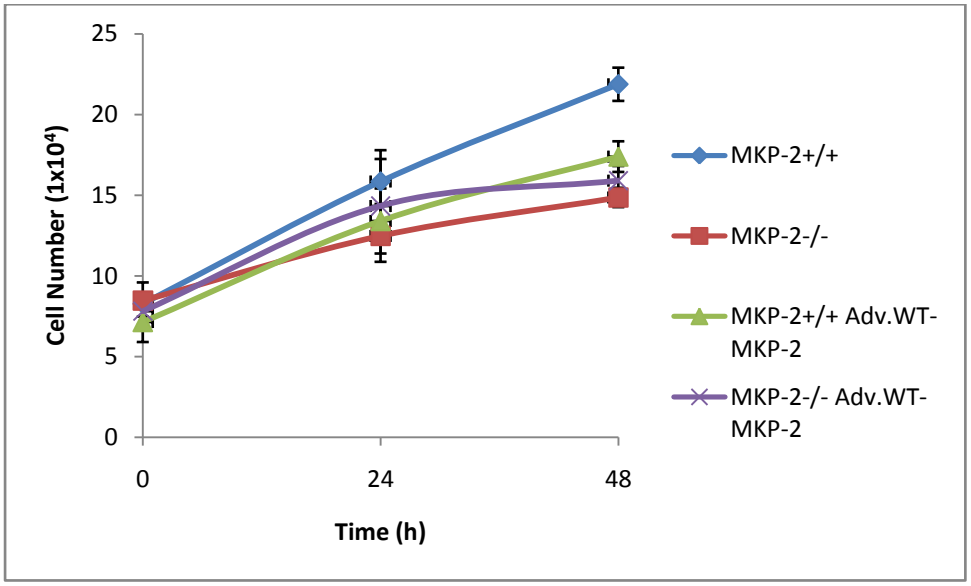

Figure 3.21: Effect of Adv. WT MKP-2 on proliferation

Subconfluent mouse aortic smooth muscle cells of both MKP-2+/+ and MKP-2−/−, were infected with Adv.WT-MKP-2 (300pfu) and rendered quiescent in 0.1% FCS for 24h prior to stimulation. Cells were then stimulated with 10% FCS for 48h over 24h time periods. Proliferation was measured by cell counting at 24h intervals over a 48h time period. These results are representative of 3 independent experiments.

3.6.3 Over-expression of Adenoviral WT-MKP-2 and CI-MKP-2 and the differential effect on ERK signalling

Following the observation of Adv.WT-MKP-2 having a detrimental effect on cell proliferation, opportunity arises to question the mechanism by which this occurs and how, or if this relates to MKP-$2^{-/-}$ smooth muscle cells exhibiting cytokinetic phenotypic differences. The use of a constitutively-inactive (CI) adenoviral MKP-2, allows for exploration into the non-catalytic effect of MKP-2. Figure 3.22 displays the effect of both the Adv.WT-MKP-2 and Adv.CI-MKP-2 on ERK signalling. It can be seen that over-expression of WT-MKP-2 abolishes ERK signalling; however this effect is not seen with over-expression of CI-MKP-2 (Figure 3.22), confirming the lack of catalytic activity. It should be noted that no difference in total ERK was observed and therefore the effect observed is dependent upon the activity of ERK rather than total protein. It can therefore be concluded that Adv.CI-MKP-2 can be used as a tool to investigate the potential for MKP-2 to be acting independent of its catalytic activity.

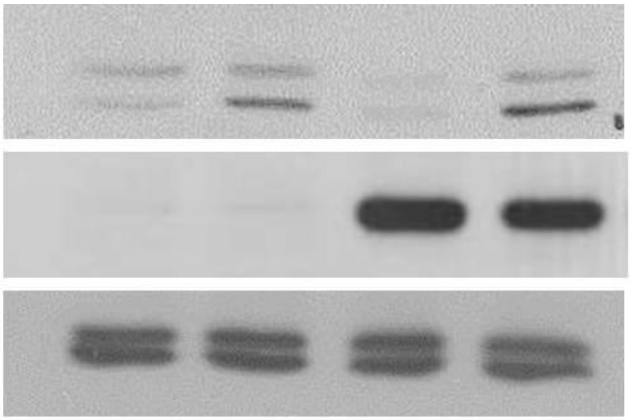

FCS (10%)	-	+	+	+
Ad.WT-MKP-2	-	-	+	-
Ad.CI-MKP-2	-	-	-	+

Figure 3.22: Adv. WT MKP-2 inhibits ERK signalling in MASMC

Confluent mouse aortic smooth muscle cells were infected with Adv.WT-MKP-2 and Adv.CI-MKP-2 300 pfu in 0.1% media. Cells were stimulated in 10% FCS, prepared, separated by SDS PAGE and probed for p-ERK (44/42kDa), MKP-2(43kDa). Blots were stripped and reprobed for T-ERK which was used a loading control (44/42kDa). These results are representative of 2 independent experiments.

3.2.7 Over-expression of CI-MKP-2 suggests a non-MAP kinase dependant role for MKP-2 in MASMC proliferation

3.2.7.1 Over-expression of Adenoviral CI-MKP-2 decreased proliferation rates in both wild-type and MKP-2 deficient MASMCs

Having established from previous experiments that WT-MKP-2 over-expression significantly inhibited proliferation in MASMCs, a gain of function study was conducted to determine whether over-expression of Adv. CI-MKP-2 could reverse this deficit in cell growth by reintroducing the capacity for MKP-2 to bind to known or unknown substrates. For this purpose MASMCs were infected with increasing concentration of Adv. CI-MKP-2 (200-500 pfu) and assessed for MKP-2 expression by Western blotting (see figure 3.23). Maximum expression was achieved between 300 and 500 pfu. Based on this result the cells derived from MKP-$2^{-/-}$ were infected with Adv. MKP-2 at 300 pfu and cellular proliferation assessed at this concentration.

Assessment of Adv.CI-MKP-2 over-expression in reversing the G2/M accumulation in MKP-$2^{-/-}$ MASMC was conducted using flow cytometric cell cycle analysis. Initial results depicted in Figure 3.24, imply over-expression of CI-MKP-2 has the capacity to reverse the G2/M accumulation observed in MKP-$2^{-/-}$ MASMCs, with a significant reduction of 16% ($p<0.05$). However, also notable was the slight, albeit not significant reduction of adenovirally infected MKP-$2^{+/+}$ cells in G2/M phase of the cell cycle. This could therefore suggest that over-expression of a catalytically-inactive mutant of MKP-2 may have an effect on the proliferation of both wild-type and MKP-2 knockout MASMCs. To investigate this possibility, the effect of Adv.CI-MKP-2 on cellular proliferation was assessed using haemocytometer counting (as described in Materials and Methods section). In concordance with previously described data, MKP-$2^{-/-}$ MASMCs have a slower proliferative growth when compared with MKP-$2^{+/+}$ MASMCs (Figure 3.25). However, it can be seen that once overexpressed with CI-MKP-2 both wild-type and knockout MASMCs exhibit a marked reduction in proliferation, comparable MKP-$2^{-/-}$ cells (WT 21.87±0.665 $x10^4$ cell number, WT + Adv.WT-MKP-2 18.14±1.02 $x10^4$ cell number; KO 14.859± 0.907 $x10^4$ cell number,

KO + Adv.WT-MKP-2 16.15± 1.54 $x10^4$ cell number). Due to lack of ERK dephosphorylation in Adv.CI-MKP-2 cells, it can be deduced that this proliferative defect is not an ERK-dependant signalling deficit but does suggest MKP-2 requires its catalytic activity for a successful proliferative profile.

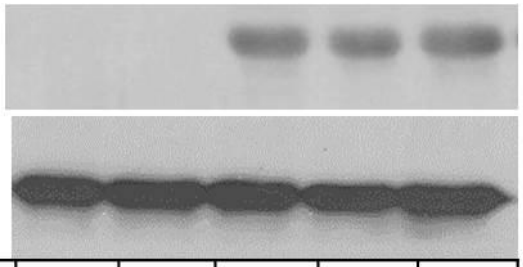

PFU	-	-	200	300	500
LacZ	-	+	-	-	-
Adv.WT-MKP-2	-	-	+	+	+
FCS	+	+	+	+	+

Figure 3.23 PFU curve of Adv.CI-MKP-2

Subconfluent mouse aortic smooth muscle cells were infected with Adv.CI-MKP-2 in concentrations varying from 200-500 pfu in 0.1% media. Cells were stimulated in 10% FCS, prepared, separated by SDS PAGE and probed for MKP-2 (43 kDa) and stripped and reprobed for GAPDH which was used a loading control GAPDH (37kDa).

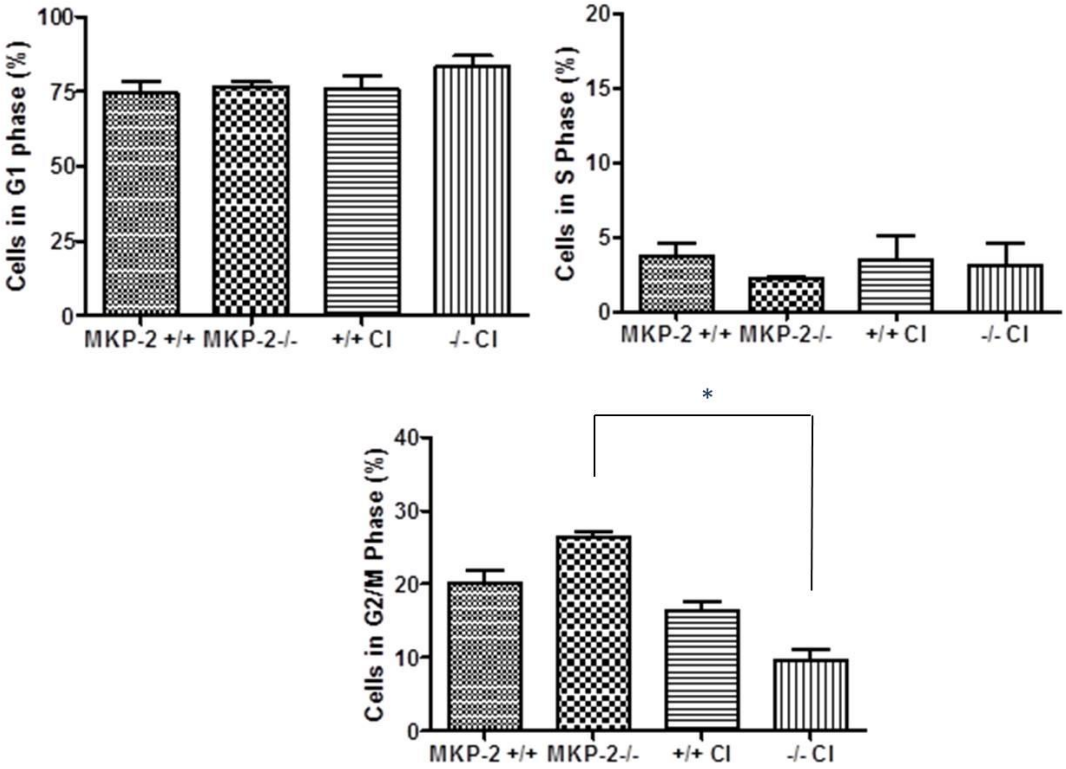

Figure 3.24 Effect of Adv.CI-MKP-2 on MASMC Cell Cycle

Subconfluent mouse aortic smooth muscle cells were infected with Adv.CI-MKP-2 (300pfu) rendered quiescent in 0.1% FCS for 24h prior to stimulation, both MKP-$2^{+/+}$ and $^{-/-}$ were stimulated with 10% FCS for 24h. Whole cells were harvested and fixed in 70% ethanol and stained with propidium iodide, as outlined in the Materials and Methods section. These results are representative of 3 independent experiments. *P<0.05 mean ± S.E. Statistical analysis was corrected using Bonferoni's considerations

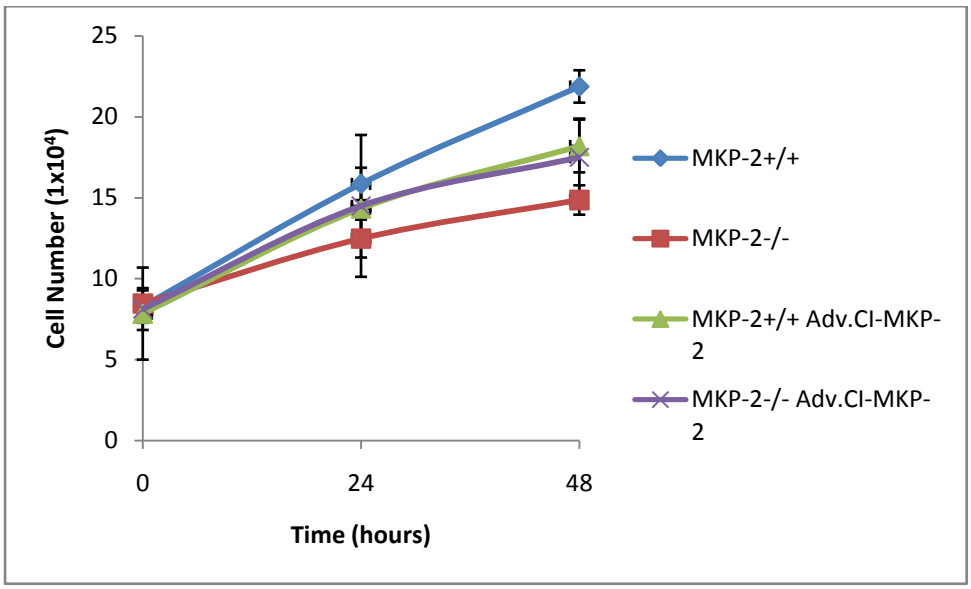

Figure 3.25 Effect of Adv.CI-MKP-2 on MASMC Proliferation

Subconfluent mouse aortic smooth muscle cells of both MKP-$2^{+/+}$ and $^{-/-,}$ were infected with Adv.CI-MKP-2 (300pfu) and rendered quiescent in 0.1% FCS for 24h prior to stimulation. Cells were then stimulated with 10% FCS for 48h over 24h time periods. Proliferation was measured by cell counting at 24h intervals over a 48h time period. These results are representative of 2 independent experiments.

3.2.7.2 Over-expression of Adenoviral CI-MKP-2 decreased expression of proteins required for cytokinesis in both wild-type and MKP-2 deficient MASMCs

From previous experiments it has been established that an MKP-2 catalytically-inactive mutant results in a proliferative deficit, however the effect on proteins required for cytokinesis are yet to be elucidated. Using a combination of nocodazole and Adv.CI-MKP-2 treatment, the effect of CI-MKP-2 on synchronised cells in mitosis was conducted. It can be seen from Figure 3.26, asynchronous MKP-$2^{-/-}$MASMCs exhibit a significant lower expression of phospho-Histone H3 when compared with wild-type cells (WT 1, KO 0.71±0.09; p=0.05). Upon infection with Adv.CI-MKP-2, a modest reduction in Histone H3 expression was consistent in MKP-2 deficient MASMCs (WT + Adv.CI-MKP-2 0.63±0.1; KO + Adv.CI-MKP-2 0.57±0.002; p=0.122). Once synchronised both MKP-$2^{+/+}$ and MKP-$2^{-/-}$ MASMCs exhibit a marked reduction in Histone H3 (ser10) phosphorylation once infected with Adv.CI-MKP-2 (WT 0.789±0.09, WT + Adv.CI-MKP-2 0.5±0.04; KO 0.742±0.084, KO + Adv.CI-MKP-2 0.34±0.009). This reduction of phosphorylation shown in Histone H3 is consistent over the 0h and 2h time point (WT 0.6±0.02, KO 0.54 ±0.04; p=0.003) post-release from nocodazole, suggesting that the catalytic activity of MKP-2 is required for cells in prometaphase and cytokinesis. Interestingly, ERK phosphorylation was shown to be upregulated in cytokinesis timepoints when compared to asynchronous cells and cells in prometaphase of mitosis. This requirement of ERK is exhibited in MASMCs derived from both wild-type and MKP-2 knockout mice; however the Adv.CI-MKP-2 had no effect on ERK phosphorylation. Collectively these data suggest that MKP-2 requires its catalytic activity for full proliferative capacity but may not involve the inactivation of ERK or JNK.

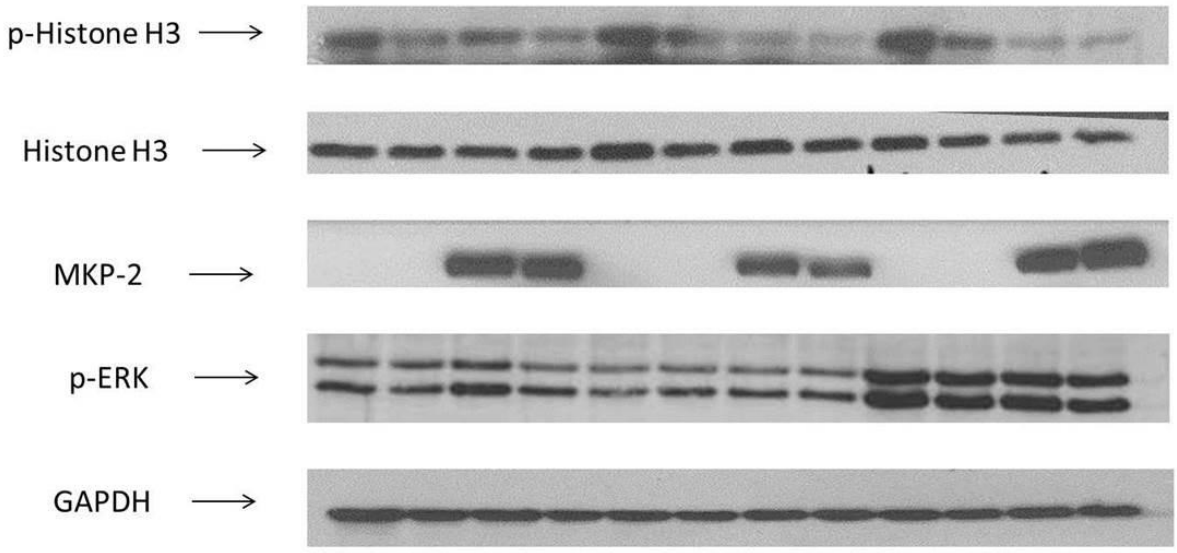

Time (hours)	24				0				2			
Nocodazole (50ng/ml)	-	-	-	-	+	+	+	+	+	+	+	+
FCS 10%	+	+	+	+	+	+	+	+	+	+	+	+
Adv. CI- MKP-2	-	-	+	+	-	-	+	+	-	-	+	+
MKP-2	+	-	+	-	+	-	+	-	+	-	+	-

Figure 3.26 Effect of Adv.CI-MKP-2 on MASMCs in proteins required for cytokinesis

Subconfluent mouse aortic smooth muscle cells were infected with Adv.CI-MKP-2 (300pfu). Once infected, cells they were treated with nocodazole (50ng/ml) for 16h. Cells were washed twice in PBS and stimulated with 10% FCS for the noted timepoint. Whole cell lysates were prepared, separated by SDS PAGE and probed for p-Histone H3 (ser10) (17kDa), p-ERK1/2 (44/42kDa)GAPDH (37kDa) as described in the Material and Methods section. These results are representative of 3 independent experiments.

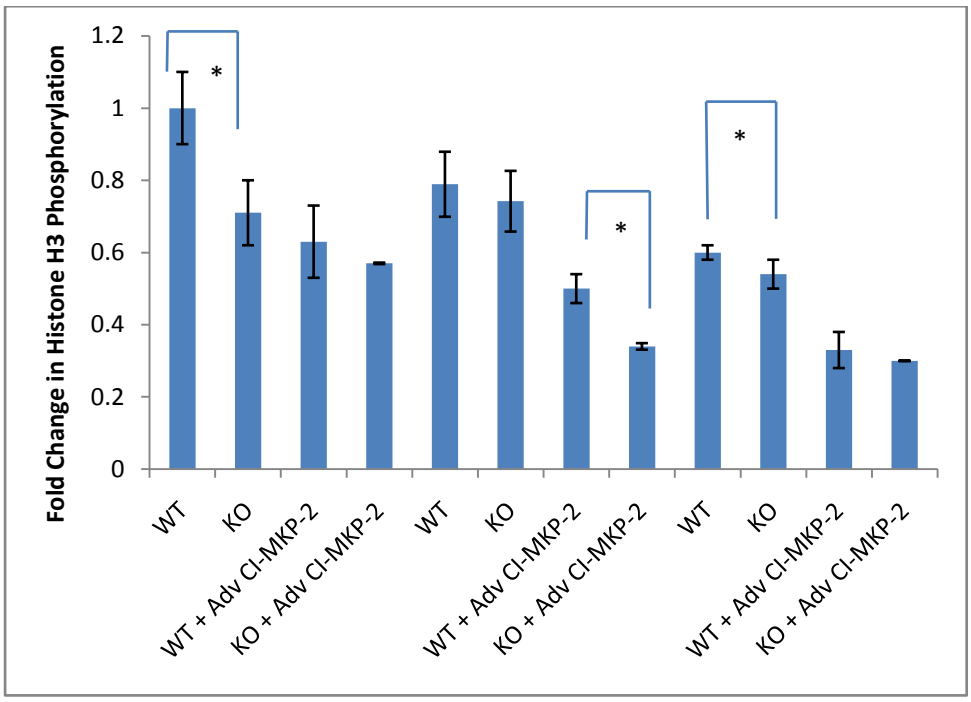

Figure 3.26Cont. Effect of Adv.Ci-MKP-2 on MASMCs in proteins required for cytokinesis

Subconfluent mouse aortic smooth muscle cells were infected with Adv.CI-MKP-2 (300pfu). Once infected, cells were treated with nocodazole (50ng/ml) for 16h. Cells were washed twice in PBS and stimulated with 10% FCS for the noted timepoint. Whole cell lysates were prepared, separated by SDS PAGE and probed for p-Histone H3 (ser10) (17 kDa)as described in the Material and Methods section. These results are representative of 3 independent experiments. . *P<0.05 mean ± SEM

3.3 Discussion

MAP kinase phosphatase-2 (MKP-2) is a type 1 dual specificity phosphatase (DUSP) which has been previously shown to regulate the activities of MAP kinase substrates, ERK and JNK *in vitro* (Misra-Press *et al*. 1995; Owens and Keyse, 2007; Lawan *et al*., 2012). However, unlike other DUSP family members, the cellular functions of MKP-2 are not well described within the literature. This chapter focused upon the use of a novel MAP kinase phosphatase-2 knockout (MKP-2) mouse and investigated the consequences of deletion on both, MAP kinase regulation and cellular growth. MKP-2 is often overshadowed by the prototypic phosphatase, MKP-1 largely due to their significantly similar sequence homology and function as type 1 DUSPs. Considerations have also implied that there is potential for overlapping or compensatory functions between MKP-1 and MKP-2. Indeed, as previously the MKP-2 knockout mouse generated did not display an obvious phenotypic change; they were of normal weight, fertile and displayed no developmental, growth or behavioural abnormalities (Lawan *et al*., 2011). This is consistent with mice lacking MKP-1, which show no phenotypic abnormalities and cells generated from these mice demonstrate no sign of irregular regulation of ERK signalling (Dorfman *et al*., 1996).

Firstly, aortae dissected from wild-type and knockout MKP-2 mice were assessed to investigate their endogenous structural phenotypes. As discussed within the results text, there are no major structural differences exhibited between MKP-$2^{+/+}$ and $MKP^{-/-}$ aortae. There have yet to be published data to support this, as no histology of the aorta has previously been conducted in Dusp4 mice. It should be recognised that the aortae staining shown in Figure 3.1 were carried out using basic haematoxylin and eosin which highlights merely nucleus and cytoplasm. However time permitting, further investigative stains such as Masson's trichrome for collagen composition or smooth muscle actin to assess a possible difference in cellular composition with the vessel. In order to confirm the cells grown in culture were specifically smooth muscle cells originating from the medial layer of the aorta, they were probed for SMA-α by both immunofluorescence and Western blotting. Both methods resulted in a positive result

of the smooth muscle actin marker, confirming that both MKP-$2^{+/+}$and MKP-$2^{-/-}$ cells in question possessed the specific contractile phenotype associated with MASMCs. Further analysis was carried out in order compare the ability of both wild-type and MKP-2 knockout cells to differentiate from contractile to synthetic, proliferative MASMCs driven by PDGF stimulation. As displayed in Figure 3.2 both wild-type and MKP-2 knockout cells display a comparable level of differentiation denoted by the reduction of SMA-α expression. No study has previously investigated the effect of MKP-2 on SMA-α expression; however SMC differentiation was shown to be altered in MKP-1 knockout mice. Lung slices obtained from an MKP-1 deficient mouse expressed higher levels of SMA-α when compared with MKP-$1^{+/+}$ mice under hypoxic conditions (Shields et al., 2011). This study suggests exaggerated SMA expression in the vascular wall of MKP-1-null lung, may be due to chronic exposure to hypoxia triggering structural remodelling of the wall (Shields et al., 2011). The contradiction between these studies may implicate differential roles for MKP-1 and MKP-2 despite the similarity in the sequence homology; however it may also indicate merely a difference in response of SMA expression to PDGF and hypoxia.

The induction of MKP-2 was attained using established activation agents, fetal calf serum (Sloss et al., 2005). The induction of MKP-2 was observed 4h after serum stimulation in wild type MASMCs (figure 3.6). This in contrast to MKP-1 induction which is normally detected as early as 30 min to 1 h after treatment with serum and other activating agents (Wu and Bennett, 2005; Manetsch et al., 2013), suggesting that the mechanisms of induction of these phosphatases may not be the same. However, MKP-1 has been described as an early response gene and thus it is not surprising for the rapid activation to be evident. This compares well with work published by Lawan et al., (2011), in which mouse embryonic fibroblasts cultured from MKP-2 knockout mice; similar to the smooth muscle cell primary culture process utilised in this study. The induction of MKP-2 was observed 2 h after serum stimulation in wild type MEFs, suggesting a similar activation of MKP-2 in smooth muscle cells and fibroblasts.

In this current study, induction of MKP-2 expression was exclusively controlled by ERK signalling but not by JNK or p38 MAPK, indicating that activation of ERK pathway is sufficient to promote the expression of MKP-2 (figure 3.7). Like MKP-1, MKP-2 contains a X(S/T)P motif (X, any neutral or basic amino acid; S/T, serine or threonine; P, proline), which can be usually recognized and phosphorylated by ERK (Clark-Lewis et al., 1991; Gonzalez et al., 1991; Zhang et al., 2007). Although MKP-2 can be regulated by ERK, the mechanism underlying its regulation is not fully understood. Peng et al., (2010) investigated activation of MKP-2 in MDA231 breast cancer cell lines, where they detail MKP-2 to be completely inhibited by the MEK inhibitor U0126, and partially inhibited by the p38 inhibitor SB203580. However, the JNK inhibitor SP600125 had no effect on phosphorylation of MKP-2. This group further describe how SB203580 partially inhibited the activation of ERK, which could explain why SB203580 has some effects on phosphorylation of MKP-2. Taken together, it can be deduced that MKP-2 activation is primarily controlled by ERK signalling. This further supports earlier studies implicating MKP-2 as part of a negative feedback loop for down regulating ERK phosphorylation and hence mitogenic signalling (Guan and Butch, 1995). Interestingly, it should not be overlooked that although the U0126 inhibitor resulted in a reduction in MKP-2 activation in MASMCs, it was not completely abolished. This could suggest a potential role for non-MAP kinase involvement in the activation of MKP-2 in smooth muscle cells. However it must not be overlooked that the inhibition of ERK may alter the stability of MKP-2 and therefore would suggest a possible accountability for the reduction in ERK expression.

MAP kinases also regulate the stability of DUSPs at the protein level by binding to MAP kinase substrates (Camps, et al. 1998). Interestingly MKP-1 has conflicting roles in protein stabilisation, where MAP kinase binding can decrease protein stability and promote MKP-1 proteolysis through the ubiquitin ligase SCFSkp2 (Lin and Yang et al., 2006). However, ERK-mediated phosphorylation of C-terminal residues (Ser359 and Ser364 in DUSP1⁄ MKP-1) in DUSP1⁄MKP-1 has been shown to result in increased protein stability, thus resulting in positive reinforcement of phosphatase activity and autoregulatory negative feedback control. Further examples include how DUSP5

expression has been found to be reduced by incubation with the MEK inhibitor U0126, post protein induction (Kucharska et al., 2009), suggesting a requirement for ERK activity. Similarly, treatment with U0126 also decreased MKP-3 mRNA and protein expression (Zeliadt et al., 2008). Moreover, a dual effect of mTOR phosphorylation of MKP-3 on Ser159 and ERK phosphorylation of Ser197 residues results a threefold reduction in MKP-3 half-life, forming a positive feedback loop following mitogenic stimulation (Marchetti et al., 2005). Thus a general pattern has emerged suggesting that ERK binding to MKPs is essential for full protein expression. Work from our laboratory detailed a variant of MKP-2 lacking the ERK binding was more prone to proteolytic degradation (Cadalbert et al., 2010). Recent work has detailed how ERK-mediated phosphorylation of C-terminal residues on MKP-2 increased protein stability (Cagnol and Rivard, 2012). However, it is notable that the ERK-dependent phosphorylation sites on MKP-1 and MKP-2 are at the C-terminus, close to the catalytic site of ERK when associated via the N-terminal KIM domain.

Initial experiments have demonstrated that deletion of MKP-2 resulted in a slight increase in baseline ERK activity in cultured MASMCs (figure 3.9). This is supported by similar studies in MKP-3 knockout fibroblasts which reported higher basal ERK phosphorylation (Maillet et al. 2008). However, SMC derived from human carotid artery with MKP-1 over-expression displayed no difference in baseline ERK phosphorylation, thus suggesting that certain MKPs may function to regulate the baseline tone of some of the MAP kinases. It was also found that ERK phosphorylation did not increase in response to PDGF or FCS in MKP-$2^{-/-}$ MASMCs over a time course that was similar to that of MKP-2 induction (Figure 3.5). The surprising lack of difference in ERK signalling between MKP-$2^{+/+}$ and MKP-$2^{-/-}$ MASMC was supported by a report by Al- Mutairi et al., (2010) of which observed in macrophages, ERK signalling was not enhanced subsequent to MKP-2 deletion. This is contrast to work published by Lawan et al., (2011) where PDGF stimulated MKP-$2^{-/-}$MEFs resulted in a significant, albeit slight increase in ERK phosphorylation. Smooth muscle cell ERK phosphorylation has been shown to be sustained upon stimulation (McDonald et al., 2010). It should be recognised that despite the seeming lack of change of ERK in

MKP-2 deficient smooth muscle cells, further experimentation should be carried out to investigate the subcellular location of the active ERK; this could be completed by simple immunofluorescent microscopy or crude nuclear extracts. Furthermore, the surprising unaltered ERK signalling in MKP-$2^{-/-}$ MASMCs may be due to a reconditioning of the smooth muscle cell phenotype, when residing in the aorta they do not proliferative endogenously but do so in response to injury. However, due to the mechanical stress endured throughout the primary culture process, combined with constant serum treatment may have conditioned the smooth muscle cells to have a sustained ERK activation, thus it is likely that the magnitude of activation obscured the potential regulatory effects of MKP-2 deletion.

An initial important finding in this study was the observation that the loss of MKP-2 protein caused alteration in the proliferation of MASMCs. Smooth muscle cells derived from MKP-$2^{-/-}$ exhibited significantly reduced cell growth compared with MKP-$2^{+/+}$ counterparts (figure 3.10 & 3.11). In contrast, further studies utilising a Dusp4 knockout mouse in an immunological setting, observed that CD4 T-cells deficient in MKP-2 were hyperproliferative with enhanced IL-2/IL-2R expression; nonetheless, no effect was exhibited of the knockout on the MAP kinase signalling profile (Huang et al., 2012). However, the finding in this present study is similar to more recent data which showed that deletion of MKP-2 inhibited the proliferation of fibroblasts (Lawan et al., 2011) therefore the proliferative alterations by MKPs may act in cell-type specific manner. It has been demonstrated that in response to serum, MKP-1 over-expression in vascular smooth muscle cells (VSMC) led to an inhibition of DNA synthesis thereby inhibiting VSMC proliferation (Li et al., 1999). This was supported by Chai et al., (2002) who detail how over-expression of MKP-1 in smooth muscle cells derived from spontaneously hypertensive rats result in a reduction in proliferation. Another report also demonstrated that fibroblasts derived from MKP-1 knockout mice displayed equal levels of ERK activity and cell proliferation with that of MKP-$1^{+/+}$ MEF (Dorfman et al., 1996). The authors concluded that MKP-1 plays a redundant role in the control of ERK activity and cell proliferation, yet this hypothesis does not correlate with the current study nor numerous other published data as described above.

These studies and the data presented in this chapter indicate that deletion the of some MKPs can lead to alteration in cell growth; whether it results in a hyperproliferative or hypoproliferative phenotype.

The decrease in proliferation in MKP-2 deficient MASMCs correlated with a significant accumulation of cells in G2/M phase (Figure 3.12). This is consistent with work published where fibroblasts derived from MKP-$2^{-/-}$mice exhibit a G2/M accumulation (Lawan et al., 2011). Indeed, it was reported that siRNA mediated knock down of MKP-2 protein expression attenuated the proliferation of MKK-f cells in vitro and in vivo, which was correlated with the inhibition of cyclin B1 expression and cdc-2 phosphorylation (Hasegawa et al., 2008) Other MKPs have been implicated in cell cycle progression, where MKP-4 over-expression resulted in an ERK-independent G2/M associated cell death and microtubule disruption (Liu et al., 2006).

However, in the current study analysis of some of the cell cycle regulatory proteins were not consistent with G2/M phase arrest, for example the expression patterns of cyclin B1 and p-cdc-2 were unaltered in MKP-$2^{-/-}$ MASMCs (Figure 3.13). The findings outlined in this chapter could possibly be due to only a proportion of cells were delayed in this phase of the cycle and that a large proportion of the cells progressed through the cycle normally and change in protein may be concealed. This limitation could be overcome by refining the population using cell sorting techniques and extracting the viable cells and subsequently assessing cdc-2 and cyclinB1 expression. Interestingly, a mechanism known as “mitotic slippage” is of increasing interest within the cancer chemotherapy field, a process by which cells can eventually override mitotic arrest without the completion of cytokinesis, resulting in hyperploid formation independent of cyclin B1 and p53 regulation (Huang et al., 2010; Toda et al., 2012). Therefore it could be hypothesised that MKP-$2^{-/-}$ MASMCs may undergo mitotic slippage. Accounting for the G2/M accumulation of these cells despite the molecular expression of cyclin B1 and cdc-2 remaining comparable between MKP-$2^{-/-}$ and MKP-$2^{+/+}$ MASMCs. Nevertheless, early work published details of how

butyrolactone, a cdc-2 specific inhibitor resulted in a G2/M accumulation but had no effect on mitotic slippage (Tsuiki et al., 2001).

Furthermore, it could also be suggested that the notable dysfunction in MKP-$2^{-/-}$ MASMCs could be very late in mitosis; the stage at which both cdc-2 and cyclin B1 are degraded thus MKP-2 deletion may be involved in late-stage mitosis. In order to investigate this possibility, time-lapse microscopy was utilised to build a more complex profile of smooth muscle cells in mitosis. Previous studies involving MKPs have failed to assess late mitotic function despite a reduction in proliferative capacity. By use of real-time imaging in MKP-$2^{-/-}$ MASMCs, a marked time increase in abscission completion was observed (Fig 3.18). Overall, the success rate of cells deficient in MKP-2 completing cytokinesis was markedly reduced in comparison with wild-type. Notably, the extension of the intercellular bridge was longer in length for the MKP-2 knockout in comparison with the wild-type suggesting dysfunction in the final stage of cytokinesis, known as abscission (Figure 3.15). No previous data has been published to investigating a role for MKPs in cytokinesis, or more specifically abscission. Following abscission, the residual midbody structure, known as the midbody derivative, possesses cell-type specific fates. The midbody derivative is either released to the extracellular medium (Ettinger et al., 2011), degraded by autophagy (Pohl & Jentsch, 2009) or persists in the cytoplasm (Ettinger et al., 2011). Therefore it could be suggested that MKP-2 may play a role in autophagy in the final processing of the midbody derivative. To date, no studies investigating a role for MKPs in autophagy have been conducted. However, autophagy is driven by Akt/mTOR signalling which is known to be MAP kinase-induced (Olsen et al., 2012), therefore regulation of MAP kinase signalling by MKPs could suggest a potential regulatory role for MKPs in autophagy.

Despite these suggestions for a possible regulatory role for MKP-2, the effect of MKP-2 deletion should not be overlooked. As previously discussed, the seeming lack of change of ERK in MKP-2 deficient smooth muscle cells, does not investigate the subcellular location of the active ERK. This could be important as MKP-2 may have

the potential to act as a shuttle protein and therefore phosphorylation may appear unchanged, when in fact the phosphorylated ERK could be accumulating in the cytoplasm. When discussing cytokinesis, ERK has shown to be crucial in the completion of abscission; where treatment with U0126, an ERK pathway inhibitor, decreases tyrosine phosphorylation levels at the midbody, leading to abscission failure in HeLa cells (Kasahara et al., 2007). Further study details how Src kinase activity during the early mitosis mediates ERK activation in late cytokinesis, indicating that Src-mediated signalling for abscission is spatially and temporally transmitted (Kasahara et al., 2007). Therefore, with the apparent unaltered ERK signalling in MKP-$2^{-/-}$ MASMCs, there is a possibility of MKP-2 acting upon Src kinase mediating cytokinesis in an indirect manner. This would not be their first interaction between Src kinase and a member of the MKP family; by use of pharmacological tools, a Src kinase inhibitor (PP1) completely blocked both VEGF- and thrombin-induced MKP-1 expression (Kinney et al., 2008). The result of this study may merely suggest that Src kinase activates ERK, which is required for MKP-1 activation and therefore inhibiting this kinase would result in a downregulation of ERK and subsequently, MKP-1 expression. However, this theory is neither confirmed nor disputed. Therefore a potential role for MKP-2 in regulating cytokinesis via Src kinase could be viable option for further investigation.

In addition to the late mitotic phenotypic changes, molecular levels correlated with a reduction Aurora B phosphorylation in the MKP-$2^{-/-}$ synchronised MASMCs. Severson et al., (2000) describe the requirement for Aurora B activity in order for the effective execution of cytokinesis, supporting data obtained from time-lapse microscopy. A large number of studies investigating cytokinesis use a yeast interaction model where a pivotal role of Aurora B in microtubule disassembly (Buvelot et al., 2003) and abscission (Norden et al., 2006) has been elucidated. In budding yeast, Ipl1 (the yeast equivalent to mammalian Aurora B) plays a role during cytokinesis by controlling the NoCut pathway that prevents abscission. Ipl1 controls the localisation of the anillin-related proteins Boi1 and Boi2, which they can function as abscission inhibitors and prevent premature abscission and concomitant chromosome breakage (Norden et al.,

2006). Conversely, inhibition of Aurora B kinase by B181123 leads to the formation of polyploidal cells supporting the correlation of reduced Aurora B and G2/M accumulation in MKP-2 knockout MASMCs. Counterintuitively, by inhibiting Aurora B kinase, multinucleate cells formed to continue to divide however they will resultantly become senescent or undergo apoptosis (Gurtler et al., 2010). Recently, Aurora B is becoming linked as a marker in many hyperproliferative cancers where the gene is not reported to be commonly amplified nor specific mutations present (Fernandez-Miranda et al., 2011). However, over-expression at the mRNA and protein levels was reported in different types of cancer including breast, colorectal, kidney, lung and prostate carcinoma (Reviewed in Hegyi et al., 2012).

Another emerging marker of Aurora B activity is the downstream target, histone H3 (Ser10). H3 phosphorylation is believed to be involved in two structurally opposed processes: transcriptional activation (Nowak and Corces, 2000), requiring chromatin decondensation, and chromosome compaction during cell division (Kaszas and Cande, 2000). As shown in Figure 3.19, a marked reduction in Histone H3 (Ser10) phosphorylation was exhibited in synchronised MKP-$2^{-/-}$ MASMCs compared with MKP-$2^{+/+}$ cells; a result consistent with the reduction in upstream aurora B phosphorylation. Interestingly, there was no difference in phosphorylation of Histone H3 in asynchronous cells which could be significant of the multiple upstream targets of Histone H3 compensating for the lack of Aurora B activity. Recent work has described how MKP-2 regulates histone H3 phosphorylation in response to oxidative stress in mitosis, however does not act via direct dephosphorylation (Jeong et al., 2013). Instead, it has been described that MKP-2 interacts with VRK1, another mitotic kinase similar to aurora B, to modulate histone H3 activity regardless of MKP-2 phosphatase activity. Conversely, histone H3 was deemed a novel substrate of MKP-1 in endothelial cells; where MKP-1-substrate complexes were immunoprecipitated, which yielded four bands of 17, 15, 14, and 10 kDa identified by mass spectrometry as histones H3, H2B, H2A, and H4, respectively (Kinney et al., 2009). Collectively these data depict the potential for MKPs to interact with histone H3 in modulating gene

expression and mitotic function- whether the interaction be via direct dephosphorylation or otherwise.

In this study the adenoviral mediated over-expression of WT-MKP-2 was utilised as an experimental pharmacological tool to reverse the proliferative dysfunction observed in MKP-$2^{-/-}$ MASMC. In the current study however this is not the case, over-expression of WT-MKP-2 in wild-type and MKP-2 redundant MASMCs resulted in a reduction in proliferation in both cell types when compared to wild-type cells. This supports data described earlier in this chapter, where MKP-2 is noted to be essential in proliferation and thus modulating MKP-2 expression has a detrimental effect on cellular growth. However, somewhat contradictory evidence has been published. MEFs derived from our MKP-2 knockout mouse and treated with Adv.WT-MKP-2, exhibited a recovery of proliferative capacity (Lawan et al., 2011) an effect not seen in the current study. Interestingly, the published work did not detail the effect of MKP-2 over-expression on wild-type cells, where it was evident in MASMCs that MKP-2 over-expression was detrimental to the capacity of both MKP-$2^{+/+}$ and MKP-$2^{-/-}$ cells to proliferate.

Further investigations detail how MKP-2 over-expression results in a G1/S accumulation in both MKP-$2^{+/+}$ and MKP-$2^{-/-}$ MASMCs. No previous study has assessed the cell cycle progression profile of cells infected with Adv.WT-MKP-2. However, in rat arterial smooth muscle cells overexpressing MKP-1, growth was arrested in the G1 phase and entry into the S phase was blocked, supporting the findings of the current study. They believe the reduction in MKP-1 expression may contribute in part to proliferation of smooth muscle cells after vascular injury, possibly through a decrease in dephosphorylation of ERK (Lai et al., 1996). As shown in Figure 3.23, Adv.WT-MKP-2 ablates ERK signalling and could therefore account for the G1/S accumulation observed. The detrimental effect of ERK inhibition has been well documented in the prevention of S phase progression (Ussar & Voss, 2004), where following G1/S arrest, known proteins upstream of ERK, including Raf and MEK, are not activated. However, retained ERK activation under conditions in which Raf and MEK activation is lost is observed, suggesting that G1/S arrest acts at the level of ERK

dephosphorylation; suggesting action may be via MKPs. The responsibility of ERK in G1/S progression is established within the literature, a novel MEK inhibitor JTP-70902 is utilising this interaction in an antitumour setting to reduce the growth of fibrosarcoma cells (Matsui et al., 2010). Collectively, these data can explain how cells over-expressing WT-MKP-2 reduces their proliferative capacity, via ERK ablation and subsequent G1/S accumulation. Therefore, utilising Adv.WT-MKP-2 does not seem an ideal tool to assess a gain of function in MKP-$2^{-/-}$ MASMCs which display a dysfunction in late stage mitosis. Ideally, an inducible WT-MKP-2 adenovirus could have been employed which would allow for cells to surpass S phase and reach mitosis, to assess any possible regain of phenotype.

From the data discussed so far, it can be concluded that MKP-2 deficient MASMCs exhibit no apparent difference in MAP kinase signalling but do possess a significant dysfunction in cytokinesis, thus it could be suggested that the loss of proliferative capacity may act independent of MAP kinase activity. In order to investigate this hypothesis further, a constitutively-inactive adenoviral MKP-2 was utilised. Removing the catalytic activity of MKP-2 initially seemed promising with a significant reduction in G2/M accumulation in MKP-$2^{-/-}$ MASMCs over-expressing CI-MKP-2; thus we hypothesised that MKP-2 would have the capacity to bind with a substrate to promote successful mitotic exit. However, further analysis proved controversial where both MKP-$2^{+/+}$ and MKP-$2^{-/-}$ MASMC exhibited a marked reduction in proliferation, with a reduction in cytokinetic protein expression suggesting a detrimental consequence by the removal the catalytic activity of MKP-2. The current study, for the first time suggests a unique role for MKP-2 in cytokinesis requiring its phosphatase activity, albeit in a non-MAP kinase dependant manner. Therefore suggesting MKP-2 has the potential to interact with non-MAP kinase substrates in order to regulate cytokinesis. Indeed, numerous conflicting studies have shown other MKPs have targeted proteins out with their documented MAP kinase specificity; MKP-1 has been proposed to act as a phosphatase towards phosphorylated histone H3. Specifically, it was found that the dephosphorylation of histone H3 (Ser10) correlated exactly with the kinetics of MKP-1 protein induction in response to thrombin and vascular endothelial

growth factor. Both *in vitro* phosphatase assays and the results of siRNA-mediated knockdown suggested that MKP-1 was the responsible activity (Kinney et al., 2009). Controversially, the Caunt group derived MEFs from MKP-1 deficient mice and in agreement with the previous publication; they found that histone H3 dephosphorylation correlated exactly with the appearance of the MKP-1 protein. However, the kinetics of dephosphorylation were identical in cells lacking MKP-1, indicating that this phosphatase is unlikely to be the activity responsible (Staple et al., 2010). Furthermore, the ERK-specific cytoplasmic phosphatase MKP-3 has been implicated in the positive regulation of gluconeogenic gene expression and is upregulated in the livers of diet-induced obese mice. It has suggested that MKP-3 may intervene more directly in this pathway by interacting with and dephosphorylating the transcription factor forkhead box O1 (FOXO1). MKP-3 mediated dephosphorylation of Ser256 in FOXO1 is proposed to promote FOXO1 nuclear import, thus increasing its transcriptional activity. The main evidence implicating MKP-3 in the regulation of FOXO1 was its coimmunoprecipitation with FOXO1 and its ability to dephosphorylate FOXO1 when coexpressed in cells. It was therefore concluded that MAPK phosphatase-3 promotes hepatic gluconeogenesis through dephosphorylation of forkhead box O1 in mice (Wu et al., 2010). To the date, only one study has detailed MKP-2 directly interacting with a non-MAP kinase substrate, VRK1 regardless of its phosphatase activity (Jeong et al., 2013). Further investigation to elucidate the site of interaction was in the chromatin fraction; more specifically MKP-2 interacts with VRK1 in the heterochromatin fraction, where histones are abundant and MKP-2 and VRK1 exist together. This could serve as a potential mechanism of action to the cytokinetic dysfunction in MKP-$2^{-/-}$ MASMC, where cells deficient in MKP-2 lack the VRK1 interaction on heterochromatin and subsequently alter histone H3 activity.

Ultimately, throughout this chapter there have been some baseline errors that were initially overlooked which would have strengthened the impact of this data. Firstly, for all Western blots carried out, Bradford assays to quantitatively assess the amount of protein in each sample would have been advantageous. Instead, protein in each samples was estimated by comparable confluency of cells and subsequently compared

to the loading control. Furthermore, analysis of Western blotting could have been clearer by quantifying bands as a ratio to the loading control.

In conclusion, the findings in this study strongly suggest that MKP-2 is necessary for cell proliferation and more specifically, cytokinesis. It also demonstrates that the mechanism, by which MKP-2 controls mitotic progression, requires its phosphatase activity albeit possibly in a non-MAP kinase dependant manner.

Chapter 4: Effect of MKP-2 over-expression on cellular proliferation in human aortic smooth muscle cells (HASMC).

4.1 Introduction

The results in chapter 3 demonstrated a novel role for MKP-2 in mouse aortic smooth muscle cell proliferation. Adenoviral over-expression of MKP-2 was shown to result in a reduction in proliferation and failure to regain the function of MKP-$2^{-/-}$ MASMCs, serving to be a rather impractical tool for the elucidation of the mechanism of proliferative dysfunction. Nevertheless, the use of Adv.WT-MKP-2 may have the potential to be utilised as a therapeutic agent to reduce smooth muscle cell proliferation. This in itself may be a useful approach, as several cardiovascular diseases have a well-accepted pathology that underlying smooth muscle hypertrophic remodelling is also a key event in cardiovascular disease. This adaptive phenotype is a marker of atherosclerosis, (Brevetti et al., 2003), hypertension (Mulvany, 2008), balloon angioplasty and stent insertion (Coats et al., 2008), critical limb ischaemia (Coats et al., 2003) and other conditions related to impaired peripheral flow. It is well established that MAP kinases play a key role in the induction of the VSMC hyperproliferative phenotype (Schad et al., 2011). MKP-2, as a type 1 nuclear phosphatase, possesses the ability to dephosphorylate and ultimately inactivate MAP kinases ERK and JNK *in vitro* (Lawan et al., 2012). Therefore, MKP-2 may be a novel therapeutic target in cardiovascular disease.

In this chapter, human aortic smooth muscle cells were used to assess the effect of WT-MKP-2 over-expression on HASMC function. Investigation of the proliferative capacity of the human smooth muscle cells, as well as their MAP kinase signalling profiles were analysed to assess the therapeutic potential of adenoviral MKP-2 in preventing hypertrophic remodelling of the blood vessel following injury or stent implantation.

4.2 Results

4.2.1 FCS-mediated activation of ERK and c-Jun signalling in HASMCs

Firstly, the effect of FCS treatment on MAP kinase phosphorylation in HASMCs was investigated. HASMCs were grown to confluency in 6-well plates and quiesced in 0.1% FCS for 24 h. As described with MASMC in Chapter 3, the phosphorylation level of MAP kinases was measured by Western blotting with antibodies that specifically recognize both phospho-Tyr and phospho-Thr residues that are regarded to be necessary and sufficient for the activation of MAP kinases. Both ERK and c-Jun phosphorylation was examined over early time courses. Cells were rendered quiescent overnight before stimulation with 10% FCS over a period of 120min. As depicted in Figure 4.1, initial FCS stimulation resulted in a rapid increase in ERK phosphorylation from control at 30 min (1±0.0 fold stimulation, 3.48±0.275 fold stimulation; p=0.012). This was sustained until 90min (3.48±0.275 fold stimulation, 3.54±0.14 fold stimulation; p=0.894). ERK phosphorylation at 120min was significantly reduced from the 90min time point (3.54±0.14 fold stimulation, 3.27±0.168 fold stimulation; p=0.047).

FCS stimulated HASMCs were assessed for the induction of p-c-Jun, cells were rendered quiescent overnight before stimulation with 10% FCS over a period of 120 min. As depicted in Figure 4.2, initial FCS stimulation resulted in a rapid increase in c-Jun phosphorylation from control at 30min (1±0.0 fold stimulation, 1.753±0.138 fold stimulation; p=0.032). The level of c-Jun phosphorylation was sustained until a significant increase in phosphorylation at the 90min time point, achieving the experimental maximal (C 1±0.0 fold stimulation, 90 min 3.337±0.529 fold stimulation; p=0.048). Observed at 120 min, was c-Jun phosphorylation reducing towards baseline levels.

4.2.2 PDGF-mediated activation of ERK and c-Jun signalling in HASMCs

Having established the ability of FCS to induce both ERK and JNK activation it was important to confirm a similar effect using PDGF, a physiologically relevant agent. PDGF stimulated HASMCs were assessed for ERK phosphorylation as shown in Figure 4.1. Cells were rendered quiescent overnight before stimulation with PDGF over a period of 120 min. Initial PDGF stimulation resulted in a rapid increase in ERK phosphorylation from control at 30min (1±0.0 fold stimulation, 3.98±0.182 fold stimulation; p=0.004), at this point the experimental maximal time of ERK phosphorylation is noted. ERK phosphorylation is reduced at 60min from 30min, albeit non-significantly (3.98±0.182 fold stimulation, 3.56±0.31 fold stimulation; p=0.088). The trend regarding the reduction of ERK phosphorylation across the time course was consistent, however at 120min the reduction of ERK from 30min is markedly reduced, nevertheless surprisingly insignificant (3.98±0.182 fold stimulation, 2.937±0.097 fold stimulation; p=0.062).

As shown in Figure 4.2, no PDGF-induced c-Jun phosphorylation could be detected. Unfortunately, JNK phosphorylation using specific antibodies for either p-c-Jun or p-JNK was not successful, stimulation was low and hard to see over background. Ideally, JNK activity would be assessed by an *in vitro* kinase assay using GST-c-Jun as a substrate (see Materials and Methods). However, time constraints did not allow the analysis of c -Jun phosphorylation.

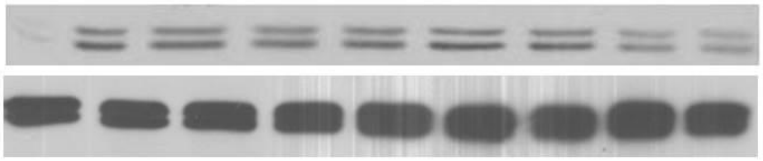

FCS (10%)	-	+	+	+	+	-	-	-	-
PDGF (10ng/ml)	-	-	-	-	-	+	+	+	+
Time (mins)	0	30	60	90	120	30	60	90	120

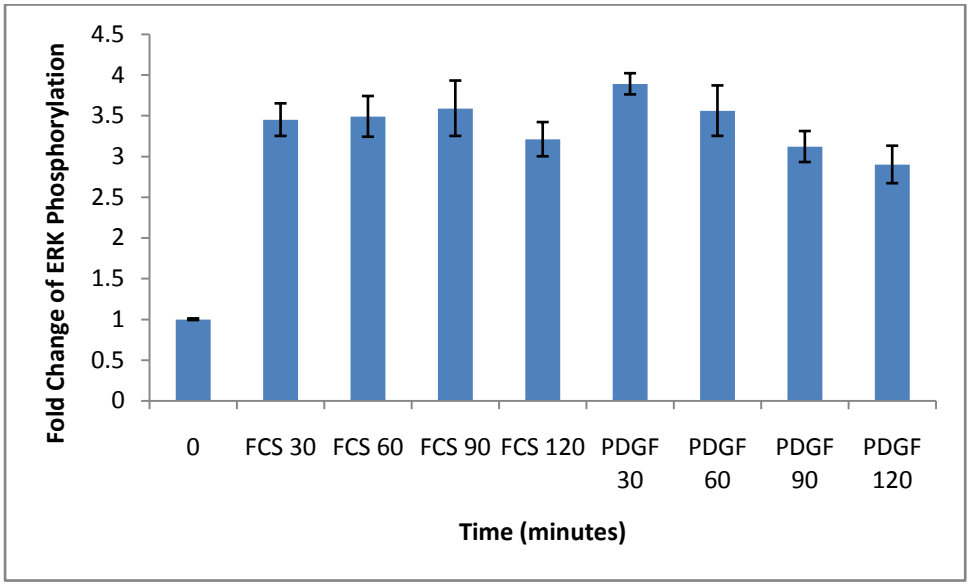

Figure 4.1: ERK signalling characterisation in HASMCs

Confluent human aortic smooth muscle cells of were rendered quiescent in 0.1% FCS for 24h prior to stimulation. Cells were then stimulated with 10% FCS or PDGF (10ng/ml) for times indicated. Cells were then lysed, run on SDS-PAGE and probed for p-ERK (44/42 kDa) and stripped and reprobed for T-ERK which was used a loading control (44/42 kDa). These results are representative of 3 independent experiments. Blots were quantified by scanning densitometry and mean ± SEM are displayed.

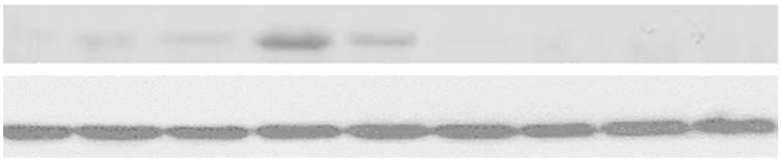

FCS (10%)	-	+	+	+	+	-	-	-	-
PDGF (10ng/ml)	-	-	-	-	-	+	+	+	+
Time (mins)	0	30	60	90	120	30	60	90	120

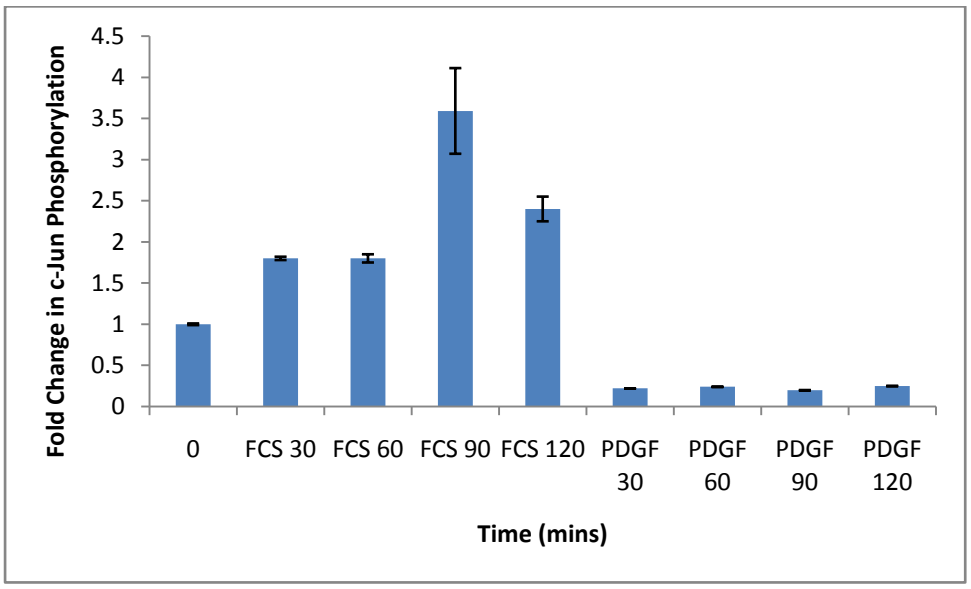

Figure 4.2: JNK signalling characterisation in HASMCs

Confluent human aortic smooth muscle cells of were rendered quiescent in 0.1% FCS for 24h prior to stimulation. Cells were then stimulated with 10% FCS or PDGF (10ng/ml) for indicated times. Cells were then lysed, run on SDS-PAGE and probed for p-c-Jun (37 kDa) and stripped and reprobed for c-Jun which was used a loading control as outlined in the Materials and Methods section. These results are representative of 3 independent experiments. Blots were quantified by scanning densitometry and mean ± SEM are displayed.

4.2.3 Proliferation of HASMC in comparison with MASMCs

Experiments assessing both human and mouse aortic smooth muscle proliferation by means of haemocytomer counting is a direct measurement of proliferation used to measure cell number at different time points (see Materials and Methods section). HASMCs were compared to MASMCs in order to ascertain appropriate comparisons with work detailed in Chapter 3. HASMCs were seeded to equal cell numbers and grown for 48h in 10% FCS.

As depicted in Figure 4.3, serum-stimulated MKP- $2^{+/+}$ MASMCs over a 48h time period, resulted in a significant increase in cell number which was apparent as early as 24 h (8.133±0.33, 15.64±1.13; p=0.016). The trend in cell number increase was observed in these cultures was alike to that exhibited in HASMC (8.84 ±0.216, 15.88±0.45; p=0.006). There were no significant difference in cell number between MASMCs and HASMCs at the 0h time point which would suggest no marked adherence difference (8.133±0.33; 8.84±0.2166; p= 0.916). At the later time point of 48h, a significant difference in proliferation was evident between MASMCs and HASMCs (Mouse 22.284±0.665x10^4 cell number, Human 17.29±1.607x10^4 cell number; p=0.02). This proliferation assay suggests HASMC proliferate at a slower rate than that of MASMCs.

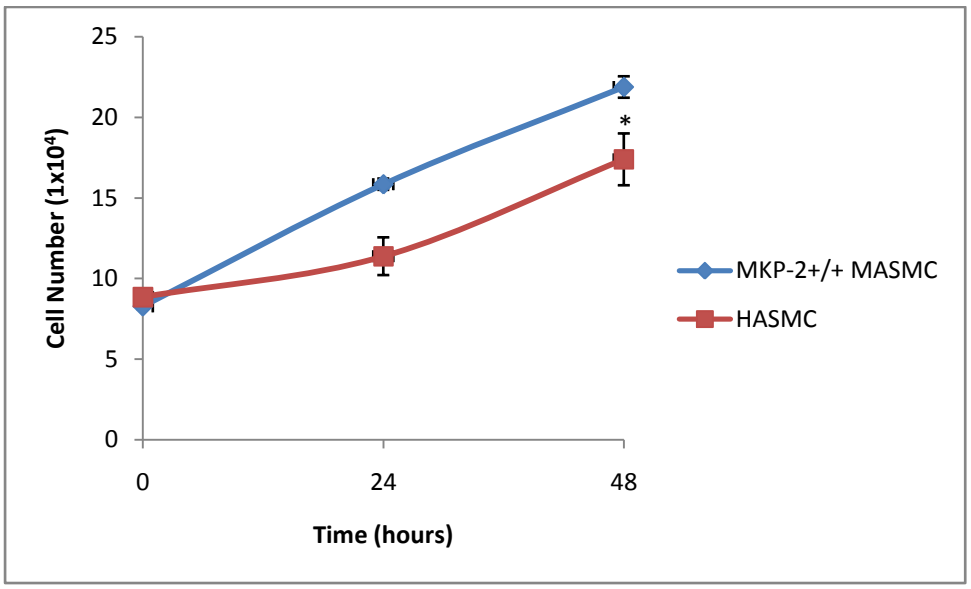

Figure 4.3 Proliferation of HASMC in comparison with MASMCs

Subconfluent mouse aortic and human aortic smooth muscle cells were rendered quiescent in 0.1% FCS for 24h prior to stimulation, both cell types were stimulated with 10% FCS for the times indicated. Proliferation was measured by cell counting at 24h intervals over a 48h time period. These results are representative of 3 independent experiments. *$p<0.05$

4.2.4 Over-expression of adenoviral WT-MKP-2 in HASMCs

Having established from previous experiments, that the over-expression of Adv. WT-MKP-2 could not reverse the deficit shown in MKP-$2^{-/-}$ MASMC cell growth and surprisingly served to be detrimental in proliferation of MKP-$2^{+/+}$ MASMCs, we assess whether Adv.WT-MKP-2 could serve as therapeutic agent in reducing SMC proliferation. For this purpose HASMCs were infected with increasing concentration of Adv.WT-MKP-2 (200-500pfu) and assessed for MKP-2 expression by Western blotting (see figure 4.4). Maximum expression was achieved between 300 and 500pfu. Based on this result HASMCs were infected with Adv.WT-MKP-2 at 300pfu the effect on MAP kinase signalling assessed at this concentration.

4.2.5 Over-expression of adenoviral WT-MKP-2 inhibits ERK signalling in human aortic smooth muscle cells

Since over-expression of MKP-2 via infection with Adv.WT-MKP-2 inhibited ERK phosphorylation in MASMCs, it was important to compare the effect of MKP-2 over expression on MAP kinase signalling profiles in HASMCs. Cells were incubated with Adv.WT-MKP-2 (300 pfu/cell) for 24h in quiescent media, prior to stimulation with FCS for times indicated. As depicted in Figure 4.5, ERK basal levels were high in both control and LacZ treated HASMCs, therefore only a modest increase in ERK phosphorylation was observed (1±0.0 fold stimulation, 1.15±0.051 fold stimulation). However, over-expression of WT-MKP-2 results in a significant inhibition, more so a complete ablation of ERK signalling, at time points as early as 15min (1.15±0.051 fold stimulation, 0.32±0.04 fold stimulation; p=0.012). This inhibition of ERK signalling was consistent across all time points assessed in HASMCs including 30 min (1.26±0.021 fold stimulation, 0.29±0.001 fold stimulation; p=0.006) and 60 min (1.18±0.03 fold stimulation, 0.362±0.09 fold stimulation; p=0.03). As described in section 4.2.2, unfortunately levels of JNK phosphorylation were deemed undetectable in either treated or untreated HASMCs. Nevertheless, it can be concluded that Adv.WT-MKP-2 possesses the ability to negate ERK signalling in HASMCs.

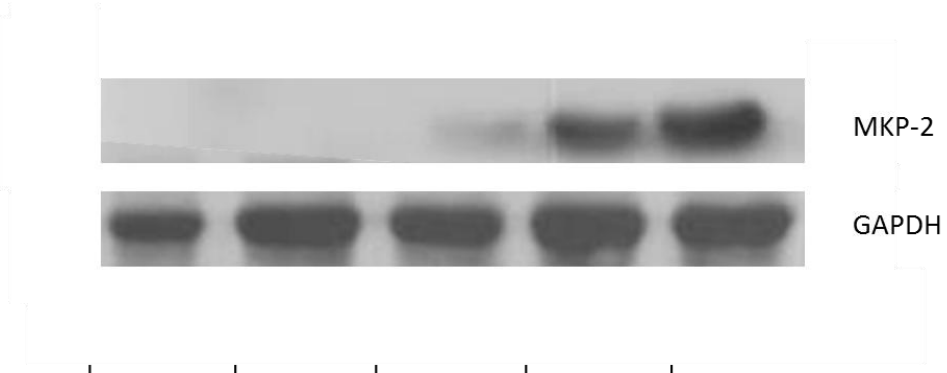

PFU			200	300	500
LacZ	-	+	-	-	-
Adv.WT-MKP-2	-	-	+	+	+

Figure 4.4 PFU curve of Adv. WT-MKP-2 in HASMCs

Subconfluent human aortic smooth muscle cells were infected with Adv.WT-MKP-2 in concentrations varying from 200-500 pfu in 0.1% media. Cells were stimulated in 10% FCS, prepared, separated by SDS PAGE and probed for MKP-2 (43 kDa) as described in the Materials and Methods section. Blots were stripped and reprobed for GAPDH which was used a loading control These results are representative of 3 independent experiments.

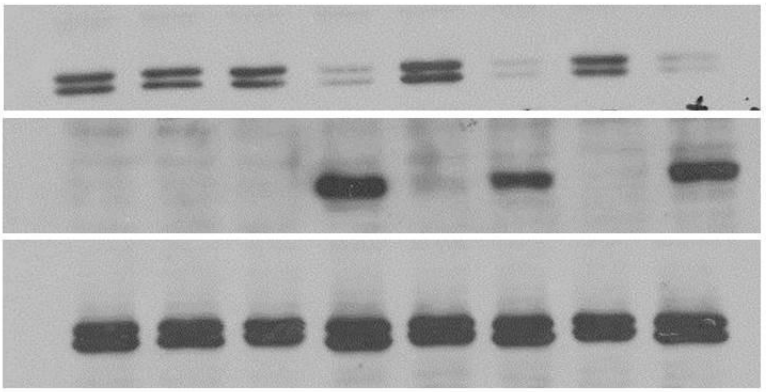

Time (mins)	0		15		30		60	
FCS (10%)	-	-	+	+	+	+	+	+
LacZ	-	+	-	-	-	-	-	-
Adv.WT-MKP-2	-	-	-	+	-	+	-	+

Figure 4.5: Effect of Adv. WT MKP-2 on ERK signalling

Subconfluent human aortic smooth muscle cells of were infected with Adv.WT-MKP-2 (300pfu) and rendered quiescent in 0.1% FCS for 24h prior to stimulation. Cells were then stimulated with 10% FCS for indicated times. Cells were then lysed, run on SDS-PAGE and probed for p-ERK (44/42kDa), T-ERK (44/42kDa) and MKP-2(43kDa) as described in the Material and Methods section. Blots were stripped and reprobed for T-ERK which was used a loading control *$p<0.05$ ***$p<0.01$ (15min $p=0.012$; 30min $p=0.006$; 60min $p=0.03$). These results are representative of 3 independent experiments. Blots were quantified by scanning densitometry and mean ± SEM are displayed.

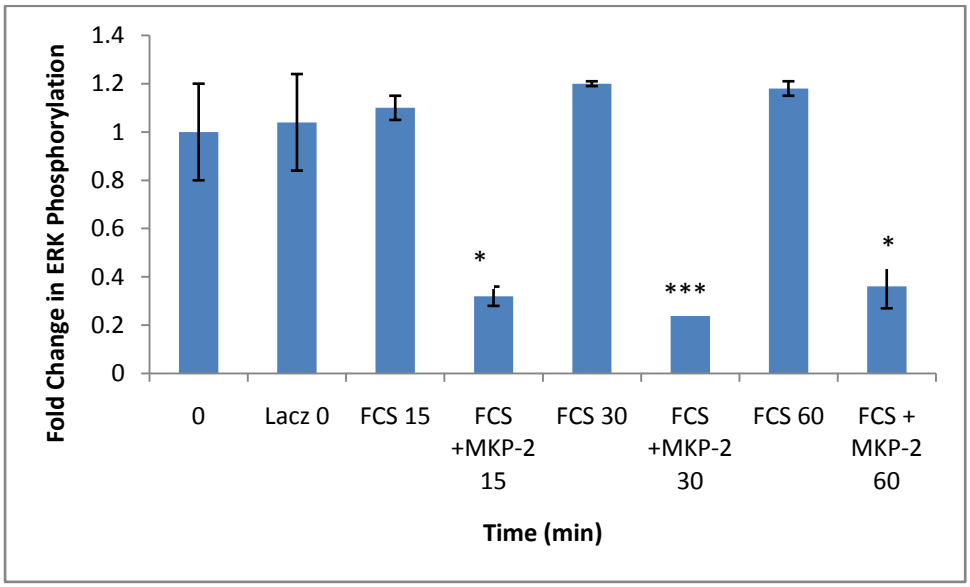

Figure 4.5: Effect of Adv. WT MKP-2 on ERK signalling

Subconfluent human aortic smooth muscle cells of were infected with Adv.WT-MKP-2 (300pfu) and rendered quiescent in 0.1% FCS for 24h prior to stimulation. Cells were then stimulated with 10% FCS for indicated times. Cells were then lysed, run on SDS-PAGE and probed for p-ERK (44/42kDa), T-ERK (44/42kDa) and MKP-2(43kDa) as described in the Material and Methods section. These results are representative of 3 independent experiments. Blots were quantified by scanning densitometry and mean ± SEM are displayed.

4.2.6 Over-expression of adenoviral WT-MKP-2 results in a reduction in human aortic smooth muscle cell proliferation

Based on the result of the pfu curve, human aortic smooth muscle cells were infected with Adv. MKP-2 at 300pfu and cellular proliferation assessed at this concentration. As depicted in Figure 4.6, serum-stimulated HASMCs of both Adv.WT-MKP-2 and uninfected cells were assessed over a 48h time period; a significant increase in cell number which was apparent as early as 24h in HASMCs (0h $8.849\pm0.33x10^4$ cell number, 24h 11.3 ± 0.31 $x10^4$ cell number; $p=0.022$). The trend in cell number increase was observed in LacZ treated human aortic smooth muscle cells and comparable to control cells (0h 9.002 ± 0.36 $x10^4$ cell number, 24h 12.92 ± 0.216 $x10^4$ cell number). There were no significant difference in cell number between Adv.WT-MKP-2 infected and uninfected HASMCs at the 0h time point which would suggest no marked adherence difference (8.849 ± 0.33 $x10^4$ cell number; 8.79 ± 0.12 $x10^4$ cell number; $p= 0.916$). Interestingly however, at the 24h time point, a marked but insignificant difference in LacZ-infected HASMC and Adv.WT-MKP-2 infected cell number was evident (LacZ 12.72 ± 1.21 $x10^4$ cell number, Adv. WT-MKP-2 10.28 ± 0.09 $x10^4$ cell number; $p= 0.074$). At the later time point of 48h, a significant difference in proliferation was observed between LacZ-infected HASMC and Adv.WT-MKP-2 infected cells (LacZ 16.75 ± 0.75 $x10^4$ cell number, Adv.WT-MKP-2 12.15 ± 1.07 $x10^4$ cell number; $p=0.005$). This proliferation assay suggests that increase of MKP-2 expression results in a reduction of human aortic smooth muscle cell proliferation.

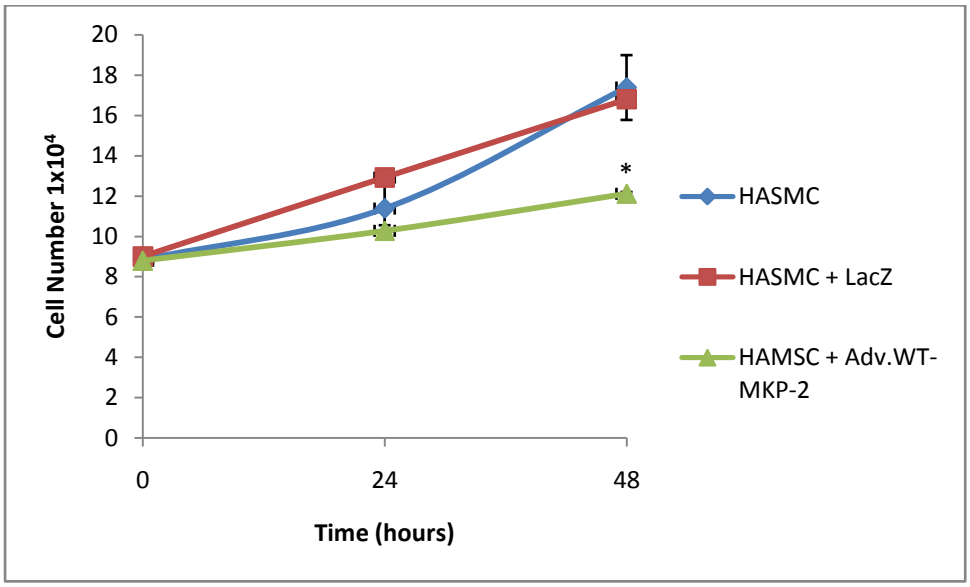

Figure 4.6: Effect of Adv. WT MKP-2 on proliferation in HASMC

Subconfluent human aortic smooth muscle cells were infected with Adv.WT-MKP-2 (300pfu) and rendered quiescent in 0.1% FCS for 24h prior to stimulation. Cells were then stimulated with 10% FCS for 48h over 24h time periods. Proliferation was measured by cell counting at 24h intervals over a 48h time period. These results are representative of 3 independent experiments. *$p<0.05$

4.2.7 Over-expression of adenoviral WT-MKP-2 inhibits G1/S progression of human aortic smooth muscle cells.

Following the observation that the over-expression of MKP-2 significantly reduced smooth muscle cell proliferation, further experiments were conducted to elucidate the difference in growth characteristics by investigating cell cycle parameters. Flow cytometric analysis using DNA propidium iodide staining was used to assess each phase of the cell cycle. The results presented in Figure 4.7 demonstrated that unsurprisingly, FCS stimulated an increase in cells in G2/M phase when compared to control (C 6.13±1.18, FCS 16.10±1.62; p=0.022). Although the induction is stark, it is currently not significant post Bonferoni's considerations. In concordance with this data, the number of HASMC residing in G1 phase of the cell cycle is significantly reduced as they drive towards mitosis (91.43±1.56, 78.93±1.39; p=0.000). The use of an empty LacZ adenoviral vector had no effect of the proliferation of HASMC cell cycle progression with a comparable of cells in G2/M phase (FCS 16.10±1.62, LacZ + FCS 16.73±0.50 p=0.768). Interestingly, over-expression of MKP-2 resulted in a significant reduction in cells in the G2/M population in comparison with LacZ control (LacZ 16.73±0.50, Adv.WT-MKP-2 16.733±0.498; p=0.009). As the data is assessed as percentage population, it does not seem surprising that as the G2/M population has decreased, the G1 population has increased. However, it should be noted that this G1 accumulation in Adv.WT-MKP-2 treated HAMSC, was not significant (p=0.081). This result supports data described in section 4.2.6 where Adv. MKP-2 over-expression proved detrimental to the ability of HASMCs to proliferate; suggesting that alteration of MKP-2 expression is responsible for the decrease in cell growth observed in these cells.

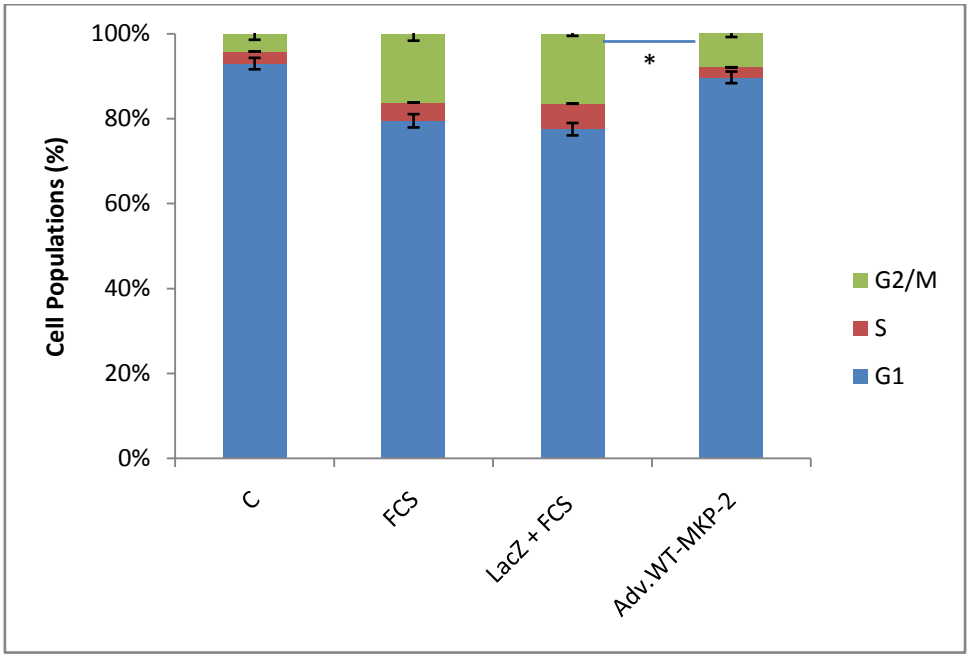

Figure 4.7 Effect of Adv.WT-MKP-2 on cell cycle progression in HASMCs

Subconfluent human aortic smooth muscle cells were infected with Adv.WT-MKP-2 (300pfu) rendered quiescent in 0.1% FCS for 24h prior to stimulation, cells were then stimulated with 10% FCS for 24h. Whole cells were harvested and stained with propidium iodide as described in the Material and Methods section. These results are representative of 3 independent experiments, mean ± S.E. Statistical analysis was corrected using Bonferoni's considerations *$p<0.0167$.

4.3 Discussion

As discussed in Chapter 3, the cellular function of this poorly studied MKP family member is not well described especially in the vascular system. In this chapter, use of adenoviral MKP-2 was utilised to assess the consequence of MKP-2 over-expression at the level of MAP kinase regulation, in relation to proliferation and also cell cycle progression. This chapter focussed upon the use of human aortic smooth muscle cells and the potential to utilise adenoviral MKP-2 in a therapeutic setting against the SMC hyperproliferative phenotype associated with many vascular disorders (Coats et al., 2008; Brevetti et al., 2003). Initial experiments in HASMCs illustrated that both FCS and PDGF activated ERK signalling in a time dependent manner with similar kinetics. These results were consistent with previous findings in human aortic smooth muscle cells where FCS and PDGF induced DNA synthesis, proliferation and differentiation (Beamier et al., 1998).

However, the JNK pathway which is well known to be activated primarily by cellular stresses and implicated in mediating apoptosis has also been demonstrated to play a role in growth factor mediated cellular proliferation in other cell types (Potapova et al., 1997, Smeal et al., 1991). In this chapter, JNK was phosphorylated in response to FCS, however we were unable to detect levels of JNK phosphorylation using specific antibodies in response to PDGF in HASMCs. There are numerous possibilities which could explain this difficulty; as described above, JNK is primarily activated in response to stress and therefore a growth factor, such as PDGF may not be regarded as an appropriate agent for such activation. However, a crosstalk between ERK and JNK pathways have been described in numerous cell lines; previous findings in vascular smooth muscle cells detail how growth factors and GPCR agonists such as ATP and Angiotensin II were able to activate JNK (Zhang et al., 2005, Robinson et al., 2006). Therefore, it would be possible to expect activation, albeit a small activation of JNK by PDGF however this was not observed in the current study. To overcome possible limitations due to antibody unreliability, GST c-Jun beads were generated in order to use an *in vitro* solid phase kinase assay however due to the hindrance of time constraints, this technique was not utilised as readily as initially aimed. Therefore the

remainder of this chapter will focus on ERK as a key member of the MAP kinase signalling pathway, detailed to be responsible for MKP-2 activation. Furthermore, the lack of MKP-2 expression detected in HASMCs, in contrast to rodent systems, is a common feature of human cellular studies (Al-Mutairi et al., 2010) and it is at present unclear as to what manipulations are required to promote protein expression. Nevertheless, it allowed the use of Adv.WT-MKP-2 without the potential of contaminating endogenous protein.

Initial characterisation of human aortic smooth muscle cells explored their endogenous proliferative phenotype. An array of literature has documented the low proliferative index of HASMCs within the artery, only reaching the threshold for the phenotypic switch upon mechanical damage (Braun-Dullaeus et al., 2011). HASMCs were plated and counted by haemocytometer as a direct measurement of cellular proliferation over a 48h time period. The cells proliferated exponentially over all time points, however when compared with MASMCs, these cells proliferate at a much slower rate. It is seems intuitive that this would be the case, as previously mentioned human smooth muscle cells physiologically exist in their quiescent state until stimulated by vessel damage (Beamish et al., 2010). This is supported by recent work which suggests that hypertension negates the activity of myocardin, in smooth muscle cells on multiple levels, hence eliminating a crucial determinant of SMC quiescence. Therefore this mechanism may control the initial switch from contractile phenotype towards the synthetic proliferative smooth muscle cell phenotype during hypertension (Pfisterer et al., 2012). Collectively, human aortic smooth muscles can proliferative in culture albeit at a slower rate than exhibited in mouse aortic smooth muscle cells.

In this study, the adenoviral mediated over-expression of WT-MKP-2 was utilised as an experimental pharmacological tool to investigate the subsequent effect on MAP kinase signalling in HASMCs. Once again, in agreement with studies in MASMCs in Chapter 3, over-expression of WT-MKP-2 significantly inhibited ERK signalling, to the point of ablation. Controversially, over-expression of WT-MKP-2 in endothelial cells was not effective in inhibiting ERK phosphorylation but exhibited significant dephosphorylative actions again JNK (Al-Harthi et al., 2010b). This strongly suggests

that the function of MKP-2, in terms of substrate specificity, may be cell type specific and agonist dependent rather than being wholly defined by *in vitro* dephosphorylation studies.

An initial important finding reported in Chapter 3, was the observation that the loss of MKP-2 protein resulted in alteration of MASMCs proliferation. Smooth muscle cells derived from Dusp4 knockout mice exhibited significantly reduced cellular growth rate compared with MKP-$2^{+/+}$ counterparts. However, over-expression of WT-MKP-2 in wild-type and MKP-2 redundant MASMCs resulted in a reduction in proliferation in both cell types when compared to wild-type cells thus we assess whether modulating MKP-2 expression in human smooth muscle cells has a detrimental effect on cellular growth. HASMCs over-expressing WT-MKP-2 display a significantly reduced proliferation rate over a 48h time course than that compared with LacZ control cells. This supports work detailed in the previous chapter which states that modulating MKP-2 expression results in detrimental effects on cellular proliferation. A link between the inhibition of ERK signalling and a subsequent reduction in cellular proliferation has been well-established in smooth muscle cells. Treatment of bovine smooth muscle cells with an established ERK inhibitor results in a significant reduction in proliferation (Abe et al., 2011). Supportingly, a recent study investigated a curcumin analogue, bisdemethoxycurcumin which inhibited migration and proliferation of smooth muscle cells by the suppression of PDGF-induced ERK signalling (Hua et al., 2013). Collectively, it can be deduced that ERK inhibition dependant on MKP-2 over-expression is responsible for the reduction in human smooth muscle cellular proliferation.

Investigating the mechanism by which MKP-2 over-expression results in a reduction in proliferative capacity, exhibited a G1/S accumulation HASMC cell cycle progression. The only previous data to describe the cell cycle progression of cells infected with Adv.WT-MKP-2 was discussed in Chapter 3. However as mentioned in the previous chapter, rat arterial smooth muscle cells overexpressing MKP-1 arrested in the G1/S border, supporting the findings of the current study. The authors believe the reduction in MKP-1 expression may contribute in part to proliferation of smooth muscle cells

after vascular injury, possibly through a decrease in dephosphorylation of ERK (Lai et al., 1996). This was supported by Chai et al., (2002) who detail how over-expression of MKP-1 in smooth muscle cells derived from spontaneously hypertensive rats result in a reduction in proliferation. Moreover, inhibition of ERK by olive oil polyphenol oleuropein exhibited a proliferative G1/S block of smooth muscle cells. This was reversed by the removal of treatment, and the smooth muscle cells in question possessed the ability to regain their full proliferative capacity.

Due to the fundamental progress in elucidating the molecular mechanisms of human diseases, increasing numbers of therapeutic genes and cellular targets are available for gene therapy. In the meantime, the challenge is to develop gene delivery vectors that exhibit high target cell selectivity and efficiency *in vivo*. The most commonly used vector system to transduce cells is based on adenovirus. Where adenoviruses have

the ability to infect dividing and non-dividing cells (Douglas, 2004) and after administration, they do not integrate into the host genome (Waehler et al., 2007). This property makes them particularly attractive for gene therapeutic applications, where temporary gene over-expression is acceptable or even beneficial.

A critical study investigating Adv.WT-MKP-2 over-expression in endothelial cells showed that MKP-2 was able to negate TNFα-stimulated apoptosis by regulating not only nuclear events such as phosphorylation of H2AX, but also cytosolic events such as caspase-3 cleavage. The authors believe that Adv.WT-MKP-2 has a potential therapeutic use in clinical conditions where JNK-mediated endothelial apoptosis is a feature (Al-Mutairi et al., 2010). Taken together with results from this chapter, it could be suggested that the differential effects of Adv.WT-MKP-2 on both human endothelial and smooth muscle cells would serve as a viable clinical aide in vascular disorders, such as atherosclerosis and restenosis. The aetiology of these disorders is somewhat alike; disease progression initiates from insult to the endothelium, triggering smooth muscle cell proliferation. As described previously, Adv.WT-MKP-2 has shown to be successful not only in the reduction of endothelial apoptosis but also in the reduction of smooth muscle cell proliferation, emphasising the two-tier targeting potential of this

adenovirus in vascular disease. Therefore, here we discuss the therapeutic options for utilising MKP-2 over-expression in reducing progression of vascular disease, notably smooth muscle cell restenosis.

Restenosis is the most important long-term vascular limitation of stent implantation for coronary artery disease, occurring in 15–60% of patients (Adams et al., 2000). As discussed within the introduction section of this thesis, many different biological mechanisms contribute to restenosis an array of systemically administered drugs have been clinically tested, such as antiplatelet agents, anticoagulants, calcium-channel blockers, angiotensin converting-enzyme inhibitors cholesterol-lowering agents, and antioxidants, which have been proven almost universally negative (Reviewed by Fattori and Piva, 2003). Interestingly, many other agents were previously tested in animal models and found to be beneficial (George et al., 2011). It is possible that the lack of efficacy exhibited in human subjects may be due, in part at least, to insufficient dosing of the drug to the site. Therefore the development of drug-eluting stents avoids systemic toxicity, by local drug-release at the site of vascular injury via a polymeric-coated stent and is therefore an attractive therapeutic method to achieve an effective local concentration of drug for a designed period. One of the first drugs approved in stent elution was rapamycin, which blocks G1/S cell-cycle progression (Javier et al., 1997) and expression of inflammatory cytokines, thus inhibiting cellular proliferation; similar to the action of over-expressed MKP-2 in smooth muscle cells. It is hypothesised that Adv.WT-MKP-2 would serve as a good clinically translational therapeutic agent. This adenovirus has the potential to be delivered with stent implantation linked to the stent surface, embedded and released from within polymer materials, or more complexly surrounded by and released through a carrier (Schwartz et al., 2002). Furthermore, the Baker group developed adenoviral-TIMP3 in a porcine vein-graft bypass model, however they utilised a novel method by luminally infecting a vessel for thirty minutes prior to surgery (George et al., 2011). Recent work describes magnetically targeted delivery as a promising experimental strategy for site-specific therapy of vascular disease. Carrier particles containing a therapeutic agent, in this case possibly Adv.WT-MKP-2, are guided by one or several properly positioned magnetic field sources that help concentrate the therapy to a specific site in the body.

(Chorny et al., 2012). This novel technique has been currently studied in rats and has the potential to upscale into a novel human therapeutic delivery system. Nevertheless, the authors believe that a more sophisticated, alternative two-source strategy can be utilised through the use of uniform, deep-penetrating magnetic fields in conjunction with vascular stents included as part of the magnetic setup and the platform for targeted delivery to injured arteries in humans. This would seem a viable delivery method for MKP-2 adenoviral therapeutic over-expression.

In conclusion, the findings in this study strongly suggest that Adv.WT-MKP-2 could serve as a potential therapeutic in reducing smooth muscle cell proliferation by the inhibition of ERK signalling. The differential effects of over-expressing MKP-2 in endothelial and HASMCs, has potential for application in vascular disorders by reducing both endothelial apoptosis and smooth muscle cell proliferation.

General Discussion

In this thesis the characteristics of a novel Dusp4 (MKP-2) knockout mouse were examined in smooth muscle cell function, where novel data was generated in relation to changes in cell cycle progression and cytokinetic exit. Preliminary observations were made in relation to the use of MKP-2 over-expression in human smooth muscle cell proliferation. This was part of a longer term objective to explore MKP-2 as a possible tool for use in cardiovascular disease such as atherosclerosis or in conditions such as restenosis following interventions such as balloon angioplasty. However, a number of key questions remain to be answered and the implications of the findings of this thesis require to be put into context of the field as whole.

Many questions regarding the function of MKP-2 *in vitro* in the context of kinase signalling must be posed. A number of studies, largely from our laboratory suggest specificity of MKP-2 for JNK and ERK in particular the former (Cadalbert et al., 2005; Sloss et al., 2005). However, in this thesis MKP-2 deletion did not give rise to any consistent changes in kinase signalling. Whilst this might be unexpected it is recognised that MKPs have overlapping specificities and therefore redundancy may be a feature. One possibility to explain these results, not examined in this thesis, was the potential for MKP-2 deletion to affect the retention of phosphorylated MAP kinase within the nucleus which has been found to be a feature of the MKPs (Keyse, 2008). As touched upon in the discussion of Chapter 3, this possibility could be investigated by simple immunofluorescent microscopy, or crude nuclear extracts to compare the subcellular localisation of ERK in MASMCs. Furthermore, MKP-2 has shown to compete with the pseudophosphatase STYX for binding to ERK, where STYX acts as a nuclear anchor that regulates ERK nuclear export (Reiterer et al., 2013). It could therefore be proposed that the removal of MKP-2 may result in STYX-mediated ERK retention in the nucleus and therefore would obscure differences in ERK signalling in MKP-2 deficient MASMCs. A second possibility is that MKP-2 may have functions distinct from the dephosphorylation of MAP kinases. Kinney et al., (2009) has demonstrated recently that MKP-1 is able to dephosphorylate histone H3, similarly MKP-3 directly interacts and dephosphorylates the transcription factor forkhead box

O1 (FOXO1) (Wu et al., 2010). It should not be overlooked that RNA interference for MKP-2 should be utilised in MASMCs to confirm the findings observed in smooth muscle cells derived from MKP-$2^{-/-}$ mice.

A related issue concerns the possibility of compensation by other MAP kinase phosphatases. As mentioned above, MKP-2 has recently been shown to compete with STYX in the modulation of spatio-temporal regulation of ERK signalling (Reiterer et al., 2013). It has been demonstrated that MKP-1 induction is increased in MKP-$2^{-/-}$ bone marrow-derived macrophages in response to LPS and this results increased ERK signalling (Cornell et al., 2010). Thus further work would be required to investigate the level of endogenous MKP-1 expression in MKP-$2^{-/-}$ smooth muscle cells in order to establish whether MKP-1 levels are increased in these cells to compensate for the loss of MKP-2. Nevertheless, if an MKP compensatory mechanism is in place it is not sufficient to overrule the striking proliferative defect exhibited in MKP-$2^{-/-}$ MASMCs.

For the first time, MKP-2 has been shown to play a critical role in the completion of smooth muscle cell cytokinesis; nevertheless this is not the first study to note a proliferative deficit in MKP-2 deficient cells. Earlier work has described an accumulation of MKP-2 knockout MEFs in the G2/M phase of the cell cycle (Lawan et al., 2011), supporting the work presented in this thesis. Interestingly however, cell cycle regulatory proteins were not consistent with G2/M phase arrest between the two studies, for example the expression patterns of cyclin B1 and p-cdc-2 were unaltered in MKP-$2^{-/-}$ MASMCs. This could suggest that the MKP-$2^{-/-}$ MEFs exhibit a proliferative defect prior to cytokinesis, unlike MASMCs; raising questions over the cell-type specific effects of Dusp4 deletion.

At present there is a substantial amount of information about the biochemical structure of MKPs however, more work is required to fully determine the specific MAP kinase substrates which individual members deactivate in order to exert their physiological functions both *in vitro* and *in vivo*. Emerging data would suggest that the specificities of MKPs for their MAP kinases would be cell–type specific (Al-Mutairi et al., 2010;

Lawan et al., 2011). Furthermore, multiple ERK binding sites on MKP-2 have been postulated, which would suggest a far more complex role for MKP-2 than first envisaged (Cadalbert et al., 2005). Such information is crucial in the targeting of MKP-2 as a potential novel therapeutic in hyperproliferative diseases such as vascular disease, as discussed within this thesis but also may serve as a novel target in a cancer setting.

The current study, for the first time suggests a unique role for MKP-2 in cytokinesis requiring its phosphatase activity, albeit in a non-MAP kinase dependant manner. Therefore proposing a novel mechanism by which MKP-2 has the potential to interact with non-MAP kinase substrates in order to regulate cytokinesis. Indeed, numerous conflicting studies have shown other MKPs have targeted proteins out with their documented MAP kinase specificity; MKP-1 has been proposed to act as a phosphatase towards phosphorylated histone H3, where MKP-3 may directly interact with transcription factor forkhead box O1 (FOXO1) (Kinney et al., 2009; Wu et al., 2010). To the date, only one study has detailed MKP-2 directly interacting with a non-MAP kinase substrate, VRK1 regardless of its phosphatase activity (Jeong et al., 2013). However, only a weak reduction in VRK1 expression could be established in MKP-$2^{-/-}$ MASMCs, when compared with the other mitotic kinase Aurora B. Taken together, it could be hypothesised that MKP-2 has the ability to bind with a substrate upstream of both VRK1 and Aurora B, resulting in the marked reduction of Aurora B and p-Histone H3in MASMCs. To further investigate this possibility, a full microarray of mitotic proteins could be used to assess the up-or down-regulation of possible interactive targets. A previous study suggested cross-talk interaction between the Aurora B and VRK1 (Kim et al., 2012), which may account for the inconsistencies of Aurora B and VRK1 specificities in different cell lines and thus the potential for MKP-2 to bind to either Aurora B or VRK1 should also be considered. This could be assessed by immunoprecipitation of MKP-2 with both of these mitotic kinases, with further peptide array analysis to ascertain the potential binding site. This would be wholly beneficial in the development of MKP-2 inhibitors for use, not only in a number of disease conditions but also as an aide in the elucidation of their physiological role. Future work

employing computational modelling will go a long way in helping to interpret the data generated regarding their exact physiological role.

Global knockout mouse models, like the Dusp4 model utilised in this study, prove to be key in the physiological investigation of poorly studied target proteins; phenotypes caused by loss of target gene function are likely to provide insight into the physiological roles of these gene products. However, global deletion of factors essential for embryonic development will result in embryonic or neonatal lethality, preventing the investigation of these factors in postnatal and adult life (Davey and MacLean, 2006). At times, loss of activity during development may mask the role of the gene in the adult state, especially if the gene is involved in numerous processes spanning development. Inducible knockout approaches may be insightful to first allow the mouse to develop and mature normally prior to ablation of the gene of interest. In the current study, offspring from Dusp4 knockout mice survive a full lifespan, which would seem surprising regarding the striking cytokinetic deficit observed in MASMCs derived from these knockout mice. It could be argued, as previously mentioned, smooth muscle cells do not endogenously proliferate but will be activated to do so in response to stress or damage. Therefore, this phenotype may only be exhibited in response to activating factors, redundant in embryogenesis. Furthermore, it could be proposed that the phenotype observed in MKP-$2^{-/-}$ is exclusive to smooth muscle cells, and in order to investigate this, MKP-2 tissue-specific knockout mouse models may be utilised. It should not be disregarded that there is a distinct possibility that the cytokinetic deficit phenotype observed *in vitro* may not be translated to an *in vivo* setting.

The work in Chapter 4 of this thesis discussed a potential role for utilising an MKP-2 over-expression system as therapeutic in vascular disorders; however the endogenous role of MKP-2 in this sub-class of disease has yet to be studied. Currently, the mouse is the most frequently used species for atherosclerosis studies; most readily accomplished by the genetic ablation of ApoE or LDLR. Although ApoE deficiency in humans is rare, it serves as good model to investigate atherosclerosis (Getz and

Reardon, 2012). In order to assess the endogenous role in atherosclerosis, an ApoE$^{-/-}$ model could be backcrossed with a Dusp4 knockout mouse. This double knockout would allow for a role of MKP-2 in atherosclerotic disease progression to be assessed. Furthermore, although *in vitro* MKP-2$^{-/-}$ smooth muscle cells have shown a reduced proliferative capacity but have yet to be assessed if this phenotype translates *in vivo*. In order to stimulate SMC growth, a restenosis model would ideal for investigation (Zaragoza et al., 2011). The use of mouse models in restenosis are somewhat infrequent, due to the size of the subject, thus larger models of restenosis are often used such as rat, rabbit, pig and dog of which results have been projected into clinical study. (Touchard and Schwartz, 2006). However, elucidation of an endogenous role for MKP-2 in these models would serve extremely difficult due the lack of large genetically altered models. Nevertheless, the experimental animals used for the study of in-stent restenosis usually lack the phenotypes for acquired heritable metabolic disorders which preclude studies of important risk factors for the disease such as diabetes, obesity, and systemic hypertension. A novel method of deploying a microvascular stent in the abdominal aorta of ApoE$^{-/-}$ mice was described (Rodriguez-Menocal et al., 2011). This relatively simple method could be deployed in a double ApoE$^{-/-}$MKP-2$^{-/-}$ mouse model to investigate the *in vivo* aspect of SMC proliferation. Furthermore, this model would be advantageous as an extension to the current study, due to arterial damage, compared to the large number of venous studies. It is unknown if the smooth muscle cells of artery and vein of the MKP-2$^{-/-}$ mouse model would differ upon damage due to the difference in medial layer composition; thus the aortic damage model described by Rodriguez-Menocal et al., (2011) would serve as in ideal model for the investigation of vascular remodelling in MKP-2 deficient mice.

An emerging body of evidence is available detailing the delivery of adenovirus *in vivo* with a therapeutic aim; successful inhibition of intracranial human glioblastoma growth has been described utilising systemic adenoviral delivery of soluble endostatin and soluble vascular endothelial growth factor receptor-2, reducing cellular proliferation and increasing tumour apoptosis (Szentirmai et al., 2008). One study conducted local vascular specific gene transfer by adenoviral delivery of human ABCG1 (Ad-ABCG1-

GFP) in cholesterol-fed atherosclerotic rabbits *in vivo*. Endothelial over-expression of ABCG1 markedly reduced atheroprogression and almost blunted vascular inflammation, as shown by markedly reduced macrophage and smooth muscle cell invasion into the vascular wall (Munch et al., 2008). Pre-clinical studies indicate that gene delivery to the vasculature could potentially be utilised to treat a range of cardiovascular diseases such as vein graft failure (George et al., 2011), in-stent restenosis (Johnson et al., 2005) and peripheral vascular disease (Ishii et al, 2004). To date, no serious side-effects have been noted throughout any Phase II or Phase III clinical trials utilising therapeutic adenovirus, nevertheless they have failed to exhibit the potential efficacy shown *in vitro* (Lopes et al., 2012; Hedman et al., 2009). However, recent work developed a successful two-step entry pathway of adenoviral vectors which is initiated by the particle binding to cellular coxsackie and adenovirus receptor (CAR), followed by the interaction of the arginine-glycine-aspartate (RGD) sequence on the adenovirus penton base. Using this technique, adenoviral-mediated targeting of hepatic stellate cells *in vivo* via p75NTR, was successful in concurrently avoiding its binding to hepatocytes. Thus, this new adenoviral targeting technique may provide a potentially feasible, selective and effective mechanism for therapeutic gene delivery to activated hepatic stellate cells (Reetz et al., 2013). We therefore question whether over-expression of MKP-2 would be an attractive application in reducing smooth muscle cell hyperproliferation associated with numerous vascular disorders.

Future work using a smooth muscle cell specific MKP-2 knockout during cardiac vascular disease will build upon the current data and will provide a crucial mechanistic understanding of how MKP-2 at a cellular level impacts on the remodelling process. The tissue specific knockout would be an ideal model in order to selectively analyse MKP-2, rather than the current global Dusp4 knockout model utilised in the current study. As discussed previously, vascular disorders including atherosclerosis and restenosis are often characterised as diseases of inflammation; due to the multiple implications of inflammatory mediators acting upon the vessel itself (Rudijanto et al., 2006). However, in the current Dusp4 global knockout model, not only surrounding cells but critical inflammatory mediators are also deficient in MKP-2; a key factor

which may distort the real effect exhibited by MKP-2 in smooth muscle cell proliferation. There has been some interesting data regarding MKP-2 in an immunological setting, where systemic infection of *Leishmania mexicana* is enhanced in MKP-$2^{-/-}$ macrophages due to an increased uptake of the parasite and reduced Th1 responses, facilitated by high levels of arginase-1 and low levels of NO production (Al-Mutairi et al., 2010). Furthermore, T cell hypo-responsiveness against *Leishmania major* in Dusp4-knockout mice does not alter the healer disease phenotype (Schroeder et al., 2013). From these studies, it would seem that altering the inflammatory responsiveness may serve as an aide in reducing smooth muscle hyperproliferation in vascular disease states. This is supported by work which has detailed that nitric oxide can inhibit SMC proliferation and reduce the injury responses within the blood vessel wall (Yu et al., 2011). Controversially, nitric oxide has shown to also induce apoptosis in smooth muscle cells (Perales et al., 2010), a process which in recent years, has displayed negative consequences both *in vitro* and *in vivo* emerging as an activator of smooth muscle cell hyperproliferation. SMCs release specific cytokines dependent upon the mode of cell death; IL-1β predominates during apoptosis, whilst IL-1α predominates during necrosis. Both IL-1α and β promote release of further cytokines from adjacent live cells, in particular IL-6 and MCP-1. The balance of cytokines results in a pathology with differing compositions, including inflammation or neointima formation, via direct promotion of SMC proliferation (Bennett et al., 2012).

In conclusion, the work presented in this thesis suggests a novel role for MKP-2 in mouse aortic smooth muscle cell proliferation, providing new insights into the understanding of MKP-2 in the completion of cytokinesis. Furthermore, the MKP-2 kinase binding domain is required for successful completion of cytokinesis but may not involve the inactivation of ERK or JNK. Furthermore, an early investigation into the possible use of Adv.WT-MKP-2 as a vascular therapeutic in human aortic smooth muscle cells (HASMCs) was conducted. The over-expression of MKP-2 negated ERK signalling and consequently resulted in a reduction in cellular proliferation. Furthermore, the reduction in cellular proliferation was shown to be caused by a G1/S accumulation in the cell cycle. Collectively, these data may suggest that modification

of MKP-2 expression or function may represent a new approach in reducing SMC hyperproliferation in vascular disease states.

Abe, R., Beckett, J., Nixon, A, Rochier, A, Yamashita, N. and Sumpio, B., 2011. Olive oil polyphenol oleuropein inhibits smooth muscle cell proliferation. Eur. J. Vasc. Endovasc. Surg. 41, 814–20.

Adams, M.R., 2013. Coronary artery revascularisation: selecting the appropriate strategy. Intern. Med. J. 43, 18–22.

Adams, M.R., Kinlay, S., Blake, G.J., Orford, J.L., Ganz, P., and Selwyn, P., 2000. Pathophysiology of atherosclerosis: development, regression, restenosis. Curr. Atheroscler. Rep. 2, 251–8.

Agarwal, M.L., Agarwal, a, Taylor, W.R., and Stark, G.R., 1995. p53 controls both the G2/M and the G1 cell cycle checkpoints and mediates reversible growth arrest in human fibroblasts. Proc. Natl. Acad. Sci. U. S. A. 92, 8493–7.

Agarwal, M.L., Taylor, W.R., Chernov, M. V, Chernova, O.B., and Stark, G.R., 1998. The p53 network. J. Biol. Chem. 273, 1–4.

Akiyama T, and Moussa I,., 1998. Angiographic and clinical outcome following coronary stenting of small vessels: A comparison with coronary stenting of large vessels. J Am Coll Cardiol 32, 1610–1618.

Albinsson S, Suarez Y, Skoura A, Offermanns S, and Miano G, 2010. MicroRNAs are necessary for vascular smooth muscle growth, differentiation, and function. Arter. Thromb Vasc Biol 30, 1118 –1126.

Alessi DR, and Smythe C., 1993. The human CL100 gene encodes a tyr/thr-protein phosphatase which potently and specifically inactivates MAP kinase and suppresses its activation by oncogenic ras in xenopus oocyte extracts. Oncogene. 8, 2015–20.

Alexander RW, G.K., 1996. Signal transduction in vascular smooth muscle. J Hypertens Suppl. 14, 51–4.

Al-Mutairi, M., Al-Harthi, S., Cadalbert, L. and Plevin, R., 2010. Over-expression of mitogen-activated protein kinase phosphatase-2 enhances adhesion molecule expression and protects against apoptosis in human endothelial cells. Br. J. Pharmacol. 161, 782–98.

Al-Mutairi, M.S., Cadalbert, L.C., McGachy, H.A., Shweash, M., Schroeder, J., Kurnik, M., Sloss, C.M., Bryant, C.E., Alexander, J., and Plevin, R., 2010. MAP kinase phosphatase-2 plays a critical role in response to infection by Leishmania mexicana. PLoS Pathog. 6, e1001192.

Alonso A, Sasin J, Bottini N, Friedberg I, Friedberg I, Osterman A, G.A., Hunter T, and Dixon J, 2004. Protein tyrosine phosphatases in the human genome. Cell 117, 699–711.

Arellano, M., and Moreno, S., 1997. Regulation of CDK/cyclin complexes during the cell cycle. Int. J. Biochem. Cell Biol. 29, 559–573.

Auger, F., D'Orléans-Juste, P., and Germain, L., 2007. Adventitia contribution to vascular contraction: hints provided by tissue-engineered substitutes. Cardiovasc. Res. 75, 669–78.

Avruch J, Alexander MC, Palmer JL, Pierce MW, Nemenoff R,A, Blackshear PJ, and Tipper J., 1982. Role of insulin-stimulated protein phosphorylation in insulin action. Fed Proc 41, 2629–2633.

Avruch, J., 2007. MAP kinase pathways: the first twenty years. Biochim. Biophys. Acta 1773, 1150–60.

Baluska F,and Menzel D., 2006. Cytokinesis in plant and animal cells: endosomes "shut the door". Dev Biol. 294, 1–10.

Barry, O.P., Mullan, B., Sheehan, D., Kazanietz, M.G., Shanahan, F., Collins, J.K., and O'Sullivan, G.C., 2001. Constitutive ERK1/2 activation in esophagogastric rib bone marrow micrometastatic cells is MEK-independent. J. Biol. Chem. 276, 15537–46.

Bartkova J, Thullberg M, Slezak P, Jaramillo E, Rubio C, and Thomassen LH, 2001. Aberrant expression of G1-phase cell cycle regulators in flat and exophytic adenomas of the human colon. Gastroenterology. 120, 1680–8.

Bastos RN, 2010. Plk1 negatively regulates Cep55 recruitment to the midbody to ensure orderly abscission. J Cell Biol. 191, 751–60.

Bayliss, R., Fry, A., Haq, T., Yeoh, S., 2012. On the molecular mechanisms of mitotic kinase activation. Open Biol. 2, 120136.

Beamish. J., 2010. Molecular Regulation of Contractile Smooth Muscle Cell Phenotype : Implications for Vascular Disease. J Cell Biol. 191, 751–60.

Bennett, M., Yu, H., and Clarke, M., 2012. Signalling from dead cells drives inflammation and vessel remodelling. Vascul. Pharmacol. 56, 187–92.

Bennett, M.R., Evan, G.I., and Newby, A.C., 1994. Deregulated expression of the c-myc oncogene abolishes inhibition of proliferation of rat vascular smooth muscle cells by serum reduction, interferon-gamma, heparin, and cyclic nucleotide analogues and induces apoptosis. Circ Res 74, 525–536.

Berasi., 2006. Inhibition of gluconeogenesis through transcriptional activation of EGR1 and DUSP4 by AMP-activated kinase. J Biol Chem. 281, 27167–77.

Bermudez, O., Pagès, G., and Gimond, C., 2010. The dual-specificity MAP kinase phosphatases: critical roles in development and cancer. Am. J. Physiol. Cell Physiol. 299, C189–202

Bicknell, K.A., Surry, E.L., and Brooks, G., 2003. Targeting the cell cycle machinery for the treatment of cardiovascular disease 571–591.

Blackshear PJ, and Nemenoff RA., 1983. Insulin and growth factors stimulate the phosphorylation of a Mr-22000 protein in 3T3 L1 adipocytes. Biochem J 214, 11–19.

Bokemeyer, D., Lindemann, M., and Kramer, H.J., 1998. Regulation of Mitogen-Activated Protein Kinase Phosphatase-1 in Vascular Smooth Muscle Cells. Hypertension 32, 661–667.

Boutros, T., Chevet, E., and Metrakos, P., 2008. Mitogen-activated protein (MAP) kinase/MAP kinase phosphatase regulation: roles in cell growth, death, and cancer. Pharmacol Rev 60, 261–310.

Bowen-Pope DF,., 1982. Platelet-derived growth factor.II. Specific binding to cultured cells. J Biol Chem 257, 5161–5171.

Braun-Dullaeus, R.C., Mann, M.J., Sedding, D.G., Sherwood, S.W., von der Leyen, H.E., and Dzau, V.J., 2004. Cell cycle-dependent regulation of smooth muscle cell activation. Arterioscler. Thromb. Vasc. Biol. 24, 845–50.

Braun-Dullaeus RC, and Mann MJ., 1998. Cell cycle progression: new therapeutic target for vascular proliferative disease. Circulation 98, 82– 89.

Brondello, J., Brunet, A., Pouysse, J. and Mckenzie, F.R., 1997. The Dual Specificity Mitogen-activated Protein Kinase Phosphatase- 1 and -2 Are Induced by the p42 / p44 MAPK Cascade *. Biochemistry 272, 1368 –1376.

Brondello JM, and Pouyssegur J, M.F., 1999. Reduced MAP kinase phosphatase-1 degradation after p42/p44MAPKdependent phosphorylation. Science 286, 2514–2517.

Brunet, A., Roux, D., Lenormand, P., Dowd, S., Keyse, S., and Pouyssegur, J., 1999. Nuclear translocation of p42/p44 mitogen-activated protein kinase is required for growth factor-induced gene expression and cell cycle entry. EMBO J 18, 664–674.

Bui, Q.T., Prempeh, M., and Wilensky, R.L., 2009. Atherosclerotic plaque development. Int J Biochem Cell Biol 41, 2109–2113..

Burke B, E.J., 2002. Remodelling the walls of the nucleus. Nat Rev Mol Cell Biol. 3, 487–97.

Butler, T., Paul, J., Europe-Finner, N., Smith, R., and Chan, E.-C., 2013. Role of serine-threonine phosphoprotein phosphatases in smooth muscle contractility. Am. J. Physiol. Cell Physiol. 304, 485–504.

Buvelot S, Tatsutani SY, and Vermaak D., 2003. The budding yeast Ipl1/Aurora protein kinase regulates mitotic spindle disassembly. J Cell Biol 160, 329–339.

Cadalbert, L., Sloss, C.M., Cameron, P., and Plevin, R., 2005. Conditional expression of MAP kinase phosphatase-2 protects against genotoxic stress-induced apoptosis by binding and selective dephosphorylation of nuclear activated c-jun N-terminal kinase. Cell Signal 17, 1254–1264.

Cadalbert, L.C., Sloss, C.M., Cunningham, M.R., Al-Mutairi, M., McIntire, A., Shipley, J., and Plevin, R.,. Differential regulation of MAP kinase activation by a novel splice variant of human MAP kinase phosphatase-2. Cell Signal 22, 357–365.

Cagnol S, R.N., 2013. Oncogenic KRAS and BRAF activation of the MEK/ERK signaling pathway promotes expression of dual-specificity phosphatase 4 (DUSP4/MKP2) resulting in nuclear ERK1/2 inhibition. Oncogene 32, 564–576.

Camps M, Nichols A, Gillieron C, Antonsson B, Muda M, and Chabert C, 1998. Catalytic activation of the phosphatase MKP-3 by ERK2 mitogen-activated protein kinase. Science 280, 1262–1265.

Caplice NM, Bunch TJ, Stalboerger PG, Wang S, Simper D, Miller DV, Russell SJ, and Litzow MR, E.W., 2003. Smooth muscle cells in human coronary atherosclerosis can originate from cells administered at marrow transplantation. Proc Natl Acad Sci U S A 100, 4754 – 4759.

Carlton JG, 2009. The ESCRT machinery: new functions in viral and cellular biology. Biochem Soc Trans 37, 198–9.

Carmena M, 2012. Abscission checkpoint control: stuck in the middle with Aurora B. Open Biol. 2, 120095.

Carnero, A., Hannon, G.J., 1998. The INK4 family of CDK inhibitors. Curr Top Microbiol Immunol 227, 43–55.

Carrillo-Sepulveda MA., 2010. Phenotypic modulation of cultured vascular smooth muscle cells: a functional analysis focusing on MLC and ERK1/2 phosphorylation. Mol Cell Biochem 341, 279–289.

Carrozza JP Jr., and Kuntz RE,., 1992. Angiographic and clinical outcome of intracoronary stenting: Immediate and long-term results from a large single-center experience. J Am Coll Cardiol 20, 328–337.

Caunt, C.J., and Keyse, S.M., 2013. Dual-specificity MAP kinase phosphatases (MKPs): shaping the outcome of MAP kinase signalling. FEBS J. 280, 489–504.

Chambard, J.-C., Lefloch, R., Pouysségur, J., and Lenormand, P., 2007. ERK implication in cell cycle regulation. Biochim. Biophys. Acta 1773, 1299–310.

Chan, D.W., Liu, V.W., Tsao, G.S., Yao, K.M., Furukawa, T., Chan, K.K., and Ngan, H.Y., 2008. Loss of MKP3 mediated by oxidative stress enhances tumorigenicity and chemoresistance of ovarian cancer cells. Carcinogenesis 29, 1742–1750.

Chang, L., Kamata, H., Solinas, G., Luo, J.L., Maeda, S., Venuprasad, K., Liu, Y.C., and Karin, M., 2006. The E3 ubiquitin ligase itch couples JNK activation to TNFalpha-induced cell death by inducing c-FLIP(L) turnover. Cell 124, 601–613.

Charles CH, and Abler AS., 1992. cDNA sequence of a growth factorinducible immediate early gene and characterization of its encoded protein. Oncogene 7, 187–190.

Charron, T., Nili, N., and Strauss, B.H., 2006. The cell cycle: a critical therapeutic target to prevent vascular proliferative disease. Can J Cardiol 22 Suppl B, 41B–55B.

Chaudhury, H., Zakkar, M., Boyle, J., Cuhlmann, S., van der Heiden, K., Luong, L.A., Davis, J., Platt, A., Mason, J.C., Krams, R., Haskard, D.O., Clark, A.R., and Evans, P.C., 2010. c-Jun N-terminal kinase primes endothelial cells at atheroprone sites for apoptosis. Arterioscler. Thromb. Vasc. Biol. 30, 546–53.

Cheah, P.L., Kunaseegaran, R., and Looi, L.M., 2001. Expression of proliferating cell associated protein, Ki-67, supports cellular proliferation in WHO Class IV lupus nephritis. Malays J Pathol 23, 27–30.

Chen C, Hu SY, Luo DQ, and Zhu SY, 2013. Potential antitumor agent from the endophytic fungus Pestalotiopsis photiniae induces apoptosis via the mitochondrial pathway in HeLa cells. Oncol Rep 1773–81.

Chen, H., Li, X., and Ljungdahl, L.G., 1994. Isolation and properties of an extracellular beta-glucosidase from the polycentric rumen fungus Orpinomyces sp. strain PC-2. Appl Env. Microbiol 60, 64–70.

Chen, L.C., Matsumura, K., Deng, G., Kurisu, W., Ljung, B.M., Lerman, M.I., Waldman, F.M., and Smith, H.S., 1994. Deletion of two separate regions on chromosome 3p in breast cancers. Cancer Res 54, 3021–3024.

Chen, P., Hutter, D., Yang, X., Gorospe, M., Davis, R.J., and Liu, Y., 2001a. Discordance between the binding affinity of mitogen-activated protein kinase subfamily members for MAP kinase phosphatase-2 and their ability to activate the phosphatase catalytically. J. Biol. Chem. 276, 29440–9.

Chen, N., Nomura, M., She, Q.B., Ma, W.Y., Bode, A.M., Wang, L., Flavell, R.A. and Dong, Z., 2001. Suppression of skin tumorigenesis in c-Jun NH2-terminal kinase-2-deficient mice. Cancer Res. 61, 3908–3912.

Chin, P.C., Liu, L., Morrison, B.E., Siddiq, A., Ratan, R.R., Bottiglieri, T., and D'Mello, S.R., 2004. The c-Raf inhibitor GW5074 provides neuroprotection in vitro and in an animal model of neurodegeneration through a MEK-ERK and Akt-independent mechanism. J Neurochem 90, 595–608.

Chitale M., 2009. An integrated genomic analysis of lung cancer reveals loss of DUSP4 in EGFR-mutant tumors. Oncogene 28, 2773–83.

Chorny, M., Fishbein, I., Adamo, R.F., Forbes, S.P., Folchman-Wagner, Z., and Alferiev, I.S., 2012. Magnetically targeted delivery of therapeutic agents to injured blood vessels for prevention of in-stent restenosis. Methodist Debakey Cardiovasc. J. 8, 23–7.

Christie, G.R., Williams, D.J., Macisaac, F., Dickinson, R.J., Rosewell, I., and Keyse, S.M., 2005. The Dual-Specificity Protein Phosphatase DUSP9 / MKP-4 Is Essential for Placental Function but Is Not Required for Normal Embryonic Development †. Society 25, 8323–8333.

Christov, K., Chew, K.L., Ljung, B.M., Waldman, F.M., Goodson 3rd, W.H., Smith, H.S., and Mayall, B.H., 1994. Cell proliferation in hyperplastic and in situ carcinoma lesions of the breast estimated by in vivo labeling with bromodeoxyuridine. J Cell Biochem Suppl 19, 165–172.

Chu, Y., Solski, P.A., Khosravi-Far, R., Der, C.J., and Kelly, K., 1996. The mitogen-activated protein kinase phosphatases PAC1, MKP-1, and MKP-2 have unique substrate specificities and reduced activity in vivo toward the ERK2 sevenmaker mutation. J Biol Chem 271, 6497–6501.

Chung, E., and Chen, R.H., 2003. Phosphorylation of Cdc20 is required for its inhibition by the spindle checkpoint. Nat Cell Biol 5, 748–753.

Clarke, M., and Bennett, M., 2006. Defining the role of vascular smooth muscle cell apoptosis in atherosclerosis. Cell Cycle 5, 2329–31.

Clark-Lewis I, and Sanghera JS, P.S., 1991. Definition of a consensus sequence for peptide substrate recognition by p44mpk, the meiosis-activated myelin basic protein kinase. J Biol Chem 266, 15180–4.

Clemmons DR,., 1985. Evidence for a functional role of endogenously produced somatomedinlike peptides in the regulation of DNA synthesis in cultured human fibroblasts and porcine smooth muscle cells. J Clin Invest 75, 1914–1918.

Clemmons DR., 1984. Interaction of circulating cell-derived and plasma growth factors in stimulating cultured smooth muscle cell replication. J Cell Physiol 121, 425–430.

Clowes AW, and Reidy MA, C.M., 1983. Kinetics of cellular proliferation after arterial injury, I: smooth muscle growth in the absence of endothelium. Lab Invest. 49, 327–333.

Cobb M., 1983. Description of a protein kinase derived from insulin-treated 3T3-L1 cells thatcatalyzes the phosphorylation of ribosomal protein S6 and casein. J. Biol. Chem 258, 12472–12481.

Collins, N.L., Reginato, M.J., Paulus, J.K., Sgroi, D.C., Labaer, J., and Brugge, J.S., 2005. G 1 / S Cell Cycle Arrest Provides Anoikis Resistance through Erk-Mediated Bim Suppression † 25, 5282–5291.

Connell JW, Lindon C, and Luzio JP., 2009. Spastin couples microtubule severing to membrane traffic in completion of cytokinesis and secretion. Traffic 10, 42–56.

Cooper JA, and Sefton MB., 1984. Diverse mitogenic agents induce the phosphorylation of two related 42,000-dalton proteins on tyrosine in quiescent chick cells. Mol. Cell. Biol 4, 30–37.

Cornell, T.T., Rodenhouse, P., Cai, Q., Sun, L., and Shanley, T.P., 2010. Mitogen-activated protein kinase phosphatase 2 regulates the inflammatory response in sepsis. Infect. Immun. 78, 2868–76.

Costa MA, S.D., 2005. Molecular basis of restenosis and drug-eluting stents. Circulation. 111, 2257–2273.

Cox RH, 1979. Contribution of smooth muscle to arterial wall mechanics. Basic Res Cardiol. 74, 1–9.

Cremer T., 2001. Chromosome territories, nuclear architecture and gene regulation in mammalian cells. Nat Rev Genet 2, 292–301.

Crowther, M. 2005. Pathogenesis of atherosclerosis. Hematology Am. Soc. Hematol. Educ. Program 436–41.

Curcio, A., Torella, D., and Indolfi, C., 2011. Mechanisms of Smooth Muscle Cell Proliferation and Endothelial Regeneration After Vascular Injury and Stenting. Circ. J. 75, 1287–1296.

Cyert, M.S., 2001. Regulation of nuclear localization during signaling. J Biol Chem 276, 20805–20808.

Daniel JM., 2011. Circulating smooth muscle progenitor cells in arterial remodeling. J Mol Cell Cardiol. 50, 273–9.

Datta, N.S., Kolailat, R., Fite, A., Pettway, G., and Abou-Samra, A.B., Distinct roles for mitogen-activated protein kinase phosphatase-1 (MKP-1) and ERK-MAPK in PTH1R signaling during osteoblast proliferation and differentiation. Cell Signal 22, 457–466.

Davey, R. and MacLean, H.E., 2006. Current and future approaches using genetically modified mice in endocrine research. Am. J. Physiol. Endocrinol. Metab. 291, E429–38.

David, A.R., Kershaw, A., and Heagerty, A., Atherosclerosis and diet in ancient Egypt. Lancet 375, 718–719.

Davies, C. and Tournier, C., 2012. Exploring the function of the JNK (c-Jun N-terminal kinase) signalling pathway in physiological and pathological processes to design novel therapeutic strategies. Biochem. Soc. Trans. 40, 85–9.

Davies MK., 1996. Leonardo da Vinci (1452-1519). Heart 76, 464.

Davis-Dusenbery, B.N., Wu, C., and Hata, A., 2011. Micromanaging vascular smooth muscle cell differentiation and phenotypic modulation. Arterioscler. Thromb. Vasc. Biol. 31, 2370–7.

Dhanasekaran, D.N., and Reddy, E.P., 2008. JNK signaling in apoptosis. Oncogene 27, 6245–6251.

Dong, P., Zhou, J.-Y., and Wu, G.S., 2010. Post-translational regulation of mitogen-activated protein kinase phosphatase-2 (MKP-2) by ERK. Cell Cycle 9, 4650–4655.

Dorfman K, Carrasco D, Gruda M, Ryan C, and Lira SA,., 1996. Disruption of the erp/mkp-1 gene does not affect mouse development: normal MAP kinase activity in ERP/MKP-1-deficient fibrolasts. Oncogene 13, 925–931.

Douglas, J.S., 2007. Pharmacologic approaches to restenosis prevention. Am. J. Cardiol. 100, 10K–6K.

Drechsler, H., and Mcainsh, A.D., 2012. Exotic mitotic mechanisms Exotic mitotic mechanisms.

Du, L., Lyle, C.S., Obey, T.B., Gaarde, W.A., Muir, J.A., Bennett, B.L., and Chambers, T.C., 2004. Inhibition of cell proliferation and cell cycle progression by specific inhibition of basal JNK activity: evidence that mitotic Bcl-2 phosphorylation is JNK-independent. J Biol Chem 279, 11957–11966.

Duff, J.L., Monia, B.P., and Berk, B.C., 1995. Mitogen-activated protein (MAP) kinase is regulated by the MAP kinase phosphatase (MKP-1) in vascular smooth muscle cells. Effect of actinomycin D and antisense oligonucleotides. J Biol Chem 270, 7161–7166.

Dumesic, P., Scholl, F., Barragan, D.I., and Khavari, P., 2009. Erk1/2 MAP kinases are required for epidermal G2/M progression. J. Cell Biol. 185, 409–22.

Emmert-buck, M.R., Vocke, C.D., Pozzatti, R.O., Duray, P.H., Jennings, S.B., Florence, C.D., Zhuang, Z., Bostwick, D.G., Liotta, L.A., and Linchan, W.M., 1995. Allelic Loss on Chromosome 8p12 − 21 in Microdissected Prostatic Intraepithelial Neoplasia Advances in Brief Prostatic. Cancer Res. 2959–2962.

Ettinger AW, Wilsch-Bräuninger M, Marzesco AM, Bickle M, Lohmann A, Maliga Z, Karbanová J, Corbeil D, and Hyman AA,., 2011. Proliferating versus differentiating stem and cancer cells exhibit distinct midbody-release behaviour. Nat Commun 2.

Evans, D.R., and Guy, H.I., 2004. Mammalian pyrimidine biosynthesis: fresh insights into an ancient pathway. J Biol Chem 279, 33035–33038.

Farooq A, Chaturvedi G, Mujata S, Plotnikova O, Zeng L, and Dhalluin C, 2001. Solution structure of ERK2 binding domain of MAPK phosphatase MKP-3: structural insights into MKP-3 activation by ERK2. Mol Cell 7, 387–399.

Fattori, R., and Piva, T., 2003. Rapid review Drug-eluting stents in vascular intervention 361, 18–20.

Feng, H., Xiang, H., Mao, Y.W., Wang, J., Liu, J.P., Huang, X.Q., Liu, Y., Liu, S.J., Luo, C., Zhang, X.J., and Li, D.W., 2004. Human Bcl-2 activates ERK signaling pathway to regulate activating protein-1, lens epithelium-derived growth factor and downstream genes. Oncogene 23, 7310–7321.

Fernandez-Miranda G, Trakala M, Martin J, Escobar B, Gonzalez A, Ghyselinck NB, Ortega S, Canamero M, and Perez de Castro I, M.M., 2011. Genetic disruption of aurora B uncovers an essential role for aurora C during early mammalian development. Development 138 138, 2661–2672.

Ferns, G.A., Raines, E.W., Sprugel, K.H., Motani, A.S., Reidy, M.A., and Ross, R., 1991. Inhibition of neointimal smooth muscle accumulation after angioplasty by an antibody to PDGF. Science (80-.). 253, 1129–1132.

Fey, D., Croucher, D.R., Kolch, W. and, Kholodenko, B.N., 2012. Crosstalk and signaling switches in mitogen-activated protein kinase cascades. Front. Physiol. 3, 355.

Fielding AB, Schonteich E, Matheson J, Wilson G, Yu X, Hickson GR, Srivastava S, Baldwin SA, and Prekeris R, G.G., 2005. Rab11-FIP3 and FIP4 interact with Arf6 and the exocyst to control membrane traffic in cytokinesis. EMBO J 24, 3389–99.

Fisher P., 2012. Phosphorylation network dynamics in the control of cell cycle transitions. J Cell Sci 125, 4703–11.

Freestone, B., Krishnamoorthy, S., and Lip, G.Y. Assessment of endothelial dysfunction. Expert Rev Cardiovasc Ther 8, 557–571.

Freshney, R., 1994. Culture of Animal Cells: A manual of basic technique. In: Ed. Wiley-Liss, Inc., 605 Third Avenue, New York, NY 10158-002.

Furukawa T, and Horii A., 2004. Molecular pathology of pancreatic cancer: in quest of tumor suppressor genes. Pancreas 28, 253–256.

Gabella G, 1984. Structural apparatus for force transmission in smooth muscles. Physiol Rev 64, 455–77.

Gachet, Y., Tournier, S., Millar, J.B., and Hyams, J.S., 2001. A MAP kinase-dependent actin checkpoint ensures proper spindle orientation in fission yeast. Nature 412, 352–355.

Galaktionov, K., Chen, X., and Beach, D., 1996. Cdc25 cell-cycle phosphatase as a target of c-myc. Nature 382, 511–517.

Gao, T., Zhang, Z., Yu, W., and Wang, Y., 2009. Atherosclerotic carotid vulnerable plaque and subsequent stroke: a high-resolution MRI study. Cerebrovasc Dis 27, 345–352.

Gelfant S, 1977. A new concept of tissue and tumor cell proliferation. Cancer Res. 37, 3845–3852.

George, S.J., Wan, S., Hu, J., MacDonald, R., Johnson, J.L., and Baker, A.H., 2011. Sustained reduction of vein graft neointima formation by ex vivo TIMP-3 gene therapy. Circulation 124, S135–42.

Getz, G.S., and Reardon, C. , 2012. Animal models of atherosclerosis. Arterioscler. Thromb. Vasc. Biol. 32, 1104–15.

Gilmore T, M.G., 1983. Phorbol ester and diacylglycerol induces protein phosphorylation at tyrosine. Nature 306, 253–266.

Glading, A., Chang, P., Lauffenburger, D.A., and Wells, A., 2000. Epidermal growth factor receptor activation of calpain is required for fibroblast motility and occurs via an ERK/MAP kinase signaling pathway. J Biol Chem 275, 2390–2398.

Goel, S. a, Guo, L.-W., Liu, B., and Kent, K.C., 2012. Mechanisms of post-intervention arterial remodelling. Cardiovasc. Res. 96, 363–71.

Gomez, D., and Owens, G.K., 2012. Smooth muscle cell phenotypic switching in atherosclerosis. Cardiovasc. Res. 95, 156–64.

Gong, K.Z., Zhang, Z.G., Li, A.H., Huang, Y.F., Bu, P., Dong, F., and Liu, J., 2004. ROS-mediated ERK activation in delayed protection from anoxic preconditioning in neonatal rat cardiomyocytes. Chin Med J 117, 395–400.

Gonzalez FA, and Raden DL., 1991. Identification of substrate recognition determinants for human ERK1 and ERK2 protein kinases. J Biol Chem 266, 22159–63.

Gordon RE., 1980. Wound repair in rat tracheal epithelium: division of G1 and G2-arrested cells following injury. Lab Invest 42, 616–621.

Gorski DH, LePage DF, Patel CV, Copeland NG, and Jenkins NA,., 1993. Molecular cloning of a diverged homeobox gene that is rapidly down-regulated during the G0/G1 transition in vascular smooth muscle cells. Mol Cell Biol. 13, 3722–33.

Green, R. a, Paluch, E., and Oegema, K., 2012. Cytokinesis in animal cells. Annu. Rev. Cell Dev. Biol. 28, 29–58.

Griendhing KK,., 1997. Oxidative stress and cardiovascular disease. Circulation. 96, 3264–3265.

Gromley A, Yeaman C, Rosa J, Redick S, Chen CT, Mirabelle S, Guha M, and Sillibourne J, D.S., 2005. Centriolin anchoring of exocyst and SNARE complexes at the midbody is required for secretory-vesicle-mediated abscission. Cell 123, 75–87.

Groom, L.A., Sneddon, A.A., Alessi, D.R., Dowd, S., and Keyse, S.M., 1996. Differential regulation of the MAP, SAP and RK/p38 kinases by Pyst1, a novel cytosolic dual-specificity phosphatase. EMBO J 15, 3621–3632.

Groom LA, Sneddon AA, and Alessi DR., 1996. Differential regulation of the MAP, SAP and RK/p38 kinases by Pyst1, a novel cytosolic dual-specificity phosphatase. EMBO J 15, 3621–3632.

Grown, W., 1958. Atherosclerosis and Myocardial Infarction. Can Med Assoc J 79, 1007–1008.

Guan Z and Butch B, 1995. Isolation and characterization of a novel dual specific phosphatase, HVH2, which selectively dephosphorylates the mitogen-activated protein kinase. J Biol Chem. 270, 7197–7203.

Guan, Z., Buckman, S.Y., Springer, L.D., and Morrison, A.R., 1999. Both p38alpha(MAPK) and JNK/SAPK pathways are important for induction of nitric-oxide synthase by interleukin-1beta in rat glomerular mesangial cells. J Biol Chem 274, 36200–36206.

Guizetti J, G.D., 2010. Cytokinetic abscission in animal cells. Semin Cell Dev Biol. 21, 909–16.

Gutierrez GJ, Tsuji T, Cross JV, Davis RJ, Templeton DJ, and Jiang W, R.Z., 2010. JNK-mediated phosphorylation of Cdc25C regulates cell cycle entry and G(2)/M DNA damage checkpoint. J Biol Chem. 285, 14217–28.

Halilovic, E., and Solit, D.B., 2008. Therapeutic strategies for inhibiting oncogenic BRAF signaling. Curr Opin Pharmacol 8, 419–426.

Halka, A.T., Turner, N.J., Carter, A., Ghosh, J., Murphy, M.O., Kirton, J.P., Kielty, C.M., and Walker, M.G., 2008. The effects of stretch on vascular smooth muscle cell phenotype in vitro. Cardiovasc. Pathol. 17, 98–102.

Hallstrom, T.C., and Nevins, J.R., 2009. Balancing the decision of cell proliferation and cell fate. Cell Cycle 8, 532–535.

Hamzah, J., Batty, K.T., Davis, W.A., Mori, T.A., Ching, S.Y., Croft, K.D., and Davis, T.M., 2007. Retinol supplementation in murine Plasmodium berghei malaria: effects on tissue levels, parasitaemia and lipid peroxidation. Int J Parasitol 37, 525–537.

Han ZS, Enslen H, Hu X, Meng X, Wu IH, Barrett T, and Davis RJ, I.Y., 1998. A conserved p38 mitogen-activated protein kinase pathway regulates Drosophila immunity gene expression. Mol Cell Biol 18, 3527–39.

Hans, F., and Dimitrov, S., 2001. Histone H3 phosphorylation and cell division. Oncogene 20, 3021–7.

Hao, H., Gabbiani, G., and Bochaton-Piallat, M.L., 2003. Arterial smooth muscle cell heterogeneity: implications for atherosclerosis and restenosis development. Arter. Thromb Vasc Biol 23, 1510–1520.

Harris TJ, 2010. The molecular pathology of cancer. Nat Rev Clin Oncol 7, 251–265.

Hartwell, L.H., 1974. Saccharomyces cerevisiae cell cycle. Bacteriol. Rev. 38, 164–98.

Hartwell, L.H., and Kastan, M.B., 1994. Cell cycle control and cancer. Science 266, 1821–8.

Hartwell LH, and Culotti J, R.B., 1970. Genetic control of the cell-division cycle in yeast. I. Detection of mutants. Proc Natl Acad Sci U S A 66, 352–9.

Hasegawa, T., Enomoto, A., Kato, T., Kawai, K., Miyamoto, R., Jijiwa, M., Ichihara, M., Ishida, M., Asai, N., Murakumo, Y., Ohara, K., Niwa, Y., Goto, H., and Takahashi, M., 2008. Roles of induced expression of MAPK phosphatase-2 in tumor development in RET-MEN2A transgenic mice. Oncogene 27, 5684–5695.

Hayashi, M., and Lee, J.-D., 2004. Role of the BMK1/ERK5 signaling pathway: lessons from knockout mice. J. Mol. Med. (Berl). 82, 800–8.

He, X., Wang, J., Guo, Z., Liu, Q., Chen, T., Wang, X., and Cao, X., 2005. Requirement for ERK activation in sinomenine-induced apoptosis of macrophages. Immunol Lett 98, 91–96.

Hedman M, Muona K, Hedman A, Kivela A, Syvanne M, Eranen J, Rantala A, Stjernvall J, Nieminen MS, and Hartikainen J., 2009. Eight-year safety follow-up of coronary artery disease patients after local intracoronary VEGF gene transfer. Gene Ther. 16, 629–634.

Hegyi, K., and Méhes, G., 2012. Mitotic failures in cancer: Aurora B kinase and its potential role in the development of aneuploidy. Pathol. Oncol. Res. 18, 761–9.

Heldin C-H, and Westermark B, W.A., 1981. Specific receptors for platelet-derived growth factor on cells derived fromconnective tissue and glia. Proc Natl Acad Sci USA 78, 3664–3668.

Hengst, L., Gopfert, U., Lashuel, H.A., and Reed, S.I., 1998. Complete inhibition of Cdk/cyclin by one molecule of p21(Cip1). Genes Dev 12, 3882–3888.

Hetzer, M.W., 2010. The nuclear envelope. Cold Spring Harb. Perspect. Biol. 2, a000539.

Hirose, M., Kosugi, H., Nakazato, K., and Hayashi, T., 1999. Restoration to a quiescent and contractile phenotype from a proliferative phenotype of myofibroblast-like human aortic smooth muscle cells by culture on type IV collagen gels. J. Biochem. 125, 991–1000.

Holis ND., 2013. Preconception folic acid supplementation and risk for chromosome 21 nondisjunction: a report from the National Down Syndrome Project. Am J Med Genet A 3, 438–44.

Hosang M, R.M., 1989. Human vascular smooth muscle cells have at least two distinct PDGF receptors and can secrete PDGF-AA. J Cardiovasc Pharmacol 14, 22–26.

Ho-Tin-Noé, B., and Michel, J.-B., 2011. Initiation of angiogenesis in atherosclerosis: smooth muscle cells as mediators of the angiogenic response to atheroma formation. Trends Cardiovasc. Med. 21, 183–7.

Hua Y, Dolence J, Ramanan S, and Ren J, N.S., 2013. Bisdemethoxycurcumin inhibits PDGF-induced vascular smooth muscle cell motility and proliferation. Mol Nutr Food Res 57, 1611–1618.

Huang CY, Lin YC, Hsiao WY, Liao FH, and Huang PY, T.T., 2012. DUSP4 deficiency enhances CD25 expression and CD4+ T-cell proliferation without impeding T-cell development. Eur J Immunol. 42, 476–488.

Huang, H.-C., Mitchison, T.J., and Shi, J., 2010. Stochastic competition between mechanistically independent slippage and death pathways determines cell fate during mitotic arrest. PLoS One 5, e15724.

Hui, L., Zatloukal, K., Scheuch, H., Stepniak, E. and Wagner, E.., 2008. Proliferation of human HCC cells and chemically induced mouse liver cancers requires JNK1-dependent p21 downregulation. J. Clin. Invest 118, 3943–3953.

Hunter T, C.J., 1985. Protein-tyrosine kinases. Annu. Rev. Biochem. 54, 897–930.

Hurley JH, H.P., 2010. Membrane budding and scission by the ESCRT machinery: it's all in the neck. Nat Rev Mol Cell Biol. 11, 556–66.

Hutter D, Chen P, and Barnes J, L.Y., 2000. Catalytic activation of mitogen-activated protein (MAP) kinase phosphatase-1 by binding to p38 MAP kinase: critical role of the p38 C-terminal domain in its negative regulation. Biochem J 352, 155–163.

Hutter, D., Chen, P., Li, J., Barnes, J., and Liu, Y., 2002. The carboxyl-terminal domains of MKP-1 and MKP-2 have inhibitory effects on their phosphatase activity. Mol Cell Biochem 233, 107–117.

Hutter, M.C., Krebs, J., Meiler, J., Griesinger, C., Carafoli, E., and Helms, V., 2002. A structural model of the complex formed by phospholamban and the calcium pump of sarcoplasmic reticulum obtained by molecular mechanics. Chembiochem 3, 1200–1208.

Ihara E, M.J., 2007. The regulation of smooth muscle contractility by zipper-interacting protein kinase. Can J Physiol Pharmacol 85, 79–87.

Imaizumi S, Grijalva V, Priceman S, Wu L, Su F, Farias-Eisner R, Hama S, Navab M, and Fogelman AM., 2010. Mitogen- activated protein kinase phosphatase-1

deficiency decreases atherosclerosis in apolipoprotein E null mice by reducing monocyte chemoattractant protein-1 levels. Mol Genet Metab 101, 66–75.

Imaizumi, S., Grijalva, V., Priceman, S., Wu, L., Su, F., Farias-eisner, R., Hama, S., Navab, M., Fogelman, A.M., and Reddy, S.T., 2010. Mitogen-activated protein kinase phosphatase-1 deficiency decreases atherosclerosis in apolipoprotein E null mice by reducing monocyte chemoattractant protein-1 levels. Mol. Genet. Metab. 101, 66–75.

Indolfi C, Avvedimento EV, Rapacciuolo A, Di Lorenzo E, and EspositoG, S.E., 1995. Inhibition of cellular ras prevents smooth muscle cell proliferation after vascular injury in vivo. Nat Med 541–545.

Indolfi C, and Curcio A, 2003. Simvastatin reduces neointimal thickening after experimental angioplasty. Circulation 107, e25.

Indolfi C, Esposito G, Di Lorenzo E, Rapacciuolo A, and Feliciello A, P.A., 1995. Smooth muscle cell proliferation is proportional to the degree of balloon injury in a rat model of angioplasty. Circulation 92, 1230–1235.

Indolfi, C., Torella, D., Coppola, C., Stabile, E., Esposito, G., Curcio, A., Pisani, A., Cavuto, L., Arcucci, O., Cireddu, M., Troncone, G., and Chiariello, M., 2002. Rat carotid artery dilation by PTCA balloon catheter induces neointima formation in presence of IEL rupture. Am. J. Physiol. Heart Circ. Physiol. 283, H760–7.

Ip JH, Fuster V, Israel D, Badimon L, and Badimon J., 1991. The role of platelets, thrombin and hyperplasia in restenosis after coronary angioplasty. J Am Coll Cardiol. 17, 77B– 88B.

Isaacs WB, 1995. Molecular genetics of prostate cancer. Cancer Surv. 25, 357–79.

Isenovic, E.R., Kedees, M.H., Haidara, M. a, Trpkovic, A., Mikhailidis, D.P., and Marche, P., 2010. Involvement of ERK1/2 kinase in insulin-and thrombin-stimulated vascular smooth muscle cell proliferation. Angiology 61, 357–64.

Ishibe, S., Joly, D., Liu, Z.X., and Cantley, L.G., 2004. Paxillin serves as an ERK-regulated scaffold for coordinating FAK and Rac activation in epithelial morphogenesis. Mol Cell 16, 257–267.

Ishii S, Koyama H, Miyata T, Nishikage S, Hamada H, and Miyatake S-I, S.H., 2004. Appropriate control of ex vivo gene therapy delivering basic fibroblast growth factor promotes successful and safe development of collateral vessels in rabbit model of hind limb ischemia. J Vasc Surg 39, 629–638.

Ito M, Nakano T, and Erdodi F,., 2004. Myosin phosphatase: structure, regulation and function. Mol Cell Biochem 259, 197–209.

Iwasa H, and Han J, I.F., 2003. Mitogen-activated protein kinase p38 defines the common senescence-signalling pathway. Genes Cells. 8, 131–44.

Izumi Y, Kim S, Namba M, Yasumoto H, Miyazaki H, Hoshiga M, Kaneda Y, Morishita R, and Zhan Y, I.H., 2001. Gene transfer of dominant-negative mutants of extracellular signal-regulated kinase and c- Jun NH2-terminal kinase prevents neointimal formation in balloon-injured rat artery. Circ.Res. 88, 1120–1126.

Jawień J., 2012. Atherosclerosis in 2012: what is new? Pol Arch Med Wewn. 122, 170–3.

Jeong DG, Yoon TS, Kim JH, Shim MY, Jung SK, Son JH, and Ryu SE, K.S., 2006. Crystal structure of the catalytic domain of human MAP kinase phosphatase 5: structural insight into constitutively active phosphatase. J Mol Biol. 360.

Jeong, M.-W., Kang, T.-H., Kim, W., Choi, Y.H., and Kim, K.-T., 2013. Mitogen-activated protein kinase phosphatase 2 regulates histone H3 phosphorylation via interaction with vaccinia-related kinase 1. Mol. Biol. Cell 24, 373–84.

Jessup M, Greenberg B, Mancini D, Cappola T, Pauly DF, Jaski B, Yaroshinsky A, Zsebo KM, and Dittrich H, H.R., 2011. Calcium upregulation by percutaneous administration of gene therapy in cardiac disease (CUPID): A phase trial of intracoronary gene therapy of sarcoplasmic reticulum Ca 2 +−ATPas in patients with advanced heart failure. Circulation 124, 304–313.

Jin, Y., Calvert, T.J., Chen, B., Chicoine, L.G., Joshi, M., Bauer, J.A., Liu, Y., and Nelin, L.D., 2010. Mice deficient in Mkp-1 develop more severe pulmonary hypertension and greater lung protein levels of arginase in response to chronic hypoxia. Am. J. Physiol. Heart Circ. Physiol. 298, H1518–28.

Johnson, G.L., and Lapadat, R., 2002. Mitogen-Activated Protein Kinase Pathways Mediated by ERK , JNK , and p38 Protein Kinases The Protein Kinase Complement of the Human Genome. Science (80-.). 298, 1911–1912.

Kaneko H, and Watanabe H,., 1984. The presence of G1 and G2 populations in normal epithelium of rat urinary bladder. Basic Appl Histochem 28, 41–57.

Kasahara, K., Nakayama, Y., Nakazato, Y., Ikeda, K., Kuga, T., and Yamaguchi, N., 2007. Src signaling regulates completion of abscission in cytokinesis through ERK/MAPK activation at the midbody. J. Biol. Chem. 282, 5327–39.

Kastrati A, and Schomig A, E.S., 1997. Predictive factors of restenosis after coronary stent placement. J Am Coll Cardiol 30, 1428–1463.

Kaszas E and Cande WZ., 2000. Kaszas E and Cande WZ. J. Cell Sci. 113, 3217–3226.

Katz, M., Amit, I., and Yarden, Y., 2007. Regulation of MAPKs by growth factors and receptor tyrosine kinases. Biochim. Biophys. Acta 1773, 1161–76.

Kearney, M.T., 2010. Targeting the endothelium to prevent diabetes-related atherosclerosis. Diab Vasc Dis Res 7, 177.

Kennedy, N.J., and Davis, R.J., 2003. Role of JNK in tumor development. Cell Cycle 2, 199–201.

Kerr, J.F., Wyllie, A.H., and Currie, A.R., 1972. Apoptosis: a basic biological phenomenon with wide-ranging implications in tissue kinetics. Br J Cancer 26, 239–257.

Keyse, S.M., 2008. Dual-specificity MAP kinase phosphatases (MKPs) and cancer. Cancer Metastasis Rev 27, 253–261.

Keyse SM, G.M., 1993. Amino acid sequence similarity between CL100, a dual-specificity MAP kinase phosphotase and cdc25. Trends Biochem Sci. 3, 377–378.

Kim, E.K., and Choi, E.-J., 2010. Pathological roles of MAPK signaling pathways in human diseases. Biochim. Biophys. Acta 1802, 396–405.

Kim, H.S., Ullevig, S.L., Zamora, D., Lee, C.F., and Asmis, R., 2012. Redox regulation of MAPK phosphatase 1 controls monocyte migration and macrophage recruitment. Proc. Natl. Acad. Sci. U. S. A. 109, E2803–12.

Kim, M.S., and Dean, L.S., 2011. In-stent restenosis. Cardiovasc. Ther. 29, 190–8.

Kim, S., and Iwao, H., 2003. Stress and vascular responses: mitogen-activated protein kinases and activator protein-1 as promising therapeutic targets of vascular remodeling. J Pharmacol Sci 91, 177–181.

Kinney, C.M., Chandrasekharan, U.M., Mavrakis, L., and DiCorleto, P.E., 2008. VEGF and thrombin induce MKP-1 through distinct signaling pathways: role for MKP-1 in endothelial cell migration. Am. J. Physiol. Cell Physiol. 294, C241–50.

Klimova, T.A., Bell, E.L., Shroff, E.H., Weinberg, F.D., Snyder, C.M., Dimri, G.P., Schumacker, P.T., Budinger, G.R., and Chandel, N.S., 2009. Hyperoxia-induced premature senescence requires p53 and pRb, but not mitochondrial matrix ROS. FASEB J 23, 783–794.

Kockx, M.M., 1998. Apoptosis in the atherosclerotic plaque: quantitative and qualitative aspects. Arter. Thromb Vasc Biol 18, 1519–1522.

Kockx, M.M., and Herman, G., 2000. Apoptosis in atherosclerosis: beneficial or detrimental? Cardiovasc. Res. 45, 736–46.

Kohno M., 1985. Diverse Mitogenic agents induce a rapid phosphorylation of a common set of cellular proteins at tyrosine in quiescent mammalian cells. J. Biol. Chem 260, 1771–1779.

Kovanen, P.T., 2007. Mast cells and degradation of pericellular and extracellular matrices: potential contributions to erosion, rupture and intraplaque haemorrhage of atherosclerotic plaques. Biochem Soc Trans 35, 857–861.

Koyama N, Kinsella MG, Wight TN, and Hedin U., 1998. Heparan sulfate proteoglycans mediate a potent inhibitory signal for migration of vascular smooth muscle cells. Circ Res 83, 305–13.

Krishna M, N.H., 2008. The complexity of mitogen-activated protein kinases (MAPKs) made simple. Cell Mol Life Sci. 65, 3525–44.

Kruman II, Ilyasova EN, and Rudchenko SA, K.Z., 1988. The intestinal epithelial cells of ground squirrel (Citellus undulatus) accumulate at G2 phase of the cell cycle throughout a bout of hibernation. Comp Biochem Physiol A Comp Physiol 90, 233–236.

Kucharska A, Linda KR, Christopher S, and Nick AM, 2009. Regulation of the inducible nuclear dual-specificity phosphatase DUSP5 by ERK MAPK. Cell. Signal. 21, 1794–1805.

Kyriakis JM,. Mammalian MAPK signal transduction pathways activated by stress and inflammation: a 10-year update. Physiol Rev 92, 689–737.

Lacolley, P., Regnault, V., Nicoletti, A., Li, Z., and Michel, J.-B., 2012. The vascular smooth muscle cell in arterial pathology: a cell that can take on multiple roles. Cardiovasc. Res. 95, 194–204.

Lacroix B, van Dijk J, Gold ND, Guizetti J, Aldrian-Herrada G, Rogowski K, and Gerlich DW, J.C., 2010. Tubulin polyglutamylation stimulates spastin-mediated microtubule severing. J Cell Biol 189, 945–54.

Lafaurie-Janvore, J., Maiuri, P., Wang, I., Pinot, M., Manneville, J.-B., Betz, T., Balland, M., and Piel, M., 2013. ESCRT-III Assembly and Cytokinetic Abscission Are Induced by Tension Release in the Intercellular Bridge. Science (80-.). 339, 1625–1629.

Lai, K., Wang, H., Lee, W.S., Jain, M.K., Lee, M.E., and Haber, E., 1996. Mitogen-activated protein kinase phosphatase-1 in rat arterial smooth muscle cell proliferation. J. Clin. Invest. 98, 1560–7.

Lang, R., Hammer, M., and Mages, J., 2006. DUSP meet immunology: dual specificity MAPK phosphatases in control of the inflammatory response. J. Immunol. 177, 7497–504.

Larsson, P., Roos, G., Stenling, R., and Ljungberg, B., 1994. Proliferation of human renal cell carcinoma studied with in vivo iododeoxyuridine labelling and immunohistochemistry. Scand J Urol Nephrol 28, 135–140.

Laskey WK, and Kimmel S,., 2000. Contemporary trends in coronary intervention: A report from the Registry of the Society for Cardiac Angiography and Interventions. Catheter Cardiovasc Interv 49, 19–22.

Lawan, A., Al-Harthi, S., Cadalbert, L., McCluskey, A.G., Shweash, M., Grassia, G., Grant, A., Boyd, M., Currie, S., and Plevin, R., 2011. Deletion of the Dual Specific Phosphatase-4 (DUSP-4) Gene Reveals an Essential Non-redundant Role for MAP Kinase Phosphatase-2 (MKP-2) in Proliferation and Cell Survival . J. Biol. Chem. 286, 12933–12943.

Lawan, A., Shi, H., Gatzke, F., and Bennett, A.M., 2013. Diversity and specificity of the mitogen-activated protein kinase phosphatase-1 functions. Cell. Mol. Life Sci. 70, 223–37.

Lawan, A., Torrance, E., Al-Harthi, S., Shweash, M., Alnasser, S., Neamatallah, T., Schroeder, J., and Plevin, R., 2012. MKP-2: out of the DUSP-bin and back into the limelight. Biochem. Soc. Trans. 40, 235–9.

Lee, B., and Moon, S.-K., 2005. Ras/ERK signaling pathway mediates activation of the p21WAF1 gene promoter in vascular smooth muscle cells by platelet-derived growth factor. Arch. Biochem. Biophys. 443, 113–9.

Li, B., Yang, L., Shen, J., Wang, C., and Jiang, Z., 2007. The antiproliferative effect of sildenafil on pulmonary artery smooth muscle cells is mediated via upregulation of mitogen-activated protein kinase phosphatase-1 and degradation of extracellular signal-regulated kinase 1/2 phosphorylation. Anesth. Analg. 105, 1034–41, table of contents.

Li C, Yanhua Hu, Manuel Mayr, and Q.X., 1999. Cyclic Strain Stressinduced Mitogen-activated Protein Kinase (MAPK) Phosphatase 1 Expression in Vascular Smooth Muscle Cells Is Regulated by Ras/Rac-MAPK Pathways. J Biol Chem. 23, 25273–25280.

Li, C., and Xu, Q., 2000. Mechanical stress-initiated signal transductions in vascular smooth muscle cells. Cell. Signal. 12, 435–45.

Liao, D.F., Duff, J.L., Daum, G., Pelech, S.L., and Berk, B.C., 1996. Angiotensin II stimulates MAP kinase kinase kinase activity in vascular smooth muscle cells, Role of Raf. Circ Res 79, 1007–1014.

Liao Q, Guo J, Kleeff J, Zimmermann A, Büchler MW, and Korc M., 2003. Down-regulation of the dual-specificity phosphatase MKP-1 suppresses tumorigenicity of pancreatic cancer cells. Gastroenterology. 124, 1830–45.

Libby, P., Sukhova, G., Lee, R.T., and Liao, J.K., 1997. Molecular biology of atherosclerosis. Int J Cardiol 62 Suppl 2, S23–9.

Lin YW,., 2006. Cooperation of ERK and SCFSkp2 for MKP-1 destruction provides a positive feedback regulation of proliferating signaling. J Biol Chem. 281, 915–926.

Liu S, 2007. Structural basis of docking interactions between ERK-2 and MAP kinase phosphatase 3. Proc Natl Acad Sci USA 103, 5326–5331.

Liu, X., Yan, S., Zhou, T., Terada, Y. and Erikson, R.L., 2004. The MAP kinase pathway is required for entry into mitosis and cell survival. Oncogene 23, 763–776.

Liu, Y., Asakura, M., Inoue, H., Nakamura, T., Sano, M., Niu, Z., Chen, M., Schwartz, R.J., and Schneider, M.D., 2007. Sox17 is essential for the specification of cardiac mesoderm in embryonic stem cells. Mouse Genome 104, 3859–3864.

Liu, Y., Lagowski, J., Sundholm, A., Sundberg, A., and Kulesz-Martin, M., 2007. Microtubule disruption and tumor suppression by mitogen-activated protein kinase phosphatase 4. Cancer Res. 67, 10711–9.

Lobjois, V., Jullien, D., Bouché, J.-P., and Ducommun, B., 2009. The polo-like kinase 1 regulates CDC25B-dependent mitosis entry. Biochim. Biophys. Acta 1793, 462–8.

Loda 1996. Expression of mitogen-activated protein kinase phosphatase-1 in the early phases of human epithelial carcinogenesis. Am J Pathol. 149, 1553–64.

Lohka, M.J., and Maller, J.L., 1985. Induction of nuclear envelope breakdown, chromosome condensation, and spindle formation in cell-free extracts. J. Cell Biol. 101, 518–23.

Lopes RD, Williams JB, Mehta RH, Reyes EM, Hafley GE, Allen KB, Mack MJ, Peterson ED, Harrington RA, and Gibson CM, 2012. Edifoligide and long-term outcomes after coronary artery bypass grafting: PRoject of Ex-vivo Vein graft ENgineering via Transfection IV (PREVENT IV) 5-year results. Am Hear. J 164, 379–386.

Luo, L.-J., Liu, F., Wang, X.-Y., Dai, T.-Y., Dai, Y.-L., Dong, C., and Ge, B.-X., 2012. An essential function for MKP5 in the formation of oxidized low density lipid-induced foam cells. Cell. Signal. 24, 1889–98.

M. Kyriakis, H. App, X.F. Zhang, P. Banerjee, D.L. Brautigan, U.R. and Rapp, J.A., 1992. Raf-1 activates MAP kinase–kinase. Nature 358, 417–421.

MacCorkle, R., and Tan, T.-H., 2005. Mitogen-activated protein kinases in cell-cycle control. Cell Biochem. Biophys. 43, 451–61.

Mackay DR, and Makise M, U.K., 2010. Defects in nuclear pore assembly lead to activation of an Aurora B-mediated abscission checkpoint. J Cell Biol 191, 923–31.

Maillet M, Purcell NH, Sargent MA, York AJ, and Bueno OF., 2008. DUSP6 (MKP3) Null Mice Show Enhanced ERK1/2 Phosphorylation at Baseline and Increased Myocyte Proliferation in the Heart Affecting Disease Susceptibility. J Biol Chem 283, 31246–31255.

Manchado, E., Guillamot, M., and Malumbres, M., 2012. Killing cells by targeting mitosis. Cell Death Differ. 19, 369–77.

Manetsch, M., Rahman, M.M., Patel, B.S., Ramsay, E.E., Rumzhum, N.N., Alkhouri, H., Ge, Q., and Ammit, A.J., 2013. Long-acting β2-agonists increase fluticasone propionate-induced mitogen-activated protein kinase phosphatase 1 (MKP-1) in airway smooth muscle cells. PLoS One 8, e59635.

Mao, L., Tang, Q., Samdani, S., Liu, Z., and Wang, J.Q., 2004. Regulation of MAPK/ERK phosphorylation via ionotropic glutamate receptors in cultured rat striatal neurons. Eur J Neurosci 19, 1207–1216.

Marchetti S, Gimond C, Chambard JC, Touboul T, and Roux D,., 2005. Extracellular signal-regulated kinases phosphorylate mitogen-activated protein kinase phosphatase 3/DUSP6 at serines 159 and 197, two sites critical for its proteasomal degradation. Mol Cell Biol 25, 854–864.

Margadant, C., Cremers, L., Sonnenberg, A., and Boonstra, J., 2013. MAPK uncouples cell cycle progression from cell spreading and cytoskeletal organization in cycling cells. Cell. Mol. Life Sci. 70, 293–307.

Marshall, C.J., 1994. Signal transduction. Hot lips and phosphorylation of protein kinases. Nature 367, 686.

Marx, S.O., Totary-Jain, H., and Marks, A.R., 2011. Vascular smooth muscle cell proliferation in restenosis. Circ. Cardiovasc. Interv. 4, 104–11.

Matsui, T., Murata, H., Sowa, Y., Sakabe, T., Koto, K., Horie, N., Tsuji, Y., Sakai, T., and Kubo, T., 2010. A novel MEK1 / 2 inhibitor induces G 1 / S cell cycle arrest in human fibrosarcoma cells 329–333.

Mayerl C, Lukasser M, Sedivy R, Niederegger H, and Seiler R, W.G., 2006. Atherosclerosis research from past to present–on the track of two pathologists with opposing views, Carl von Rokitansky and Rudolf Virchow. Virchows Arch 446, 96–103.

McAleenan A, Clemente-Blanco A, Cordon-Preciado V, Sen N, and Esteras M., 2013. Post-replicative repair involves separase-dependent removal of the kleisin subunit of cohesin. Nature 493, 250–4.

McAlpine CS,., 2013. The Development and Progression of Atherosclerosis: Evidence supporting a Role for Endoplasmic Reticulum (ER) Stress Signaling. Cardiovasc Hematol Disord Drug Targets. 13, 158–64.

McDonald, R. , Pyne, S., Pyne, N.J., Grant, A., Wainwright, C.L., and Wadsworth, R.M., 2010. The sphingosine kinase inhibitor N,N-dimethylsphingosine inhibits neointimal hyperplasia. Br. J. Pharmacol. 159, 543–53.

Michel, J.-B., Li, Z. and Lacolley, P., 2012. Smooth muscle cells and vascular diseases. Cardiovasc. Res. 95, 135–7.

Mill, C., and George, S.J., 2012. Wnt signalling in smooth muscle cells and its role in cardiovascular disorders. Cardiovasc. Res. 95, 233–40.

Misra-Press A, Rim CS, Yao H, and Roberson MS, 1995. A novel mitogen-activated protein kinase phosphatase. Structure, expression and regulation. J Biol Chem 270, 14587–96.

Montagnoli, A., Fiore, F., Eytan, E., Carrano, A.C., Draetta, G.F., Hershko, A., and Pagano, M., 1999. Ubiquitination of p27 is regulated by Cdk-dependent phosphorylation and trimeric complex formation. Genes Dev. 13, 1181–1189.

Moore RK,., 2005. Molecular biology and physiological role of the oocyte factor, BMP-15. Mol Cell Endocrinol. 234, 67–73.

Morel DW, and Hessler JR, C.G., 1983. Low density lipoprotein cytotoxicity induced by free radical peroxidation of lipid. J Lipid Res. 24, 1070–1076.

Morrison DK,., 2003. Regulation of MAP kinase signaling modules by scaffold proteins inmammals. Annu. Rev. Cell Dev. Biol 19, 91–118.

Muda M, Theodosiou A, Rodrigues N, Boschert U, Camps M, Gillieron C, and Davies K,., 1996. The dual specificity phosphatases M3⁄6 and MKP-3 are highly selective for inactivation of distinct mitogen-activated protein kinases. J Biol Chem 271, 27205–27208.

Münch, G., Bültmann, A., Li, Z., Holthoff, H.-P., Ullrich, J., Wagner, S., and Ungerer, M., 2012. Overexpression of ABCG1 protein attenuates arteriosclerosis and endothelial dysfunction in atherosclerotic rabbits. Heart Int. 7, e12.

Muslin AJ, 2008. MAPK signalling in cardiovascular health and disease: molecular mechanisms and therapeutic targets. Clin Sci (Lond). 115, 203–18.

Muto, A., Fitzgerald, T.N., Pimiento, J.M., Maloney, S., Teso, D., Paszkowiak, J.J., and Tormod, S., 2008. biology for vascular surgeons 45, 15–24.

Nakamura KD, and Martinez R., 1983. Tyrosine phosphorylation of specific proteins after mitogen stimulation of chicken embryo fibroblasts. Mol Cell Biol 3, 380–390.

Nasmyth, K., 2002. Segregating sister genomes: the molecular biology of chromosome separation. Science 297, 559–65.

Newby, A.C., and George, S.J., 1996. Proliferation, migration, matrix turnover, and death of smooth muscle cells in native coronary and vein graft atherosclerosis. Curr Opin Cardiol 11, 574–582.

Niba, E.T.E., Nagaya, H., Kanno, T., Tsuchiya, A., Gotoh, A., Tabata, C., Kuribayashi, K., Nakano, T., and Nishizaki, T., 2013. Crosstalk between PI3 kinase/PDK1/Akt/Rac1 and Ras/Raf/MEK/ERK pathways downstream PDGF receptor. Cell. Physiol. Biochem. 31, 905–13.

Niiro N., 2001. Zipper-interacting protein kinase induces Ca2+-free smooth muscle contraction via myosin light chain phosphorylation. J Biol Chem 276, 29567–74.

Nitta M, 1997. Heat shock induces transient p53-dependent cell cycle arrest at G1/S. Oncogene 15, 561–5.

Nizamutdinova, I.T., Kim, Y.M., Lee, J.H., Chang, K.C., and Kim, H.J., 2012. MKP-7, a negative regulator of JNK, regulates VCAM-1 expression through IRF-1. Cell. Signal. 24, 866–72.

Noguchi M, Tashiro H, Shirasaki R, Gotoh M, and Kawasugi K,2007. Dual-specificity phosphatase 10 is fused to MDS1/EVI1-like gene 1 in a case of acute myelogenous leukemia with der1t1;1(p36.3;q21). Int J Hematol 85, 175–176.

Norden C, Mendoza M, D.J, 2006. The NoCut pathway links completion of cytokinesis to spindle midzone function to prevent chromosome breakage. Cell 125, 85–98.

Novak-Hofer I, T.G., 1984. An activated S6 kinase in extracts from serum-and epidermal growth factorstimulated Swiss 3T3 cells. J.Biol. Chem 259, 5995–6000.

Nowak SJ and Corces V, 2000. Nowak SJ and Corces V. Genes Dev. 14, 3003 –3013.

Nurse PM, 2002. Cyclin dependent kinases and cell cycle control. Biosci Rep 22, 487–99.

Oktay, K., Buyuk, E., Oktem, O., Oktay, M., and Giancotti, F.G., 2008. The c-Jun N-terminal kinase JNK functions upstream of Aurora B to promote entry into mitosis. Cell Cycle 7, 533–41.

Olsen, B.B., Svenstrup, T.H., and Guerra, B., 2012. Downregulation of protein kinase CK2 induces autophagic cell death through modulation of the mTOR and MAPK signaling pathways in human glioblastoma cells. Int. J. Oncol. 41, 1967–76.

Owens GK, 1995. Regulation of differentiation of vascular smooth muscle cells. Physiol Rev 75, 487–517.

Palm-Leis, A., Singh, U.S., Herbelin, B.S., Olsovsky, G.D., Baker, K.M., and Pan, J., 2004. Mitogen-activated protein kinases and mitogen-activated protein kinase phosphatases mediate the inhibitory effects of all-trans retinoic acid on the hypertrophic growth of cardiomyocytes. J. Biol. Chem. 279, 54905–17.

Patterson, C., 2002. Things have changed: cell cycle dysregulation and smooth muscle cell dysfunction in atherogenesis. Ageing Res. Rev. 1, 167–79.

Patterson KI, Brummer T, and O'Brien PM,., 2009. Dual-specificity phosphatases: critical regulators with diverse cellular targets. Biochem J 418, 475–489.

Perales, S., Alejandre, M.J., Palomino-Morales, R., Torres, C., and Linares, A., 2010. Influence of cholesterol and fish oil dietary intake on nitric oxide-induced apoptosis in vascular smooth muscle cells. Nitric Oxide 22, 205–12.

Pfeifle B, Boeder H, D.H., 1987. Interaction of receptors for insulin-like growth factor I, platelet-derived growth factor, and fibroblast growth factor in rat aortic cells. Endocrinology 120, 2251–2258.

Pfisterer, L., Feldner, A., Hecker, M., and Korff, T., 2012. Hypertension impairs myocardin function: a novel mechanism facilitating arterial remodelling. Cardiovasc. Res. 96, 120–9.

Pines J, 2006. Mitosis: a matter of getting rid of the right protein at the right time. Trends Cell Biol. 16, 55–63.

Pohl C, J.S., 2009. Midbody ring disposal by autophagy is a post-abscission event of cytokinesis. Nat. Cell. Biol. 11, 65–70.

Potapova, O., and A. Haghighi1997. The Jun kinase/stress-activated protein kinase pathway functions to regulate DNA repair and inhibition of the pathway sensitizes tumor cells to cisplatin. J Biol Chem 272, 14041–14044.

Proctor BM, Ren J, Chen Z, Schneider JG, Coleman T, Lupu TS, and Semenkovich CF, M.A., 2007. Grb2 is required for atherosclerotic lesion formation. Arter. Thromb. Vasc. Biol 27, 1361–1367.

Qi G, Ogawa I, Kudo Y, MiyauchiM, Siriwardena BS, Shimamoto F, and Tatsuka M, T.T., 2007. Aurora-B expression and its correlation with cell proliferation and metastasis in oral cancer. Virchows Arch 450, 297–302.

Qian LB, Fu JY, and Cai X.,2012. Betulinic acid inhibits superoxide anion-mediated impairment of endothelium-dependent relaxation in rat aortas. Indian J Pharmacol. 44, 588–592.

Quemeneur, L., Beloeil, L., Michallet, M.C., Angelov, G., Tomkowiak, M., Revillard, J.P., and Marvel, J., 2004. Restriction of de novo nucleotide biosynthesis interferes with clonal expansion and differentiation into effector and memory CD8 T cells. J Immunol 173, 4945–4952.

Rahaman SO, Lennon DJ, Febbraio M, Podrez EA, and Hazen SL, S.R., 2006. A CD36-dependent signaling cascade is necessary for macrophage foam cell formation. Cell Metab. 4, 211–221.

Rahmouni, S., Cerignoli, F., Alonso, A., Tsutji, T., Henkens, R., Zhu, C., Louis-dit-sully, C., Moutschen, M., Jiang, W., and Mustelin, T., 2006. Loss of the VHR dual-specific phosphatase causes cell-cycle arrest and senescence. Group 8.

Rauhala HE, Porkka KP, Tolonen TT, and Martikainen PM,., 2005. Dual-specificity phosphatase 1 and serum/glucocorticoid-regulated kinase are downregulated in prostate cancer. Int J Cancer. 117, 738–745.

Ray LB, 1988. Insulin-stimulated microtubule-associated protein kinase is phosphorylated on tyrosine and threonine in vivo. Proc. Natl. Acad. Sci. USA 85, 3753–3757.

Reddy SM, 2004. Potential role for mitogen-activated protein kinase phosphatase-1 in the development of atherosclerotic lesions in mouse models. Arter. Thromb Vasc Biol. 24, 1676–81.

Reetz, J., Genz, B., Meier, C., Kowtharapu, B.S., Timm, F., Vollmar, B., Herchenröder, O., Abshagen, K., and Pützer, B.M., 2013. Development of Adenoviral Delivery Systems to Target Hepatic Stellate Cells In Vivo. PLoS One 8, e67091.

Reiterer, V., Fey, D., Kolch, W., Kholodenko, B.N., and Farhan, H., 2013. Pseudophosphatase STYX modulates cell-fate decisions and cell migration by spatiotemporal regulation of ERK1/2. Proc. Natl. Acad. Sci. U. S. A. 110, E2934–43.

Rekhter, M.D., and Gordon, D., 1994. Cell proliferation and collagen synthesis are two independent events in human atherosclerotic plaques. J Vasc Res 31, 280–286.

Rensen, S.S., Doevendans, P.A., and van Eys, G.J., 2007. Regulation and characteristics of vascular smooth muscle cell phenotypic diversity. Neth Hear. J 15, 100–108.

Reynisdottir, I., Polyak, K., Iavarone, A., and Massague, J., 1995. Kip/Cip and Ink4 Cdk inhibitors cooperate to induce cell cycle arrest in response to TGF-beta. Genes Dev 9, 1831–1845.

Ricci R, Sumara G, Sumara I, Rozenberg I, Kurrer M, Akhmedov A, Hersberger M, Eriksson U,Eberli FR, Becher B, Borén J, Chen M, Cybulsky MI, Moore KJ, Freeman MW, Wagner EF, and MatterCM, L.T., 2004. Requirement of JNK2 for scavenger receptor A-mediated foam cell formation in atherogenesis. Science (80-.). 206, 1558–1561.

Rieder, C.L., 2011. Mitosis in vertebrates: the G2/M and M/A transitions and their associated checkpoints. Chromosome Res. 19, 291–306.

Rigas JD, Hoff RH, and Rice AE., 2001. Transition state analysis and requirement of Asp-262 general acid/base catalyst for full activation of dual-specificity phosphatase MKP3 by extracellular regulated kinase. Biochemistry 40, 4398–4400.

Robinson, C.J.M., Sloss, C.M., and Plevin, R., 2001. Inactivation of JNK activity by mitogen-activated protein kinase phosphatase-2 in EAhy926 endothelial cells is dependent upon agonist-specific JNK translocation to the nucleus 13, 29–41.

Rodriguez-Menocal, L., Wei, Y., Pham, S.M., St-pierre, M., Li, S., Goldschmidt-clermont, P., and Vazquez-padron, R.I., 2011. A Novel Mouse Model of In-Stent Restenosis 209, 359–366.

Rojo F, González-Navarrete I, and Bragado R., 2009. Mitogen-activated protein kinase phosphatase-1 in human breast cancer independently predicts prognosis and is repressed by doxorubicin. Clin Cancer Res. 15, 3530–9.

Rosini P, De Chiara G, Bonini P, Lucibello M, Marcocci ME, Garaci E, 2004. Nerve growth factor-dependent survival of CESS B cell line is mediated by increased expression and decreased degradation of MAPK phosphatase 1. J Biol Chem 279, 14016–14023.

Rosner, M.R., 2007. MAP kinase meets mitosis: a role for Raf Kinase Inhibitory Protein in spindle checkpoint regulation. Cell Div. 2, 1.

Ross, R., 1999. Atherosclerosis--an inflammatory disease. N Engl J Med 340, 115–126.

Rössig, L., Haendeler, J., Hermann, C., Malchow, P., Urbich, C., Zeiher, a M., and Dimmeler, S., 2000. Nitric oxide down-regulates MKP-3 mRNA levels:

involvement in endothelial cell protection from apoptosis. J. Biol. Chem. 275, 25502–7.

Rossomando AJ, Payne DM, and Weber MJ, S.T., 1989. Evidence that pp42, a major tyrosine kinase target protein, is a mitogen-activated serine/threone protein kinase. Proc Natl Acad Sci USA 86, 6940–6943.

Rudijanto, A.,. The role of vascular smooth muscle cells on the pathogenesis of atherosclerosis. Acta Med. Indones. 39, 86–93.

SaccoP., 2012. Mapping the human phosphatome on growth pathways. Mol Syst Biol. 8.

Sagona, A.P., and Stenmark, H., 2010. Cytokinesis and cancer. FEBS Lett. 584, 2652–61.

Sakakura, K., Nakano, M., Otsuka, F., Ladich, E., Kolodgie, F.D., and irmani, R., 2013. Pathophysiology of atherosclerosis plaque progression. Heart. Lung Circ. 22, 399–411.

Sakurai H, Miyoshi H, and Mizukami J, 2000. Phosphorylation-dependent activation of TAK1 mitogen-activated protein kinase kinase kinase by TAB1. FEBS Lett 474, 141–5.

Sata M, Saiura A, Kunisato A, Tojo A, Okada S, Tokuhisa T, Hirai H, Makuuchi M, and Hirata Y,., 2002. Hematopoietic stem cells differentiate into vascular cells that participate in the pathogenesis of atherosclerosis. Nat Med. 8, 403– 409.

Schoen FJ, 2005. Cardiac valves and valvular pathology: update on function, disease, repair, and replacement. Cardiovasc Pathol. 14, 189–94.

Schroeder, J., McGachy, H.A., Woods, S., Plevin, R., and Alexander, J., 2013. T cell hypo-responsiveness against Leishmania major in MAP kinase phosphatase (MKP) 2 deficient C57BL/6 mice does not alter the healer disease phenotype. PLoS Negl. Trop. Dis. 7, e2064.

Schubbert, S., Shannon, K., and Bollag, G., 2007. Hyperactive Ras in developmental disorders and cancer. Nat Rev Cancer 7, 295–308.

Schwartz RS, and Edelman E, ., 2002. Drug-eluting stents in preclinical studies: recommend end evaluation from a consensus group. Circulation 106, 1867–73.

Schwartz SM, and Campbell GR, C.J., 1986. Replication of smooth muscle cells in vascular disease. Circ Res. 58, 427– 444.

Senolt, L., Vencovsky, J., Pavelka, K., Ospelt, C., and Gay, S., 2009. Prospective new biological therapies for rheumatoid arthritis. Autoimmun Rev 9, 102–107.

Serruys PW, de Jaegere P, Kiemeneij F, Macaya C, and Rutsch W, H.G., 1994. A comparison of balloon-expandable-stent implantation with balloon angioplasty in patients with coronary artery disease: Benestent Study Group. N Engl J Med 331, 489–495.

Severson AF, Hamill DR, Carter JC, and Schumacher J,., 2000. The aurora-related kinase AIR-2 recruits ZEN-4/CeMKLP1 to the mitotic spindle at metaphase and is required for cytokinesis. Curr Biol. 10, 1162–1171.

Sirois MG, and Simons M,., 1997. Antisense oligonucleotide inhibition of PDGFR-beta receptor subunit expression directs suppression of intimal thickening. Circulation 95, 669–76.

Skop P., 2004. Dissection of the mammalian midbody proteome reveals conserved cytokinesis mechanisms. Science (80-.). 305, 61–6.

Slack DN, Seternes OM, and Gabrielsen M,., 2001. Distinct binding determinants for erk2/p38alpha and jnk mapkinases mediate catalytic activation and substrate selectivity ofmap kinase phosphatase-1. J Biol Chem 19, 16491–165002.

Slijkhuis, W., Mali, W., and Appelman, Y., 2009. A historical perspective towards a non-invasive treatment for patients with atherosclerosis. Neth. Heart J. 17, 140–4.

Sloss, C.M., Cadalbert, L., Finn, S.G., Fuller, S.J., and Plevin, R., 2005. Disruption of two putative nuclear localization sequences is required for cytosolic localization of mitogen-activated protein kinase phosphatase-2. Cell. Signal. 17, 709 – 716.

Smeal, T., 1991. "Oncogenic and transcriptional cooperation with Ha-Ras requires phosphorylation of c-Jun on serines 63 and 73. Nature 354, 494–496.

Smith, A., Price, C., Cullen, M., Muda, M., King, A., Ozanne, B., Arkinstall, S., and Ashworth, A., 1997. Chromosomal Localization of Three Human Dual Specificity Phosphatase Genes (DUSP4 , DUSP6 , and DUSP7). Cancer Res. 527, 524–527.

Smith, T.G., Sweetman, D., Patterson, M., Keyse, S.M., and Münsterberg, A., 2005. Feedback interactions between MKP3 and ERK MAP kinase control scleraxis expression and the specification of rib progenitors in the developing chick somite. Biomed. Res. 1305–1314.

Somlyo AP., 2003. Ca2+ sensitivity of smooth muscle and nonmuscle myosin II: modulated by G proteins, kinases, and myosin phosphatase. Physiol Rev 83, 1325–58.

Song, L., Li, D., Liu, R., Zhou, H., Chen, J., and Huang, X., 2007. Ser-10 phosphorylated histone H3 is involved in cytokinesis as a chromosomal passenger. Cell Biol. Int. 31, 1184–90.

Stewart AE, and Dowd S1999. Crystal structure of the MAPK phosphatase Pyst1 catalytic domain and implications for regulated activation. Nat Struct Biol 6, 174–181.

Sturgill TW,., 1986. Muscle proteins related to microtubule associated protein-2 are substrates for an insulin-stimulatable kinase. Biochem. Biophys. Res. Comm 134, 565–571.

Subramanian, S., Jaffer, F.A., and Tawakol, A. Optical molecular imaging in atherosclerosis. J Nucl Cardiol 17, 135–144.

Sumara, G., Belwal, M., and Ricci, R., 2005. "Jnking" atherosclerosis. Cell Mol Life Sci 62, 2487–2494.

Sun, H., Charles, C.H., Lau, L.F., and Tonks, N.K., 1993. MKP-1 (3CH134), an immediate early gene product, is a dual specificity phosphatase that dephosphorylates MAP kinase in vivo. Cell 75, 487–493.

Tang, N., Liu, L., Kang, K., Mukherjee, P.K., Takahara, M., Chen, G., McCormick, T.S., Cooper, K.D., and Ghannoum, M., 2004. Inhibition of monocytic interleukin-12 production by Candida albicans via selective activation of ERK mitogen-activated protein kinase. Infect Immun 72, 2513–2520.

Tanoue T, Maeda R, and Adachi M, N.E., 2001. Identification of a docking groove on ERK and p38 MAP kinases that regulates the specificity of docking interactions. EMBO J. 200, 466–479.

Taylor DA., 1988. Calcium dependence of myosin light chain phosphorylation in smooth muscle cells. J Biol Chem 263, 14456–62.

Teeling, M., 2004. Regulation of innate and adaptive immune responses by MAP kinase. Nature 430, 793–797.

Teng, C., Huang, W., and Meng, T., 2007. Several Dual Specificity Phosphatases Coordinate to Control the Magnitude and Duration of JNK Activation in Signaling Response to Oxidative Stress * □. J. Biol. Chem. 282, 28395–28407.

Thakar, R.G., Cheng, Q., Patel, S., Chu, J., Nasir, M., Liepmann, D., Komvopoulos, K., and Li, S., 2009. Cell-shape regulation of smooth muscle cell proliferation. Biophys. J. 96, 3423–32.

Thompson, R.C., Allam, A.H., Lombardi, G.P., Wann, L.S., Sutherland, M.L., Sutherland, J.D., Soliman, M.A.-T., Frohlich, B., Mininberg, D.T., Monge, J.M., Vallodolid, C.M., Cox, S.L., Abd el-Maksoud, G., Badr, I., Miyamoto, M.I., el-Halim Nur el-Din, A., Narula, J., Finch, C.E., and Thomas, G.S., 2013. Atherosclerosis across 4000 years of human history: the Horus study of four ancient populations. Lancet 381, 1211–22.

Thornton, T.M., and Rincon, M., 2009. Non-Classical P38 Map Kinase Functions : Cell Cycle Checkpoints and Sur- vival. Cell 5.

Thyberg, J., Hedin, U., Sjolund, M., Palmberg, L., and Bottger, B. 1990. Regulation of differentiated properties and proliferation of arterial smooth muscle cells. Arterioscler. Thromb. Vasc. Biol. 10, 966–990.

Tigalis M, B.A., 2007. Protein tyrosine phophatase function: the substrate perspective. Biochem J. 402, 1–15.

Toda, K., Naito, K., Mase, S., Ueno, M., Uritani, M., Yamamoto, A., and Ushimaru, T., 2012. APC/C-Cdh1-dependent anaphase and telophase progression during mitotic slippage. Cell Div. 7, 4.

Tonks, N.K., 2006. Protein tyrosine phosphatases: from genes, to function, to disease. Nat. Rev. Mol. Cell Biol. 7, 833–846.

Torres, C., Francis, M.K., Lorenzini, A., Tresini, M., and Cristofalo, V.J., 2003. Metabolic stabilization of MAP kinase phosphatase-2 in senescence of human fibroblasts. Exp. Cell Res. 290, 195–206.

Touchard AG, S.R., 2006. Preclinical restenosis models: challenges and successes. Toxicol Pathol. 34, 11–18.

Touny LH., 2006. Identification of both Myt-1 and Wee-1 as necessary mediators of the p21-independent inactivation of the cdc-2/cyclin B1 complex and growth inhibition of TRAMP cancer cells by genistein. Prostate 66, 1542–55.

Tresini M, Lorenzini A, Torres C, and C.V., 2007. Modulation of replicative senescence of diploid human cells by nuclear ERK signaling. J Biol Chem. 282, 4136–4151.

Tritto, I., and Ambrosio, G., 2004. The multi-faceted behavior of nitric oxide in vascular “inflammation”: catchy terminology or true phenomenon? Cardiovasc Res 63, 1–4.

Tsigkas, G., 2011. Review Article Stent Restenosis, Pathophysiology and Treatment Options: A 2010 Update 149–157.

Tsuiki, H., Nitta, M., Tada, M., Inagaki, M., Ushio, Y., and aya, H., 2001. Mechanism of hyperploid cell formation induced by microtubule inhibiting drug in glioma cell lines. Oncogene 20, 420–9.

Ussar, S., and Voss, T., 2004. MEK1 and MEK2, different regulators of the G1/S transition. J Biol Chem 279, 43861–43869.

Vagnarelli P, 2012. Repo-Man-PP1: a link between chromatin remodelling and nuclear envelope reassembly. Nucleus 3, 138–42.

Vagnarelli, P., 2012. Mitotic chromosome condensation in vertebrates. Exp. Cell Res. 318, 1435–41.

Vas, A.C., and Clarke, D.J., 2008. Aurora B kinases restrict chromosome decondensation to telophase of mitosis. Cell Cycle 7, 293–6.

Venter, D.J., Ramus, S.J., Hammet, F.M.A., Silva, M. De, Hutchins, A., Petrovic, V., Price, G., and Armes, J.E., 2005. Complex CGH alterations on chromosome arm 8p at candidate tumor suppressor gene loci in breast cancer cell lines 160, 134–140.

Ventura, J.J., Cogswell, P., Flavell, R.A., Baldwin Jr., A.S., and Davis, R.J., 2004. JNK potentiates TNF-stimulated necrosis by increasing the production of cytotoxic reactive oxygen species. Genes Dev 18, 2905–2915..

Waehler R, and Russell SJ, C.D., 2007. Engineering targeted viral vectors for gene therapy. Nat Rev Genet 8, 573–586.

Waha, A., Felsberg, J., Hartmann, W., von dem Knesebeck, A., Mikeska, T., Joos, S., Wolter, M., Koch, A., Yan, P.S., Endl, E., Wiestler, O.D., Reifenberger, G., Pietsch, T., and Waha, A., 2010. Epigenetic downregulation of mitogen-activated protein kinase phosphatase MKP-2 relieves its growth suppressive activity in glioma cells. Cancer Res. 70, 1689–99.

Wancket LM, Meng X, and Rogers LK, L.Y., 2012. Mitogen-activated protein kinase phosphatase (Mkp)-1 protects mice against acetaminophen-induced hepatic injury. Toxicol Pathol. 40, 1095–105.

Wang W., 2013. Zygotic G2/M Cell Cycle Arrest Induced by ATM/Chk1 Activation and DNA Repair in Mouse Embryos Fertilized with Hydrogen Peroxide-Treated Epididymal Mouse Sperm. PLoS One 8, 73987.

Wang, H., Lu, Y., Huang, W., Papoutsakis, E.T., Fuhrken, P., and Eklund, E.A., 2007. HoxA10 Activates Transcription of the Gene Encoding Mitogen-activated Protein Kinase Phosphatase 2 (Mkp2) in Myeloid Cells *. J. Biol. Chem. 282, 16164 – 16176.

Weston, C.R., and Davis, R.J., 2007. The JNK signal transduction pathway. Curr. Opin. Cell Biol. 19, 142–9.

Weston, C.R., Lambright, D.G., Davis, R.J., 2002. Signal transduction. MAP kinase signaling specificity. Science 296, 2345–2347.

White, K.M., Alba, R., Parker, A.L., Wright, A.F., Bradshaw, A.C., Delles, C., McDonald, R. and Baker, A.H., 2013. Assessment of a novel, capsid-modified adenovirus with an improved vascular gene transfer profile. J. Cardiothorac. Surg. 8, 183.

Wilhelm, S.M., Carter, C., Tang, L., Wilkie, D., McNabola, A., Rong, H., Chen, C., Zhang, X., Vincent, P., McHugh, M., Cao, Y., Shujath, J., Gawlak, S., Eveleigh, D., Rowley, B., Liu, L., Adnane, L., Lynch, M., Auclair, D., Taylor, I., Gedrich, R., Voznesensky, A., Riedl, B., Post, L.E., Bollag, G., and Trail, P.A., 2004. BAY 43-9006 exhibits broad spectrum oral antitumor activity and targets the RAF/MEK/ERK pathway and receptor tyrosine kinases involved in tumor progression and angiogenesis. Cancer Res 64, 7099–7109.

Willard, F.S., and Crouch, M.F., 2001. MEK, ERK, and p90RSK are present on mitotic tubulin in Swiss 3T3 cells: a role for the MAP kinase pathway in regulating mitotic exit. Cell Signal 13, 653–664.

Woods, S., Schroeder, J., McGachy, H. a, Plevin, R., Roberts, C.W., and Alexander, J., 2013. MAP Kinase Phosphatase-2 Plays a Key Role in the Control of Infection with Toxoplasma gondii by Modulating iNOS and Arginase-1 Activities in Mice. PLoS Pathog. 9, e1003535.

Wu, J.J., and Bennett, A.M., 2005. Essential role for mitogen-activated protein (MAP) kinase phosphatase-1 in stress-responsive MAP kinase and cell survival signaling. J Biol Chem 280, 16461–16466.

Wu, Q., and Brown, M.R., 2006. Signaling and function of insulin-like peptides in insects. Annu Rev Entomol 51, 1–24.

Wu, Z., Jiao, P., Huang, X., Feng, B., Feng, Y., Yang, S., Hwang, P., Du, J., Nie, Y., Xiao, G., and Xu, H., 2010. MAPK phosphatase – 3 promotes hepatic gluconeogenesis through dephosphorylation of forkhead box O1 in mice 120, 3901–3911.

Xu, H., Yang, Q., Shen, M., Huang, X., Dembski, M., Gimeno, R., Tartaglia, L.A., Kapeller, R., and Wu, Z., 2005. Dual specificity MAPK phosphatase 3 activates PEPCK gene transcription and increases gluconeogenesis in rat hepatoma cells. J Biol Chem 280, 36013–36018.

Xu J, Ismat FA, Wang T, and Yang J, E.J., 2007. NF1 regulates a Ras-dependent vascular smooth muscle proliferative injury response. Circulation 116, 2148–56.

Xu, L., Liu, T., Han, F., Zong, Z., Wang, G., Yu, B., and Zhang, J., 2012. AURKB and MAPK involvement in the regulation of the early stages of mouse zygote development. Sci. China. Life Sci. 55, 47–56.

Y. Yarden, A. and Ullrich, 1988. Growth factor receptor tyrosine kinases. Annu. Rev. Biochem. 57, 443–478.

Yang D, Rismanchi N, Renvoisé B, Lippincott-Schwartz J, and Blackstone C, 2008. Structural basis for midbody targeting of spastin by the ESCRT-III protein CHMP1B. Nat Struct Mol Biol. 15, 1278–86.

Yang, D., Xie, P., Guo, S., and Li, H., 2010. Induction of MAPK phosphatase-1 by hypothermia inhibits TNF-alpha-induced endothelial barrier dysfunction and apoptosis. Cardiovasc. Res. 85, 520–9.

Yang, K.L., Chang, W.T., Chuang, C.C., Hung, K.C., and Li, E.I., 2008. Antagonizing TGF-beta induced liver fibrosis by a retinoic acid derivative through regulation of ROS and calcium influx. Biochem Biophys Res Commun 365, 484–489.

Yang, S.-H., Sharrocks, A.D., and Whitmarsh, A.J., 2013. MAP kinase signalling cascades and transcriptional regulation. Gene 513, 1–13.

Yu PJ, Ferrari G, Pirelli L, Gulkarov I, Galloway AC, and Mignatti P, P.G., 2007. Vascular injury and modulation of MAPKs: a targeted approach to therapy of restenosis. Cell Signal 19, 1359–71.

Zakkar, M., Chaudhury, H., Sandvik, G., Enesa, K., Luong, L.A., Cuhlmann, S., Mason, J.C., Krams, R., Clark, A.R., Haskard, D.O. and Evans, P.C., 2008. Increased endothelial mitogen-activated protein kinase phosphatase-1 expression suppresses proinflammatory activation at sites that are resistant to atherosclerosis. Circ. Res. 103, 726–32.

Zama, T., Aoki, R., Kamimoto, T., Inoue, K., Ikeda, Y., and Hagiwara, M., 2002. Scaffold Role of a Mitogen-activated Protein Kinase Phosphatase , SKRP1 , for the JNK Signaling Pathway *. Biochemistry 277, 23919 –23926.

Zaragoza, C., Gomez-Guerrero, C., Martin-Ventura, J.L., Blanco-Colio, L., Lavin, B., Mallavia, B., Tarin, C., Mas, S., Ortiz, A., and Egido, J., 2011. Animal models of cardiovascular diseases. J. Biomed. Biotechnol. 2011, 497841.

Zardi, E.M., and Afeltra, A., Endothelial dysfunction and vascular stiffness in systemic lupus erythematosus: Are they early markers of subclinical atherosclerosis? Autoimmun Rev 9, 684–686.

Zecevic, M., Catling, A.D., Eblen, S.T., Renzi, L., Hittle, J.C., Yen, T.J., Gorbsky, G.J., and Weber, M.J., 1998. Active MAP kinase in mitosis: localization at kinetochores and association with the motor protein CENP-E. J Cell Biol 142, 1547–1558.

Zeliadt NA, and Maurob LJ,., 2008. Reciprocal Regulation of Extracellular Signal Regulated Kinase 1/2 and Mitogen Activated Protein Kinase Phosphatase-3. Toxicol Appl Pharmacol. 232, 408–417.

Zetterberg AH, and Pettersson RF, L.S., 2001. Hartwell, Hunt and Nurse share the 2001 Nobel Prize in physiology or medicine. CDK and cyclin--molecular motors of cell cycle. Lakartidningen 98, 4544–50.

Zhan, Y., 2002. Effects of Dominant-Negative c-Jun on Platelet-Derived Growth Factor-Induced Vascular Smooth Muscle Cell Proliferation. Arterioscler. Thromb. Vasc. Biol. 22, 82–88.

Zhan, Y., 2003. Role of JNK, p38, and ERK in Platelet-Derived Growth Factor-Induced Vascular Proliferation, Migration, and Gene Expression. Arterioscler. Thromb. Vasc. Biol. 23, 795–801.

Zhang L, Zhou Y, and Zhu J, X.Q., 2012. An updated view on stem cell differentiation into smooth muscle cells. Vasc. Pharmacol 56, 280–287.

Zhang S, Weinheimer C, Courtois M, Kovacs A, Zhang CE, Cheng AM, and Wang Y,., 2003. The role of the Grb2-p38 MAPK signaling pathway in cardiac hypertrophy and fibrosis. J. Clin. Invest 111, 833–841.

Zhang, T., Mulvaney, J.M., and Roberson, M.S., 2001. Activation of mitogen-activated protein kinase phosphatase 2 by gonadotropin-releasing hormone. Mol. Cell. Endocrinol. 172, 79 – 89.

Zhang, W., and Liu, H.T., 2002. MAPK signal pathways in the regulation of cell proliferation in mammalian cells. Cell Res 12, 9–18.

Zhang Y, D.C., 2007. Regulatory mechanisms of mitogen activated kinase signaling. Cell Mol Life Sci 64, 2771–89.

Zhang Z-Y., 2001. Protein tyrosine phosphatases: prospects for therapeutics. Curr. Opin. Chem. Biol 5, 416–423.

Zhao M, Liu Y, Wang X, New L, and Han J, B.U., 2002. Activation of the p38 MAP kinase pathway is required for foam cell formation from macrophages exposed to oxidized LDL. APMIS 110, 458–468.

Zhao, Y., 2003. Suppression of mitogen-activated protein kinase phosphatase-1 (MKP-1) by heparin in vascular smooth muscle cells. Biochem. Pharmacol. 66, 769–776.

Zheng, H., Xue, S., Lian, F., and Wang, Y.-Y., 2011. A novel promising therapy for vein graft restenosis: overexpressed Nogo-B induces vascular smooth muscle cell

apoptosis by activation of the JNK/p38 MAPK signaling pathway. Med. Hypotheses 77, 278–81.

Zhou B and Zhang ZY, 1999. Mechanism of mitogen activated protein kinase phosphatase-3 activation by ERK2. J Biol Chem 274, 35526–35534.

Zhou, J., Ma, J., Zhang, B.C., Li, X.L., Shen, S.R., Zhu, S.G., Xiong, W., Liu, H.Y., Huang, H., Zhou, M., and Li, G.Y., 2004. BRD7, a novel bromodomain gene, inhibits G1-S progression by transcriptionally regulating some important molecules involved in ras/MEK/ERK and Rb/E2F pathways. J Cell Physiol 200, 89–98.